

PDF hosted at the Radboud Repository of the Radboud University Nijmegen

The following full text is a publisher's version.

For additional information about this publication click this link.

<http://hdl.handle.net/2066/148935>

Please be advised that this information was generated on 2018-11-05 and may be subject to change.

Familial macular disease

*Clinical and genetic studies on age-related macular degeneration
and inherited macular dystrophies*



Nicole T.M. Saksens

Familial macular disease

*Clinical and genetic studies on age-related macular degeneration
and inherited macular dystrophies*

Nicole T.M. Saksens

Research described in this thesis was a Salentein fellowship.

It was funded by the Diana Hermes stichting, Foundation Fighting Blindness USA, Nederlandse Oogonderzoek Stichting, Macula Fonds, Oogfonds, Algemene Nederlandse Vereniging ter Voorkoming van Blindheid, Stichting Nederlands Oogheelkundig Onderzoek, and Gelderse Blindenstichting. Financial contribution to the publication of this thesis from Radboud University Nijmegen, Stichting Leids Oogheelkundig Ondersteuningsfonds, Rotterdamse Stichting Blindenbelangen, Stichting Blindenhulp, Stichting voor Ooglijders, Landelijke Stichting voor Blinden en Slechtzienden, Elvea Low Vision B.V., Ergra Low vision B.V., Santen Pharma, Abbott Medical Optics B.V., Allergan B.V., Bayer Healthcare B.V., Chipsoft B.V., DORC, Genzyme Europe B.V., Lameris Ootech B.V., Low Vision Totaal B.V., Rockmed, Sanmed B.V., Synga medical B.V., Théa pharma B.V., Ophtec B.V., Haags Kunstogen Laboratorium, Simovision B.V., Carl Zeiss B.V., Koninklijke Visio, Novartis pharma, Oculenti B.V., Urspharm Benelux B.V. is gratefully acknowledged.

None of the above-mentioned organizations or companies could influence or bias the content of this thesis.

The work presented in this thesis was carried out within the Radboud Institute for Health Sciences.

Institute for Health Sciences
Radboudumc



Copyright © 2015, N.T.M. Saksens, Nijmegen, the Netherlands

Design: Nicole Nijhuis

Cover art: Joel Lammerink

Printed by: Gildeprint, Enschede

ISBN: 978-94-6233-058-0

No part of this thesis may be reproduced in any form without written permission from the author.

Familial macular disease

*Clinical and genetic studies on age-related macular degeneration
and inherited macular dystrophies*

Een wetenschappelijke proeve
op het gebied van de Medische Wetenschappen

Proefschrift

ter verkrijging van de graad van doctor
aan de Radboud Universiteit Nijmegen
op gezag van de Rector Magnificus,
volgens besluit van het College van Decanen
in het openbaar te verdedigen op 18 december 2015
om 10:30 uur precies

Door

Nicole Theresia Maria Saksens

geboren op 3 januari 1987
te Haaksbergen

Promotoren:

Prof. dr. C.B. Hoyng

Prof. dr. A.I. den Hollander

Copromotor:

Dr. C.J.F. Boon (Leids Universitair Medisch Centrum)

Manuscriptcommissie:

Prof. dr. B. Franke (Voorzitter)

Prof. dr. L.A.L.M. Kiemeny

Dr. M.J. van Schooneveld (Academisch Medisch Centrum)



Trots 'een echte Saksens' te zijn

CONTENTS

	List of abbreviations	11
Chapter 1:	General introduction	15
Chapter 2:	Age-related macular degeneration and macular dystrophies mimicking AMD	45
	Macular dystrophies mimicking age-related macular degeneration <i>Prog Retin Eye Res 2014;39:23-57</i>	
Chapter 3:	Age-related macular degeneration	
3.1	Clinical characteristics of familial and sporadic age-related macular degeneration: differences and similarities <i>Invest Ophthalmol Vis Sci 2014;55:7085-92</i>	125
3.2	Predictive value of family history versus genetic risk variants in age-related macular degeneration <i>Manuscript in preparation</i>	143
3.3	Analysis of risk alleles and complement activation levels in familial and non-familial age-related macular degeneration <i>PLoS One; Under review</i>	159
3.4	Rare variants associated with age-related macular degeneration result in a lower age at onset and higher familial occurrence <i>JAMA Ophthalmol; Under review</i>	177
3.5	Analysis of rare variants in the <i>CFH</i> gene in patients with the cuticular drusen subtype of age-related macular degeneration <i>Mol Vis 2015;21:285-92</i>	193
Chapter 4:	Dominant cystoid macular dystrophy	211
	Dominant cystoid macular dystrophy <i>Ophthalmology 2015;122:180-91</i>	
Chapter 5:	Butterfly-shaped pigment dystrophy	235
	Mutations in α -catenin 1 cause butterfly-shaped pigment dystrophy and perturbed retinal pigment epithelium integrity <i>Nature Genet; accepted</i>	
Chapter 6:	General discussion	267
Chapter 7:	Summary / Samenvatting	287
	List of publications	293
	Dankwoord	297
	About the author / PhD portfolio	300

LIST OF ABBREVIATIONS

A2E	N-retinylidene-N-retinylethanolamine
aHUS	atypical hemolytic-uremic syndrome
AFVD	adult-onset foveomacular vitelliform dystrophy
AMD	age-related macular degeneration
anti-VEGF	anti-vascular endothelial growth factor
AREDS	Age-Related Eye Disease Study
ARMS2	age-related maculopathy susceptibility protein 2
AUC	area under the curve
BCVA	best corrected visual acuity
BMI	body mass index
BSPD	butterfly-shaped pigment dystrophy
BVMD	Best vitelliform macular dystrophy
C2	complement component 2
C3	complement component 3
C9	complement component 9
CACD	central areolar choroidal dystrophy
CCP	complement control protein
CD	cuticular drusen
CFB	complement factor B
CFCs	cystoid fluid collections
CFH	complement factor H
CFI	complement factor I
CI	confidence interval
CIRCL	Cologne Image Reading Center and Laboratory
CME	cystoid macular edema
CNBP	CCHC-type zinc finger, nucleic acid-binding protein
CNV	choroidal neovascularization
CSC	central serous chorioretinopathy
cSLO	confocal scanning laser ophthalmoscopy
CTNNA1	α -catenin 1
D	diopters
DA	dark adaptation
DCMD	dominant cystoid macular dystrophy
DMPK	dystrophia myotonica protein kinase
DNA	deoxyribonucleic acid
EOG	electro-oculography
ERG	electroretinography
ETDRS	Early Treatment Diabetic Retinopathy Study

EUGENDA	European Genetic Database
EVS	Exome Variant Server
FA	fluorescein angiography
FAF	fundus autofluorescence
FF-ERG	full-field ERG
FO	fast oscillation
GA	geographic atrophy
HGVS	Human Genome Variation Society
ICGA	indocyanine green angiography
iPsc	induced pluripotent stem cells
ISCEV	International Society for Clinical Electrophysiology of Vision
logMAR	logarithm of the minimal angle of resolution
LORD	late-onset retinal degeneration
LP	light peak
MAC	membrane attack complex
MacTel	macular telangiectasia
MAF	minor allele frequency
MELAS	mitochondrial encephalopathy lactic acidosis and stroke-like episodes
MIDD	maternally inherited diabetes and deafness
ML	malattia leventinese
MPGN II	membranoproliferative glomerulonephritis type II
NCMD	North Carolina macular dystrophy
OCT	optical-coherence tomography
OD	oculus dexter
ONL	outer nuclear layer
OR	odds ratio
OS	oculus sinister
PCR	polymerase chain reaction
Polyphen	polymorphism phenotyping
<i>PRPH2</i>	peripherin-2
PXE	pseudoxanthoma elasticum
RNA	ribonucleic acid
ROC	receiver operating characteristics
RPD	reticular pseudodrusen
RPE	retinal pigment epithelium
RV	rare variant
SD	standard deviation
SD-OCT	spectral-domain optical coherence tomography
SE	spherical equivalents
SEM	standard error of the mean

SFD	Sorsby fundus dystrophy
SIFT	sorting intolerant from tolerant
SNPs	single nucleotide polymorphisms
SNVs	single nucleotide variants
<i>TIMP3</i>	tissue inhibitor of metalloproteinase 3
VA	visual acuity
VEGF	vascular endothelial growth factor

Visual acuity conversion chart

Snellen VA in decimal	Snellen VA in Foot	VA in LogMAR
1.25	20/16	-0.10
1.00	20/20	0.00
0.80	20/25	0.10
0.63	20/32	0.20
0.50	20/40	0.30
0.40	20/50	0.40
0.32	20/63	0.50
0.25	20/80	0.60
0.20	20/100	0.70
0.16	20/125	0.80
0.125	20/160	0.90
0.10	20/200	1.00
0.05	20/400	1.30

Chapter 1

General introduction





1.1 Anatomy of the eye

When light enters the front of the eye through the cornea, the light waves are refracted by several tissues in the eye and ultimately focus on the central retina at the back of the eye (**Figure 1.1**). The axial length of the adult human eyeball is 21-26 mm. Short eyes (axial length <20 mm) have their focal point behind the retina and are called hyperopic, whereas long eyes (axial length >26 mm) have their focal point in front of the retina and are called myopic.

In eyes that have a short axial length, the anterior chamber angle (the angle formed between the cornea and the iris) is also narrow and can close, resulting in acute angle-closure glaucoma, like in some patients with dominant cystoid macular dystrophy (DCMD).

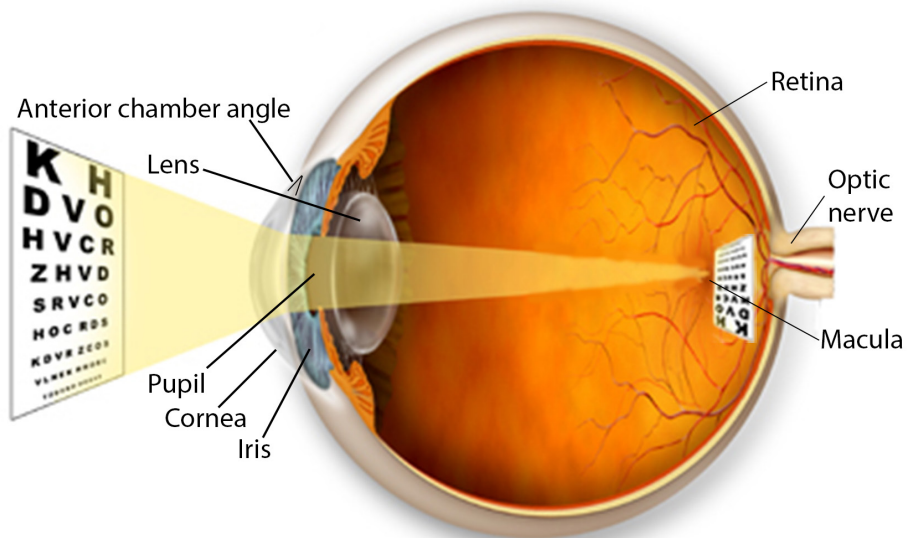


Figure 1.1 Anatomy and visual pathway of the human eye. (Figure derived from <http://www.lasik.md/learnaboutlasik/refractiveerrors.php>)

1.1.1 The retina

The retina is subdivided into the overlying neurosensory retina and the underlying retinal pigment epithelium (RPE) (layer 1). The neurosensory retina consists of several layers of neurons that are interconnected by synapses and supporting cells, which are arranged in a highly organized manner and form eight distinct layers (**Figure 1.2**). The photoreceptor layer (layer 2) contains the outer and inner segments of the rod and cone cells. The outer nuclear layer (layer 3) contains the nuclei of the photoreceptor cells. The inner segments of the photoreceptor cells are connected to interneurons via synapses in the outer plexiform layer (layer 4). The inner nuclear layer (layer 5) is composed of the nuclei of the supporting Müller cells and the interneurons (amacrine cells, bipolar cells, and horizontal cells). These

cells are connected via synapses in the inner plexiform layer (layer 6) to the ganglion cells (layer 7). The axons of the ganglion cells in the nerve fiber layer (layer 8) are oriented towards the optic disc. The Müller cells have long processes spanning from the outer nuclear layer to the internal limiting membrane (layer 9) and serve as supporting cells, helping to protect and repair retinal neurons.¹

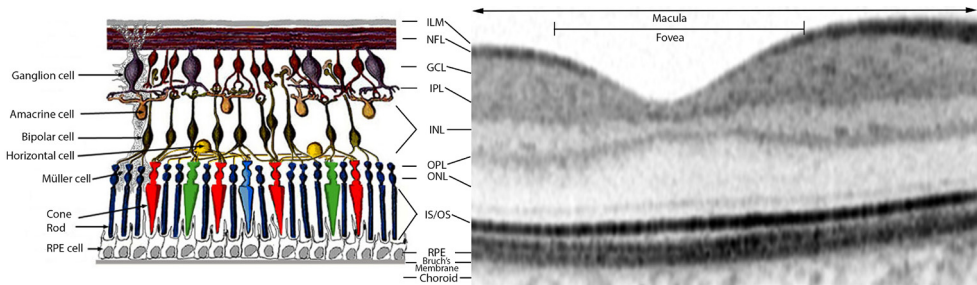


Figure 1.2 Schematic representation of the cellular organization and layers of the human central retina (left), with a corresponding transverse image of the central macula by optical coherence tomography (right). The following layers of the retina can be seen in the image. 1: retinal pigment epithelium (RPE); 2: inner segment (IS) and outer segment (OS) of the photoreceptors; 3: outer nuclear layer (ONL); 4: outer plexiform layer (OPL); 5: inner nuclear layer (INL); 6: inner plexiform layer; 7: ganglion cell layer (GCL); 8: nerve fiber layer (NFL); 9: internal limiting membrane (ILM). (Adapted from <http://webvision.med.utah.edu/imageswv/schem.jpeg>)

The visual function of the retina is based upon the anatomical location in the central macula and the peripheral retina. The macula, which is the central part of the retina, is located inside the temporal vascular arcades and is typically 5-6 mm in diameter. The macula contains cones and rods and is responsible for high visual acuity, color vision, and contrast sensitivity; the macula subserves the central 15-20° of the visual field. Thus, impaired function in the macula results in a loss of sharp vision, altered color vision, and the development of a central scotoma. The center of the macula contains a 1.5 mm wide circular depression called the fovea, which contains primarily cone cells. Although the fovea accounts for only 0.5% of the retina's surface, approximately 50% of the nerve fibers in the optic nerve carry information from the fovea, due to the high density of cone photoreceptors.

In contrast, the peripheral retina contains predominantly rod cells, thus providing vision in dim lighting. The peripheral retina also supports the peripheral visual field. Consequently, retinal diseases affecting the peripheral retina cause impaired night vision (nyctalopia) and constricted peripheral visual field.

The RPE is the deepest layer in the retina and is attached—albeit tenuously—to the sensory retina by interdigitation of the apical processes of the RPE cells.² RPE cells have many physical, optical, metabolic, and molecular transport functions, which together play an essential role in the visual process. Melanin absorbs scattered light and is expressed

in RPE cells, with the highest density in the foveal region. RPE cells actively transport nutrients and growth factors to the photoreceptor cells, and they regulate the transport of waste products, water, and ions between choroidal vessels and the subretinal space. In addition, the RPE layer plays a key role in the regeneration of visual pigments and the phagocytosis of outer segments shed by cone and rod photoreceptors. Finally, the RPE secretes several factors, including vascular endothelial growth factor (VEGF), tissue inhibitor of metalloproteinases-3 (TIMP-3), and complement-associated factors. Overexpression of VEGF promotes the formation of choroidal neovascularization in several conditions, including age-related macular degeneration (AMD).

1.1.2 Blood-retina barrier

The retina is provided with oxygen by the choriocapillaris and the retinal vessels. The choroidal capillaries are 40–60 μm in diameter, providing the highest rate of blood flow in the body compared to other tissues; ^{3,4} these capillaries have thin, fenestrated walls that enable the diffusion of molecules to nourish the outer part of the retina (i.e., the RPE and photoreceptors). To regulate the movement of solutes and nutrients from the choroid to the subretinal space, RPE cells are tightly interconnected via tight cellular junctions, thus forming the outer blood-retina barrier. A breach in this barrier can cause a serous exudative detachment. The non-fenestrated blood vessels of the central retinal artery lie in the nerve fiber layer, close to the internal limiting membrane of the retina; these vessels connect with the retinal veins via an extensive capillary network that extends outward to the external border of the inner nuclear layer. This network supplies blood to the internal layers of the retina. The endothelial cells in the retinal vessels are also tightly connected to one another by tight cellular junctions, forming the inner blood-retina barrier. This barrier mediates the highly selective diffusion of molecules between the blood and the retina and is essential for maintaining retinal homeostasis. Specifically, retinal homeostasis is based on a balance between osmotic force, hydrostatic force, capillary permeability, and tissue compliance, yielding a capillary filtration rate that is balanced by the rate of fluid removal from extracellular retinal tissue (for example, by glia and RPE cells). Perturbations in the outer and inner blood-retina barriers can increase the level of extracellular fluid in the retina, leading to cystoid spaces in the retina. These cystoid fluid collections are located primarily within the inner nuclear layer and the outer plexiform layer, as the anatomical avascular zone has relatively few retinal vessels that provide a pathway for extracellular fluid to return to the intravascular compartment.⁵ Müller cells may also play a role in the development of cystoid macular edema (CME), as the outer cell processes of Müller cells contain tight junctions, providing a partial barrier against the passage of subretinal exudates into the retina.² Thus, CME may be associated with a deterioration in the cellular integrity—and subsequent swelling—of Müller cells.⁶



1.1.3 The aging retina

The retina is particularly susceptible to the effects of aging due to several intrinsic factors. First, because most cell types in the retina are non-dividing, damaging effects are cumulative. Second, photoreceptors and RPE cells are metabolically highly active; indeed, these cells are among the highest energy-consuming cells in the body. Third, the retina is highly oxygenated and directly exposed to light; together, these two factors increase the organ's susceptibility to oxidative damage. With age, reactive oxygen species are formed in RPE cells, thereby causing damage to the retina. In addition, RPE cells lose the light-absorbing pigment melanin, reducing their antioxidant capacity. As a result of phagocytosis of photoreceptor outer segments and oxidative stress, with age, lipofuscin—and its toxic constituent *N*-retinylidene-*N*-retinyl-ethanolamine (A2E)—accumulates in the RPE.^{7, 8} Lipofuscins are a heterogeneous group of lipids, proteins, and various fluorescent compounds that are formed primarily from incompletely digested retinoids in the visual cycle.⁹⁻¹¹

In the RPE, the highest concentration of lipofuscin occurs at the parafoveal zone, where the density of rod cells is highest. In this zone, the rods are particularly vulnerable to age-related changes,¹² leading to a decline in the density of rod cells. Thus, the parafoveal zone has been suggested as the area in which atrophic AMD typically originates.^{8, 13}

The choriocapillaris is closely related to the RPE. RPE-derived VEGF can influence the choriocapillaris, and with increasing age both the density and diameter of the choriocapillaris decrease in the macula, resulting in reduced blood flow. With RPE thinning, the choriocapillaris can become atrophic and become less fenestrated, thereby reducing its molecular transport capacity.^{14, 15}

Bruch's membrane separates the RPE from the underlying choriocapillaris. With aging, this membrane becomes thicker due to the deposition of collagen lipids and other substances such as complement components.¹⁶⁻¹⁸ This accumulation of substances reduces the transepithelial transport of fluid and nutrients. In addition, Bruch's membrane—which is thinnest in the macula—becomes more fragile with increasing age, making it more susceptible to neovascular ingrowth.¹⁹ Extracellular deposits such as drusen preferentially develop between Bruch's membrane and the basement membrane of the RPE. Drusen are subretinal deposits that are mainly situated in the macula, and they contain a mixture of lipids, cellular debris, and/or inflammatory components. Taken together, the combination of its extremely high metabolism, oxidative stress caused by the local phagocytosis of photoreceptor outer segments by the RPE, and the accumulation of waste products predisposes the macula to develop drusen.

1.2 Clinical evaluation of retinal anatomy and function

An ophthalmological examination often begins with a measure of visual acuity in order to determine visual function. The aspect of the retina on ophthalmoscopy (**Figure 1.3A**) provides important clues regarding the nature of the disease. However, a complete

evaluation of the retina's anatomy and function can often provide important information useful for making a differential diagnosis and can shed light on the severity of the disease. Such an examination can include conventional diagnostic techniques as well as recently developed specialized (multimodal) imaging techniques.

1.2.1 Retinal imaging

1.2.1.1 Fluorescein angiography

Fluorescein angiography (FA) is an imaging technique that enables the practitioner to image the choroidal and retinal vasculature following an intravenous injection or oral dose of sodium fluorescein (**Figure 1.3B**). The fluorescein dye diffuses from the large fenestrated capillaries of the choriocapillaris, but normally cannot pass either the outer blood-retina barrier of the RPE or the inner barrier of the retinal vessels.

1.2.1.2 Optical coherence tomography

Optical coherence tomography (OCT) provides a cross-sectional high-resolution image of the retina (**Figure 1.3C**). This non-invasive imaging technique measures differences in light reflectivity between different tissue components and can reveal the anatomical location of structural abnormalities.

1.2.1.3 Fundus autofluorescence

Another non-invasive imaging technique is fundus autofluorescence (FAF), which provides a topographical map of lipofuscin distribution within the RPE. FAF uses short-wavelength (i.e., blue) light to excite lipofuscin, which autofluoresces (**Figure 1.3D**). FAF can reveal metabolic changes at the level of the RPE and can therefore provide functional information that cannot be obtained using conventional imaging techniques such as FA and OCT.

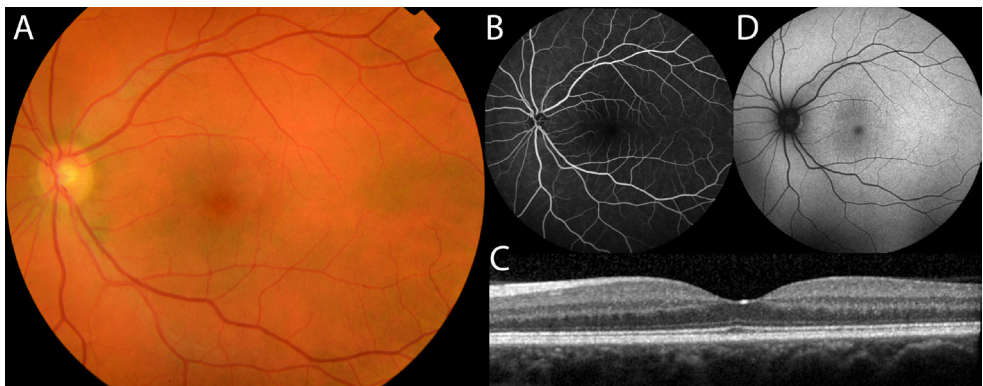


Figure 1.3 Examples of techniques used to image the fundus. The examples show a healthy fundus imaged using color fundus photography (A), fluorescein angiography (B), spectral domain optical coherence tomography (SD-OCT) (C), and fundus autofluorescence imaging (D).

1.2.2 Retinal function tests

1.2.2.1 Electro-oculography

Electro-oculography (EOG) measures the function of the entire RPE-photoreceptor complex. EOG displays the positive electrical potential generated in the eye during repeated eye movements; this potential is photosensitive, decreasing in the dark and recharging during light adaptation. The difference in electrical potential between dark and light is called the Arden ratio. The conditions for performing electrophysiological tests in the eye have been standardized by the International Society for Clinical Electrophysiology of Vision (ISCEV).

1.2.2.2 Electroretinography

Full-field electroretinography (ERG) records the total electrical activity generated by the retina in response to a flash of light. A flash stimulus is followed by an initial negative 'a-wave', which arises from the photoreceptors, and then by a 'b-wave', which arises from the bipolar and Müller cells. Under scotopic (dark-adapted) conditions, a weak flash is used to stimulate the rods, and this is followed by a very strong flash, which stimulates both the rods and cones. After exposing the eye to light-adapted conditions, a strong flash is then used to measure the photopic potential arising from the cones, and the cone-derived flicker response is obtained using a 30-Hz white light flicker stimulus.

1.2.2.3 Dark adaptation

Dark adaptation measurement is used to evaluate the absolute thresholds of cone and rod sensitivity in complete darkness. The sensitivity of cones recovers more rapidly than rods; however, the sensitivity of rods eventually exceeds the sensitivity of cones and can therefore be used as an indicator of rod photoreceptor dysfunction.

1.2.2.4 Color vision

Our ability to perceive colors is based on the retina's ability to discriminate light of different wavelengths. This is achieved by the presence of three types of cones (red, green, and blue cones), which are located primarily in the macula.

1.2.2.5 Visual field testing

Visual field testing measures decreased (or absent) sensitivity to light stimuli in both the central and peripheral visual fields. A region with decreased light sensitivity surrounded by a zone of relatively normal sensitivity is called a scotoma. Dynamic perimetry (e.g., Goldmann perimetry) can be used to define the peripheral visual field (and its borders) by confrontation of a moving light stimulus into the visual field; this technique can also be used to roughly locate a relative or absolute central scotoma. Static perimetry (e.g., Humphrey visual field testing) measures the sensitivity of the retina within the central visual field by applying several non-moving spots of light of varying brightness.



1.3 Molecular genetics

1.3.1 DNA structure and function

Deoxyribonucleic acid (DNA) is comprised of a double-helical sequence containing four different nucleotides (adenine, A; thymine, T; guanine, G; and cytosine, C). This sequence is organized in 23 pairs of chromosomes, with each pair containing one maternal chromosome and one paternal chromosome. Because we inherit our chromosomes from our parents, we also inherit many of our traits—and therefore diseases—from our parents.

The human genome encodes approximately 20,000 to 25,000 genes, which are specific DNA sequences that encode instructions for the formation of proteins. The transcription of genes into messenger ribonucleic acid (mRNA) is controlled by regulatory sequences such as promoters and enhancers. Prior to protein translation, the non-coding parts of a gene (i.e., the introns) are excised from the nascent RNA by an event called splicing, leading to the concatenation of the coding parts of the gene (exons). Combinations of three adjacent nucleotides (i.e., codons) in the mRNA code for specific amino acids to adhere to the peptide chain during translation. Finally, the formation of a protein is terminated by the presence of a 'stop' codon, a specific sequence of three nucleotides (TAG, TAA, or TGA) that does not encode an amino acid, but forms the code to stop the translation of a protein.

1.3.2 Genetic variants

DNA is subject to various forms of heritable alterations. These variations can affect an entire chromosome or chromosomal region (for example, in trisomy 21, which is more commonly known as Down syndrome) or only an individual gene. Changes that affect an individual gene can be roughly categorized into two types: single-nucleotide polymorphisms (SNPs) and mutations.

1.3.2.1 Single-nucleotide polymorphisms

SNPs are natural variations in the DNA sequence, which affect only one single nucleotide, and occur in at least 1% of the population. When a SNP occurs within an exon of a gene or in a regulatory region near a gene, it can affect the gene's function or expression. Although individual SNPs do not usually cause disease, individuals carrying several SNPs can have an increased risk of developing certain diseases, for example AMD (see **Chapter 3**).

1.3.2.2 Mutations

A pathogenic mutation is a relatively rare alteration of the DNA sequence that gives rise to disease, for example by impairing protein function. Heterozygous individuals have one mutant allele and one unaffected (i.e., 'wild-type') allele, whereas homozygous individuals have two mutant alleles (i.e., both copies of the gene contain the mutation). Based on the effect they have on the resulting amino acid sequence, DNA variations in exons can be either synonymous or non-synonymous. A synonymous variant does not change the amino

acid sequence of the protein, whereas a non-synonymous variant changes the protein sequence. Several types of non-synonymous mutations can occur. A *missense* mutation replaces the wild-type amino acid with a different amino acid, and this can change the protein's structure and/or function. A *frameshift* mutation arises from the insertion or deletion of one or more (but not a multiple of 3) nucleotides in an exon. This shifts the mRNA's reading frame, giving rise to a change in the resulting amino acid sequence in the protein. This can cause a significant change in the protein's structure and often results in a non-functional protein product. If the replacement of a single nucleotide creates a stop codon, this mutation is called a *nonsense* mutation, which causes a prematurely terminated protein and can have severe phenotypic consequences. Unlike mutations in exons, variants that occur in the introns do not usually affect the protein's function, unless they occur in DNA sequences involved in gene regulation. Mutations in regulatory elements can affect the level of gene expression, and mutations in or near a splice site can cause altered splicing between introns and exons and can result in exonic sequences being removed from—or intronic sequences being added to—the mRNA.

1.3.2.3 Pathogenicity

It is often difficult to determine whether a specific genetic variant is the cause of a particular disease. In order to establish a causal relationship, the sequence variant in question should segregate with the disease in the family as expected for dominant or recessive mutations. The effect of a genetic variant on the structure and/or function of the resulting protein can often be predicted using various bioinformatics programs such as PhyloP, Grantham, Sorting Intolerant From Tolerant (SIFT), and Polymorphism Phenotyping (PolyPhen). The effect of variants in or near splice sites can be predicted with splice site prediction software. Other arguments to suggest pathogenicity of a genetic variant may arise when a specific genetic variant is conserved in many species throughout evolution (suggesting that the variant is disadvantageous) and by the absence of the variant in control subjects who do not have the disease.

1.3.2.4 Mode of inheritance

Diseases may be inherited in several ways. In autosomal dominant inheritance, a variant or mutation in one of the two gene copies is sufficient to inherit a specific trait or disorder. A carrier of an autosomal dominant mutation has a 50% likelihood of passing the mutation to his/her offspring and therefore, theoretically 50% of the children would inherit the disease. This is only the case if the mutation is fully penetrant and thus results in a disease in all carriers of the mutation, like in DCMD. Reduced penetrance results in some carriers who have the mutation but not the corresponding phenotype; this can occur due to the presence of additional modifying genetic factors and/or interactions with environmental factors. Thus, reduced penetrance can mask the dominant mode of inheritance.



In autosomal recessive inheritance, the mutation must be present on both gene copies (allele) in order to cause the disease. When an affected patient carries an identical mutation on both alleles, the mutation is homozygous; a carrier of different mutations on each allele is referred to as compound heterozygous. If both parents are heterozygous carriers of a mutation, each child has a 25% chance of inheriting both mutant copies (50% chance of inheriting the paternal mutant allele and 50% chance of inheriting the maternal mutant allele) and developing the disease phenotype. If the mutation occurs on an X chromosome, female heterozygous carriers are usually unaffected, as they also have a second, wild-type X chromosome. Male offspring have a 50% probability of inheriting the mutation from their carrier mother and will develop disease as they carry only one (affected) X chromosome. Finally, mutations can be located in the mitochondrial DNA, which is maternally inherited, and can affect both male and female offspring if the mother is affected.

1.3.3 Mutation detection

1.3.3.1 Monogenic diseases

The identification of the underlying mutation in a monogenic disease can confirm or establish a clinical diagnosis, which will help to provide the patient with adequate information regarding the prognosis of the disease, and it can facilitate genetic counseling in the family members of the patient. To date, knowing the precise genetic cause of a disease rarely has therapeutic consequences, as gene therapy is still being developed. Nevertheless, this information can help clinicians understand the pathogenesis of the disease.

The identification of the underlying disease-causing genetic defect in a monogenic disease of unknown cause can be started with linkage analysis in order to determine the chromosomal location of the defect; for example, this approach was used to determine that the DCMD locus is located on chromosome 7 (7p15.3).²⁰ The genetic defect and surrounding polymorphisms tend to inherit together during meiosis, and these so-called 'polymorphic markers' can be used to link the phenotype to a specific chromosomal locus. To identify a disease locus with genome-wide significance, a relatively large family with multiple affected individuals is required. To find the disease-causing mutation within the identified locus, candidate genes with a function related to the disease process can be screened for mutations by performing DNA sequence analysis. Traditionally, Sanger sequencing has been used for this approach, which is labor-intensive and expensive if a large number of candidate genes must be analyzed. Therefore, new 'next-generation' sequencing technologies can now be used to sequence all of the genes located in the chromosomal interval (targeted sequencing) or even all of the genes in the entire genome (exome sequencing). If a mutation is found, segregation of this mutation with the disease must be confirmed in the affected family.

In patients with a retinal phenotype in which the genetic defect cannot be mapped to a specific locus (for example, due to small family size), currently identified mutations and/or other gene variants can be screened using a microarray ('gene chip'), providing a

rapid, cost-effective method for testing hundreds of known mutations in multiple genes. If no mutations are found, exome sequencing can be applied to attempt to detect novel mutations in known retinal disease-related genes, or even to identify new disease-related genes.

1.3.3.2 Complex diseases

In complex diseases such as AMD, identifying the underlying genetic variants can provide information regarding the pathways involved in the development of the disease and can therefore provide a possible therapeutic target. Additionally, factors playing a role in the development of the disease can be incorporated into prediction models to estimate more precisely someone's risk of developing the disease.

In complex or multifactorial diseases, genetic variants in multiple genes can increase the risk of developing the disease, in addition to environmental factors. Family and twin studies may be used to estimate the inherited component of the disease. Previously, twin studies clearly suggested the importance of genetic factors in the pathogenesis of AMD, as monozygotic twins showed a higher concordance of disease features in intermediate and late-stage AMD compared to dizygotic twins.^{21,22} Detecting genetic variants in complex disease such as AMD can be difficult due to the relatively small contribution of individual genetic factors and phenotypic variability. Some clinical features have a more significant genetic component than others, like small peripheral drusen and cuticular drusen.²³⁻²⁵ Genome-wide association studies in large cohorts have already identified several AMD-associated SNPs.²⁶ Simulation studies showed a significantly lower mean genotypic load of common AMD risk alleles in densely affected families than expected, suggesting that these families may carry rare, highly penetrant genetic variants.²⁷ However, the question remains, How can we identify these genetic variants?

To analyze a complex disease, linkage studies are often problematic, as they require large, multi-generation families, which is challenging when studying an age-related disease such as AMD. In addition, the inheritance pattern is often not clear, genetic variants may not be fully penetrant, and phenocopies may occur due to the contribution of other genetic (and environmental) factors. Exome sequencing may be used to identify new genetic causes by sequencing all 180,000 exons of the human genome.²⁸ For each individual subject, exome sequencing generally provides approximately 40,000 variants that differ from the reference sequence; therefore, after several filtering steps have been applied, several affected and non-affected family members must be analyzed in order to identify variants that segregate in the family.²⁸ For example, filtering can be performed by inclusion of only coding variants of high and moderate impact on protein sequence (missense, nonsense, frameshift, and splice variants), exclusion of variants with a minor allele frequency >0.1% in the '1000 Genomes Project' or the Exome Sequencing Project (ESP), and inclusion of missense variants that are annotated as 'probably damaging' by PolyPhen or 'deleterious' by SIFT.

Screening all exons in the genome provides a small chance (<4%) that potentially pathogenic gene variants associated with an increased risk of other unrelated diseases (for example, cancer or a neurological disorder) will be identified by chance.²⁹ This could have important consequences for patients and their family members. Therefore, patients must be counseled thoroughly by their clinician on the chance of such incidental findings, and patients must provide written consent before exome sequencing is performed.

1.4 Age-related macular degeneration

AMD affects 30-50 million people worldwide and is the most common cause of visual impairment and blindness in the Western world.³⁰⁻³³ As the name suggests, AMD primarily affects the macula, leading to a progressive loss of the central visual field and a decline in visual acuity and color vision. AMD can have a profound impact on quality of life, as affected patients can no longer read, recognize faces, or discriminate colors.^{34, 35}

1.4.1 Stages of AMD

Pathologically, AMD is characterized initially by changes in the RPE, followed by a loss of RPE and photoreceptor cells and/or secondary angiogenesis. Based on the anatomic abnormalities that develop in the fundus, AMD can be divided into early AMD and advanced AMD.

1.4.1.1 Early AMD

In early AMD, a spectrum of changes is observed in the aging macula despite relatively preserved visual acuity. The presence of drusen is the most characteristic early fundoscopic finding in AMD. Drusen usually present after the age of 50 years and appear on fundoscopy as focal white/yellow subretinal deposits. Histologically, drusen are focal extracellular deposits between the inner collagenous zone of Bruch's membrane and the basal lamina of the RPE, consisting of cellular remnants and debris derived from degenerated RPE cells.³⁶⁻³⁹ The molecular composition of drusen indicates that they may be the result of a chronic inflammatory stimulus that exacerbates the effect of primary pathogenic stimuli.³⁹

Based on their characteristics and appearance, drusen can be distinguished as 'hard', 'soft', 'crystalline', 'reticular', or 'cuticular'. Hard drusen are defined as small (<63 μm), sharply defined structures, whereas soft drusen are larger (>63 μm) and irregularly shaped with poorly demarcated borders. The progression of early AMD to intermediate AMD is characterized by an increase in the number and/or size of drusen, which also increases the risk of progressing to advanced AMD.⁴⁰ Both hard drusen and soft drusen can undergo calcification (crystalline drusen). On the other hand, reticular pseudodrusen (RPD) and cuticular drusen (CD) are defined based on the drusen patterns. RPD are defined as multiple 'drusen-like structures' that form poorly defined networks of broad interlacing ribbons.⁴¹ RPD can be identified easily using blue-channel examination, OCT, near-infrared imaging, red-free photography, or FAF imaging. OCT imaging shows clearly that RPD



are located above the RPE and that subretinal drusenoid deposits can cross the inner/outer segment of the retina.⁴² The presence of RPD is strongly associated with the risk of developing advanced AMD.⁴³⁻⁴⁵ On funduscopy, CD appear as innumerable small, yellow lesions that are scattered throughout the fundus; these lesions have a typical ‘stars in the sky’ appearance on fluorescein angiography. Anatomically, CD are located between the RPE and Bruch’s membrane.

1.4.1.2 Advanced AMD

Early AMD can progress to advanced AMD, which can be classified as geographic atrophy (GA) or neovascular AMD. GA is characterized by the development of one or more sharply delineated regions of atrophy of the RPE and photoreceptors in the macula. GA accounts for the majority of advanced AMD cases. Neovascular AMD is due to choroidal neovascularization (CNV), which is the formation of new blood vessels that arise primarily from the choroidal vessels; these vessels grow through defects in Bruch’s membrane and infiltrate the retinal and/or subretinal space. These newly developed fenestrated vessels are friable and can cause serous RPE detachment, hemorrhage, and secondary fibrous scarring in the macula, resulting in rapid and severe loss of vision.

1.4.2 Risk factors

AMD is a complex, multifactorial disease and has been associated with several demographic, environmental, and genetic risk factors. Advanced age is the major risk factor associated with AMD.³¹ The prevalence of AMD increases with age and is more prevalent among females than males.^{31, 46, 47} The aging population will result in an increasing prevalence of AMD, leading to a higher social and healthcare burden. Therefore, new advances in preventive and therapeutic options—and the ability to predict high-risk individuals before disease onset—are urgently needed.

1.4.2.1 Environmental risk factors

Current cigarette smoking is the most important modifiable risk factor that has consistently been associated with a 2-3-fold increased risk in the development and progression of AMD.⁴⁸⁻⁵⁰ Although the precise mechanism is still unknown, oxidative damage, vascular inflammation, changes in choroidal blood flow, hypoxia, and antioxidant depletion have all been implicated in the retinal change that occurs in AMD patients secondary to smoking cigarettes.⁵⁰⁻⁵² Quitting can reduce the risk of AMD, but even after 20 years the risk still remains higher than among individuals who never smoked.⁵³ Several other modifiable risk factors have also been associated with AMD and include obesity,^{54, 55} low physical activity, sunlight exposure,⁵⁶ cardiovascular disease,⁴⁸ and certain dietary factors.⁵⁰ With respect to diet, the consumption of omega 3, carotenoids (e.g., lutein and zeaxanthin), vitamin A, vitamin E, and antioxidants such as zinc may protect against the development of AMD.⁵⁷



1.4.2.2 Family history

Approximately one-third of all patients with AMD have a positive family history for the disease.⁵⁸⁻⁶¹ Familial and twin-based studies initially revealed that genetic factors are strongly associated with developing AMD.^{21, 62-64} The heritability of AMD is estimated between 45% and 70%; the heritability of advanced cases is 67-71%.²² Since then, AMD-associated SNPs have been identified at 19 distinct loci; together, these SNPs can explain up to 65% of the heritability.^{26, 65} Part of the missing heritability may be explained by rare, more penetrant genetic variants.⁶⁶⁻⁶⁹ Genetic testing of AMD families seems to be the ideal approach for identifying these rare variants, as the aggregation of AMD in families cannot be attributed entirely to the clustering of known genetic and/or environmental risk factors.⁷⁰ In patients with familial AMD, genetic factors seem to play a more important role.⁷¹ To date, rare variants have been identified in a small number of families with AMD.^{28, 67, 72, 73} Thus, the genetic variants that explain familial occurrence still need to be identified in the majority of families with AMD families.

1.4.2.3 Genetic risk factors

Genome-wide association studies have identified several common genetic variants that are associated with AMD; these variants have relatively small effect sizes and are found in or near several genes that play a role in AMD-associated pathways (**Table 1.1**).²⁶ The two major AMD-associated SNPs are the Ala69Ser variant in *ARMS2* (which encodes age-related maculopathy susceptibility protein 2) and the Tyr402His variant in *CFH* (which encodes complement factor H); each of these variants causes a nearly three-fold increase in the risk of developing AMD.²⁶ The function of the *ARMS2* protein is not currently known, although mitochondrial dysfunction in photoreceptors and a defect in the extracellular matrix have been suggested;^{74, 75} this protein may also be associated with increased complement activation.⁷⁶ The *CFH* gene encodes the principal regulator of the alternative complement pathway.⁷⁷⁻⁷⁹ Other complement system genes have been associated with AMD and include complement component 2 (*C2*),⁸⁰ complement component 3 (*C3*),^{81, 82} complement component 9 (*C9*),⁸² complement factor B (*CFB*),⁸⁰ and complement factor I (*CFI*).^{26, 82, 83}

Table 1.1 Loci that are significantly associated with age-related macular degeneration

Chromosome	Gene	SNP	Risk allele	EAF	OR [95% CI]
10	<i>ARMS2/HTRA1</i>	rs10490924	T	0.30	2.76 [2.72–2.80]
1	<i>CFH</i>	rs10737680	A	0.64	2.43 [2.39–2.47]
6	<i>C2/CFB</i>	rs429608	G	0.86	1.74 [1.68–1.79]
19	<i>C3</i>	rs2230199	C	0.20	1.42 [1.37–1.47]
22	<i>TIMP3</i>	rs5749482	G	0.74	1.31 [1.26–1.36]
19	<i>APOE</i>	rs4420638	A	0.83	1.30 [1.24–1.36]
3	<i>COL8A1/FILIP1L</i>	rs13081855	T	0.10	1.23 [1.17–1.29]
16	<i>CETP</i>	rs1864163	G	0.76	1.22 [1.17–1.27]
6	<i>IER3/DDR1</i>	rs3130783	A	0.79	1.16 [1.11–1.20]
8	<i>TNFRSF10A</i>	rs13278062	T	0.48	1.15 [1.12–1.19]
6	<i>VEGFA</i>	rs943080	T	0.51	1.15 [1.12–1.18]
22	<i>SLC16A8</i>	rs8135665	T	0.21	1.15 [1.11–1.19]
4	<i>CFI</i>	rs4698775	G	0.31	1.14 [1.10–1.17]
9	<i>TGFBR1</i>	rs334353	T	0.73	1.13 [1.10–1.17]
15	<i>LIPC</i>	rs920915	C	0.48	1.13 [1.09–1.17]
14	<i>RAD51B</i>	rs8017304	A	0.61	1.11 [1.08–1.14]
6	<i>COL10A1</i>	rs3812111	T	0.64	1.10 [1.07–1.14]
3	<i>ADAMTS9/MIR548A2</i>	rs6795735	T	0.46	1.10 [1.07–1.14]
13	<i>B3GALT1</i>	rs9542236	C	0.44	1.10 [1.07–1.14]

SNP = single-nucleotide polymorphism; EAF = allele frequency of the risk-increasing allele; OR = odds ratio; CI = confidence interval. (Table derived from Fritsche et al.²⁶)

Other genes that harbor AMD-associated SNPs are located in the high-density lipoprotein cholesterol pathway (*APOE*,^{84, 85} *ABCA1*,⁸⁶ *CETP*,⁸⁶ *FADS1_3*,⁸⁷ *LIPC*,⁸⁷ and *LPL*⁸⁶), the extracellular collagen matrix pathway (*COL8A1*,⁸⁷ *COL10A1*,⁸⁸ and *TIMP3*⁸⁶), and vascular endothelial growth factors (*VEGFA* and *TGFBR1*). In addition, rare, highly penetrant variants with a strong association with AMD were recently identified by performing sequence analysis of complement genes and exome sequencing in patients with sporadic or familial AMD (Figure 1.4).^{28, 67, 69, 82, 89}

1.4.3 Pathogenesis

The pathogenesis of AMD is complex and incompletely understood. Genetic association studies have implicated several biological pathways in which the immune system and inflammation play a central causative role in the pathogenesis of AMD. A growing body of evidence suggests that the complement system plays a key role in the pathogenesis of AMD.⁹¹ Histopathology studies indicate that chronic inflammation in response to cellular debris derived from degenerated RPE cells leads to the formation of drusen.³⁹ This notion is supported by the finding of genetic associations between AMD and several common and rare variants in genes that encode complement components.^{74, 77-81, 83}

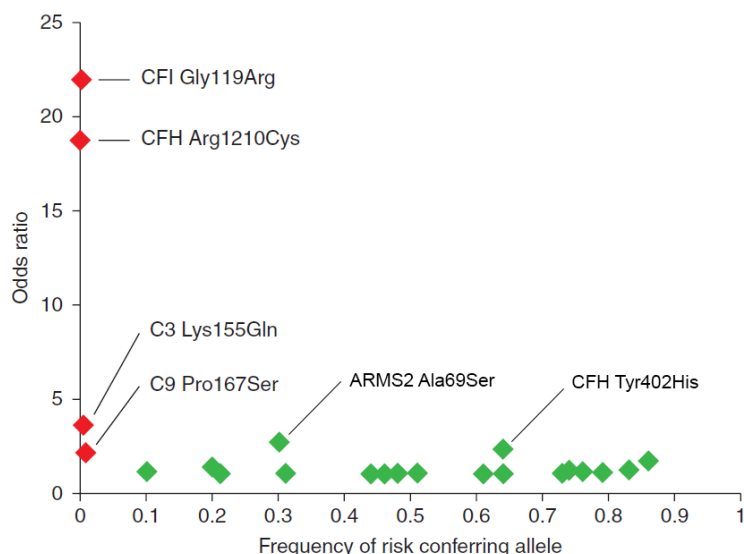


Figure 1.4 Genetic architecture of age-related macular degeneration. The effect size (odds ratio) of common and rare AMD-associated variants is plotted against minor allele frequency (MAF). Common variants with a relatively small effect size are shown in green.²⁶ Rare variants with low population allele frequencies and large effect sizes are shown in red: CFI Gly119Arg (MAF: 0.001, OR: 22.0);⁸⁹ CFH Arg1210Cys (MAF: 0.0002, OR: 18.8);⁶⁹ C3 Lys155Gln (MAF: 0.004, OR: 3.7);⁶⁶ and C9 Pro167Ser (MAF: 0.008, OR: 2.2).⁸² MAF was calculated from the NHLBI Exome Sequencing Project based on alleles in populations of European ancestry. (figure derived from den Hollander et al.⁹⁰)

1.4.3.1 The complement system

The complement system is part of the innate immune system (**Figure 1.5**) and can be activated via three distinct pathways (the classical, the alternative and the lectin pathway). Activation of the complement system leads to the removal of potentially harmful materials such as cellular debris and generates the production of inflammatory chemotactic proteins that trigger inflammation (e.g., complement components C3a and C5a) and opsonized proteins that attract other immune cells (e.g., C3b). The complement system is tightly regulated by several proteins such as complement factor H (CFH) and CFI. Dysregulated complement activation can cause substantial damage to self-tissues, leading to a variety of diseases, including AMD.⁹² Increased levels of complement components (e.g., CFB) and complement activation products (e.g., C3d and C3a) have been found in the plasma of AMD patients.⁹³⁻⁹⁵ In addition, chronic continuous activation of the complement system occurs in the eyes of elderly individuals. Activation of the complement system may lead to the formation of drusen and to degeneration of the RPE and photoreceptor cells.¹⁸ Consistent with this hypothesis, several components of the complement system have been detected in drusen.^{96,97} Drusen and RPE degeneration can in turn activate the complement system, and this vicious cycle causes further damage to RPE cells and the retina.

The complement system can also affect other mechanisms associated with the pathophysiology of AMD. For example, the chemotaxis of macrophages causes a release of reactive oxygen species, thus causing oxidative damage, which plays an important role in the development of AMD. In addition, the membrane attack complex (MAC), a final component in the complement cascade that results in cell lysis, can disrupt the delicate balance between anti-angiogenic and pro-angiogenic factors in the choroid and retina, thus causing CNV.⁹⁸

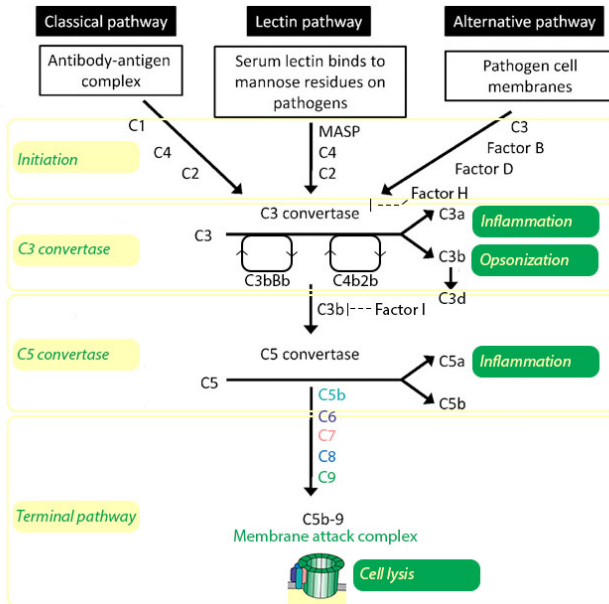


Figure 1.5 Schematic representation of the complement system. The complement system can be activated by three different pathways: the classical, the lectin, and the alternative pathway. Activation of the system initiates the formation of component 3 (C3) convertase (Initiation). This enzyme cleaves C3 into C3a and C3b (C3 convertase). C3b generates C3bBb, which amplifies the C3 convertase. If activation of the system progresses, C5 convertase, which cleaves C5 into C5a and C5b, is generated. C5b can initiate the terminal pathway, which recruits components C6, C7, C8, and C9 and forms the membrane attack complex. Overall, complement activation results in three effector responses: 1) the anaphylactic peptides C3a and C5a cause inflammation; 2) C3b causes opsonization of the foreign surface, leading to phagocytosis; and 3) the membrane attack complex is inserted into the membrane, resulting in cell lysis. (Figure modified according to Kandhadia et al.⁹⁹)

1.4.4 Prevention and therapy

With the identification of several AMD susceptibility genes and the revealed inflammatory pathways playing a critical role in the pathophysiology of AMD, genetic studies of AMD may contribute to our ability to prevent the progressive loss of central vision and may facilitate the development of new treatments. This is very important as the prevalence of AMD will increase over time by aging of the population, and visual impairment reduces quality of life.



Drugs that target the complement system are currently being tested for their efficacy in AMD,^{100, 101} and future work on rare variants and non-coding DNA in the pathogenesis of AMD will likely reveal additional biochemical pathways with AMD-associated genetic variants. Pharmacologic targets in these pathways may lead to rational, effective therapeutic approaches for preventing and treating this sight-threatening disease.¹⁰²

The only therapeutic approach currently available for reducing the risk of progressing to advanced AMD is the consumption of certain dietary supplements (e.g., vitamin C, vitamin E, zinc, beta-carotene, and/or lutein/zeaxanthin), which can reduce the risk of progression by up to 25%.¹⁰³ Although neovascular AMD can be treated successfully with anti-VEGF drugs, some patients with neovascular AMD do not benefit from anti-VEGF therapy. Clinical factors such as age, baseline visual acuity, and baseline CNV lesion size appear to be important predictors of whether a patient with neovascular AMD will respond to anti-VEGF treatment;¹⁰⁴ in addition, response to treatment may also depend on the genotype of several AMD-associated genes, including *CFH*,¹⁰⁴⁻¹⁰⁶ *VEGFA*,^{104, 107, 108} and *ARMS2*.¹⁰⁹ However, the pharmacogenetic relationship was not consistently replicated for all AMD-associated genes.^{106, 110} Currently, no therapeutic option is available for geographic atrophy.

1.5 Dominant cystoid macular dystrophy

DCMD is an extremely rare retinal dystrophy with an autosomal dominant inheritance pattern. However, in the Netherlands, one large family with DCMD exists in which the disease can be traced back to a single common ancestor in the early 18th century. In the 1970s, Pinckers and Deutman collected clinical and electrophysiological data from this family, and to date a large body of clinical data has been collected from 97 affected members and 52 unaffected family members.

DCMD typically presents within the first or second decade of life, with intraretinal cystoid fluid collections (CFCs) as the most remarkable finding (**Figure 1.6**); in addition, patients can present with a (highly) hypermetropic refraction error. The degree of CFCs can vary widely, corresponding with a variable visual acuity over time. During disease progression, CFCs diminish and are replaced by chorioretinal atrophy, eventually resulting in a visual acuity at the level of legal blindness. Corresponding with the progression of structural abnormalities in the retina, the retinal function becomes impaired, expressed by an abnormal EOG and full-field ERG. DCMD can be classified into three stages, as discussed in **Chapter 4**.

Linkage analysis showed a shared DCMD haplotype (i.e., a combination of alleles at a certain chromosomal locus) located on the short arm of chromosome 7 (7p15-p21).²⁰ DCMD is a monogenic, autosomal dominant disease; however, the causative genetic defect has not yet been identified. Advanced next-generation sequencing techniques are currently being used in an attempt to identify the genetic cause of this devastating disease.

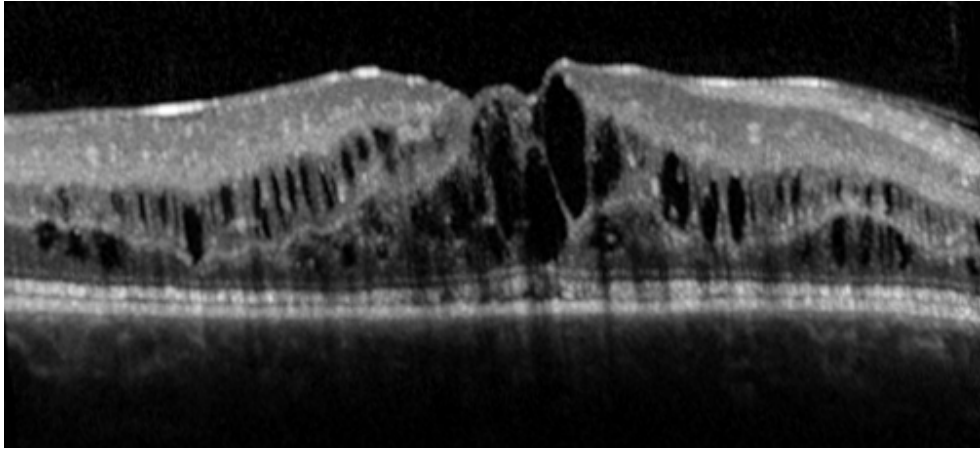


Figure 1.6 Optical coherence tomography image of cystoid fluid collections in the macula of a 23-year-old patient with dominant cystoid macular dystrophy.

1.6 Butterfly-shaped pigment dystrophy

Butterfly-shaped pigment dystrophy (BSPD) was first described in 1970 by Deutman et al.¹¹¹ BSPD is one of the autosomal dominant pattern dystrophies,¹¹² which have been subdivided into five groups based on the pattern of pigment distribution. Pattern dystrophies are clinically heterogeneous diseases, as the shape of the central yellow lesions can vary considerably. Thus, members of a single family with a given genetic mutation can have several different patterns, and an individual patient can have different patterns in the left and right eyes or can even progress from one pattern to another pattern.¹¹³⁻¹¹⁵ BSPD is characterized by the deposition of pigment at the level of the RPE; these deposits are arranged symmetrically in a triradiate pattern confined to the center of the macula, resembling the shape of a butterfly.¹¹¹ BSPD has also been called butterfly-shaped macular dystrophy. The pigment figure is generally surrounded by a zone of depigmentation, which corresponds to hyperfluorescence in the early phases of fluorescein angiography, thus outlining the hypofluorescent pigment shape in the macula (**Figure 1.7**).¹¹² Usually BSPD causes a mild loss of central vision in midlife, and it has a relatively good prognosis. Patients often present with an abnormal EOG, but the ERG remains normal. In addition to phenotypic heterogeneity, BSPD also shows marked genetic heterogeneity. BSPD is inherited as an autosomal dominant disease and can be partly explained by mutations in the peripherin-2 (*PRPH2*) gene.¹¹⁶⁻¹¹⁹ The *PRPH2* gene is located on chromosome 6 (6p21.2) and encodes an integral membrane protein that plays an important role in the morphogenesis of rod outer segment discs and cone lamellae.¹²⁰



Figure 1.7 Fluorescein angiograph of a 36-year-old patient with butterfly-shaped pigment dystrophy.

1.7 Aims and outline of this thesis

The aim of this thesis is to increase our understanding of the clinical and genetic characteristics of AMD and other macular diseases. Specifically, we studied the importance of a positive family history of AMD with respect to clinical, phenotypic, and genetic aspects, and our results will likely facilitate the development of reliable models for predicting AMD. This may provide more accurate information regarding the individual risk for AMD, particularly for individuals in which AMD has a strong familial component. In addition, the identification of genetic variants in familial AMD and BSPD will facilitate risk assessment and genetic counseling of family members and will aid to elucidate the pathophysiology of these diseases.

Chapter 1 provides the reader with information on the basic aspects of the retina, as well as the clinical and genetic methods that may be applied in the analysis of retinal disease. In addition, the general characteristics of AMD, DCMD and BSPD are described with emphasis on the importance of the familial occurrence in macular disease.

Chapter 2 discusses the characteristics of AMD and macular dystrophies that may mimic AMD and provides a practical differential diagnostic guideline based on overlapping and distinguishing clinical and genetic characteristics.

Chapter 3 concerns the clinical and genetic analysis of AMD with respect to the presence or absence of a family history of AMD.

Chapter 3.1 starts with an evaluation of the differences and similarities between familial and sporadic AMD with respect to risk factors, clinical characteristics, and phenotypes.

Chapter 3.2 provides an analysis of the family history of AMD and the importance of family history in AMD prediction models that are based on the density of a positive family history and family size. The non-significant additive value of common SNPs in an AMD prediction model for familial patients may be explained by the contribution of additional rare genetic factors that segregate within these families.

Chapter 3.3 presents the differences in the contribution of common genetic variants and complement activation levels between familial and sporadic AMD. A better understanding of the factors that interact with family history will aid in reliable prediction for AMD.

Chapter 3.4 describes the clinical differences between affected carriers of a rare variant in the *CFI*, *C9*, or *C3* complement gene compared to non-carriers with AMD. In addition, the presence of a rare variant has been analyzed with respect to a positive family history.

Chapter 3.5 reveals the identification of novel rare variants in the *CFH* gene in patients with cuticular drusen, a subtype of AMD, and describes the clinical features of individuals carrying these genetic variants.

Chapter 4 provides a system for classifying DCMD into three distinct stages based on the clinical characteristics and long-term follow-up data obtained from a large Dutch family with DCMD. Additionally, we discuss our evaluation of the efficacy of therapeutic options and the penetrance of the genetic locus in this family.

Chapter 5 presents the identification of rare mutations in the *CTNNA1* gene as a novel cause of BSPD, followed by functional studies to investigate the impact of these mutations on protein function. In addition, mouse models are used to evaluate the impact of this mutated gene on retinal architecture and function.

In **Chapter 6** the studies described in this thesis are further discussed and placed in a broader perspective. Finally, a summary of the findings is provided in **Chapter 7**.

REFERENCES

1. Dyer MA, Cepko CL. Regulating proliferation during retinal development. *Nat Rev Neurosci* 2001;2:333-342.
2. Agarwal A. *Gass' Atlas of Macular diseases*: Elsevier; 2012:6-8.
3. Parver LM, Auker C, Carpenter DO. Choroidal blood flow as a heat dissipating mechanism in the macula. *Am J Ophthalmol* 1980;89:641-646.
4. Parver LM, Auker CR, Carpenter DO. The stabilizing effect of the choroidal circulation on the temperature environment of the macula. *Retina* 1982;2:117-120.
5. Agarwal A, *Gass' Atlas of Macular diseases*: Elsevier; 2012:44.
6. Yanoff M, Fine BS, Brucker AJ, Eagle RC, Jr. Pathology of human cystoid macular edema. *Surv Ophthalmol* 1984;28 Suppl:505-511.
7. Feeney-Burns L, Hilderbrand ES, Eldridge S. Aging human RPE: morphometric analysis of macular, equatorial, and peripheral cells. *Invest Ophthalmol Vis Sci* 1984;25:195-200.
8. Wing GL, Blanchard GC, Weiter JJ. The topography and age relationship of lipofuscin concentration in the retinal pigment epithelium. *Invest Ophthalmol Vis Sci* 1978;17:601-607.
9. Boulton M, McKechnie NM, Breda J, Bayly M, Marshall J. The formation of autofluorescent granules in cultured human RPE. *Invest Ophthalmol Vis Sci* 1989;30:82-89.
10. Feeney-Burns L, Eldred GE. The fate of the phagosome: conversion to 'age pigment' and impact in human retinal pigment epithelium. *Trans Ophthalmol Soc U K* 1983;103 (Pt 4):416-421.
11. Katz ML. Incomplete proteolysis may contribute to lipofuscin accumulation in the retinal pigment epithelium. *Adv Exp Med Biol* 1989;266:109-116; discussion 116-108.
12. Curcio CA. Photoreceptor topography in ageing and age-related maculopathy. *Eye (Lond)* 2001;15:376-383.
13. Curcio CA, Millican CL, Allen KA, Kalina RE. Aging of the human photoreceptor mosaic: evidence for selective vulnerability of rods in central retina. *Invest Ophthalmol Vis Sci* 1993;34:3278-3296.
14. Korte GE, Reppucci V, Henkind P. RPE destruction causes choriocapillary atrophy. *Invest Ophthalmol Vis Sci* 1984;25:1135-1145.
15. Neuhardt T, May CA, Wilsch C, Eichhorn M, Lutjen-Drecoll E. Morphological changes of retinal pigment epithelium and choroid in rd-mice. *Exp Eye Res* 1999;68:75-83.
16. Feeney-Burns L, Ellersieck MR. Age-related changes in the ultrastructure of Bruch's membrane. *Am J Ophthalmol* 1985;100:686-697.
17. Guymer R, Luthert P, Bird A. Changes in Bruch's membrane and related structures with age. *Prog Retin Eye Res* 1999;18:59-90.
18. Hageman GS, Luthert PJ, Victor Chong NH, Johnson LV, Anderson DH, Mullins RF. An integrated hypothesis that considers drusen as biomarkers of immune-mediated processes at the RPE-Bruch's membrane interface in aging and age-related macular degeneration. *Prog Retin Eye Res* 2001;20:705-732.
19. Chong NH, Keonin J, Luthert PJ, et al. Decreased thickness and integrity of the macular elastic layer of Bruch's membrane correspond to the distribution of lesions associated with age-related macular degeneration. *Am J Pathol* 2005;166:241-251.
20. Kremer H, Pinckers A, van den Helm B, Deutman AF, Ropers HH, Mariman EC. Localization of the gene for dominant cystoid macular dystrophy on chromosome 7p. *Hum Mol Genet* 1994;3:299-302.
21. Klein ML, Mauldin WM, Stoumbos VD. Heredity and age-related macular degeneration. Observations in monozygotic twins. *Arch Ophthalmol* 1994;112:932-937.



22. Seddon JM, Cote J, Page WF, Aggen SH, Neale MC. The US twin study of age-related macular degeneration: relative roles of genetic and environmental influences. *Arch Ophthalmol* 2005;123:321-327.
23. Grassi MA, Folk JC, Scheetz TE, Taylor CM, Sheffield VC, Stone EM. Complement factor H polymorphism p.Tyr402His and cuticular Drusen. *Arch Ophthalmol* 2007;125:93-97.
24. Postel EA, Agarwal A, Schmidt S, et al. Comparing age-related macular degeneration phenotype in probands from singleton and multiplex families. *Am J Ophthalmol* 2005;139:820-825.
25. van de Ven JP, Smailhodzic D, Boon CJ, et al. Association analysis of genetic and environmental risk factors in the cuticular drusen subtype of age-related macular degeneration. *Mol Vis* 2012;18:2271-2278.
26. Fritsche LG, Chen W, Schu M, et al. Seven new loci associated with age-related macular degeneration. *Nat Genet* 2013;45:433-439, 439e431-432.
27. Sobrin L, Maller JB, Neale BM, et al. Genetic profile for five common variants associated with age-related macular degeneration in densely affected families: a novel analytic approach. *Eur J Hum Genet* 2010;18:496-501.
28. Yu Y, Triebwasser MP, Wong EK, et al. Whole-exome sequencing identifies rare, functional CFH variants in families with macular degeneration. *Hum Mol Genet* 2014;23:5283-5293.
29. Dorschner MO, Amendola LM, Turner EH, et al. Actionable, pathogenic incidental findings in 1,000 participants' exomes. *Am J Hum Genet* 2013;93:631-640.
30. Ambati J. Age-related macular degeneration and the other double helix. The Cogan Lecture. *Invest Ophthalmol Vis Sci* 2011;52:2165-2169.
31. Smith W, Assink J, Klein R, et al. Risk factors for age-related macular degeneration: Pooled findings from three continents. *Ophthalmology* 2001;108:697-704.
32. Klein R, Wang Q, Klein BE, Moss SE, Meuer SM. The relationship of age-related maculopathy, cataract, and glaucoma to visual acuity. *Invest Ophthalmol Vis Sci* 1995;36:182-191.
33. Klaver CC, Wolfs RC, Vingerling JR, Hofman A, de Jong PT. Age-specific prevalence and causes of blindness and visual impairment in an older population: the Rotterdam Study. *Arch Ophthalmol* 1998;116:653-658.
34. de Jong PT. Age-related macular degeneration. *N Engl J Med* 2006;355:1474-1485.
35. Miskala PH, Bass EB, Bressler NM, et al. Surgery for subfoveal choroidal neovascularization in age-related macular degeneration: quality-of-life findings: SST report no. 12. *Ophthalmology* 2004;111:1981-1992.
36. Rudolf M, Clark ME, Chimento MF, Li CM, Medeiros NE, Curcio CA. Prevalence and morphology of druse types in the macula and periphery of eyes with age-related maculopathy. *Invest Ophthalmol Vis Sci* 2008;49:1200-1209.
37. Al-Hussaini H, Schneiders M, Lundh P, Jeffery G. Drusen are associated with local and distant disruptions to human retinal pigment epithelium cells. *Exp Eye Res* 2009;88:610-612.
38. Curcio CA, Presley JB, Malek G, Medeiros NE, Avery DV, Kruth HS. Esterified and unesterified cholesterol in drusen and basal deposits of eyes with age-related maculopathy. *Exp Eye Res* 2005;81:731-741.
39. Anderson DH, Mullins RF, Hageman GS, Johnson LV. A role for local inflammation in the formation of drusen in the aging eye. *Am J Ophthalmol* 2002;134:411-431.
40. Buitendijk GH, Rochtchina E, Myers C, et al. Prediction of age-related macular degeneration in the general population: the Three Continent AMD Consortium. *Ophthalmology* 2013;120:2644-2655.
41. Mimoun G, Soubrane G, Coscas G. Macular drusen. *J Fr Ophthalmol* 1990;13:511-530.

42. Zweifel SA, Spaide RF, Curcio CA, Malek G, Imamura Y. Reticular pseudodrusen are subretinal drusenoid deposits. *Ophthalmology* 2010;117:303-312 e301.
43. Arnold JJ, Sarks SH, Killingsworth MC, Sarks JP. Reticular pseudodrusen. A risk factor in age-related maculopathy. *Retina* 1995;15:183-191.
44. Klein R, Meuer SM, Knudtson MD, Iyengar SK, Klein BE. The epidemiology of retinal reticular drusen. *Am J Ophthalmol* 2008;145:317-326.
45. Marsiglia M, Boddu S, Bearely S, et al. Association between geographic atrophy progression and reticular pseudodrusen in eyes with dry age-related macular degeneration. *Invest Ophthalmol Vis Sci* 2013;54:7362-7369.
46. Rudnicka AR, Jarrar Z, Wormald R, Cook DG, Fletcher A, Owen CG. Age and gender variations in age-related macular degeneration prevalence in populations of European ancestry: a meta-analysis. *Ophthalmology* 2012;119:571-580.
47. Klein R, Klein BE, Knudtson MD, et al. Prevalence of age-related macular degeneration in 4 racial/ethnic groups in the multi-ethnic study of atherosclerosis. *Ophthalmology* 2006;113:373-380.
48. Chakravarthy U, Wong TY, Fletcher A, et al. Clinical risk factors for age-related macular degeneration: a systematic review and meta-analysis. *BMC Ophthalmol* 2010;10:31.
49. Thornton J, Edwards R, Mitchell P, Harrison RA, Buchan I, Kelly SP. Smoking and age-related macular degeneration: a review of association. *Eye (Lond)* 2005;19:935-944.
50. Velilla S, Garcia-Medina JJ, Garcia-Layana A, et al. Smoking and age-related macular degeneration: review and update. *J Ophthalmol* 2013;2013:895147.
51. Cano M, Thimmalappula R, Fujihara M, et al. Cigarette smoking, oxidative stress, the anti-oxidant response through Nrf2 signaling, and Age-related Macular Degeneration. *Vision Res* 2010;50:652-664.
52. Swaroop A, Chew EY, Rickman CB, Abecasis GR. Unraveling a multifactorial late-onset disease: from genetic susceptibility to disease mechanisms for age-related macular degeneration. *Annu Rev Genomics Hum Genet* 2009;10:19-43.
53. Vingerling JR, Hofman A, Grobbee DE, de Jong PT. Age-related macular degeneration and smoking. The Rotterdam Study. *Arch Ophthalmol* 1996;114:1193-1196.
54. Klein BE, Klein R, Lee KE, Jensen SC. Measures of obesity and age-related eye diseases. *Ophthalmic Epidemiol* 2001;8:251-262.
55. Schaumberg DA, Christen WG, Hankinson SE, Glynn RJ. Body mass index and the incidence of visually significant age-related maculopathy in men. *Arch Ophthalmol* 2001;119:1259-1265.
56. Mitchell P, Smith W, Wang JJ. Iris color, skin sun sensitivity, and age-related maculopathy. The Blue Mountains Eye Study. *Ophthalmology* 1998;105:1359-1363.
57. Ho L, van Leeuwen R, Witteman JC, et al. Reducing the genetic risk of age-related macular degeneration with dietary antioxidants, zinc, and omega-3 fatty acids: the Rotterdam study. *Arch Ophthalmol* 2011;129:758-766.
58. Assink JJ, Klaver CC, Houwing-Duistermaat JJ, et al. Heterogeneity of the genetic risk in age-related macular disease: a population-based familial risk study. *Ophthalmology* 2005;112:482-487.
59. Klein ML, Francis PJ, Ferris FL, 3rd, Hamon SC, Clemons TE. Risk assessment model for development of advanced age-related macular degeneration. *Arch Ophthalmol* 2011;129:1543-1550.
60. Shahid H, Khan JC, Cipriani V, et al. Age-related macular degeneration: the importance of family history as a risk factor. *Br J Ophthalmol* 2012;96:427-431.
61. Silvestri G, Johnston PB, Hughes AE. Is genetic predisposition an important risk factor in age-related macular degeneration? *Eye (Lond)* 1994;8 (Pt 5):564-568.



62. Heiba IM, Elston RC, Klein BE, Klein R. Sibling correlations and segregation analysis of age-related maculopathy: the Beaver Dam Eye Study. *Genet Epidemiol* 1994;11:51-67.
63. Meyers SM, Greene T, Gutman FA. A twin study of age-related macular degeneration. *Am J Ophthalmol* 1995;120:757-766.
64. Hammond CJ, Webster AR, Snieder H, Bird AC, Gilbert CE, Spector TD. Genetic influence on early age-related maculopathy: a twin study. *Ophthalmology* 2002;109:730-736.
65. Maller J, George S, Purcell S, et al. Common variation in three genes, including a noncoding variant in CFH, strongly influences risk of age-related macular degeneration. *Nat Genet* 2006;38:1055-1059.
66. Helgason H, Sulem P, Duvvari MR, et al. A rare nonsynonymous sequence variant in C3 is associated with high risk of age-related macular degeneration. *Nat Genet* 2013;45:1371-1374.
67. Zhan X, Larson DE, Wang C, et al. Identification of a rare coding variant in complement 3 associated with age-related macular degeneration. *Nat Genet* 2013;45:1375-1379.
68. Manolio TA, Collins FS, Cox NJ, et al. Finding the missing heritability of complex diseases. *Nat New Biol* 2009;461:747-753.
69. Raychaudhuri S, Iartchouk O, Chin K, et al. A rare penetrant mutation in CFH confers high risk of age-related macular degeneration. *Nat Genet* 2011;43:1232-1236.
70. Klaver CC, Wolfs RC, Assink JJ, van Duijn CM, Hofman A, de Jong PT. Genetic risk of age-related maculopathy. Population-based familial aggregation study. *Arch Ophthalmol* 1998;116:1646-1651.
71. Khoury MJ, Beaty TH, Liang KY. Can familial aggregation of disease be explained by familial aggregation of environmental risk factors? *Am J Epidemiol* 1988;127:674-683.
72. Ratnapriya R, Zhan X, Fariss RN, et al. Rare and common variants in extracellular matrix gene Fibrillin 2 (FBN2) are associated with macular degeneration. *Hum Mol Genet* 2014;23:5827-5837.
73. Hoffman JD, Cooke Bailey JN, D'Aoust L, et al. Rare complement factor H variant associated with age-related macular degeneration in the Amish. *Invest Ophthalmol Vis Sci* 2014;55:4455-4460.
74. Fritsche LG, Loenhardt T, Janssen A, et al. Age-related macular degeneration is associated with an unstable ARMS2 (LOC387715) mRNA. *Nat Genet* 2008;40:892-896.
75. Kortvely E, Hauck SM, Duetsch G, et al. ARMS2 is a constituent of the extracellular matrix providing a link between familial and sporadic age-related macular degenerations. *Invest Ophthalmol Vis Sci* 2010;51:79-88.
76. Smailhodzic D, Klaver CC, Klevering BJ, et al. Risk alleles in CFH and ARMS2 are independently associated with systemic complement activation in age-related macular degeneration. *Ophthalmology* 2012;119:339-346.
77. Edwards AO, Ritter R, 3rd, Abel KJ, Manning A, Panhuysen C, Farrer LA. Complement factor H polymorphism and age-related macular degeneration. *Science* 2005;308:421-424.
78. Klein RJ, Zeiss C, Chew EY, et al. Complement factor H polymorphism in age-related macular degeneration. *Science* 2005;308:385-389.
79. Haines JL, Hauser MA, Schmidt S, et al. Complement factor H variant increases the risk of age-related macular degeneration. *Science* 2005;308:419-421.
80. Gold B, Merriam JE, Zernant J, et al. Variation in factor B (BF) and complement component 2 (C2) genes is associated with age-related macular degeneration. *Nat Genet* 2006;38:458-462.
81. Yates JR, Sepp T, Matharu BK, et al. Complement C3 variant and the risk of age-related macular degeneration. *N Engl J Med* 2007;357:553-561.
82. Seddon JM, Yu Y, Miller EC, et al. Rare variants in CFI, C3 and C9 are associated with high risk of advanced age-related macular degeneration. *Nat Genet* 2013;45:1366-1370.

83. Fagerness JA, Maller JB, Neale BM, Reynolds RC, Daly MJ, Seddon JM. Variation near complement factor I is associated with risk of advanced AMD. *Eur J Hum Genet* 2009;17:100-104.
84. Baird PN, Guida E, Chu DT, Vu HT, Guymer RH. The epsilon2 and epsilon4 alleles of the apolipoprotein gene are associated with age-related macular degeneration. *Invest Ophthalmol Vis Sci* 2004;45:1311-1315.
85. Klaver CC, Kliffen M, van Duijn CM, et al. Genetic association of apolipoprotein E with age-related macular degeneration. *Am J Hum Genet* 1998;63:200-206.
86. Chen W, Stambolian D, Edwards AO, et al. Genetic variants near TIMP3 and high-density lipoprotein-associated loci influence susceptibility to age-related macular degeneration. *Proc Natl Acad Sci USA* 2010;107:7401-7406.
87. Neale BM, Fagerness J, Reynolds R, et al. Genome-wide association study of advanced age-related macular degeneration identifies a role of the hepatic lipase gene (LIPC). *Proc Natl Acad Sci USA* 2010;107:7395-7400.
88. Yu Y, Bhangale TR, Fagerness J, et al. Common variants near FRK/COL10A1 and VEGFA are associated with advanced age-related macular degeneration. *Hum Mol Genet* 2011;20:3699-3709.
89. van de Ven JP, Nilsson SC, Tan PL, et al. A functional variant in the CFI gene confers a high risk of age-related macular degeneration. *Nat Genet* 2013;45:813-817.
90. den Hollander AI, de Jong EK. Highly Penetrant Alleles in Age-Related Macular Degeneration. *Cold Spring Harb Perspect Med* 2014.
91. Sivaprasad S, Chong NV. The complement system and age-related macular degeneration. *Eye (Lond)* 2006;20:867-872.
92. Sohn JH, Kaplan HJ, Suk HJ, Bora PS, Bora NS. Complement regulatory activity of normal human intraocular fluid is mediated by MCP, DAF, and CD59. *Invest Ophthalmol Vis Sci* 2000;41:4195-4202.
93. Scholl HP, Charbel Issa P, Walier M, et al. Systemic complement activation in age-related macular degeneration. *PLoS One* 2008;3:e2593.
94. Sivaprasad S, Adewoyin T, Bailey TA, et al. Estimation of systemic complement C3 activity in age-related macular degeneration. *Arch Ophthalmol* 2007;125:515-519.
95. Reynolds R, Hartnett ME, Atkinson JP, Giclas PC, Rosner B, Seddon JM. Plasma complement components and activation fragments: associations with age-related macular degeneration genotypes and phenotypes. *Invest Ophthalmol Vis Sci* 2009;50:5818-5827.
96. Anderson DH, Radeke MJ, Gallo NB, et al. The pivotal role of the complement system in aging and age-related macular degeneration: hypothesis re-visited. *Prog Retin Eye Res* 2010;29:95-112.
97. Johnson LV, Leitner WP, Staples MK, Anderson DH. Complement activation and inflammatory processes in Drusen formation and age related macular degeneration. *Exp Eye Res* 2001;73:887-896.
98. Bora NS, Matta B, Lyzogubov VV, Bora PS. Relationship between the complement system, risk factors and prediction models in age-related macular degeneration. *Mol Immunol* 2014.
99. Khandhadia S, Cipriani V, Yates JR, Lotery AJ. Age-related macular degeneration and the complement system. *Immunobiology* 2012;217:127-146.
100. Yehoshua Z, de Amorim Garcia Filho CA, Nunes RP, et al. Systemic complement inhibition with eculizumab for geographic atrophy in age-related macular degeneration: the COMPLETE study. *Ophthalmology* 2014;121:693-701.
101. Loyet KM, Good J, Davancaze T, et al. Complement inhibition in cynomolgus monkeys by anti-factor d antigen-binding fragment for the treatment of an advanced form of dry age-related macular degeneration. *J Pharmacol Exp Ther* 2014;351:527-537.



102. SanGiovanni JP, Chew EY. Clinical Applications of Age-Related Macular Degeneration Genetics. *Cold Spring Harb Perspect Med* 2014.
103. Evans JR. Antioxidant vitamin and mineral supplements for slowing the progression of age-related macular degeneration. *Cochrane Database Syst Rev* 2006;CD000254.
104. Finger RP, Wickremasinghe SS, Baird PN, Guymer RH. Predictors of anti-VEGF treatment response in neovascular age-related macular degeneration. *Surv Ophthalmol* 2014;59:1-18.
105. Brantley MA, Jr., Fang AM, King JM, Tewari A, Kymes SM, Shiels A. Association of complement factor H and LOC387715 genotypes with response of exudative age-related macular degeneration to intravitreal bevacizumab. *Ophthalmology* 2007;114:2168-2173.
106. Kanoff J, Miller J. Pharmacogenetics of the treatment response of age-related macular degeneration with ranibizumab and bevacizumab. *Semin Ophthalmol* 2013;28:355-360.
107. Zhao L, Grob S, Avery R, et al. Common variant in VEGFA and response to anti-VEGF therapy for neovascular age-related macular degeneration. *Curr Mol Med* 2013;13:929-934.
108. Veloso CE, de Almeida LN, Recchia FM, Pelayes D, Nehemy MB. VEGF gene polymorphism and response to intravitreal ranibizumab in neovascular age-related macular degeneration. *Ophthalmic Res* 2014;51:1-8.
109. Abedi F, Wickremasinghe S, Richardson AJ, Islam AF, Guymer RH, Baird PN. Genetic influences on the outcome of anti-vascular endothelial growth factor treatment in neovascular age-related macular degeneration. *Ophthalmology* 2013;120:1641-1648.
110. Hagstrom SA, Ying GS, Pauer GJ, et al. VEGFA and VEGFR2 gene polymorphisms and response to anti-vascular endothelial growth factor therapy: comparison of age-related macular degeneration treatments trials (CATT). *JAMA ophthalmology* 2014;132:521-527.
111. Deutman AF, van Blommestein JD, Henkes HE, Waardenburg PJ, Solleveld-van Driest E. Butterfly-shaped pigment dystrophy of the fovea. *Arch Ophthal* 1970;83:558-569.
112. Agarwal A, *Gass' Atlas of Macular diseases*: Elsevier; 2012:254-267.
113. Yang Z, Li Y, Jiang L, et al. A novel RDS/peripherin gene mutation associated with diverse macular phenotypes. *Ophthalmic Genet* 2004;25:133-145.
114. Francis PJ, Schultz DW, Gregory AM, et al. Genetic and phenotypic heterogeneity in pattern dystrophy. *Br J Ophthalmol* 2005;89:1115-1119.
115. Agarwal A, Patel P, Adkins T, Gass JD. Spectrum of pattern dystrophy in pseudoxanthoma elasticum. *Arch Ophthal* 2005;123:923-928.
116. Fossarello M, Bertini C, Galantuomo MS, Cao A, Serra A, Pirastu M. Deletion in the peripherin/RDS gene in two unrelated Sardinian families with autosomal dominant butterfly-shaped macular dystrophy. *Arch Ophthal* 1996;114:448-456.
117. Nichols BE, Drack AV, Vandenburg K, Kimura AE, Sheffield VC, Stone EM. A 2 base pair deletion in the RDS gene associated with butterfly-shaped pigment dystrophy of the fovea. *Hum Mol Genet* 1993;2:601-603.
118. Nichols BE, Sheffield VC, Vandenburg K, Drack AV, Kimura AE, Stone EM. Butterfly-shaped pigment dystrophy of the fovea caused by a point mutation in codon 167 of the RDS gene. *Nat Genet* 1993;3:202-207.
119. Zhang K, Garibaldi DC, Li Y, Green WR, Zack DJ. Butterfly-shaped pattern dystrophy: a genetic, clinical, and histopathological report. *Arch Ophthal* 2002;120:485-490.
120. Boon CJ, den Hollander AI, Hoyng CB, Cremers FP, Klevering BJ, Keunen JE. The spectrum of retinal dystrophies caused by mutations in the peripherin/RDS gene. *Prog Retin Eye Res* 2008;27:213-235.



Chapter 2

Age-related macular degeneration and macular dystrophies mimicking AMD

Macular dystrophies mimicking age-related macular degeneration

N.T.M. Saksens, M. Fleckenstein, S. Schmitz-Valckenberg, F.G. Holz,
A.I. den Hollander, J.E.E. Keunen, C.J.F. Boon, C.B. Hoyng

Published in: Progress in Retinal and Eye Research 2014;39:23-57



Age-related macular degeneration (AMD) is the leading cause of irreversible blindness in the elderly population in the Western world. AMD is a clinically heterogeneous disease presenting with drusen, pigmentary changes, geographic atrophy and /or choroidal neovascularization. Due to its heterogeneous presentation, it can be challenging to distinguish AMD from several macular diseases that can mimic the features of AMD. This clinical overlap may potentially lead to misdiagnosis. In this review, we discuss the characteristics of AMD and the macular dystrophies that can mimic AMD. The appropriate use of clinical and genetic analysis can aid the clinician to establish the correct diagnosis, and to provide the patient with the appropriate prognostic information. An overview is presented of overlapping and distinguishing clinical features.

1. INTRODUCTION

1.1 AMD

Age-related macular degeneration (AMD) is a progressive chronic disease of the central retina and the leading cause of irreversible blindness in the elderly population in industrialized countries.¹ Based on a meta-analysis of studies in white people aged 40 years and older, the prevalence of early AMD is estimated to be 6.8% and the late stages to be 1.5%.² The prevalence of AMD increases exponentially with age.³ In the Beaver Dam Eye Study that includes predominantly white participants, individuals of age 75 years and older, the fifteen year cumulative incidence of early AMD was 24.4% and of late AMD was 7.6%.⁴ The prevalence of AMD, however, differs in ethnic groups. The Baltimore Eye Study has shown that late stage AMD was nine to ten times more prevalent in the white as compared to the black participants.⁵ In the Asian population, the prevalence of late stage AMD appears to be largely similar to that in white people.⁶

Different cell layers are involved in the disease process: the photoreceptors, the retinal pigment epithelium (RPE), Bruch's membrane and the choriocapillaris. Different stages and phenotypic manifestations of AMD have been categorized⁷: The early stages (early and intermediate AMD) are characterized by pigmentary alterations and/or the formation of so called 'drusen', extracellular material located between the RPE and the Bruch's membrane. Patients with early AMD are usually asymptomatic. AMD may progress to exudative (neovascular) AMD and non-exudative (atrophic) AMD, both resulting in vision loss. Typically, patients with neovascular AMD describe sudden worsening of central vision with distortion of straight lines or a dark patch in their central vision. In atrophic AMD progressive loss of vision develops over many years. Neovascular AMD and atrophic AMD may also occur in combination. The most severe decline of visual acuity from AMD is caused by these advanced forms of the disease. In addition, psychophysical studies have demonstrated that several parameters of visual function, in particular contrast sensitivity, visual adaptation, central visual field, and color discrimination, deteriorate already in the early stages of AMD.⁸ Since the disturbance in psychophysical function in AMD is not limited to the macular region, but extends well into the retinal periphery, it appears that there is a global impairment of retinal function.^{9,10}

The pathogenesis of AMD is incompletely understood. As a complex, multifactorial disease, it is thought to involve variations in a number of genetic, systemic and environmental factors. Aging itself appears to be the major risk factor that renders the retina more susceptible to environmental effects.¹¹

Biochemical, histological and genetic studies have indicated several pathways in AMD pathogenesis, including excessive accumulation of lipofuscin, oxidative damage, malfunctioning of the complement system, and chronic low-grade inflammation and possible sequences of events have been proposed.



Lipofuscin accumulates in postmitotic RPE cells with age apparently due to incomplete lysosomal degradation of photoreceptor outer segments (reviewed by Boulton).¹² Lipofuscin consists of a multitude of molecules including the dominant fluorophore N-retinyl-N-retinylidene ethanolamine (A2E), a by-product of the visual cycle.^{13, 14} Exposure of lipofuscin containing RPE cells to blue light (390-520nm) results in a lipofuscin-dependent lipid peroxidation, protein oxidation, loss of lysosomal integrity, mitochondrial DNA damage, and RPE cell death (reviewed by Boulton).¹² It has further been suggested that products of the photooxidation of A2E in RPE cells could serve as a trigger for complement activation.¹⁵ An aberrant complement regulation - that is implicated by the association of the risk for AMD with DNA sequence variants in genes encoding for complement factors (see below) - appears to contribute to chronic inflammation. Herein, drusen are thought to form as a product of those local inflammatory processes.^{16, 17}

In recent years, major progress was made in elucidating the genetic basis of AMD through the identification of two common variants on chromosome 1 and 10, together likely accounting for approximately 50% of cases. On chromosome 1, a strong association was identified with variants in the complement factor H (*CFH*) gene, suggesting an involvement of the complement cascade in AMD pathogenesis.¹⁸⁻²¹ Subsequently, AMD risk variants in other genes involved in the complement cascade were identified, for example in the complement component 2/factor B,²² component 3 (*C3*),²³ and complement factor I genes.²³ The second major AMD risk locus was identified on chromosome 10. Disease associated variants support a region harbouring two genes in strong linkage disequilibrium, named the age-related maculopathy susceptibility 2 gene and the high temperature requirement factor A1 gene.^{24, 25} However, the functional implications of the chromosome 10 locus on AMD pathology are still unclear. A genomic wide association study recently performed by the AMD Gene Consortium found in total 19 loci associated with AMD, including seven new loci.²⁶ Recently, rare, highly penetrant mutations in the *CFH* and *Complement Factor I* genes have been identified besides the common genetic variants, conferring a high risk of AMD.²⁷⁻³⁰ Rare variants may play an important role in the pathogenesis of AMD particularly in case of densely affected families.

Recently, a predictive model for late stage AMD based on data from population-based studies (the Rotterdam Study, the Beaver Dam Eye Study, and the Blue Mountains Eye Study) has been reported. It has been shown that best prediction for late AMD was based on age, sex, 26 genetic variants, 2 environmental variables, and early AMD phenotype.^{31, 32}

1.2 Differentiating macular dystrophies from AMD: difficulties and relevance

There are no pathognomonic clinical characteristics for AMD, despite the fact that drusen are a hallmark feature. Different clinical manifestations may be present, leading to a broad phenotypic spectrum of AMD. Due to this clinical variability of AMD, there is a considerable overlap with a number of macular dystrophies that are often monogenic with specific inheritance patterns. Also, AMD and the macular dystrophies show a considerable variation

in their clinical presentation and severity. Flecks that may resemble drusen can be present in several hereditary macular conditions. Many macular dystrophies may show chorioretinal atrophy comparable to geographic atrophy (GA) in AMD. Choroidal neovascularization (CNV) can also occur in macular dystrophies, although it is rare and appears to have a relatively favourable prognosis as compared to CNV in AMD.³³

A differentiation between AMD and other macular disorders is important as the exact diagnosis can have implications for the prognosis and genetic counselling as well as for preventive and therapeutic strategies.

This review aims to give an overview of macular dystrophies that may mimic AMD. For every disease we describe the symptoms, multimodal imaging and psychophysical and electrophysiological testing. In addition, we also summarize the genetic background and the pathophysiology of each disease. Based on these specific clinical and genetic characteristics, we provide a practical differential diagnostic guideline.

2. FUNDOSCOPIC FINDINGS IN AMD AND MACULAR DYSTROPHIES

2.1 Drusen and ‘drusen-like lesions’

Drusen are considered as the phenotypic hallmark of AMD, but they are not pathognomonic of AMD.³⁴ Drusen are focal deposits of extracellular debris located between the basal lamina of the RPE and the inner collagenous layer of Bruch’s membrane.^{35,36} Drusen are known to contain carbohydrates, zinc, and at least 129 different proteins, including apolipoproteins and excluding extracellular matrix.³⁷⁻⁴³

Fundoscopically, drusen are yellowish nodular lesions located at the posterior pole. Previous classifications of AMD have included the following qualities of drusen: drusen size (e.g., large vs. small), character (e.g., soft vs. hard), location, number, and area.⁴⁴⁻⁴⁶ The recently reported AMD classification by Ferris et al. again stresses the importance of drusen size in AMD patients, particularly with regards to the prognostic relevance for late-stage disease development. Hereby, small drusen ($\leq 63 \mu\text{m}$) are considered to represent normal aging changes and should be differentiated from early AMD.⁷ Medium sized drusen ($>63 \mu\text{m}$ and $\leq 125 \mu\text{m}$) without associated pigment abnormalities represent early while large drusen ($> 125 \mu\text{m}$) and/or any AMD-related pigmentary abnormality (i.e. any definite hyper- or hypopigmentary abnormalities associated with medium or large drusen) represent intermediate AMD (**Figure 2.1A**).⁷ Drusen may present as clusters and become confluent (‘confluent drusen’). Large confluent drusen may form clinically evident pigment epithelial detachments without underlying CNV (‘drusenoid pigment epithelium detachment’).⁴⁷ On fluorescein angiography (FA), small drusen may show a focal hyperfluorescence in the late-stage, whereas larger drusen usually show a hypofluorescence due to the blockage of choroidal background fluorescence. Fundus autofluorescence (FAF) does not allow clear distinction of most AMD-related drusen because drusen exhibit a similar signal compared



to the background (**Figure 2.1B**). One exception is large, confluent drusen that show a mildly increased signal. Compared to fundus photography, the area involved by soft drusen appears to be better detectable by FAF imaging. On spectral-domain optical coherence tomography (SD-OCT) imaging, drusen typically present as ‘dome-shaped’ elevations of variable size of the outer retinal layers and the RPE (**Figure 2.1D**). SD-OCT herein enables to reveal differential reflectivity of the drusen material by itself⁴⁸. This may point to differences in the biochemical composition of drusen.

Cuticular drusen, formerly known as ‘basal laminar drusen’ that have been firstly described by Gass in 1977.⁴⁹ It has been estimated that the cuticular drusen phenotype comprises approximately 10% of the AMD spectrum.²⁸ Cuticular drusen are usually 25 - 75 μm in size and are discretely round, slightly raised, yellow, subretinal pigment epithelium nodules that initially may be randomly scattered in the macular area in young adults, but later often become more numerous and in some patients are grouped in clusters of 15 - 20 drusen (**Figure 2.1E**).⁴⁹ These clusters, in turn, may be closely arranged in a knit pattern giving the entire macula and the paramacula an orange-peel appearance.⁴⁹ FA is particularly helpful for the visualization of cuticular drusen. They fluoresce discretely during the early arterio-venous phase and in many patients they give the fundus a ‘stars-in-the-sky’ picture (**Figure 2.1G**).⁴⁹ FAF shows cuticular drusen as areas of ill-defined autofluorescence centered by punctate hypo-autofluorescent lesions (**Figure 2.1F**).⁵⁰⁻⁵² Besides correlating with ‘dome-shaped’ elevations, cuticular drusen have been reported to further appear as irregular slight thickening of RPE/Bruch’s membrane complex or as a ‘sawtooth’ RPE elevation on SD-OCT scans (**Figure 2.1H**).⁵⁰

A higher allele frequency of the *CFH* Y402H risk allele in patients with cuticular drusen suggests that activation of the alternative pathway of the complement system may play a larger role in the pathogenesis of the cuticular drusen phenotype than in the remainder of the AMD phenotypes.⁵³⁻⁵⁵ This is supported by previous studies that identified rare pathogenic *CFH* mutations in a subset of families with cuticular drusen.^{28, 30}

In addition, reticular (pseudo-)drusen have been described. Initially reported by Mimoun et al. as ‘pseudodrusen visible en lumière bleu’ [‘the pseudo-drusen visible in blue light’].⁵⁶ It has been described by others using different terms, including ‘reticular drusen’.⁵⁷ There is still an ongoing debate whether reticular drusen are located anterior or posterior to the RPE. Reticular drusen are subtle, fundoscopically hardly detectable individual lesions showing an interlacing network of round or oval shaped multiple, yellowish irregularities with an approximately size between 50 and 250 μm (**Figure 2.1I**). Several studies, for instance the Beaver Dam Eye study, identified reticular drusen as a risk factor for the development of late-stage AMD.^{58, 59} On FA reticular drusen may show a discrete hypofluorescence towards the later phases. The reticular pattern is typical for reticular drusen by FAF imaging showing multiple spots with decreased intensity surrounded by mildly increased intensity (**Figure 2.1J**). The reticular drusen pattern in cSLO (confocal scanning laser ophthalmoscopy) images correlates with marked changes at a level anterior to the RPE/Bruch’s membrane

complex.⁶⁰⁻⁶² By scanning precisely through a row of reticular lesions by SD-OCT, accumulation of material between the ellipsoid zone of the photoreceptors and the RPE/Bruch's membrane complex is visible (**Figure 2.1K**)⁶⁰⁻⁶² (anatomical correlations of SD-OCT bands are according to the nomenclature proposed by the 'International Nomenclature for Optical Coherence Tomography Panel').

Large colloid drusen are large (200 to 300 μm) lesions associated with an early age at onset and a relatively good vision.⁶³ The lesions show increased autofluorescence on FAF and are mildly hyperfluorescent in the early phases of FA, with a progressive staining in late phases.⁶³ On indocyanine green angiography (ICGA), large colloid drusen are hypofluorescent in the early phase, and in later phases the hypofluorescent centre is surrounded by a hyperfluorescent halo bordered by a thin hypofluorescent ring.⁶³

Irregular flecks: Fundus flavimaculatus is characterized by the presence of irregular yellowish flecks in the deeper retinal layers of the posterior pole. The flecks are variable in size, shape and distribution. In the midperipheral retina, these yellowish flecks can be interconnected to form a reticular pattern.⁶⁴

Vitelliform lesions: The term 'vitelliform' is aspecific, referring to a round, yellowish lesion that looks like an egg yolk. Vitelliform lesions show intense hyperautofluorescence on FAF and hypofluorescence on FA, due to the accumulation of hyperreflective material between the neuroretina and RPE, which is visible on SD-OCT.^{65,66} Vitelliform lesions can be seen in a broad range of macular conditions, such as adult-onset foveomacular vitelliform dystrophy (AFVD), Best vitelliform macular dystrophy (BVMD), drusenoid vitelliform RPE detachments, mitochondrial retinal dystrophy associated with the m.3243A>G mutation, vitreofoveal traction, acute vitelliform polymorphous exudative maculopathy, and paraneoplastic vitelliform retinopathy.^{67,68}

2.2 Pigmentary changes

Pigmentary changes appear on clinical examination either as hypopigmentary changes, which are seen as depigmented areas of the RPE or hyperpigmentary changes, which are deposits of grey or black pigment within the retina or at the level of the RPE.^{46,69} Hyperpigmentation in AMD is presumed to result from RPE displacement, migration, or degeneration.^{46,69} Any hyper- or hypopigmentary abnormality associated with medium or large drusen is a defining feature of intermediate AMD.⁷

On FA, hyperpigmentations usually appear hypofluorescent due to blocked background fluorescence, while on FAF, there is frequently a correlating increased signal (**Figure 2.1B**). On SD-OCT, hyperpigmentary alterations usually correlate with hyperreflective foci (**Figure 2.1C**). These foci may be located at the level of the RPE or in more inner retinal layers.^{60,70} Serial examinations *in vivo* by high-resolution OCT imaging have shown migration of these hyperreflective foci into more inner retinal layers with time.^{71,72}



2.3 Geographic atrophy

Fundoscopically, GA appears as a sharply demarcated area with depigmentation and typically enhanced visualisation of deep choroidal vessels (**Figure 2.1L**). GA may occur as uni-focal or multi-focal lesion. The configuration of atrophy may vary from round or oval to lobular. Histologically, areas of GA in AMD are characterized by loss of the RPE, of outer layers of the neurosensory retina and the choriocapillaris.^{73, 74}

On FA, GA typically presents with late well-defined hyperfluorescence. Due to the loss of the RPE, the hyperfluorescent signal derives from the staining of the exposed deep choroid and sclera ('window defect').

Due to RPE atrophy and thus loss of intrinsic fluorophores, GA in AMD presents as well-demarcated lesion with decreased FAF signal (**Figure 2.1M**). FAF imaging allows for more precise delineation of the atrophy process as compared to fundus photography. Furthermore, in the area surrounding the GA, different patterns of abnormal FAF may be differentiated.^{75, 76} This allows for phenotypic sub-classification of GA. Herein, the 'banded' and the 'diffuse' GA sub-types have been shown to be associated with a significantly faster progression of the GA lesions as compared to the 'none' and 'focal' sub-types.⁷⁵

On SD-OCT imaging, GA is characterized by loss of the outer retinal layers, including the outer nuclear layer, the external limiting membrane, ellipsoid zone, myoid zone, and interdigitation zone, respectively, and by loss of the inner part of the RPE/Bruch's membrane complex (assumed RPE-layer) (**Figure 2.1N**).⁶⁰ The GA border in AMD usually shows marked alterations of the outer retinal SD-OCT layers. In the area surrounding GA, SD-OCT imaging may reveal various microstructural alterations that may also be found in eyes with only drusen and hyperpigmentation.⁶⁰

2.4 Choroidal neovascularization

CNV is the in-growth of pathologic new blood vessels through Bruch's membrane into the sub-RPE and/or the subretinal space originating from the choriocapillaris. Leakage of plasma or blood into the surrounding tissue is characteristic of CNV lesion. The natural course of CNV is evolution to fibrovascular scar formation. Retinal Angiomatous Proliferation (RAP) has recently been recognized as a variant of neovascular AMD that is characterized by the formation of pathologic new vessels within the retina that may secondarily invade into the subretinal space or into the choroid.⁷⁷ Polypoidal choroidal vasculopathy (PCV) is characterized by branching vascular networks terminating in polypoidal dilations that appear as reddish-orange structures beneath the RPE.⁷⁸ It is still debated if PCV is a sub-form of AMD or if it is a separate clinical entity. CNV may present fundoscopically as greyish subretinal lesion (**Figure 2.1O**). Other fundoscopic changes that suggest CNV include macular edema, subretinal fluid, hard exudates, haemorrhage, and RPE detachment.

It has been shown that CNV may be associated with normal, increased, or decreased focal RPE autofluorescence.⁷⁹⁻⁸³ Abnormal FAF intensities visible in eyes with CNV often extend beyond the edge of a lesion defined by FA, which indicates a more widespread

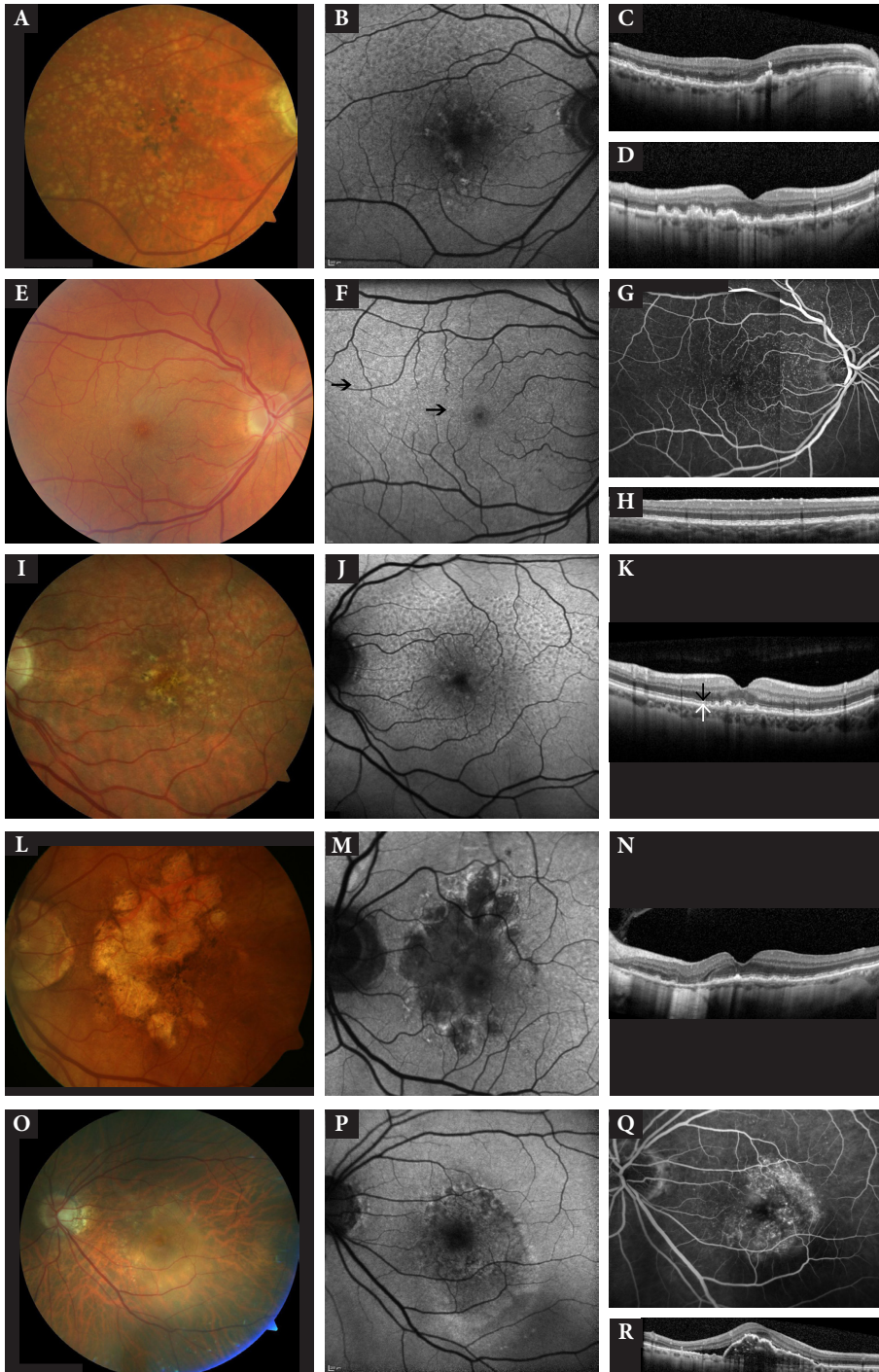
disease process, over and above that witnessed on conventional angiograms (**Figure 2.1P**). It has been speculated that this observation may reflect the proliferation of RPE cells around the CNV.⁸⁴

Fluorescence angiography is the gold standard for visualization of CNV and differentiation of CNV variants. According to its appearance during FA, CNV can be classified into classic or occult lesion types. The classic type shows well-defined margins and homogeneous leakage of dye within the entire lesion, whereas occult lesions demonstrate irregular margins with heterogeneous leakage of fluorescein within the lesion (**Figure 2.1Q**).⁸⁵ Originally, the differences in leakage pattern were assumed to be explained by the anatomic location – subretinal or sub-RPE – of the CNV. However, clinico-pathological correlations indicated a lack of strong correlation between fluorescein angiography pattern and anatomic localization of the CNV.⁸⁶

For the diagnosis and visualization of PCV and RAP, indocyanine green (ICG) angiography is superior to other imaging modalities.

High-resolution OCT imaging allows for precise visualization of subretinal and intraretinal fluid and other CNV-associated characteristics (**Figure 2.1R**). Furthermore, detection of changes in retinal thickness by OCT imaging has become an important indicator in the monitoring of therapeutic effects in CNV.





► **Figure 2.1 (A-D)** Drusen and hyperpigmentation in a 67-year-old patient with intermediate Age related macular degeneration (AMD). The color fundus image (A) shows medium and large sized drusen associated with hyperpigmentation. Fundus autofluorescence (FAF) imaging (B) shows an increased signal that is mainly associated with the hyperpigmentary changes. Drusen are associated with increased, decreased or normal FAF. Note the 'reticular drusen' FAF pattern pronounced superior-temporally. Optical coherence tomography (OCT) imaging reveals hyperreflective foci that correspond to the hyperpigmentary changes (C) or shows the characteristic dome-shaped appearance of drusen (D). The images (E-H) show cuticular drusen in a 38-year-old patient. (E) Color fundus photograph showing small yellow cuticular drusen in the macula and peripheral retina. (F) FAF image showing increased autofluorescence of the deposits in the posterior pole (black arrows). (G) Fluorescein angiography (FA) image showing the hyperfluorescent deposits as a typical 'stars-in-the-sky' picture in the early phase. (H) Horizontal OCT scan showing the cuticular drusen corresponding to hyperreflective elevations of the retinal pigment epithelium (RPE). The images (I-K) show reticular drusen in an 80-year-old patient associated with intermediate AMD. The color fundus image (I) shows the superior central area with drusen and hyperpigmentation in an interlacing network of round and oval shaped yellowish irregularities. FAF imaging (J) shows multiple spots with decreased intensity surrounded by mildly increased intensity. SD-OCT imaging (K) reveals a wavy pattern of the ellipsoid zone (black arrow) with accumulation of highly reflective material between the ellipsoid zone and the RPE/Bruch's membrane complex (white arrow) corresponding to the reticular pattern in the IR image. The images (L-N) show a multifocal geographic atrophy (GA) secondary to AMD, in a 77-year-old patient. Fundoscopically (L), the GA appears as a sharply demarcated area with depigmentation and typically enhanced visualisation of deep choroidal vessels. On FAF imaging (M) there is a well-demarcated area with decreased FAF corresponding to the GA lesion. On SD-OCT imaging (N), GA is characterized by loss of the outer retinal layers and a signal enhancement within the choroid. (O-R) Choroidal neovascularization (CNV) in a 68-year-old patient with occult CNV secondary to AMD. In the fundus image (O), there is a PED and drusen. In the FAF image (P), the lesion extends beyond the edge of the lesion defined by FA (Q). On SD-OCT imaging (R), there is a PED visible with subretinal fluid in the inferior part of the lesion.



3. DIFFERENTIAL DIAGNOSTIC TOOLS

The most important differential diagnostic findings and genetic associations of each macular dystrophy are summarized in **Table 2.1**. With the advancements in multimodal retinal imaging and genetic testing, a spectrum of diagnostic tools is currently available to establish the correct diagnosis. An overview of important differentiating findings with the available differential diagnostic tools is given below.

3.1 Symptoms and fundoscopy

Patients with early AMD usually present with normal central visual acuity. Impaired dark adaptation upon moving from brightly lit to dim environments, however, is commonly reported by patients with early AMD, although central visual acuity remains normal.⁸⁷ Furthermore, distinct drusen may cause metamorphopsia. Progression of the disease generally results in vision loss, increased metamorphopsia and/or a dark patch in central vision. The course of visual symptoms and the age of onset may help to discriminate AMD from macular dystrophies.

North Carolina macular dystrophy (NCMD) patient for instance, typically present with visual complaints during their childhood and complaints and fundoscopic features have a stable course. The visual acuity is relatively good and stable, like in patients with late-onset Stargardt and pseudo-Stargardt pattern dystrophy. Patients with late-onset retinal degeneration (LORD), Sorsby fundus dystrophy (SFD) and pseudo-Stargardt pattern dystrophy may also present with night vision problems or loss of peripheral vision. Some macular diseases discussed in this review are multisystemic disorders presenting with additional multisystemic symptoms. Patients with maculopathy in myotonic dystrophy often present with muscle weakness and myotonia and patients with pseudoxanthoma elasticum (PXE) may suffer from cardiovascular disease, gastro-intestinal bleeding and skin papules. Hearing loss and diabetes in maternally inherited diabetes and deafness (MIDD) patients and renal disease in membranoproliferative glomerulonephritis type II (MPGN II) patients are also systemic symptoms, which may help to come to the correct diagnosis.

In AMD, fundoscopic features are present mainly in the macular area. In contrast, deposits in SFD patients are present in the entire posterior pole, extending to the equator. The presence of comet tail lesions, angioid streaks and peau d'orange point to PXE-related dystrophy. In addition, the aspect of the optic disc and the peripapillary region may provide distinguishing information like drusen of the optic disc in PXE dystrophies, and juxtapapillary drusenoid lesions in Malattia Leventinese (ML).



Table 2.1 Summary of distinguishing features of macular dystrophies in comparison with AMD

Clinical characteristics	Diagnosis	Distinguishing features	Gene/locus
Drusen and drusen-like deposits	ML	- Earlier age at onset (30-40y)	<i>EFEMP1</i>
		- Positive family history (AD inheritance pattern)	
		- Presence of typical radially oriented macular drusen, sometimes with nodular peripapillary drusen, which evolve to large densely packed and confluent drusen	
SFD		- Earlier age at onset (30-50y)	<i>TIMP3</i>
		- Positive family history (AD inheritance pattern)	
		- Delayed choroidal filling on FA	
		- Extramacular chorioretinal disease	
NCMD		- Early age at onset (in childhood or possibly congenital)	<i>(MCDR1 locus on chr 6q16)</i>
		- Positive family history (AD inheritance pattern and Irish-American ancestry)	
		- Relatively stationary course, except in rare cases of CNV	
		- Absence of sub-RPE deposits on SD-OCT	
		- Relatively preserved visual acuity despite sometimes marked atrophy	
		- Onset of night vision problems before the age of 50	
LORD		- Positive family history (AD inheritance pattern)	<i>C1QTNF5</i>
		- Extensive scalloped areas of chorioretinal atrophy	
		- Long anteriorly inserted lens zonules and peripapillary iris transillumination	
		- Evidence of widespread retinal disease on dark adaptation and full-field ERG in advanced LORD.	

(Continued)



Table 2.1 Continued

Clinical characteristics		Diagnosis	Distinguishing features	Gene/locus
Yellowish flecks	Irregular	Late-onset Stargardt	<ul style="list-style-type: none"> - Flecks are more irregularly shaped and do not cluster in the central macula - Intense autofluorescence of flecks on FAF images - Dark choroid on FA 	<i>ABCA4</i>
		Pseudo-Stargardt pattern dystrophy	<ul style="list-style-type: none"> - Early age at onset (<55y) - Positive family history (AD inheritance pattern) - Flecks show intense autofluorescence on FAF images and hyperfluorescence with a central hypofluorescent spot on FA. - Constriction of peripheral visual field 	<i>PRPH2/RDS</i>
		Pattern dystrophy	<ul style="list-style-type: none"> - Earlier age at onset (20-50y) - Positive family history (AD inheritance pattern may be masked) - Absence of typical soft drusen - Specific AF and FAF patterns 	<i>PRPH2/5q21.2-q33.2</i>
	Vitelliform	AFVD	<ul style="list-style-type: none"> - Central vitelliform lesion without surrounding drusen - Marked autofluorescence changes within AFVD lesions - Lesion corresponding to hyperreflective accumulation above the RPE on SD-OCT 	<i>PRPH2/BEST1</i>
		BVMD	<ul style="list-style-type: none"> - Age at onset before the age of 50 - Positive family history (AD inheritance pattern) - Central vitelliform lesion without surrounding drusen - Marked autofluorescence changes within BVMD lesion - Lesion corresponding to hyperreflective accumulation above the RPE on SD-OCT - Markedly abnormal EOG 	<i>BEST1</i>



Table 2.1 Continued

Clinical characteristics	Diagnosis	Distinguishing features	Gene/locus
Atrophy without drusen or flecks	CACD	<ul style="list-style-type: none"> - Relatively early age at onset (30-50y) - Positive family history (AD inheritance pattern) - Absence of genuine drusen on ophthalmoscopy and SD-OCT - More pronounced FAF changes than in atrophic AMD - Earlier age at onset (30-60y) - No drusen - Temporal optic disc pallor - ERG findings typical for cone dystrophy - Relatively early age at onset - History of serous neuroretinal detachment without drusen on ophthalmoscopy and SD-OCT - Gravitational tracks on FA and FAF - Earlier age at onset (>40y) - Absence of drusen - Capillary dilatation on FA, particular temporally to the fovea - Parafoveal hyperreflectivity in blue reflectance - Retinal thinning and cavities on SD-OCT 	<i>PRPH2</i>
	Late-onset cone dystrophy	<ul style="list-style-type: none"> - Positive family history (maternal inheritance pattern) - Speckled hypo- and hyperautofluorescence that may spread along the temporal retinal vascular arcades and surround the optic disc - Concomitant symptoms such as hearing loss and diabetes 	<i>m.3243A>G</i>
Dystrophy associated with syndrome or systemic disease	MIDD/ MELAS associated macular dystrophy	<ul style="list-style-type: none"> - Earlier age at onset (in adolescents) - Angioid streaks on near infrared-, FA-, FAF-, and SD-OCT-imaging. - Accompanied ocular findings such as peau d' orange and comet tail lesions - Accompanied systemic symptoms such as skin abnormalities, cardiovascular disease, gastro-intestinal bleeding 	<i>ABCC6</i>
	MPGN II	<ul style="list-style-type: none"> - Earlier age at onset (in childhood) - Stars in the sky appearance on FA - Accompanied renal disease 	<i>C3 + CFH</i>
	Maculopathy in Myotonic dystrophy	<ul style="list-style-type: none"> - Positive family history of myotonic dystrophy - Associated ocular symptoms such as posterior subcapsular cataracts, ptosis, ophthalmoplegia, and low intraocular pressure - Generalized muscle weakness and myotonia 	<i>DMPK + CNBP</i>

Abbreviations: ML, Malattia Leventinese; AD, autosomal-dominant; SFD, Sorsby Fundus Dystrophy; FA, fluorescein angiography; NCMMD, North Carolina Macular Dystrophy; CNV, choroidal neovascularization; RPE, retinal pigment epithelium; SD-OCT, spectral-domain optical coherence tomography; LORD, Late Onset Retinal Macular Dystrophy; ERG, electroretinography; FAF, fundus autofluorescence; AFVD, Adult-onset Foveo Macular dystrophy; BVMD, Best Vitelliform Macular Dystrophy; EOG, electro-oculography; CACD, Central Areolar Choroidal Dystrophy; AMD, Age-related Macular Degeneration; CSC; Central Serous Chorioretinopathy; MacTel, Macular Telangiectasia; MIDD, Maternally Inherited Diabetes and Deafness; MELAS, Mitochondrial Encephalopathy, Lactic Acidosis and Stroke-like episodes.



3.2 Fundus autofluorescence

Besides funduscopy, FAF is probably the most valuable differentiating tool to distinguish the different macular dystrophies from each other and from AMD. Abnormalities on FAF are often more extensive than the abnormalities seen on funduscopy or FA. FAF gives an indirect reflection of metabolic changes and lipofuscin accumulation at the level of the RPE and allows topographical mapping of lipofuscin distribution in the RPE. Lesions with increased FAF often corresponds to fundoscopically visible yellow lesions that contain lipofuscin, either due to accumulation of abnormally increased amounts of lipofuscin in the RPE (such as the flecks seen in Stargardt disease), and/or accumulation of autofluorescent material between the neuroretina and RPE that contains lipofuscin precursors (such as in BVMD).^{66, 88} Decreased FAF is observed for instance in areas of RPE atrophy (**Figure 2.1M, 2.2I and 2.5F**). Lesions in AMD show increased, decreased or normal autofluorescence, but generally to a more modest degree than in macular dystrophy (**Figure 2.1M, 2.1F, 2.5B and 2.5F**). In contrast, macular dystrophies often have very marked FAF abnormalities because of the higher and earlier-onset overload of autofluorescent lipofuscin due to the underlying effects of the genetic defect. As will be discussed below in the disease-specific sections, FAF imaging is able to identify fairly disease-specific distributions of FAF that strongly point to specific macular dystrophies. In a way, FAF can show a certain ‘genetic fingerprint’. For instance, markedly autofluorescent irregular flecks in the posterior pole are very suggestive of either autosomal-recessive Stargardt macular dystrophy or autosomal-dominant pseudo-Stargardt pattern dystrophy.⁸⁹

3.3 Fluorescein angiography

Fluorescein angiography (FA) permits the study of the retinal and choroidal circulation by administration of fluorescein dye. Although FA is used less frequently in the era of FAF and OCT, it can sometimes still be useful in the diagnosis and follow-up of specific macular dystrophies. Although CNV is rare present in most macular dystrophies, it is a prominent and early-onset feature for instance in SFD.⁹⁰

FA can also show a typical pattern of flecks, such as a ‘stars in the sky’ appearance in cuticular drusen and MPGN II, and a ‘dot-and-halo’ or ‘solar eclipse’ lesion in AFVD. Moreover, FA can show other hallmark features such as an absence of choroidal background fluorescence (‘dark choroid’) in Stargardt disease and delayed choroidal filling in SFD.^{88, 91}

3.4 Optical coherence tomography

Spectral-domain optical coherence tomography (SD-OCT) allows a high-resolution analysis of the anatomical location of deposits and/or flecks in or under the retina/RPE. Deposits located under the RPE, like drusen in AMD, can be found in several macular dystrophies such as, LORD, ML and cuticular drusen.⁹² Deposits in ML and cuticular drusen appear as sawtooth RPE elevations or dome-shaped elevations and may also present as thickening of the RPE/Bruch’s membrane complex. Thickening of the RPE may also be found on SD-OCT

in patients with SFD, NCMD, and MIDD. In contrast to AMD drusen, the subretinal deposits in pattern dystrophy, AFVD, BVMD and reticular pseudodrusen are located anterior to the RPE.^{65,93} In addition to the localizing value of OCT in the analysis of deposits, SD-OCT will also show the location of atrophic lesions. Finally, SD-OCT is able to visualize evidence of intraretinal and subretinal fluid accumulation, such as in CNV.

3.5 Psychophysical and electrophysiological testing

Despite the fact that most of the discussed dystrophies predominantly affect the macula, the full-field electroretinography (ERG) - which reflects panretinal cone and rod function - can become progressively abnormal in some diseases, such as in pseudo-Stargardt pattern dystrophy. Multifocal ERG and pattern ERG can become abnormal early in the course of the disease, although these examinations are of limited differential diagnostic value. The electro-oculography (EOG), which reflects panretinal function of the RPE, can be performed to distinguish between BVMD and AFVD, as the EOG response is markedly abnormal in BVMD in contrast to AFVD.^{67,94} These examples illustrate that the so-called 'macular' dystrophies can actually affect photoreceptor and/or RPE function of the entire retina in selected entities.

3.6 Genetics

AMD is a multifactorial disease in which several genetic as well as environmental factors play a role. Although the majority of AMD cases are sporadic, the disease may also run in the family.⁹⁵ Some families are very densely affected, and it has been suggested that such families may carry rare genetic variants that confer a large risk on developing AMD.⁹⁶ Most disease discussed in this review are monogenic diseases caused by a known genetic mutation or locus, which may help in the diagnostic procedure.

A thorough family history and drawing of a pedigree can be pivotal in the identification of an inheritance pattern in a specific macular disorder. Patients with an autosomal-dominant macular dystrophies, like Central areolar choroidal dystrophy, ML, NCMD, LORD, AFVD and butterfly-shaped pattern dystrophy, frequently have family members with a history of macular disease. However, incomplete penetrance and variable expression can complicate the recognition of inheritance patterns

Some genes and their defects are associated with a certain degree of genotype-phenotype correlation, such as the *ABCA4* gene and its associated phenotypes,⁹⁷ although the spectrum of clinically defined *ABCA4* disease is notably broad.^{98,99} Mutations in other genes, such as the *PRPH2* and *BEST1* gene, are associated with marked phenotypic heterogeneity and show relatively limited genotype-phenotype correlation.^{67,100}

Genetic testing may play an important role in the diagnostic procedure, as the identification of the causative gene in many cases can be the definitive confirmation of a specific macular dystrophy. This is especially helpful in patients with early and end-stage disease, with less specific, ophthalmoscopic abnormalities, as it may be difficult to



discern macular diseases. Genetic confirmation of a clinically suspected diagnosis can aid in providing a clinical prognosis for the patient, and the identification of a causative gene will facilitate genetic counselling. **Table 2.2** provides an overview of identified genes and loci and the associated macular dystrophies that are discussed in this review.

Table 2.2 Summary of macular dystrophies associated with identified genes and loci

Gene or locus	Associated diseases
5q21.2-q33.2	Pattern dystrophy
<i>ABCA4</i>	Late-onset Stargardt
<i>ABCC6</i>	Angioid streaks related dystrophy
<i>BEST1</i>	Adult-onset foveomacular vitelliform dystrophy Best-vitelliform macular dystrophy
<i>C1QTNF5</i>	Late-onset retinal degeneration
<i>C3</i>	Cuticular drusen Membranoproliferative glomerulonephritis type II
<i>CFH</i>	Cuticular drusen Membranoproliferative glomerulonephritis type II
<i>CNBP</i>	Maculopathy in Myotonic dystrophy
<i>DMPK</i>	Maculopathy in Myotonic dystrophy
<i>EFEMP1</i>	Malattia leventinese
<i>m.3243A>G</i>	MIDD/MELAS associated macular dystrophy
<i>MCDR1</i> locus	North Carolina macular dystrophy
<i>PRPH2/RDS</i>	Central areolar choroidal dystrophy Pseudo-Stargardt pattern dystrophy Pattern dystrophy Adult-onset foveomacular vitelliform dystrophy
<i>TIMP3</i>	Sorsby fundus dystrophy

Abbreviations: MIDD, *Maternally Inherited Diabetes and Deafness*; MELAS, *Mitochondrial Encephalopathy, Lactic Acidosis and Stroke-like episodes*.

4. MACULAR DYSTROPHIES MIMICKING AMD

4.1 Drusen and ‘drusen-like deposits’

4.1.1 Malattia leventinese

4.1.1.1 Introduction

Malattia leventinese (ML), also known as Doyme honeycomb retinal dystrophy, is an autosomal-dominantly inherited macular dystrophy. Some authors refer to this entity as ‘dominant drusen’, although this term is not specific as there are more forms of dominantly inherited drusen, such as cuticular drusen.^{28, 101-103}

4.1.1.2 Clinical characteristics

The onset of ML is generally in the third to fourth decade of life, but shows a wide variation.^{63, 92, 102, 104} Most patients are asymptomatic until the age of 30 to 40 years, when they may start to experience a variety of early visual symptoms, including central vision loss, paracentral scotomata, photophobia, color vision problems, and metamorphopsia.^{105, 106} A more rapid, progressive central vision loss generally starts around the mid-40s as a result of extensive pigmentary changes, GA, and/or CNV.¹⁰² The evolution of the disease and its impact on visual function are highly variable between families and between individuals of the same family.^{102, 106, 107}

4.1.1.3 Ophthalmoscopic features

The first ophthalmoscopic signs of ML appear by the age of 20 years, through the appearance of typical small, radially oriented drusen in the macular area (**Figure 2.2A**).^{102, 103, 108} In this early stage, visual acuity is relatively preserved. With time, large round drusen appear in the macula, extending in the nasal area and around the optic disc. Centrally in the macula the drusen usually become a confluent yellow-white subretinal plaque with pigmentary changes. ML may progress to central chorioretinal atrophy in 26-69% of patients older than 45 years and may be complicated by CNV in 6-24% of these patients.^{102, 106, 108}

4.1.1.4 Fundus autofluorescence

FAF reveals an intense autofluorescence of large round drusen located around the macular area and optic disc area, whereas smaller radial drusen are faintly visible (**Figure 2.2B**).^{63, 92, 104} The association of increased autofluorescence with large drusen may be stronger in ML patients than in AMD patients.^{92, 109, 110}

4.1.1.5 Fluorescein and indocyanine green angiography (ICGA)

In the early phase of FA, the large central drusen are indistinct and hypofluorescent, whereas the small radial drusen are well demarcated and highly hyperfluorescent (**Figure 2.2C**).^{63, 92, 104} In the late phase of FA, the large round central drusen are intensely hyperfluorescent due to staining and the fluorescence of small drusen decrease.^{63, 92, 104} The fluorescence pattern on ICGA is comparable to that in FA, but the hyperfluorescent large drusen are surrounded by a hypofluorescent halo in the late phase of ICGA.^{63, 92, 104} Possible CNV on ophthalmoscopy and SD-OCT may be confirmed on FA and ICGA.

4.1.1.6 Optical coherence tomography

The small radial drusen on SD-OCT correspond to irregular slight thickening of the RPE/Bruch's membrane complex and/or 'sawtooth RPE elevation' (**Figure 2.2D**).⁹² The large round drusen correspond to focal dome-shaped or more diffuse deposition of hyperreflective material between the RPE and Bruch's membrane within the macular and peripapillary area (**Figure 2.2E**).⁹² SD-OCT also shows confluence of large focal drusen over time.⁹² Large

drusen may be associated with a relative preservation of the overlying neurosensory retina and may be compatible with relatively spared visual acuity.¹¹¹

4.1.1.7 Psychophysical and electrophysiological testing

The EOG is normal in ML, suggesting that the disease does not lead to a diffusely dysfunctional RPE.^{102, 107} Multifocal ERG abnormalities localized to the macular region may be recorded only in patients with advanced disease.^{102, 107, 112} The full-field ERG is generally normal, but the 30-Hz flicker responses may be reduced.^{102, 105, 107} Visual fields are normal or show loss of sensitivity of the central visual field.^{102, 106, 112}

4.1.1.8 Genetic association

ML and Doyme honeycomb retinal dystrophy were considered separate entities until a single autosomal-dominantly inherited mutation (p.Arg345Trp) in the *EFEMP1* gene, also known as *fibulin-3*, was identified in both conditions.^{101, 102, 113}

4.1.1.9 Pathophysiology

Histopathological studies of ML demonstrate drusenoid deposits between the RPE and Bruch's membrane with thickening of Bruch's membrane, atrophy of the RPE and structural damage to rod and cone photoreceptors.^{114, 115} The *EFEMP1* gene encodes fibulin-3, an extracellular matrix protein.^{108, 116} *Efemp1 Arg345Trp* mutation knock-in mice studies have shown aberrant EFEMP1/fibulin-3 and Tissue Inhibitor of Metalloproteinase 3 (TIMP3) protein accumulation within RPE cells and between the RPE and Bruch's membrane.^{117, 118} In this mouse model of ML, sub-RPE drusen-like deposits, RPE abnormalities, and complement activation in the RPE and Bruch's membrane are seen.^{118, 119} These findings in ML show that there is not only a clinical overlap, but also a pathophysiological overlap with AMD.

4.1.1.10 Differential diagnosis with age-related macular degeneration

ML may be confused with AMD because of:

- the presence of drusen and possible evolution to GA and CNV.^{102, 108}

Features that help to distinguish ML from AMD:

- an earlier age at onset
- a positive family history with an autosomal-dominant inheritance pattern
- the presence of drusen localized nasal of the disc and the presence of typical radially oriented macular drusen, which can evolve to large densely packed and confluent drusen in later stages, often with nodular juxtapapillary drusenoid lesions
- genetic analysis revealing a mutation in the *EFEMP1* gene



4.1.2 Sorsby fundus dystrophy

4.1.2.1 Introduction

Sorsby fundus dystrophy (SFD) is an autosomal-dominantly inherited retinal dystrophy, leading to bilateral loss of central vision secondary to CNV, pigment epithelial atrophy, or both at the macula.¹²⁰⁻¹²³ Also, the peripheral vision may be severely affected.¹²³ SFD is exceptional among the inherited retinal dystrophies mimicking AMD in that subretinal neovascularization is characteristic of the disease, whereas CNV only occurs rarely in other macular dystrophies.⁹⁰

4.1.2.2 Clinical characteristics

The majority of SFD cases present during the fourth to fifth decades of life, but with a broad range of age at onset up to the eighth decade.^{121, 124, 125} A large clinical variability is possible both within and between affected families, with regard to age at onset, disease progression and fundus appearance.^{120, 121, 126} In their early 40s, more than half of the patients have difficulties with dark adaptation as an early symptom without other visual symptoms.^{91, 127} Nyctalopia is the result of peripheral retinal dysfunction,^{120, 121, 128} which can eventually lead to progressive loss of peripheral vision.¹²⁹ Some patients remain asymptomatic until the onset of central vision loss, often in the 4th-6th decade of life, because of CNV or GA of the macula.^{91, 121, 124} In approximately 60% of patients, a CNV with rapid vision loss develops in at least one eye in the fifth decade of life, and 50% of the patients develop CNV in the second eye within a few years after the onset of CNV in the first eye.¹²¹ SFD usually leads to legal blindness in the 5th-7th decade because of marked central and peripheral vision loss.^{90, 122, 124, 128}

4.1.2.3 Ophthalmoscopic features

The first ophthalmoscopic findings are subretinal, fine, yellow drusen-like deposits, located in the entire posterior pole with extension to the equator (**Figure 2.2F**).^{121, 124} These deposits often appear after the age of twenty, with preservation of visual acuity.^{121, 124} Within a few years after the first symptoms, pigmentary changes, chorioretinal atrophy, and CNV can appear in the macula (**Figure 2.2F**), resulting in a more rapid loss of central vision.^{91, 124, 128, 129} Patients can also develop extensive and extrafoveal CNV in the macula.¹²¹ After the age of 60, extensive and peripheral chorioretinal atrophy can develop, together with a central disciform scar and atrophy that is indistinguishable from AMD.^{49, 121, 123, 124, 128}

4.1.2.4 Fundus autofluorescence

The yellow deposits on ophthalmoscopy correspond to reduced FAF, unlike drusen in AMD and yellowish deposits in most other macular dystrophies.^{109, 120, 130} Areas of stippled increased and decreased autofluorescence extend toward and sometimes beyond the vascular arcades corresponding to the areas of subretinal fluid.¹²⁰ In the late stage, FAF shows bilateral areas of central confluent decreased autofluorescence corresponding to

the areas of RPE atrophy, with hyperautofluorescent borders surrounding these atrophic areas.¹²⁰

4.1.2.5 Fluorescein and indocyanine green angiography

The earliest phenotypic marker of SFD is a delayed filling of the choriocapillaris on FA.^{91, 124} This patchy hypofluorescence may be a typical finding before the onset of CNV and becomes more profound and extend centrifugally with time.^{121, 124} The deposits in SFD are not markedly hyperfluorescent in contrast to AMD and cuticular drusen. In SFD, hyperfluorescent CNV can develop multifocally with multiple recurrences, and classic CNV is more frequent than in AMD.^{121, 129} ICGA can show early mottling and late hyperfluorescence in the peripheral retina.¹³¹

4.1.2.6 Optical coherence tomography

SD-OCT images demonstrate focal hyperreflectivity of the ellipsoid zone to the choroid layer which may represent the thickened Bruch's membrane.¹²⁰ In early stages, SD-OCT can show evidence of retinal atrophy, specifically loss of the outer nuclear layer in the perifoveal region.¹²⁰ This finding may represent early morphological changes related to the symptoms of night blindness.¹²⁰ In cases with CNV, SD-OCT can show subretinal and/or intraretinal fluid before clinical or angiographic evidence of CNV.^{91, 120, 121}

4.1.2.7 Psychophysical and electrophysiological testing

Even early in the course of the disease, EOG results show an abnormally low light rise in most SFD cases,^{128, 132} indicating a generalized RPE dysfunction. Full-field ERG results remain normal until extensive and peripheral chorioretinal atrophy become apparent.^{90, 128, 131, 132} In the early stage of SFD, a tritanomaly may be present^{126, 128, 131} with prolonged dark adaptation times in patients with nyctalopia.¹²⁸ Visual field testing may show (para)central scotoma and moderate peripheral constriction.^{90, 128, 131}

4.1.2.8 Genetic association

SFD is an autosomal-dominantly inherited fundus dystrophy with full penetrance and variable expression.^{120, 133} Several mutations in the *TIMP3* gene are associated with SFD, of which p.Ser181Cys is the most common mutation.^{134, 135} The onset and severity of SFD appears to depend roughly on the specific *TIMP3* mutation.¹³⁴

4.1.2.9 Pathophysiology

TIMP3 protein is secreted by the RPE and deposited into Bruch's membrane.¹³⁶ TIMP3 has various functions: it regulates extracellular matrix remodelling by modulating matrix metalloproteinase activity, it inhibits angiogenesis by blocking vascular endothelial growth factor (VEGF) receptors, and it regulates inflammation.^{136, 137} SFD is thought to be caused by an accumulation of abnormal TIMP3 protein, leading to a thickened and dysfunctional

Bruch's membrane.^{138, 139} This TIMP3 accumulation inhibits transport across Bruch's membrane, either by inhibiting normal turnover of the extracellular matrix or by creating a direct physical barrier.^{134, 139} Such a barrier would impair retinal nutrition, leading to atrophy of the RPE and photoreceptor death. Neovascularization may be a secondary response to retinal malnutrition, hypoxia, and VEGF upregulation.^{129, 137, 139} The clinically observed yellowish deposits in SFD are localized between the basement membrane of the RPE and the inner collagenous layer of Bruch's membrane^{127, 140} and are strongly positive for TIMP3 protein.¹⁴⁰

4.1.2.10 Differential diagnosis with age-related macular degeneration

SFD may be confused with AMD because of:

- the overlap in age at onset
- the presence of drusen-like deposits, pigmentary changes, GA and CNV

Features that help to distinguish SFD from AMD:

- a positive family history with an autosomal-dominant inheritance pattern
- the earlier age at the onset of complaints and fundoscopic findings
- delayed choroidal filling on FA
- extramacular chorioretinal atrophy and CNV
- genetic analysis revealing a mutation in the TIMP3 gene

4.1.3 North Carolina macular dystrophy

4.1.3.1 Introduction

North Carolina macular dystrophy (NCMD) is an autosomal-dominantly inherited macular dystrophy which was initially described in 1971 in a large family in North Carolina, USA.¹⁴¹

4.1.3.2 Clinical characteristics

The onset of NCMD is in early childhood and it has a stable course.^{142, 143} In most cases, there are only minor changes in clinical appearance or visual acuity over time.¹⁴⁴⁻¹⁴⁶ The visual acuity is often better than expected from the clinical examination and does not correlate significantly to the grade of the disease or to the age of the patient.^{143, 147, 148} Patients may be largely asymptomatic unless they develop CNV⁴⁹, which is rare. Atrophic lesions can result in vision loss, but even in those cases the visual acuity may be relatively preserved as a result of eccentric fixation.^{146, 149}

4.1.3.3 Ophthalmoscopic features

The phenotype is highly variable and can be subdivided in 3 grades.^{142, 145} In grade 1, fine small yellow drusen-like lesions and pigmentary changes may be observed in the central macula with relatively preserved visual acuity.⁴⁹ The yellow lesions that seem to be located at the level of the RPE, can have a radial pattern, and can also be present in the peripheral retina.^{49, 142, 145, 146} In grade 2, patients show larger, confluent macular lesions with or without



RPE atrophy, which can be associated with some visual impairment. Grade 3 NCMD is characterized by larger areas of profound chorioretinal atrophy in the macula that may even resemble a coloboma or staphyloma, with hyperpigmentation and drusen-like lesions surrounding this atrophic lesion (**Figure 2.2H**). Occasionally, NCMD is complicated by CNV resulting in a markedly central vision loss.^{142, 146}

4.1.3.4 Fundus autofluorescence

The small drusen-like yellowish lesions in NCMD patients are hyperautofluorescent.¹⁴⁷ Markedly atrophic areas on ophthalmoscopy correspond to absent autofluorescence with a hyperautofluorescent surrounding border of the lesion (**Figure 2.2I**).¹⁴⁶

4.1.3.5 Fluorescein angiography

In grade 1 and 2 NCMD, FA shows transmission defects with hyperfluorescence of the drusen-like lesions both in the early and late phases of FA.⁴⁹ In grade 3 disease, the FA highlights the remaining choroidal vessels in the atrophic area due to the RPE window defect.

4.1.3.6 Optical coherence tomography

On SD-OCT, a thickening of the ellipsoid zone to the RPE layer can be present,¹⁴⁷ but no clear accumulation of material between the RPE and Bruch's membrane is present, in contrast to drusen in AMD.^{147, 150} In grade 3 disease, SD-OCT shows a marked thinning and atrophy of the neurosensory retina, RPE, and choroid, but intact photoreceptors adjacent to the lesion (**Figure 2.2J**).^{144, 146, 150}

4.1.3.7 Psychophysical and electrophysiological testing

The EOG and full-field ERG are normal in all stages, indicating that there is both no generalised retinal or RPE dysfunction.¹⁴⁹ The multifocal ERG can show decreased amplitudes within fundoscopically visible lesions in the macular area.¹⁴⁴ Color vision is relatively well-preserved.^{147, 149}

4.1.3.8 Genetic association

NCMD is an autosomal-dominantly inherited disorder,¹⁴¹ linked to the *MCDR1* locus on chromosome 6q16,^{151, 152} but the exact gene and its function are currently unknown. An early-onset autosomal-dominant macular dystrophy (*MCDR3*) resembling NCMD has been mapped to chromosome 5.^{147, 153}

4.1.3.9 Pathophysiology

The pathogenesis of NCMD is unknown. Histopathological studies in eyes with markedly atrophic NCMD lesions have shown a complete loss of photoreceptors and RPE, attenuation of Bruch's membrane, and choroidal atrophy.^{154, 155} Adjacent to the central lesion, lipofuscin accumulation has been identified in the RPE.^{154, 155}

4.1.3.10 Differential diagnosis with age-related macular degeneration

NCMD can be confused with AMD because of:

- the association with yellow drusen-like lesions, GA and CNV

Features that help to distinguish NCMD from AMD include:

- an early age at the onset (in childhood or possibly congenital)
- a positive family history with an autosomal-dominant inheritance pattern, and Irish-American ancestry
- a relatively stationary course, except in rare cases of CNV
- no sub-RPE deposits visible on SD-OCT

4.1.4 Late-onset retinal degeneration

4.1.4.1 Introduction

Late-onset retinal degeneration (LORD) is an autosomal-dominantly inherited macular dystrophy, first described in patients with Scottish ancestry.^{156, 157}

4.1.4.2 Symptoms

Patients with LORD usually present with night blindness in the fifth to sixth decade of life,^{156, 158, 159} followed by progressive central and peripheral vision loss in the following decades.^{156, 158, 159}

4.1.4.3 Clinical features

Patients with LORD typically have long anteriorly inserted lens zonules and peripupillary iris atrophy (**Figure 2.2K and L**).^{156, 160} Fundoscopic changes become visible from the fifth decade onwards, together with the onset of night blindness, with drusenoid deposits in the mid-peripheral retina often being the first visible retinal manifestations (**Figure 2.2M**).^{156, 160} In the following decades, scalloped areas of chorioretinal atrophy in the posterior pole and beyond the vascular arcades develop.^{158, 159} When this atrophy affects the fovea, this results in marked central vision loss. In the late stages of the disease, peripheral bone-spicule hyperpigmentation as well as central or peripheral CNV may develop.^{156, 158, 159}

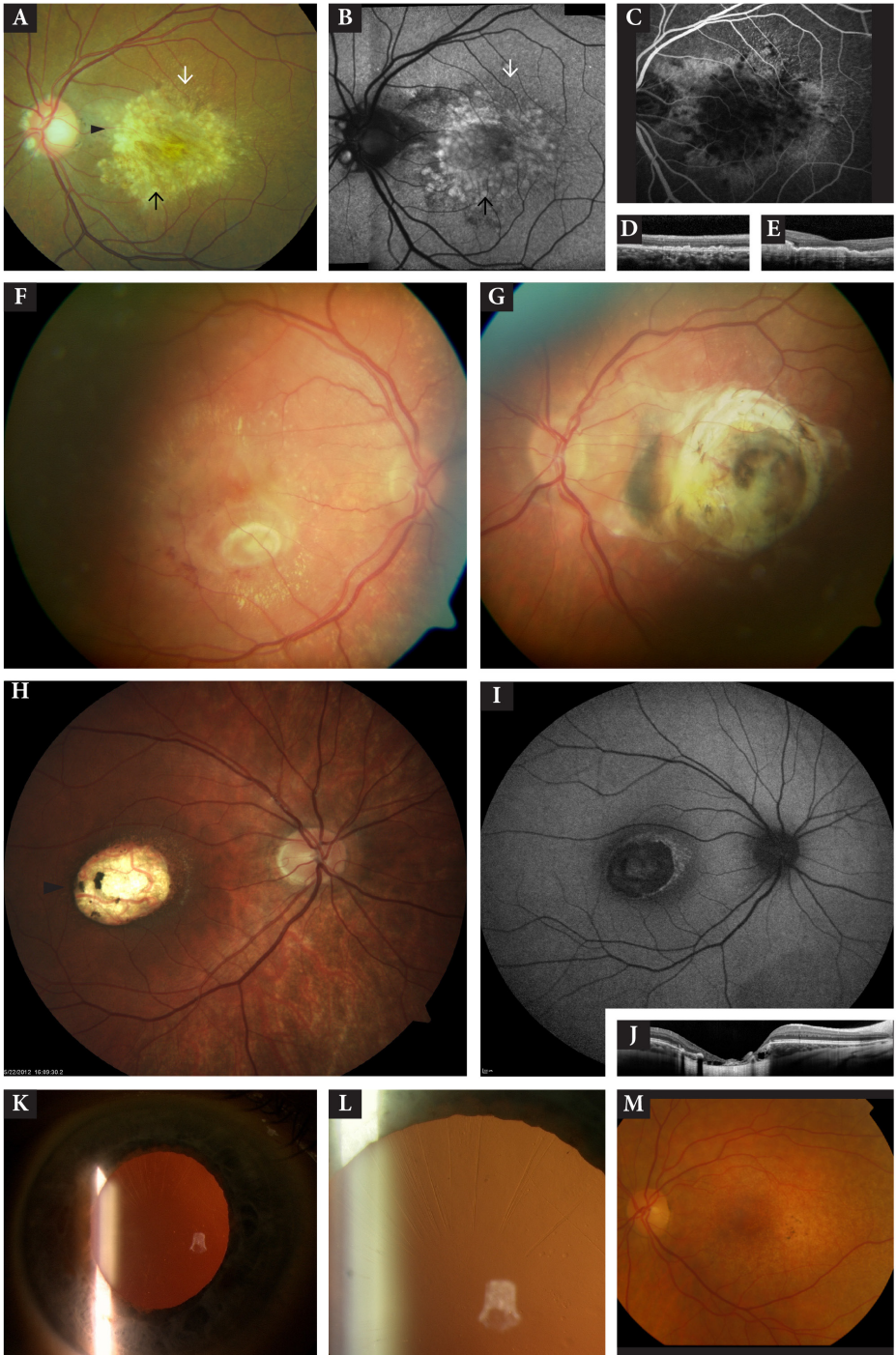
4.1.4.4 Fundus autofluorescence

The early drusenoid yellow dots in the retina may show increased FAF.¹⁵⁶ FAF highlights marked autofluorescence changes in macular atrophy by decreased autofluorescence with scalloped borders.^{159, 160}

4.1.4.5 Fluorescein angiography

The fine structure and staining characteristics of the sub-RPE deposits in early LORD may resemble those in AMD, and in advanced disease FA shows RPE window defects of the scalloped atrophic lesions.^{49, 158}





► **Figure 2.2 (A-E)** Malattia Leventinese in a 51-year-old patient who carried an EFEMP1 mutation. **(A)** Color fundus photograph showing small radiating drusen (white arrow) and larger confluent drusen in the macular area (black arrow) and around the optic disc. Centrally located large drusen confluence to a yellow-white plaque. **(B)** Fundus autofluorescence (FAF) image showing that large drusen located in the macula (black arrow) and drusenoid lesions nasally in the optic disc correspond to increased FAF, whereas the small radial drusen (white arrow) are faintly visible. **(C)** Fluorescein angiography (FA) image showing blockage of background fluorescence caused by the central large drusen and small hyperfluorescent radially oriented drusen. **(D)** Horizontal optical coherence tomography (OCT) scan showing the sawtooth elevations of the retinal pigment epithelium (RPE) corresponding to the small radial drusen. **(E)** Horizontal OCT scan (scan in the plane indicated by black arrowhead in **A**), showing diffuse deposition of hyperreflective material between the RPE and Bruch's membrane, corresponding to large round drusen. **(F-G)** Sorsby fundus dystrophy (Courtesy of SM Downes). **(F)** Color fundus photograph showing typical drusen along the arcade with a central choroidal neovascular complex. **(G)** Color fundus photograph showing poor response to previous photodynamic therapy. **(H-J)** North Carolina macular dystrophy stage 3 in a 19-year-old patient (Courtesy of Alessandro Iannaccone, MD, MS, Retinal Degeneration & Ophthalmic Genetics Service, Hamilton Eye Institute, University of Tennessee Health Science Center, Memphis, TN, USA). **(H)** Color fundus photograph showing a large circumscribed area of chorioretinal atrophy in the macula, with surrounding drusen-like lesions. **(I)** FAF image showing decreased autofluorescent in the atrophic lesion with a hyperautofluorescent surrounding edge of the lesion. **(J)** OCT scan (scan in the plane indicated by black arrowhead in **H**) showing atrophy of the neurosensory retina, RPE, and choroid, but intact photoreceptors adjacent to the lesion. **(K-M)** Late onset retinal dystrophy in an 82-year-old patient who carried the p.Ser163Arg mutation in the C1QTNF5 gene (Courtesy of Moorfields Eye Hospital). **(K)** Slit lamp examination showing long anteriorly inserted lens zonules and peripupillary atrophy. **(L)** An enlarged view of slit lamp examination image **K** clearly showing long anteriorly inserted lens zonules. **(M)** Color fundus photograph showing small drusenoid deposits in the posterior pole with some pigmentary changes.

4.1.4.6 Optical coherence tomography

Midreflective deposits located between the RPE and Bruch's membrane may be seen on SD-OCT. ¹⁵⁸⁻¹⁶⁰ In advanced cases, SD-OCT shows chorioretinal atrophy with also outer retinal abnormalities. ^{156, 159, 160}

4.1.4.7 Psychophysical and electrophysiological testing

Abnormal dark adaptation is the first manifestation of LORD, preceding subjective night blindness and fundus changes. ^{156, 158} The full-field ERG may become abnormal in advanced disease, ^{158, 160} revealing a generalized rod-cone dysfunction. ^{157, 159} In advanced LORD, the peripheral visual field also becomes constricted. ^{49, 156, 158}

4.1.4.8 Genetic association

LORD is a genetically heterogeneous disease with an autosomal-dominant inheritance pattern ^{157, 161} caused by a heterozygous p.Ser163Arg founder mutation in the C1QTNF5 gene on chromosome 11. ¹⁶¹ This mutation presumably originates from a single ancestor from south-east Scotland. ¹⁵⁶

4.1.4.9 Pathophysiology

Histopathological studies reveal loss of photoreceptors and extensive sub-RPE deposits, resembling AMD drusen in structure and lipid composition.^{157,158} Although a *C1qtnf5* knock-in mouse model closely mimics the phenotypic features of LORD,¹⁶² the exact function of the *C1QTNF5* gene is unknown. The *C1QTNF5* is highly expressed in the RPE, lens and ciliary body epithelium.¹⁶¹ Deposits may be caused by misfolded C1QTNF5 protein accumulating in the endoplasmic reticulum of the RPE, compromising the function of the RPE and resulting in sub-RPE deposits as well as impaired RPE adhesion to Bruch's membrane.^{161,163}

4.1.4.10 Differential diagnosis with age-related macular degeneration

LORD may be confused with AMD because of:

- the presence of drusenoid deposits, chorioretinal atrophy and sometimes CNV

Features that help to distinguish LORD from AMD include:

- an autosomal-dominant inheritance pattern
- onset of night vision problems before the age of 60
- extensive 'scalloped' areas of chorioretinal atrophy
- long anteriorly inserted lens zonules and peripupillary iris transillumination
- evidence of widespread retinal disease on dark adaptation and full-field ERG in advanced LORD
- mutation in the *C1QTNF5* gene

4.2 Irregular yellowish flecks

4.2.1 Late-onset Stargardt disease

4.2.1.1 Introduction

Autosomal-recessive Stargardt disease is a hereditary retinal dystrophy, usually diagnosed within the first two decades of life.¹⁶⁴ A later age at onset (≥ 50 years) has been reported in a small number of patients. Late-onset Stargardt disease belongs to the spectrum of retinal dystrophies caused by mutations in the *ABCA4* gene.⁸⁸ The estimated carrier frequency of mild *ABCA4* mutations in population studies is 1/25 individuals.^{165,166} Over 600 disease-causing mutations in the *ABCA4* gene have been identified and some *ABCA4* mutations have been associated with STGD1, cone-rod dystrophy, retinitis pigmentosa and AMD.⁹⁹

4.2.1.2 Clinical characteristics

Usually at the age of 55 patients present with progressive central vision loss and may be accompanied by metamorphopsia or oscillopsia.⁸⁸ The fundus abnormalities, however, may be coincidentally found in asymptomatic patients at ophthalmologic screening for glaucoma, diabetes or thyroid eye disease.

4.2.1.3 Ophthalmoscopic features

Fundus examination shows irregular, pisciform, flavimaculatus flecks scattered throughout the posterior pole or spread to the midperipheral retina (**Figure 2.3A**). Yellowish flecks or dots may be limited to the centre of the macula, whereas sometimes no flecks, but small yellowish spots are present in the macula. Extensive chorioretinal atrophy may be present and it is rarely complicated by CNV.¹⁶⁷⁻¹⁶⁹

4.2.1.4 Fundus autofluorescence

The yellowish flecks correspond to intense autofluorescence on FAF imaging (**Figure 2.3B**).⁸⁸ Some flecks may be surrounded by a halo of reduced autofluorescence. In up to 50% of the cases, a relatively preserved autofluorescence signal of the fovea is seen, indicating foveal spare. This difference in autofluorescence signal and degree of foveal sparing corresponded with structural findings on SD-OCT.

4.2.1.5 Fluorescein angiography

A decreased choroidal background fluorescence ('dark choroid') on FA is present in about 80% of the patients (**Figure 2.3C**).⁸⁸ In rare cases, CNV is visible by focal staining and leakage of dye in respectively the early and late phase.¹⁶⁹

4.2.1.6 Optical coherence tomography

SD-OCT shows hyperreflective thickening of the RPE layer in Stargardt disease, which is distinguishing from sub-RPE drusen in AMD (**Figure 2.3D**). The accumulation in Stargardt disease is usually associated with photoreceptor thinning.⁸⁸ In cases of foveal sparing, a near normal photoreceptor layer in the fovea may be observed explaining the late onset of visual complaints.

4.2.1.7 Psychophysical and electrophysiological testing

Photopic and scotopic full-field ERG recordings are normal in the majority of cases.⁸⁸ In contrast, multifocal ERG is in the majority of cases outside normal limits. Patients with foveal sparing have normal multifocal ERG amplitudes in the foveal area. Central visual field examinations show paracentral scotomata and central scotoma of varying extensions.

4.2.1.8 Genetic association

Homozygous or compound heterozygous mutations in the *ABCA4* gene encoding the photoreceptor-specific, ATP-binding cassette transporter A4 are responsible for STGD.¹⁷⁰ In half of the late-onset Stargardt disease patients, only one heterozygous mutation in the *ABCA4* gene may be found.^{88, 171} It is possible that the latter patients carry a second mild mutation in one of the introns or they may carry variants in modifier genes or a variant in a promoter or enhancer region near the *ABCA4* gene, which causes lower expression of the intact *ABCA4* allele.



4.2.1.9 Pathophysiology

ABCA4 defects lead to the intracellular accumulation of N-retinylidene-N-retinylethanolamine (A2E) in RPE cells.^{172, 173} A2E is cytotoxic to the RPE in high concentrations¹⁷⁴ and may be visualized in living eyes using FAF. In heterozygous *abca4* (+/-) mice, a light-dependent fourfold increase in lipofuscin compounds has been observed.¹⁷⁵ These findings in animal studies may indicate that heterozygous *ABCA4* mutations in humans eventually also lead to increased lipofuscin accumulation and possibly even retinal pathology. A study in the *Abca4* knockout mouse model for Stargardt disease has identified oxidative stress, complement activation, and down-regulation of protective complement regulatory proteins as potential mechanism of retinal dystrophy.¹⁷⁶ These animal data and the association of *ABCA4* variants with AMD could indicate that there is a pathophysiologic overlap between late-onset Stargardt disease and AMD.

4.2.1.10 Differential diagnosis with age-related macular degeneration

It is important to distinguish late-onset Stargardt disease from AMD because some AMD patients use nutritional supplements, containing the vitamin A-derivative beta-carotene, to prevent progression to advanced disease.¹⁷⁷ However, studies in *Abca4* knockout mice, an animal model for Stargardt disease, have shown that vitamin A supplementation can cause an increase of lipofuscin accumulation in the RPE.¹⁷⁸ Therefore, beta-carotene or vitamin A supplementation should be discouraged in Stargardt disease patients as it may accelerate lipofuscin accumulation and retinal degeneration.

Late-onset Stargardt disease may be confused with AMD because of:

- the late age at onset (>50 years)
- the presence of yellowish flecks, chorioretinal atrophy and rarely CNV

Features that help to distinguish late-onset Stargardt disease from AMD include:

- 'flavimaculatus' flecks are more irregularly shaped than drusen
- intense autofluorescence of flecks on FAF imaging with a surrounding halo of decreased FAF.
- 'dark choroid' on FA
- mutations in the *ABCA4* gene

4.2.2 Pattern dystrophies

4.2.2.1 Introduction

The heterogeneous group of 'pattern dystrophies' encompass a broad spectrum of inherited diseases that are characterized by various patterns of pigment distribution at the posterior pole. These include butterfly-shaped pigment dystrophy, adult-onset foveomacular vitelliform dystrophy (AFVD) (see **Chapter 4.3.1.**), reticular dystrophy of the RPE, fundus pulverulentus and pseudo-Stargardt pattern dystrophy. However, the value of this clinical classification is subject of debate,¹⁷⁹ because different types of pattern dystrophy are known to occur in different members of the same family carrying an identical mutation.

Furthermore, one form of pattern dystrophy can evolve into another within a single patient, and the type of pattern dystrophy can even be different between the two eyes of a patient.

49, 89, 100, 180, 181

4.2.2.2 Clinical characteristics

Pattern dystrophies present in midlife with mild central visual disturbances in one or both eyes. In advanced cases, patients can develop CNV and/or GA. However, many patients will retain driving vision in at least one eye well into their seventh decade of life.¹⁸²

4.2.2.3 Ophthalmoscopic features

Butterfly-shaped pigment dystrophy has first been described by Deutman and co-workers in a family with autosomal-dominant inherited pigmentation in a pattern that showed resemblance to the wings of a butterfly.¹⁸³ The pigmentation can be yellow-white or dark. The central lesion can be surrounded by depigmentation.

Reticular dystrophy of the RPE was first reported in 1950 by Sjögren as a clearly defined network of pigmented lines that resemble a fishnet with knots.¹⁸⁴

Fundus pulverulentus is characterized by coarse, punctiform mottling of the RPE in the macular area.¹⁸⁵ This rare entity is seen mostly in patients with macular dystrophy associated with PXE (for pseudoxanthoma elasticum see **Chapter 4.5.2**).¹⁸⁶

Patients with pseudo-Stargardt pattern dystrophy show irregular yellowish flecks in the posterior pole and around the retinal vascular arcades, resembling the flecks seen in fundus flavimaculatus phenotype of Stargardt disease (**Figure 2.3E**). The yellowish flecks are preceded by typical macular pattern dystrophy or by non-specific pigmentary changes in the fovea.^{89, 187}

4.2.2.4 Fundus autofluorescence

Like in most macular dystrophies, the pattern dystrophies have variable patterns of markedly abnormal autofluorescence. In pseudo-Stargardt pattern dystrophy the flecks show highly increased autofluorescence (**Figure 2.3F**). With time, the flecks tend to evolve toward a confluent atrophic area which shows larger zones of decreased FAF signal.

4.2.2.5 Fluorescein angiography

The pigmented areas in the pattern dystrophies usually show early hypofluorescence on FA, surrounded by hyperfluorescence, with some degree of late staining.^{100, 188} In pseudo-Stargardt pattern dystrophy the flecks are hyperfluorescent, sometimes with a central hypofluorescent spot (**Figure 2.3G**).^{89, 187} A dark choroid, as seen in Stargardt disease, is typically absent.



4.2.2.6 Optical coherence tomography

SD-OCT imaging reveals relatively consistent features among the different subtypes of pattern dystrophies:¹⁸⁹ hyperreflectivity between the RPE/Bruch's membrane complex and more inner retinal layers (**Figure 2.3H**); further, disruptions of the ellipsoid zone are common findings.¹⁸⁹

4.2.2.7 Psychophysical and electrophysiological testing

Full-field ERG shows normal cone and rod amplitudes and implicit times in most patients with pattern dystrophies, except in pseudo-Stargardt pattern dystrophy. Herein, the full-field photopic and scotopic ERG results can vary from normal in mild cases to non-recordable in advanced disease, and the EOG is abnormal in half of the patients.⁸⁹

The EOG in pattern dystrophies is usually normal or only moderately reduced.¹⁹⁰

4.2.2.8 Genetic association

Mutations in the *PRPH2* gene are the most common cause of the different pattern dystrophies. Recently, an association of AFVD and butterfly-shaped pigment dystrophy phenotypes has been suggested with a *high temperature requirement factor A1* risk SNP in individuals who did not carry *PRPH2* gene mutations.¹⁹¹

4.2.2.9 Pathophysiology

The *PRPH2* gene encodes a photoreceptor-specific glycoprotein that plays a role in the development and maintenance of photoreceptor outer segment discs.^{100, 192-194} Mutation in *PRPH2* could mediate pattern dystrophy disease pathogenesis by interfering with the integrity of the photoreceptor membrane.¹⁹⁵

Further, secondary atrophic changes were observed.¹⁹⁶ In a patient with butterfly-shaped pigment dystrophy due to mutation in the *PRPH2* gene, there was an abrupt transition between healthy and degenerated retina and RPE with massively lipofuscin-laden RPE cells at the transition.¹⁹⁵ Surgical specimens from a patient with a *PRPH2* mutation exhibited ultra-structural alterations in outer-segment disc structure.¹⁹⁷ Based on these genetic and histopathologic findings, the primary defect in pattern dystrophies may be assumed to be localized in the photoreceptors with subsequent changes in the RPE and choriocapillaris.

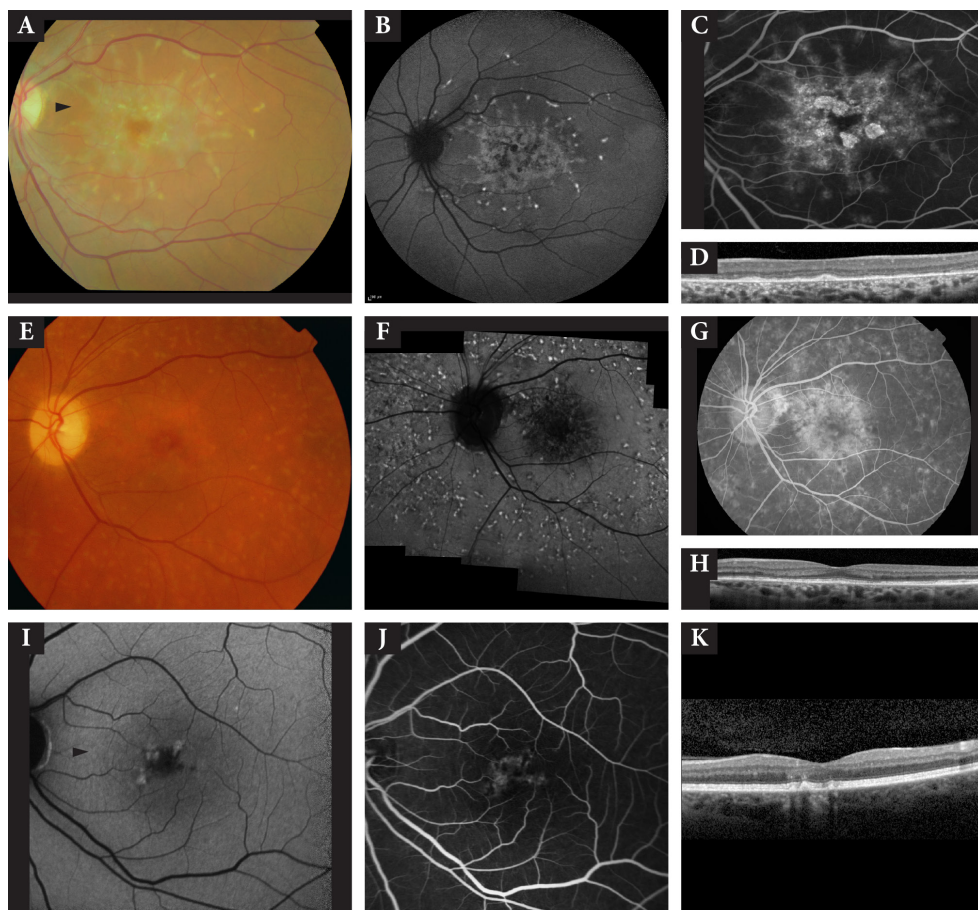


Figure 2.3 (A-D) Late-onset Stargardt in a 58-year-old patient. (A) Color fundus photograph showing irregular, pisciform, flavimaculatus flecks in the posterior pole and central irregularities of the retinal pigment epithelium. (B) Fundus autofluorescence (FAF) image showing increased autofluorescence of the flecks. (C) Fluorescein angiography (FA) image showing decreased choroidal background fluorescence causing a 'dark choroid' aspect and hyperfluorescent flecks. (D) Horizontal optical coherence tomography (OCT) scan (scan in the plane indicated by black arrowhead in A) showing hyperreflective thickening of the retinal pigment epithelium (RPE) corresponding to the flecks. The RPE thickening is associated with thinning of the photoreceptor layer. (E-H) Pseudo-Stargardt pattern dystrophy in a 57-year-old patient. (E) Color fundus photograph showing irregular yellowish flecks in the posterior pole and around the vascular arcades. (F) FAF image showing increased autofluorescence of the flecks with an adjacent hypofluorescent zone, showing the 'dot and halo' feature with enlargement of the macular hypoauflorescent zone. (G) FA image showing hyperfluorescent flecks. (H) Horizontal OCT scan showing some hyperreflective focal thickening of the photoreceptor-RPE complex, but without sub-RPE deposits. (I-K) Pattern dystrophy in a 63-year-old patient who carried a mutation in the PRPH2 gene (Courtesy of J.R.M. Cruysberg, UMC St. Radboud). (I) FAF image showing increased autofluorescence of the hyperpigmentation. (J) FA image showing hyperfluorescence that outlines the hypofluorescent figures. (K) Horizontal OCT scan (scan in the plane indicated by black arrowhead in I) showing hyperreflective material between the RPE and Bruch's membrane.

4.2.2.10 Differential diagnosis with age-related macular degeneration

Patients with pattern dystrophies may be misdiagnosed as having AMD because:

- clinically visible signs commonly present in midlife and visual complaints may manifest later in life
- secondary changes such as CNV or GA may be present

Features that help to distinguish pattern dystrophies from AMD include:

- a relatively early age at onset
- positive family history
- absence of typical sub-RPE drusen
- more pronounced autofluorescence changes than in AMD (pseudo-Stargardt pattern dystrophy)
- specific patterns on fluorescein angiography and fundus autofluorescence
- peripheral retinal abnormalities with corresponding abnormal full-field ERG (pseudo-Stargardt pattern dystrophy)
- genetic analysis revealing a mutation in the PRPH2 gene

4.3 Vitelliform lesions

4.3.1 Adult-onset foveomacular vitelliform dystrophy

4.3.1.1 Introduction

Adult-onset foveomacular vitelliform dystrophy (AFVD) was first described by Gass in 1974. According to the classification of Gass, AFVD is considered one of the pattern dystrophies.⁴⁹

4.3.1.2 Clinical characteristics

Patients experience mild loss of visual acuity and/or metamorphopsia in one or both eyes, usually after the age of 35, but may also remain asymptomatic.

4.3.1.3 Ophthalmoscopic features

In typical AFVD, bilateral small round yellow-white lesions of less than 1/3 disc diameter are seen in the fovea, without surrounding drusen (**Figure 2.4A**).⁹⁴ The central part of the lesion can be mildly pigmented. Lesions in AFVD can go through stages that are similar to BVMD (**Chapter 4.3.2**),¹⁹⁸ and can be multifocal.¹⁹⁹ Some cases can be complicated by CNV, which can respond to anti-VEGF treatment.²⁰⁰

4.3.1.4 Fundus autofluorescence

Lesions in AFVD are hyperautofluorescent, especially when the lesions have a yellowish fundoscopic aspect without significant RPE atrophy (**Figure 2.4B**).^{94, 130}



4.3.1.5 Fluorescein angiography

FA typically shows a hypofluorescent centre of the lesion, surrounded by a small hyperfluorescent ring ('dot-and-halo' or 'solar eclipse' aspect). Some larger, less pigmented lesions may show a central, patchy hyperfluorescence with late staining (**Figure 2.4C**).

4.3.1.6 Optical coherence tomography

On SD-OCT, lesions are located between the neuroretina and RPE, with a variable amount of hyperreflective material accumulated in the space between these layers (**Figure 2.4D**).⁹³ This material corresponds to the yellowish material seen on fundoscopy. Based on their high-definition OCT findings in patients with different stages of AFVD, Querques and co-workers hypothesized that early changes involve the layer between the RPE and the ellipsoid zone, first with accumulation of material beneath the sensory retina. In advanced disease, the photoreceptors and RPE layer eventually become disrupted and attenuated.²⁰¹

4.3.1.7 Psychophysical and electrophysiological testing

A characteristic differential diagnostic feature to distinguish AFVD from BVMD is the presence of a normal or only slightly subnormal light rise on the EOG,⁹⁴ whereas this light rise on EOG is often virtually absent in Best disease. The full-field ERG is normal.

4.3.1.8 Genetic association

A genetic cause may be identified in a minority of cases.²⁰² Autosomal-dominant inheritance has been described, and mutations in the *PRPH2* gene account for 2-18% of the cases, whereas mutations in the *BEST1* gene cause up to 25% of cases.²⁰³⁻²⁰⁵

4.3.1.9 Pathophysiology

Histopathologic evaluation of patients with AFVD revealed an accumulation of vitelliform material between the neuroretina and RPE beneath the fovea, consisting of photoreceptor outer segment-derived material and lipofuscin loaded pigmented cells, accounting for the vitelliform appearance.^{67, 206, 207} Lipofuscin accumulation was also seen in the RPE, with focal atrophy of the RPE bordered by hypertrophic RPE.²⁰⁸

4.3.1.10 Differential diagnosis with age-related macular degeneration

AFVD can be confused with AMD because of:

- the presence of small, round yellow-white macular lesions that may be complicated by CNV

Features that help to distinguish AFVD from AMD include:

- central vitelliform lesion without surrounding drusen
- marked autofluorescence changes within AFVD lesions
- lesion corresponding to hyperreflective accumulation above the RPE on SD-OCT

4.3.2 Best vitelliform macular dystrophy

4.3.2.1 Introduction

Best vitelliform macular dystrophy (BVMD) was first described by Friedrich Best in 1905, and is an autosomal-dominantly inherited macular dystrophy with incomplete penetrance and variable expression.⁶⁷

4.3.2.2 Clinical characteristics

The age at the onset of central vision loss is highly variable, ranging from the first to the sixth decade.^{65, 199, 209-211} Most patients become symptomatic before the age of 40. A commonly associated finding is mild to moderate hyperopia.⁶⁷

4.3.2.3 Ophthalmoscopic features

In most classifications of BVMD, the first stage is the asymptomatic carrier ('previtelliform') stage.^{67, 209, 212} In this stage, no or very mild RPE abnormalities are visible in the fundus, although the EOG is already markedly abnormal. This stage may evolve into a typical yellowish, slightly elevated, round-to-oval vitelliform lesion in the fovea, usually with a size of at least a disc diameter (as mentioned in **Chapter 2** in drusenoid vitelliform lesions). When the vitelliform material gradually shows inhomogeneous clumping, this is referred to as the vitelliruptive or 'scrambled-egg' stage (**Figure 2.4E and 2.4I**). The vitelliform material may also gravitate to the inferior part of the lesion, which corresponds to the pseudohypopyon stage. With time, a variable degree of chorioretinal atrophy and subretinal scarring may develop, to form the atrophic and cicatricial stage, respectively. Many patients show a different stage in each eye, characteristics of different stages within a single lesion, and sometimes even multifocal vitelliform lesions.^{65, 199, 209} CNV occurs in 2-9% of patients with BVMD, which tends to show a relatively benign and self-limiting course,^{209, 210, 213} although CNV in these cases also responds to intravitreal anti-VEGF treatment.²¹⁴

4.3.2.4 Fundus autofluorescence

BVMD lesions show variably-sized areas of intense hyperautofluorescence, corresponding to the vitelliform material (**Figure 2.4F and J**)⁶⁵⁻⁶⁷ (as mentioned in **Chapter 2** in drusenoid vitelliform lesions). Areas of scarring and/or RPE atrophy within a lesion show decreased autofluorescence.

4.3.2.5 Fluorescein angiography

On FA, the early phases show blocking of background fluorescence in lesions with large amounts of vitelliform material (**Figure 2.4K**), but in other cases the BVMD lesions show mild hyperfluorescence due to an RPE window defect and/or staining (**Figure 2.4G**).^{65, 66}

4.3.2.6 Optical coherence tomography

Like in AFVD, early lesions in BVMD are located between the neuroretina and RPE on SD-OCT, with a variable amount of hyperreflective material accumulated in the space between these layers (**Figure 2.4L**).^{65, 66} In more advanced lesions, hyperreflective subretinal scars and intraretinal edema may be seen (**Figure 2.4H**).

4.3.2.7 Psychophysical and electrophysiological testing

A virtually pathognomonic feature for BVMD and other *BEST1*-gene related diseases is the absence of a normal light rise on the EOG, reflected in a markedly diminished Arden ratio.⁶⁷ This abnormal EOG also allows to detect asymptomatic carriers of a *BEST1* mutation.²¹⁵ The full-field ERG is normal.

4.3.2.8 Genetic association

BVMD, a member of the group of 'bestrophinopathies', is caused by autosomal-dominantly inherited mutations in the *BEST1* gene.^{67, 216} The *BEST1* gene encodes the bestrophin-1 protein, a calcium-activated chloride channel that also influences voltage-gated calcium channels within the RPE.⁶⁷ Patients with autosomal-recessive bestrophinopathy have more extensive retinal abnormalities and carry a *BEST1* mutation on both alleles.²¹⁷

4.3.2.9 Pathophysiology

The accumulation of subretinal fluid and vitelliform material - which supposedly originates from outer photoreceptor debris - has been postulated to be the result of RPE dysfunction due to abnormal RPE ionic transport.⁶⁷ The prolonged neuroretinal detachment and lipofuscin overload of the RPE may eventually lead to photoreceptor and RPE dysfunction.

4.3.2.10 Differential diagnosis with age-related macular degeneration

BVMD may be confused with AMD because of:

- the presence of yellowish lesion(s) with chorioretinal atrophy and CNV

Features that help to distinguish BVMD from AMD include:

- an age at the onset before the age of 50
- a positive family history with an autosomal-dominant inheritance pattern
- central vitelliform lesions without surrounding drusen
- marked autofluorescence changes within BVMD lesion
- lesions corresponding to hyperreflective accumulation above the RPE on SD-OCT
- a markedly abnormal EOG
- identification of a mutation in the *BEST1* gene



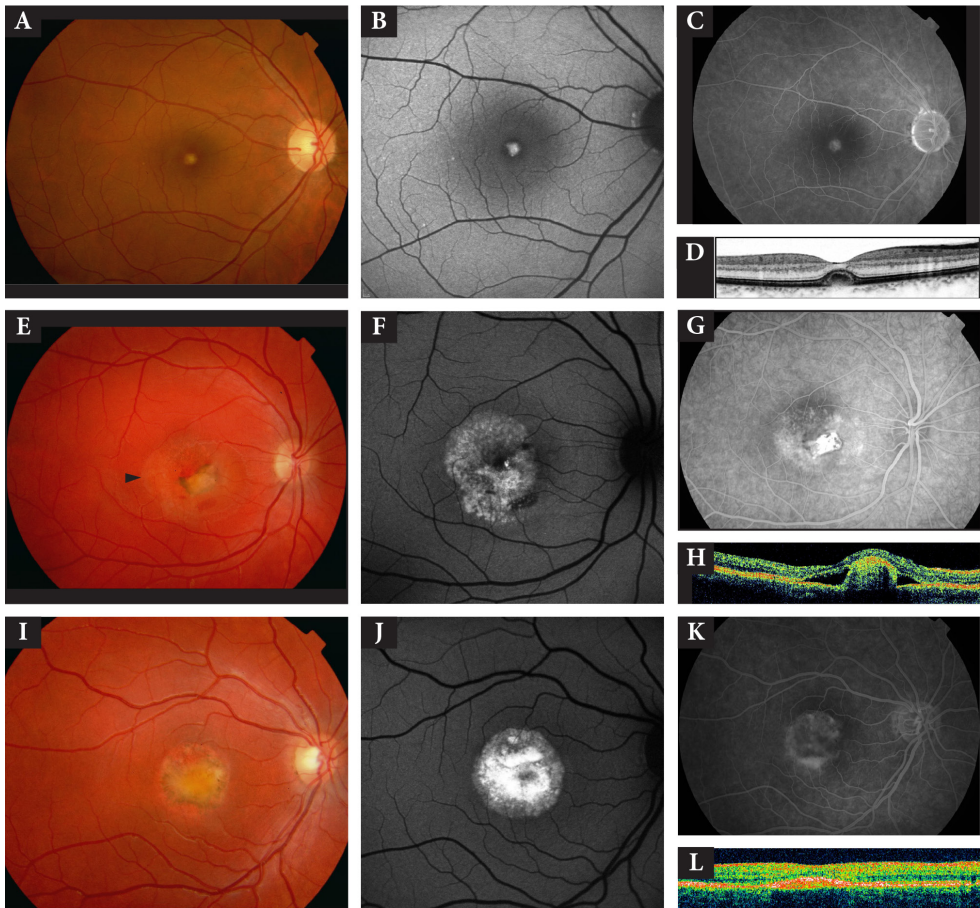


Figure 2.4 (A-D) Adult onset foveomacular vitelliform dystrophy in a 49-year-old patient who did not carry a mutation in the PRPH2 or BEST1 gene. (A) Color fundus photograph showing a round yellow lesion in the fovea with some small yellow lesions temporally in the fovea. (B) Fundus autofluorescence (FAF) image showing increased autofluorescence of the foveal round lesion and hyperautofluorescence of the smaller lesions temporally in the fovea. (C) Fluorescein angiography (FA) image showing late staining of the central lesion, as well as hyperfluorescence of some temporal small spots. (D) Horizontal optical coherence tomography (OCT) scan showing the foveal yellow lesion corresponding to accumulation of material between the neuroretina and the retinal pigment epithelium (RPE). (E-L) Best vitelliform macular dystrophy in a 15-year-old (E-H) and 13-year-old patient (I-L). (E) Color fundus photograph showing a scrambled-egg appearance with a fibrotic scar. (F) FAF image showing irregularly hyperautofluorescence of the yellow lesion in the macula. (G) FA image showing hyperfluorescence due to RPE window defects, as well as hypofluorescence caused by blocking of background fluorescence. (H) Horizontal OCT scan (scan in the plane indicated by black arrowhead in E) showing subretinal fibrous scar tissue associated with subretinal fluid. (I) Color fundus photograph showing a vitelliform/vitelliruptive lesion in the macular area. (J) FAF image showing intense hyperfluorescence of the subretinal material. (K) Two years later, the vitelliform/vitelliruptive stage has been evolved into the pseudohypopyon stage. FA image clearly shows hyperfluorescent material of the partly scrambled vitelliform lesion. (L) Vertical OCT scan showing hyperreflective material between the neuroretina and the RPE.

4.4 Miscellaneous

4.4.1 Central areolar choroidal dystrophy

4.4.1.1 Introduction

Central areolar choroidal dystrophy (CACD) is an autosomal-dominantly inherited macular dystrophy that belongs to the wide spectrum of retinal dystrophies caused by mutations in the *PRPH2* gene.¹⁰⁰ Other *PRPH2*-associated retinal dystrophies include multifocal pattern dystrophy simulating Stargardt disease/fundus flavimaculatus ('pseudo-Stargardt pattern dystrophy'),⁸⁹ pattern dystrophies such as butterfly-shaped pigment dystrophy and AFVD, as well as autosomal-dominant retinitis pigmentosa.¹⁰⁰

4.4.1.2 Clinical characteristics

The visual acuity in CACD generally deteriorates in the fourth to fifth decade of life,²¹⁸⁻²²⁰ which is earlier than in patients with AMD.²²¹ However, a later onset (after the age of 55) or even an absence of visual symptoms may be seen in up to a third of CACD patients, depending on the type of *PRPH2* mutation.^{100, 218} Therefore, late-onset CACD may be confused with atrophic AMD.^{218, 222} Visual disturbances are mainly associated with the development of GA, and marked central vision loss will eventually develop when the chorioretinal atrophy affects the fovea.²¹⁸ Besides loss of visual acuity and metamorphopsia, some CACD patients may experience mild photophobia.^{100, 218, 223} Nyctalopia is reported only rarely in CACD and seems to be associated with pigmentary changes of the peripheral retina.^{218, 223} A positive family history of vision loss is more common in CACD than in AMD.^{218, 221}

4.4.1.3 Ophthalmoscopic features

Four clinical stages of CACD have been described.^{100, 219, 220} In stage 1, fine parafoveal pigmentary RPE changes may be observed, usually under the age of 50 (**Figure 2.5A**).^{218, 224} In stage 2, an oval-to-round, mildly atrophic, hypopigmented area may be observed. Stage 3 is characterized by one or more patches of well-circumscribed RPE atrophy outside the fovea (**Figure 2.5E**). The areas of GA tend to enlarge concentrically and become confluent.^{220, 225, 226} In stage 4, the area of profound chorioretinal atrophy affects the fovea, resulting in a markedly decreased visual acuity. Patients with CACD usually do not have any flecks or drusen, but in some cases it is associated with drusen-like deposits,^{219, 225, 227} making the differential diagnosis with AMD more difficult.

4.4.1.4 Fundus autofluorescence

Like in most other macular dystrophies, marked FAF changes are a hallmark feature of CACD that distinguishes this disease entity from the more moderate FAF abnormalities in most cases of early AMD and GA in AMD.^{109, 218, 221} FAF abnormalities are more sharply demarcated, regularly oval-shaped and are confined to the central macular region, in contrast to AMD FAF abnormalities, which frequently covers the entire posterior fundus. In



early CACD, a speckled pattern of increased and decreased FAF signal predominates (**Figure 2.5B**).^{100, 221, 222} Areas of markedly decreased to absent FAF appear in stages 3 and 4 (**Figure 2.5F**).^{100, 218, 221, 222}

4.4.1.5 Fluorescein angiography

FA is helpful in detecting the earliest stage 1 abnormalities, showing pigmentary changes and small parafoveal window defects (**Figure 2.5C**).^{218, 220} In stage 2-4, hyperfluorescent window defects become more prominent.^{218, 219}

4.4.1.6 Optical coherence tomography

SD-OCT reveals reduced retinal thickness in CACD with a disruption of the ellipsoid zone of the photoreceptors, proportional to the degree of chorioretinal atrophy (**Figure 2.5D**).^{218, 221, 222} In contrast to AMD, sub-RPE deposits (drusen) are generally absent and rosette-like structures are more often present.²²¹ In eyes with atrophic lesions due to CACD, the remaining retinal layers have a relatively homogeneous aspect (**Figure 2.5G**), whereas eyes with GA due to AMD frequently have an irregular structure of the remaining retinal layers within the atrophic lesion on SD-OCT.²²¹

4.4.1.7 Psychophysical and electrophysiological testing

Tests of the macular function, such as the pattern ERG and multifocal ERG, as well as results from color vision testing usually become abnormal early in the course of CACD.^{220, 222, 223} The full-field ERG is generally normal, but may display generalized cone or cone-rod dysfunction in advanced CACD, depending on the associated *PRPH2* mutation^{100, 220, 223, 224}. The EOG is normal or slightly subnormal.²¹⁸⁻²²⁰ Early in the course visual fields are normal, but with disease progression a relative and eventually absolute paracentral scotoma may be demonstrated, corresponding to the area of advanced atrophy.^{219, 220, 222, 228} The peripheral visual field is normal.^{219, 224, 228}

4.4.1.8 Genetic association

In most cases, CACD has an autosomal-dominant inheritance pattern, caused by mutations in the *PRPH2* gene, although autosomal-recessive and sporadic cases have also been reported.^{100, 218}

4.4.1.9 Pathophysiology

Several histopathological studies on non-genotyped CACD patients have shown an absence of photoreceptors, RPE, and choriocapillaris in the area of atrophy.^{226, 229} Boon and co-workers have suggested that the abnormal peripherin/rds protein structure results in a dysmorphic cone and possibly rod outer segment structure.²¹⁸ These structural abnormalities hinder normal photoreceptor function and lead to alterations in the normal photoreceptor outer segment-RPE interaction. These changes may raise the level of

lipofuscin and toxic byproducts in the RPE cells, resulting in RPE and photoreceptor cell death through apoptosis. Atrophy of the RPE and choriocapillaris eventually lead to the typical ‘punched-out’ CACD lesions.²¹⁸ The term ‘central areolar choroidal dystrophy’ may, therefore, be a misnomer, as it suggests that the primary dystrophic focus is the choroid instead of the retina.

4.4.1.10 Differential diagnosis with age-related macular degeneration

CACD may be confused with atrophic AMD because of:

- the overlap in age at the onset (in late-onset CACD)
- the decreased penetrance and variable expression, that complicates recognition of the mode of inheritance²²³
- the association with drusen-like lesions, RPE changes, chorioretinal atrophy

Features that help to distinguish CACD from AMD:

- a relatively early onset
- a positive family history with an autosomal-dominant inheritance pattern
- absence of genuine drusen on ophthalmoscopy and SD-OCT
- more pronounced autofluorescence changes than in atrophic AMD
- genetic analysis revealing a mutation in the *PRPH2* gene

4.4.2 Late-onset cone dystrophy

4.4.2.1 Introduction

Clinical signs of cone dystrophies may develop progressively during all decades of life.²³⁰ Late onset, in the fourth^{231, 232} or even after the sixth decade,^{230, 231} however, is rare. Therefore, the diagnosis of cone dystrophy is not often considered in older patients.²³³ In addition, age-related morphological changes, such as pigment irregularities and drusen, may mask the correct diagnosis.²³³

4.4.2.2 Clinical characteristics

In cone dystrophy, patients suffer from progressive visual loss, central visual field defects, color vision impairment and photophobia.²³⁰ In cases with cone dystrophy with late onset, symptoms and signs may be mild to moderate and often non-specific, leading to misdiagnosis.²³⁴ Patients with late onset cone dystrophy develop slowly progressive loss of central or paracentral vision usually in the absence of any fundoscopic abnormalities.⁴⁹

4.4.2.3 Ophthalmoscopic features

Ophthalmoscopic findings in late-onset cone dystrophy range from normal or unspecific retinal pigment irregularities to bull’s eye maculopathy and atrophy (**Figure 2.5H**). Furthermore, pallor of the optic disc has been described.^{230, 233}



4.4.2.4 Fundus autofluorescence (cone dystrophy in general)

Fundus and near-infrared autofluorescence allow detection of retinal structural abnormalities even when findings from ophthalmoscopy are normal.²³⁵ However, in about 8.5% of patients, FAF and near-infrared autofluorescence also do not show pathological findings.²³⁵ Similar to the variability in the fundoscopic appearance of cone dystrophy, FAF and near-infrared autofluorescence may show a high heterogeneity ranging from normal signals to widespread RPE atrophy (**Figure 2.5I**).

4.4.2.5 Fluorescein angiography (cone dystrophy in general)

FA may show a dark choroid in patients with *ABCA4* associated cone dystrophy. Otherwise, FA imaging in patients with cone dystrophy does not add significant information.²³⁵

4.4.2.6 Optical coherence tomography (cone dystrophy in general)

High-resolution OCT imaging frequently reveals thinning of the retina (**Figure 2.5J**).²³⁵ In the outer retinal layers and at the RPE-level, unspecific alterations may be visible even when findings from ophthalmoscopy are normal.²³⁵

4.4.2.7 Psychophysical and electrophysiological testing

Initially, full-field ERG findings may be normal. In advanced stages, full-field ERG reveals decreased or absent photopic responses implying severe cone function impairment with normal to slightly depressed rod responses.²³⁴

4.4.2.8 Genetic association

There are only a few reports of patients with late-onset cone dystrophy. Possible familial inheritance has been reported in some of these patients.^{231, 233}

4.4.2.9 Pathophysiology

The exact pathogenesis of late-onset cone dystrophy remains unclear. The cones appear to be primarily affected with subsequent photoreceptor loss in the cone-rich central retina. The pathological changes in the underlying RPE appear to be secondary.

4.4.2.10 Differential diagnosis with age-related macular degeneration

Late-onset cone dystrophy may be confused with atrophic AMD because of:

- the age at onset (>50y)
- presence of pigmentary abnormalities

Features that help to distinguish late-onset cone dystrophy from AMD are:

- absence of drusen
- temporal optic disc pallor
- full-field and/or multifocal ERG findings typical for cone dystrophy

4.4.3 Central serous chorioretinopathy

4.4.3.1 Introduction

Central serous chorioretinopathy (CSC) is a relatively common cause of maculopathy characterized by serous fluid leakage under the neuroretina. CSC is usually sporadic, although familial cases have been described. Acute CSC often resolves spontaneously but sometimes recurs or becomes chronic.²³⁶ Risk factors for developing CSC include corticosteroid use, male sex, and type A personality.²³⁷

4.4.3.2 Symptoms

Although the chronic form of CSC may be preceded by acute CSC episodes, it is most often observed as a primary lesion.^{238, 239} Generally, chronic CSC becomes manifest before the sixth decade and may cause bilateral vision loss.^{49, 237-239} In bilateral chronic cases of CSC in which the serous subretinal fluid has eventually resorbed, the remaining central atrophic lesions may mimic AMD and atrophic macular dystrophies. Chronic CSC is more often bilateral and may be complicated by CNV, further complicating the differential diagnosis with AMD.²⁴⁰

4.4.3.3 Clinical features

In chronic CSC, persistent serous detachment or recurrent multifocal detachments of the retina and/or RPE may lead to atrophy of the RPE and the outer retina (**Figure 2.5K**).^{49, 241} Some patients develop yellowish subretinal deposits, intraretinal cystoid edema, fibrinous grey-white subretinal material, and/or CNV.^{49, 237}

4.4.3.4 Fundus autofluorescence

Areas of RPE atrophy in chronic CSC correspond to hypoautofluorescence and most long-standing CSC lesions also have speckled areas of increased FAF (**Figure 2.5L**).^{49, 242} These hyperautofluorescent areas may be explained by the accumulation of lipofuscin in the RPE, and/or from autofluorescent A2E-precursors in the subretinal space, derived from the shed outer segments of photoreceptors.²⁴²

4.4.3.5 Fluorescein angiography

On FA, chronic CSC typically shows granular areas of hyperfluorescence, often with one or more 'hot spots' of active subretinal fluid leakage (**Figure 2.5M**).²³⁷ With more extensive disease, larger hyperfluorescent RPE window defects may be seen due to RPE atrophy, sometimes with characteristic descending atrophic tracts (**Figure 2.5M**).^{49, 238} ICGA in active disease shows multiple areas of choroidal hyperfluorescence due to choroidal vascular dilation and hyperpermeability.²⁴³



4.4.3.6 Optical coherence tomography

A shallow subretinal detachment, often combined with one or more small pigment epithelial detachments may be seen on SD-OCT in chronic CSC patients (**Figure 2.5N**),^{242, 244} but – in contrast to AMD – there are no drusen.²⁴⁵ In severe cases, atrophy of the outer retinal layers and RPE remains after the serous fluid has disappeared.^{241, 242, 244} Enhanced depth imaging OCT may demonstrate a thickened choroid.²³⁷

4.4.3.7 Psychophysical and electrophysiological testing

EOG is generally normal, but mfERG reveals abnormalities even in patients with a mild course.²³⁷ Visual field testing and microperimetry may show loss of sensitivity with progression to (paracentral) scotoma,^{246, 247} and color vision testing is often abnormal.⁴⁹

4.4.3.8 Genetic association

Familial occurrence of CSC has been described, indicating that genetic factors may play a role in the pathogenesis of this disease.^{238, 248} So far, no genetic variants involved in CSC have yet been reported.

4.4.3.9 Pathophysiology

The pathophysiology of CSC remains poorly understood. There is strong evidence for a choroidal vasculopathy and hyperpermeability in CSC, leading to secondary RPE dysfunction and subretinal fluid leakage.^{237, 243} The underlying mechanism of the choroidal dysfunction remains to be determined, but it may be related to inappropriate activation of the mineralocorticoid receptor.²⁴⁹

4.4.3.10 Differential diagnosis with age-related macular degeneration

CSC may be confused with AMD because of:

- late central atrophic lesions and it may be accompanied by yellowish subretinal deposits and complicated by CNV

Features that help to distinguish CSC from AMD include:

- a relatively early age at onset
- (history of) serous neuroretinal detachment without drusen on ophthalmoscopy and SD-OCT
- gravitational tracks on FA and FAF

4.4.4 Macular telangiectasia

4.4.4.1 Introduction

The spectrum of idiopathic juxtafoveal retinal telangiectasia has been classified by Gass and Blodi in 1993.²⁵⁰ Type 2a, also called macular telangiectasia type 2 or 'MacTel', is the most common type and may show several morphological similarities to AMD. In recent years, there has been tremendous research into MacTel.²⁵¹ While the underlying cause is still not

clear, clinical features, the natural history and the correlation to retinal dysfunction have been extensively studied.

4.4.4.2 Clinical characteristics

MacTel is a bilateral disease in persons 40 years and older causing progressive visual loss. It usually presents with a slow decrease in vision, metamorphopsia, positive scotoma and reading difficulties. Symptoms may occur prior to fundoscopically visible changes.

4.4.4.3 Ophthalmoscopic features

Based on fundus photographs and FA findings, Gass and Blodi divided MacTel into five clinical stages according to the disease development.²⁵⁰ In stage 1, no abnormalities on biomicroscopy may be appreciated. FA may show minimal capillary dilatation and mild staining in the late-phase in the area temporal to the foveola.

Biomicroscopy shows in stage 2 slight greying and loss of transparency of the perifoveolar retina and no or minimal telangiectatic vessel with similar FA findings as in stage 1. The occurrence of blunted, right-angle venules that extend into the depth of the parafoveal retina, typically in the temporal fovea, characterize stage 3. Stage 4 manifests with one or several foci of black hyperplastic RPE within the retina, often beneath the blunted tips of the right angle venules and extending in some cases into the inner retina (**Figure 2.5O**). The development of subretinal neovascularization is defined as stage 5.

4.4.4.4 Fundus autofluorescence

In early disease stage, a key finding is the depletion of macular pigment in MacTel that may even occur before visible capillary dilatation in FA.^{252, 253} This finding has been confirmed by FAF imaging. In later stages, localized fundoscopically visible hyperpigmentations show a well-defined area of severely decreased FAF intensity (**Figure 2.5P**). This has been explained by RPE atrophy with loss of intrinsic fluorophores. Hyporeflexive cavities in the neurosensory retina may show an increased signal, particularly following bleaching of the retina with blue light.²⁵⁴

Blue confocal reflectance imaging is usually largely neglected in the clinical setting although it is available by standard cSLO. In MacTel, blue confocal reflectance is particularly helpful as it shows a distinctive parafoveal hyperreflectivity, already in the early stages of the disease.²⁵⁵ This characteristic signal may be caused by alterations in macular pigment and/or Müller cell loss.²⁵⁶

4.4.4.5 Fluorescein angiography

FA has traditionally been the gold-standard for the diagnosis of MacTel as it clearly demonstrates the capillary dilatations in the early phase with diffuse hyperfluorescence in the late stages (**Figure 2.5Q**). These telangiectatic vessels predominantly occur temporally to the fovea. Using stereoscopic images, these vascular alterations appear to be located in



the deeper capillary plexus.²⁵⁷ Further typical findings with FA are the hypofluorescence at the site of hyperpigmentations due to blockage (**Figure 2.5Q**) and the occurrence of leakage by retinal neovascularization in stage 5.

4.4.4.6 Optical coherence tomography

SD-OCT imaging shows intraretinal cystoid spaces or cavities without foveal thickening (**Figure 2.5R**).²⁵¹ Furthermore, disruption of the ellipsoid zone, increased reflectivity of the inner neurosensory layers, outer neurosensory atrophy, foveal detachment and laminar or full thickness macular holes may be visualized. These alterations are limited to the parafoveal macula and most prominent to the foveal centre. Gillies and co-workers have reported that the earliest subtle changes on SD-OCT imaging may be a temporal enlargement of the foveal pit that results in an asymmetry of the foveal contour with its thinnest sector temporally.²⁵⁸

4.4.4.7 Psychophysical and electrophysiological testing

Paracentral scotomata at the site of pigment hypertrophy and outer retinal cavities may be clearly confirmed by microperimetry.^{252, 259} Retinal cavities limited to the inner retina typically show preserved function. Visible disruption of the inner segment-outer segment borders as shown by SD-OCT imaging is spatially confined to reduced retinal sensitivity. Fine matrix mapping findings suggest that rod function may be more severely affected as compared to cone function and occurs earlier in the disease. By contrast, routine examinations with visual acuity testing might not be sufficient to estimate the abilities of the patient to cope with daily visual tasks particularly reading.

Standard visual field testing or ERG is usually normal or subnormal in MacTel. It would be well conceivable that the affected retinal area in MacTel is relatively small compared to the sensitivity of these modalities.

4.4.4.8 Genetic association

No causal mutation has been identified, but a genetic association of the *ATM* gene and a locus have been reported.^{260, 261} MacTel may occur in monozygotic twin, other siblings and also in families with vertical transmission, suggestive of a dominant inheritance mode.²⁵⁸

4.4.4.9 Pathophysiology

The cause of MacTel is unknown. While the name ‘macular telangiectasia’ suggest a disease of the retinal vasculature, recent findings have provided increasing evidence that MacTel is not limited to the retinal vasculature and that early neuronal involvement may be implicated in the pathogenesis of disease. Furthermore, affection of Müller cells has been discussed recently.^{256, 262-266}

4.4.4.10 Differential diagnosis with age-related macular degeneration

MacTel may be confused with AMD because of:

- similar symptoms; bilateral slow progressive loss of central vision, metamorphopsia, positive scotoma and reading difficulties
- presence of pigmentary changes and CNV may develop

Features that help to distinguish MacTel from AMD are:

- an earlier age at onset
- no drusen
- affection of abnormalities limited to the parafovea and predominantly temporal to the foveal centre
- parafoveal hyperreflectivity in confocal blue reflectance
- presence of telangiectatic vessels
- depletion of macular pigment by fundus autofluorescence
- retinal thinning (usual no thickening) and cavities by SD-OCT imaging

4.5 Dystrophies associated with a syndrome or systemic disease

4.5.1 Mitochondrial retinal dystrophy associated with the m.3243A>G mutation (maternally inherited diabetes and deafness and MELAS syndrome)

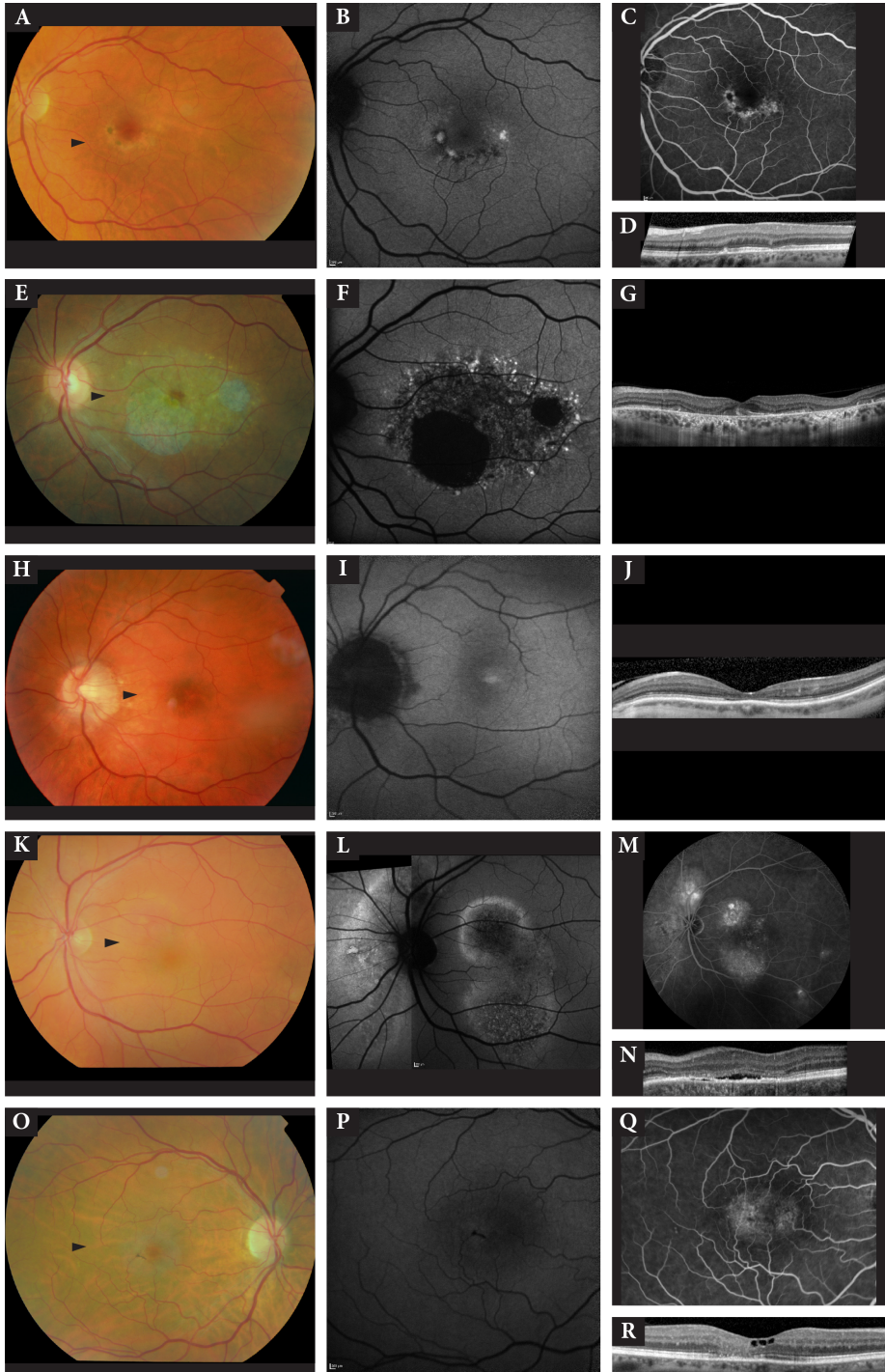
4.5.1.1 Introduction

The m.3243A>G mutation was first described in association with mitochondrial myopathy, encephalopathy, lactic acidosis and stroke-like episodes (MELAS).^{267, 268} Up to 86% of patients with the m.3243A>G mutation have evidence of retinal dystrophy.^{269, 270} Over time, more phenotypic variations of the m.3243A>G mutation have been reported, the most frequent being maternally inherited diabetes and deafness (MIDD).^{271, 272} Other systemic associations include cardiac, renal, and gastro-intestinal involvement.^{267, 268, 271, 273-275}

4.5.1.2 Clinical characteristics

Most patients have a relatively preserved central visual function because of the frequent occurrence of structural and functional sparing of the fovea.²⁷⁰ Up to 80% of patients maintain a visual acuity of 20/25 or better in at least one eye^{269, 270}. However, even if the fovea is spared, considerable visual impairment may be present as a result of paracentral scotomata in cases of progressive atrophy around the fovea.²⁷⁰





► **Figure 2.5 (A-G)** Central areolar choroidal dystrophy stage 2 in a 48-year-old patient (**A-D**) and stage 3 in a 54-year-old patient (**E-G**), both carrying a PRPH2 mutation. (**A**) Color fundus photograph showing parafoveal pigmentary changes. (**B**) Fundus autofluorescence (FAF) image showing hyperautofluorescent parafoveal changes corresponding to the pigmentary changes in **A**. (**C**) Fluorescein angiography (FA) image showing hyperfluorescence corresponding with hypopigmentation and hypofluorescence corresponding with hyperpigmentations on **A**. (**D**) Horizontal optical coherence tomography (OCT) scan (scan in the plane indicated by black arrowhead in **A**) showing a disruption of the photoreceptors corresponding to hypopigmentary changes and hyperreflective elevations of the retinal pigment epithelium (RPE) corresponding to hyperpigmentation in **A**. (**E**) Color fundus photograph showing hypopigmentation of the macula with two parafoveal, oval-to-round, atrophic areas. (**F**) Chorioretinal atrophy corresponding with severely decreased to absent FAF, bordered by speckled changes of increased and decreased FAF. (**G**) Horizontal OCT scan (scan in the plane indicated by black arrowhead in **E**) showing well-circumscribed chorioretinal atrophy. (**H-J**) Late onset cone dystrophy in a 49-year-old patient. (**H**) Color fundus photograph showing central pigmentary changes and pallor of the optic disc. (**I**) FAF image showing hyperautofluorescent foveal changes corresponding to the pigmentary changes in **H**. (**J**) Horizontal OCT scan (scan in the plane indicated by black arrowhead in **H**) showing thinning of the outer retinal layers in the fovea. (**K-N**) Central serous chorioretinopathy in a 49-year-old patient. (**K**) Color fundus photograph showing serous detachment of the retina and RPE changes. (**L**) FAF image showing speckled FAF signals of increased and decreased autofluorescence. (**M**) FA image showing a characteristic descending atrophic tract and several ‘hotspots’ of active subretinal leakage. (**N**) Horizontal OCT scan (scan in the plane indicated by black arrowhead in **K**) showing a shallow subretinal detachment combined with pigment epithelial detachment. (**O-R**) Macular telangiectasia in a 70-year-old patient. (**O**) Color fundus photograph showing greying of the perifoveolar retina. Right-angle venules extend into the depth of the temporal fovea with a lesion of black hyperplastic RPE beneath the venules. (**P**) FAF image showing decreased FAF corresponding with hyperpigmentation in **O**. (**Q**) FA image showing hyperfluorescence of the capillary dilations, predominantly temporal to the fovea located. Hyperpigmentations are hypofluorescent due to blockage. (**R**) Horizontal OCT scan (scan in the plane indicated by black arrowhead in **O**) showing intraretinal cystoid spaces without foveal thickening and disruption of the photoreceptor layers in the parafoveal macula.

4.5.1.3 Ophthalmoscopic features

The spectrum of retinal abnormalities ranges from barely discernible pigmentary abnormalities in the outer retinal layers of the macula to profound chorioretinal atrophy in the macula.²⁷⁰ Patients with the m.3243A>G mutation have retinal lesions that are localized at the posterior pole but tend to spare the fovea and often include the retina surrounding the optic disc (**Figure 2.6A**). Recently, Boon has proposed a classification system into 4 grades based on findings on ophthalmoscopy, FAF, and SD-OCT.²⁷⁰ This classification correlates both with age and visual acuity.

4.5.1.4 Fundus autofluorescence

The retinal abnormalities in m.3243A>G mutation associated macular dystrophy are clearly visible on FAF imaging.^{270, 276, 277} Mild hypofluorescent mottling correlates with the mild pigmentary abnormalities in the central fundus in grade 1 mitochondrial retinal dystrophy. In grade 2, fundoscopically visible yellow-white spots/flecks correspond to mostly increased FAF, while a decreased FAF signal is present in mildly atrophic areas (**Figure 2.6B**). In grade 3, there are one or more areas of well delineated areas of chorioretinal atrophy that present with a well-defined area of decreased FAF. Unlike grade 4 disease, these atrophic zones

may encircle the fovea but do not involve the central fovea. A diffuse speckled FAF pattern may be present that is significantly larger than would be expected from the fundoscopic appearance.^{130, 276, 277}

4.5.1.5 Fluorescein angiography

The FA signal may vary from small hyper and hypofluorescent spots to extensive RPE window defect with visibility of the underlying larger choroidal vasculature and atrophy of the choriocapillaris depending of the disease grade (**Figure 2.6C**).²⁷⁰

4.5.1.6 Optical coherence tomography

Irregular thickening or attenuation of the line corresponding to the ellipsoid zone and of the underlying RPE layer may be visualized in affected retinal area (**Figure 2.6D**). The atrophic areas correspond to a loss of the outer retinal layers on OCT imaging.²⁷⁰

4.5.1.7 Psychophysical and electrophysiological testing

The full-field ERG and EOG are normal.²⁷⁰ Multifocal ERG in mitochondrial retinal dystrophy can show reduced peak amplitudes with normal implicit times in the mfERG suggesting localized loss of function and indicating damage to the cone photoreceptor outer segments or cone photoreceptor loss in MIDD.²⁷⁸

4.5.1.8 Genetic association and pathophysiology

The m.3243A>G mutation is by far the most common cause of mitochondrial retinal dystrophy in adults²⁷⁰. The percentage of cells with the affected mitochondrial DNA in a specific tissue is referred to as 'heteroplasmy', and within a single individual, the degree of heteroplasmy may vary widely between tissues.^{270, 279} Therefore, mitochondrial disease may present at any age, with virtually any symptom or sign, and by any apparent mode of inheritance.²⁸⁰ This marked intra-individual and inter-individual variation in mitochondrial heteroplasmy explains the wide spectrum of clinical symptoms and disease severity observed between family members who share a given mitochondrial mutation.²⁸⁰ There is no clear correlation of the grade of mitochondrial retinal dystrophy with systemic heteroplasmy levels or overall systemic disease involvement.²⁷⁰

4.5.1.9 Differential diagnosis with age-related macular degeneration

m.3243A>G associated macular dystrophy may be confused with AMD because of:

- the pigmentary abnormalities and chorioretinal atrophy that can mimic drusen and GA in AMD
- the maternal inheritance pattern may be masked and the systemic disease associations may be variable or even absent

Features that help to distinguish m.3243A>G associated macular dystrophy from AMD include:

- a typical speckled FAF pattern that may spread along the temporal retinal vascular arcades and surround the optic disc ^{130, 276}
- systemic associations such as hearing loss and early-onset diabetes
- maternal inheritance of disease (no male-to-male transmission)
- genetic analysis revealing the m.3243A>G mutation

4.5.2 Dystrophies with angioid streaks

4.5.2.1 Introduction

Angioid streaks are irregular and radiating lines extending from the disc to the peripheral retina caused by breaks in the Bruch's membrane. ²⁸¹ Angioid streaks frequently occur in patients with systemic diseases, including pseudoxanthoma elasticum (PXE), osteitis deformans, sickle cell anaemia, acromegalie, Marfan syndrome, fibrodysplasia hyperelastica, thalassemia, and spherocytosis. ²⁸²

PXE is the most commonly associated systemic disorder: 59-87% of cases with angioid streaks are due to PXE. ²⁸³ It is associated with accumulation of mineralized and fragmented elastic fibers in the skin, vascular walls, and Bruch's membrane in the eye, ²⁸⁴ manifested in soft, ivory-colored papules in a reticular pattern that predominantly affect the neck and large flexor surfaces, peripheral and coronary arterial occlusive disease and gastrointestinal bleedings. ²⁸⁴

4.5.2.2 Clinical characteristics

Patients with angioid streaks usually remain asymptomatic. However, complications such as atrophy of outer retinal layers, choroidal rupture, or CNV, with or without haemorrhage and subretinal fibrosis may be associated with severe visual impairment when affecting the macula. ^{285, 286} This has been reported in 73-86% of PXE cases, ^{83, 287, 288} frequently leading to severe reduction of visual acuity as early as age 14. ²⁸⁷ By the age of 50, the majority of PXE patients have bilaterally impaired visual acuity of 20/200 or less. ^{284, 288}

4.5.2.3 Ophthalmoscopic features

Typically, there is a peripapillary ring from which irregularly radiating linear streaks extend in all directions (**Figure 2.6E**). Fibrovascular ingrowth into the angioid streaks may result in serous and/or hemorrhagic detachment of the overlying retina. In advanced stages, detachment and atrophy of the RPE and may also occur. ²⁸⁵

In PXE, first visible changes on fundoscopy are pigmentary regularities called *peau d'orange*, which are most prominently visible temporal to the fovea. ^{289, 290} These pigment irregularities have a fine, yellow, drusen-like appearance and are assumed to be localized at the level of the RPE. ^{49, 287} *Peau d'orange* typically precedes angioid streaks on average by 1 to 8 years. ²⁸⁷ Additional ocular findings in PXE are multiple small chorioretinal atrophic lesions, so called comet tail lesions, as well as drusen of the optic disc. ²⁹¹



4.5.2.4 Fundus autofluorescence

On FAF, angioid streaks may show areas of increased as well as decreased FAF (**Figure 2.6G**).^{292, 293} Focal spots of increased FAF alongside angioid streaks, consisting of pigmentations on funduscopy, constitute a parastreak phenomenon.

Macular FAF patterns in PXE patients are often similar to those observed in pattern dystrophies.²⁹³ Comet tail lesions in the midperiphery typically show an increased FAF signal and appear hyperfluorescent on FA. FAF depicts RPE atrophies, which are often more extensive than funduscopy or FA would suggest.²⁸⁴

4.5.2.5 Fluorescein angiography

Angioid streaks may show increased fluorescence if there is thinning of the RPE overlying an intact choriocapillaris. In this situation, there would be gradual fading of an early choroidal blush in the later phases of the angiogram.²⁸⁵ If there is actual separation of the choriocapillaris at the time of the separation of Bruch's membrane, one may see only hyperfluorescence along the margin of the streak with the central portion of the streak showing very little or no fluorescence.²⁸⁵ CNVs usually originate from the rim of angioid streaks and show similar angiographic pattern to that described in AMD (**Figure 2.6H**).²⁹⁴⁻²⁹⁶

4.5.2.6 Optical coherence tomography

On SD-OCT scans the pathology of angioid streaks is localized to the Bruch's membrane-RPE complex.²⁹⁷ The RPE overlying breaks in Bruch's membrane may seem unaffected, but often appears altered, focally detached, or absent. In many advanced cases, fibrovascular tissue extends from the choroidal into the subneurosensory space (**Figure 2.6I**) through the gaps in Bruch's membrane (**Figure 2.6J**). Simultaneous SD-OCT and cSLO imaging reveals the most reliable detection of angioid streaks in the near-infrared mode (**Figure 2.6F**).²⁹⁷

4.5.2.7 Psychophysical and electrophysiological testing

Full-field ERG may reveal mild to significant amplitude reduction of cone and rod responses.^{298, 299}

4.5.2.8 Genetic association

PXE is an autosomal-recessive disorder and in the majority of cases, homozygosity or compound heterozygosity is found for mutations in the *ABCC6* gene, a member of the large ATP-dependent transmembrane transporter family. Since the *ABCC6* gene is expressed primarily, if not exclusively, in the liver and kidneys, it has been suggested that PXE is a primary metabolic disorder with secondary involvement of elastic fibres.^{300, 301}

4.5.2.9 Pathophysiology

Angioid streaks represent breaks of the calcified and thickened Bruch's membrane, which are not associated with morphological changes in the overlying layers of the retina and the underlying choriocapillaris in early stages.³⁰²

4.5.2.10 Differential diagnosis with age-related macular degeneration

Angioid streaks related dystrophies may be confused with AMD because of:

- atrophy and/or CNV may occur secondary to the angioid streaks

Features that help to distinguish between angioid streaks related diseases and AMD include:

- visualization of angioid streaks by angiography, near-infrared-, AF-, and SD-OCT-imaging
- an earlier age at onset
- accompanied ocular findings such as peau d' orange and comet tail lesions in PXE
- accompanied systemic symptoms
- genetic analysis (mutations in *ABCC6*)
- skin biopsy in patients with PXE

4.5.3 Cuticular drusen in membranoproliferative glomerulonephritis II

4.5.3.1 Introduction

Membranoproliferative glomerulonephritis type II (MPGN II), also termed 'dense deposit disease', is a rare condition characterized by the deposition of abnormal electron-dense material within the glomerular basement membrane of the kidney and often within Bruch's membrane in the eye.³⁰³

4.5.3.2 Clinical characteristics

The diagnosis is made in most patients between the ages of 5 and 15 years of life. Within 10 years after diagnosis, approximately half of patients progress to end-stage renal disease, occasionally with the late co-morbidity of visual impairment.³⁰³

4.5.3.3 Ophthalmoscopic features

The majority of patients with MPGN II develop deposits at the posterior pole with the clinical appearance of cuticular drusen (**Figure 2.6L**).³⁰⁴ Visual acuity tends to be preserved until GA or CNV complicate the disease.^{182, 305-307}

4.5.3.4 Fundus autofluorescence

To the best of our knowledge, no descriptions of FAF imaging in patients with cuticular drusen and MPGN II have been published thus far. Cuticular drusen in general correspond with focal hypoautofluorescent lesions on FAF image, even when the lesions are not advanced enough to show the classic stars-in-the-sky appearance on FA.⁵¹

4.5.3.5 Fluorescein angiography

Drusen in MPGNII are identified most readily by FA. Typically, the small drusen show hyperfluorescence in the early phase of the angiogram (**Figure 2.6M**).



4.5.3.6 Psychophysical and electrophysiological testing

In long-standing cases, EOG may become abnormal due to widespread RPE atrophy.^{308, 309} In these advanced stages, color vision, dark adaptation, as well as dark adapted ERG may also become mildly abnormal.³⁰⁸

4.5.3.7 Genetic association

The pathophysiologic basis of MPGN II is associated with the uncontrolled systemic activation of the alternative pathway of the complement cascade. In most patients, loss of complement regulation is caused by C3 nephritic factor, an autoantibody directed against the C3 convertase of the alternative pathway, but in some patients, mutations in the *CFH* gene have been identified.^{303, 310}

4.5.3.8 Pathophysiology

The pathophysiologic basis for MPGN II seems to be the uncontrolled systemic activation of the alternative pathway of the complement cascade.^{311, 312} In most patients, loss of complement regulation is caused by the C3 nephritic factor, an immunoglobulin (Ig)G autoantibody that binds and prevents the inactivation of C3 convertase of the alternative pathway, thereby resulting in the perpetual breakdown of C3.³¹³ The characteristic finding in MPGN II is an intense deposition of C3 cleavage products along the glomerula capillary walls together with electron-dense deposits in the central part of the glomerula basal membrane.³⁰³ Histopathological studies on drusen in MPGN II showed both linear and focal depositions throughout the extent of the inner collagenous layer of Bruch's membrane.^{314, 315} This draws attention to the fact that the choriocapillaris-Bruch's membrane-RPE complex shows a remarkable resemblance to the capillary tuft-glomerula basal membrane-glomerular epithelial interface.^{303, 315}

4.5.3.9 Differential diagnosis with age-related macular degeneration:

MPGNII may be confused with AMD because:

- patients may develop cuticular drusen, GA and CNV

Features that help to distinguish MPGNII from AMD include:

- renal dysfunction
- retinal changes present at an early age and are often detectable in the first or second decade of life. Therefore, in patients with early onset or extensive cuticular drusen screening for renal dysfunction is reasonable.²⁸

4.5.4 Maculopathy in myotonic dystrophy

4.5.4.1 Introduction

Steinert (1909)³¹⁶ and Batten and Gibb (1909)³¹⁷ identified myotonic dystrophy as a multisystemic disorder that is now recognized as one of the most common forms of muscular dystrophy in adults.³¹⁸ This inherited disorder is accompanied by progressive

weakness of the distal muscles and myotonia. Cases of myotonic dystrophy are generally classified as one of two types based on the genetic background.³¹⁹

4.5.4.2 Clinical characteristics

In addition to muscular dystrophy and myotonia, which also may cause ptosis and weakness of the ocular muscles, myotonic dystrophy causes a consistent constellation of seemingly unrelated and rare clinical features, including cardiac conduction defects, a peculiar and specific set of endocrine changes, and posterior subcapsular iridescent cataracts.³²⁰ Further ophthalmic features include low intraocular pressure and in at least 20% to 25% of patients with myotonic dystrophy there is some evidence of retinal degeneration.^{49, 321} Most of the patients have minimal loss of visual acuity.⁴⁹

4.5.4.3 Ophthalmoscopic features

A variety of fundoscopic pictures has been described. Besides peripheral pigmentary changes, dark and yellow spots in the macular that are configured in stellae, butterfly, and reticular shape resembling pattern dystrophies may occur (**Figure 2.6N**).^{49, 321} Long-term follow-up of patients with myotonic dystrophy suggested that these pigmentary retinal changes progress slowly over time.³²²

4.5.4.4 Fundus autofluorescence

To the best of our knowledge, there are no descriptions published so far.

4.5.4.5 Fluorescein angiography

FA shows window defects and blocked fluorescence by focal pigment clumps (**Figure 2.6O**).³²³

4.5.4.6 Psychophysical and electrophysiological testing

Decreased b-wave and subnormal a-wave amplitudes in the ERG and delayed dark adaptation have been reported in patients with myotonic dystrophy.³²¹ The EOG remains normal in patients with myotonic dystrophy.³²²

4.5.4.7 Genetic association

Myotonic dystrophy type 1 is caused by the expansion of an unstable CTG trinucleotide repeat in the 3' untranslated region of the myotonic dystrophy protein kinase (*DMPK*) gene.^{320, 324} The myotonic dystrophy type 2 mutation consists in the expansion of an unstable CCTG tetranucleotide within the first intron of the CCHC-type zinc finger, nucleic acid-binding protein (*CNBP*) gene (previously named myotonia).³²⁵



4.5.4.8 Pathophysiology

Experimental evidence supports an RNA gain-of-function mechanism of expanded transcripts in myotonic dystrophy type 1 and 2.^{318, 326-329} These ‘toxic’ RNA transcripts accumulate in nuclear inclusions, interfering with the activity, localization and/or steady-state levels of RNA-interacting proteins. The exact mechanisms leading to the fundoscopic features of the disease are still unknown.

4.5.4.9 Differential diagnosis with age-related macular degeneration

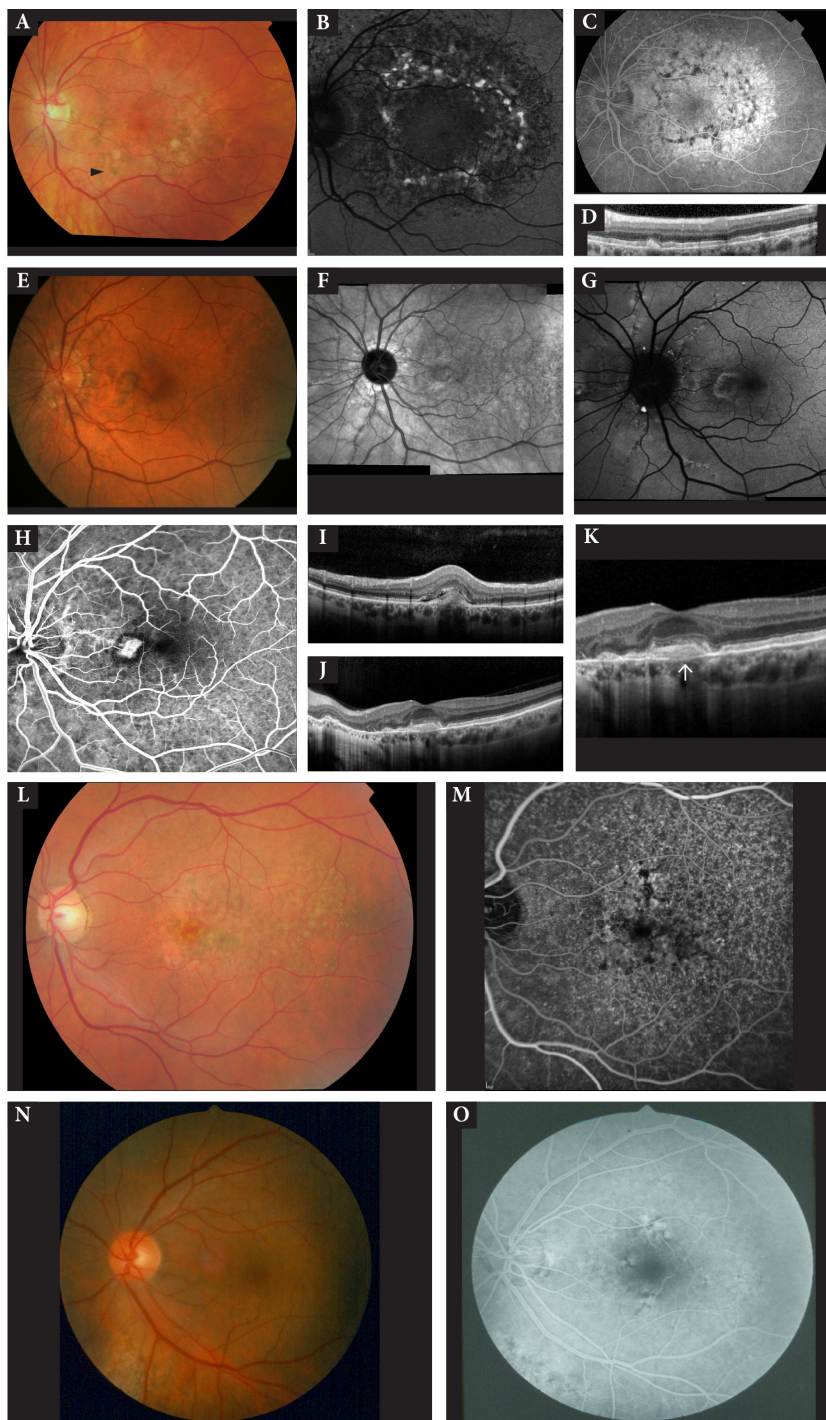
Maculopathy in myotonic dystrophy may be confused with AMD because of:

- the pattern dystrophy-like features may resemble drusen and AMD-related hyperpigmentary changes

Features that help to distinguish between myotonic dystrophy associated macular dystrophy and AMD include:

- posterior subcapsular cataracts that are present in almost all patients with myotonic dystrophy
- other associated ocular symptoms such as ptosis, ophthalmoplegia, and low intraocular pressure
- absence of typical sub-RPE or reticular drusen on SD-OCT
- generalized muscle weakness and myotonia and a positive family history
- genetic testing (*DMPK* and *CNBP*)

Figure 2.6 (A-D) *m.3243A>G* Macular dystrophy associated with MIDD in a 26-year-old patient with diabetes mellitus who carried a *m.3243 A>G* mutation. **(A)** Color fundus photograph showing hyperpigmented irregular spots in the macula and an oval area of mottled hypopigmentation that involved the macula and surrounded the optic disc. **(B)** Fundus autofluorescence (FAF) image showing that the hyperpigmented spots in the macula correspond to mainly increased FAF, whereas the hypopigmented spots and zones mainly correspond to a decreased FAF signal. **(C)** Fluorescein angiography (FA) image showing blockage of background fluorescence in the area of hyperpigmentation and hyperfluorescence due to a retinal pigment epithelium (RPE) window defect in the retinal areas that were hypopigmented and mildly atrophic on the fundus image **A**. **(D)** Horizontal optical coherence tomography (OCT) scan (scan in the plane indicated by black arrowhead in **A**) showing the hyperpigmented spot corresponding to a hyperreflective dome-shaped lesion that seemed to originate from the RPE. **(E-K)** Choroidal neovascularization (CNV) associated with angioid streaks in a 45-year-old patient with pseudoxanthoma elasticum. On fundoscopy **(E)** the identification of angioid streaks is challenging. Infra-red **(F)** or FAF **(G)** imaging might be more reliable to detect angioid streaks. FA **(H)** shows a classic CNV originating from an angioid streak. On SD-OCT image **(I)** fibrovascular invasion with subretinal fluid is visible. The OCT image **(J)** reveals a break in Bruch’s membrane associated with an angioid streak. **(K)** Magnification of image **J** highlighting the break in Bruch’s membrane (white arrow). **(L-M)** Membranoproliferative glomerulonephritis II in a 58-year-old patient who carried compound heterozygous mutations in the Complement Factor H gene. **(L)** Color fundus photograph showing widespread drusenoid lesions with irregular RPE alterations. **(M)** FA image showing stars-in-the-sky appearance with small, hyperfluorescent drusen scattered in the posterior pole. **(N-O)** Maculopathy in a 53-year-old patient with myotonic dystrophy (Courtesy of J.R.M. Cruysberg, Radboud University Nijmegen Medical Centre). **(N)** Color fundus photograph showing pigmentary changes in the macula. **(O)** FA image showing window defects and hypofluorescence corresponding with the pigmentary changes due to blockage of background fluorescence.



5. CONCLUSIONS AND FUTURE DIRECTIONS

A broad range of dystrophic macular disorders share clinical characteristics with AMD, which can make a differential diagnosis challenging. Although macular dystrophies and AMD show broad genetic and phenotypic heterogeneity, with overlapping features that may complicate a comprehensive clinical classification, there are often characteristic phenotypic features that can help in the differential diagnosis in a practical clinical setting. We propose a diagnostic flow chart in **Figure 2.7**. This flow chart inevitably is an oversimplification, and many classifications have been proposed, some based on ophthalmoscopic features, others are based on electrophysiologic findings or underlying molecular genetic defect(s).

It is clinically relevant to distinguish AMD from macular dystrophies, not only because of the prognostic implications and genetic counselling, but also because of its consequences for present and future preventive and therapeutic strategies.

A correct diagnosis can have significant implications for the prognosis. Atrophy in macular dystrophies, for example, may show a different rate of progression from that in atrophic AMD^{218, 330, 331} and CNV in macular dystrophies appears to have a relatively favourable prognosis as compared to CNV in AMD.³³

With regard to genetic counselling, it is very important to provide the patient with the correct information on the risk of affected offspring, for instance in late-onset Stargardt disease versus pseudo-Stargardt pattern dystrophy. Although these retinal dystrophies can be clinically very similar, Stargardt disease is inherited in an autosomal-recessive fashion, on contrast to autosomal-dominantly inherited pseudo-Stargardt.

An early recognition of syndrome-associated macular dystrophies paves the way to a multidisciplinary approach, a timely diagnosis, prevention and/or treatment of associated systemic disease(s). For example, it is important to recognise macular dystrophy in the constellation of pseudoxanthoma elasticum because this has implications for the prevention and treatment of cardiovascular disease. Mitochondrial retinal dystrophy associated can be the first manifestation in carriers of the m.3243A>G mutation.²⁷⁰ These patients have a very high risk of other systemic abnormalities, such as hearing loss and diabetes, for which they should be screened in a specialized centre for mitochondrial disease.

Nutritional supplements are widely used by AMD patients. However, Stargardt patients might be advised to refrain from taking vitamin A supplements, as it may accelerate the disease course. A misdiagnosis may therefore lead to recommendations which are potentially harmful.¹⁷⁸ Misdiagnosis can lead to erroneous treatment of patients.²¹⁷ Unlike in AMD, argon laser and photodynamic therapy may not be effective in the treatment of CNV in SFD patients (**Figure 2.2G**).¹²¹ On the other hand, anti-VEGF therapy may be a successful therapy,^{121, 332} as in neovascular AMD.

The development of gene therapy and stem cell based approaches for patients with retinal dystrophies patients is advancing at an accelerating pace, possibly leading to future therapeutic options in patients with retinal dystrophies in whom the affected gene has been identified. Therefore, a thorough differential diagnostic approach is essential to establish the right clinical and genetic diagnosis.



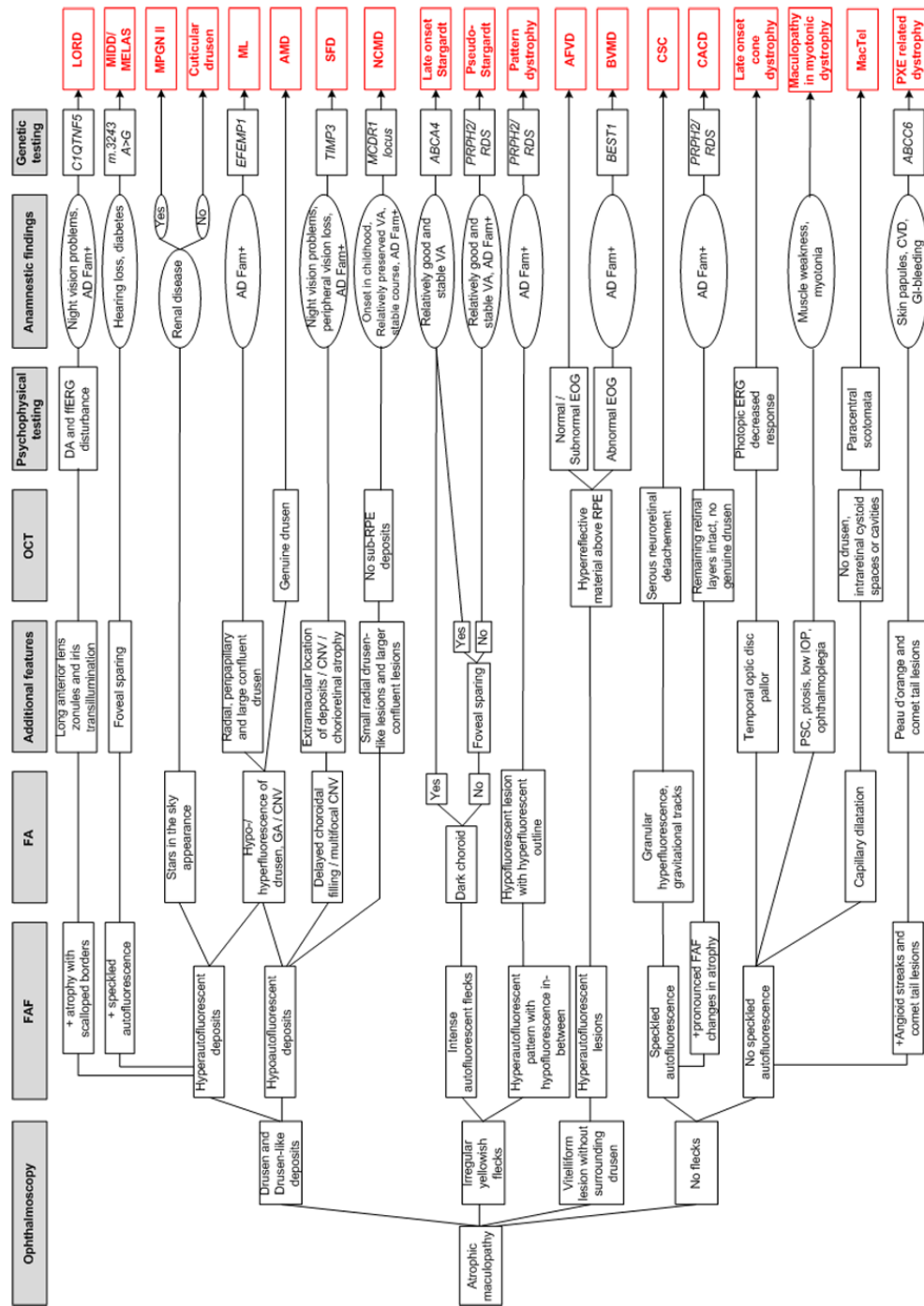




Figure 2.7 Diagnostic flowchart of atrophic macular dystrophies based on anamnesic, ophthalmoscopic, electrophysiologic and genetic findings. The flowchart indicates the most likely diagnosis, but does not exclude other diagnoses. Only most typical features and findings are included in this figure, and therefore, the absence of a finding does not exclude the diagnosis. The starting point of the flowchart is atrophic maculopathy, since atrophy can occur in all macular diseases.

Rectangles: examinational findings. Oval: anamnesic findings. Abbreviations: FAF, fundus autofluorescence; FA, fluorescein angiography; GA, geographic atrophy; CNV, choroidal neovascularization; PSC, posterior subcapsular cataracts; IOP, intraocular pressure; OCT, optical coherence tomography; DA, dark adaptation; ffERG, full-field ERG; EOG, electro-oculography; AD Fam+, positive family history with autosomal-dominant inheritance pattern; VA, visual acuity; CVD, cardiovascular disease; GI, gastro-intestinal. Figure on next page



REFERENCES

1. Lim LS, Mitchell P, Seddon JM, Holz FG, Wong TY. Age-related macular degeneration. *Lancet* 2012;379:1728-1738.
2. Smith W, Assink J, Klein R, et al. Risk factors for age-related macular degeneration: Pooled findings from three continents. *Ophthalmology* 2001;108:697-704.
3. Rudnicka AR, Jarrar Z, Wormald R, Cook DG, Fletcher A, Owen CG. Age and gender variations in age-related macular degeneration prevalence in populations of European ancestry: a meta-analysis. *Ophthalmology* 2012;119:571-580.
4. Klein R, Klein BE, Knudtson MD, Meuer SM, Swift M, Gangnon RE. Fifteen-year cumulative incidence of age-related macular degeneration: the Beaver Dam Eye Study. *Ophthalmology* 2007;114:253-262.
5. Friedman DS, Katz J, Bressler NM, Rahmani B, Tielsch JM. Racial differences in the prevalence of age-related macular degeneration: the Baltimore Eye Survey. *Ophthalmology* 1999;106:1049-1055.
6. Kawasaki R, Yasuda M, Song SJ, et al. The prevalence of age-related macular degeneration in Asians: a systematic review and meta-analysis. *Ophthalmology* 2010;117:921-927.
7. Ferris FL, 3rd, Wilkinson CP, Bird A, et al. Clinical Classification of Age-Related Macular Degeneration. *Ophthalmology* 2013;120:844-851.
8. Neelam K, Nolan J, Chakravarthy U, Beatty S. Psychophysical function in age-related maculopathy. *Surv Ophthalmol* 2009;54:167-210.
9. Walter P, Widder RA, Luke C, Konigsfeld P, Brunner R. Electrophysiological abnormalities in age-related macular degeneration. *Graefes Arch Clin Exp Ophthalmol* 1999;237:962-968.
10. Ronan S, Nusinowitz S, Swaroop A, Heckenlively JR. Senile panretinal cone dysfunction in age-related macular degeneration (AMD): a report of 52 amd patients compared to age-matched controls. *Trans Am Ophthalmol Soc* 2006;104:232-240.
11. Boulton M. Ageing of the retina and retinal pigment epithelium. In: Holz FG PD, Spaide RF, Bird AC (ed), *Age-related macular degeneration*. Heidelberg, New York, Dordrecht, London: Springer; 2013.
12. Boulton M. Ageing of the retina and retinal pigment epithelium. In: Holz FG PD, Spaide RF, Bird AC (ed), *Age-related macular degeneration*. Heidelberg, New York, Dordrecht, London: Springer; 2013:45-63.
13. Suter M, Reme C, Grimm C, et al. Age-related macular degeneration. The lipofusion component N-retinyl-N-retinylidene ethanolamine detaches proapoptotic proteins from mitochondria and induces apoptosis in mammalian retinal pigment epithelial cells. *J Biol Chem* 2000;275:39625-39630.
14. Palczewska G, Maeda T, Imanishi Y, et al. Noninvasive multiphoton fluorescence microscopy resolves retinol and retinal condensation products in mouse eyes. *Nat Med* 2010;16:1444-1449.
15. Zhou J, Jang YP, Kim SR, Sparrow JR. Complement activation by photooxidation products of A2E, a lipofuscin constituent of the retinal pigment epithelium. *Proc Natl Acad Sci U S A* 2006;103:16182-16187.
16. Hageman GS, Luthert PJ, Victor Chong NH, Johnson LV, Anderson DH, Mullins RF. An integrated hypothesis that considers drusen as biomarkers of immune-mediated processes at the RPE-Bruch's membrane interface in aging and age-related macular degeneration. *Prog Retin Eye Res* 2001;20:705-732.
17. Donoso LA, Kim D, Frost A, Callahan A, Hageman G. The role of inflammation in the pathogenesis of age-related macular degeneration. *Surv Ophthalmol* 2006;51:137-152.

18. Klein RJ, Zeiss C, Chew EY, et al. Complement factor H polymorphism in age-related macular degeneration. *Science* 2005;308:385-389.
19. Haines JL, Hauser MA, Schmidt S, et al. Complement factor H variant increases the risk of age-related macular degeneration. *Science* 2005;308:419-421.
20. Hageman GS, Anderson DH, Johnson LV, et al. A common haplotype in the complement regulatory gene factor H (HF1/CFH) predisposes individuals to age-related macular degeneration. *Proc Natl Acad Sci U S A* 2005;102:7227-7232.
21. Edwards AO, Ritter R, 3rd, Abel KJ, Manning A, Panhuysen C, Farrer LA. Complement factor H polymorphism and age-related macular degeneration. *Science* 2005;308:421-424.
22. Gold B, Merriam JE, Zernant J, et al. Variation in factor B (BF) and complement component 2 (C2) genes is associated with age-related macular degeneration. *Nat Genet* 2006;38:458-462.
23. Maller JB, Fagerness JA, Reynolds RC, Neale BM, Daly MJ, Seddon JM. Variation in complement factor 3 is associated with risk of age-related macular degeneration. *Nat Genet* 2007;39:1200-1201.
24. Jakobsdottir J, Conley YP, Weeks DE, Mah TS, Ferrell RE, Gorin MB. Susceptibility genes for age-related maculopathy on chromosome 10q26. *Am J Hum Genet* 2005;77:389-407.
25. Rivera A, Fisher SA, Fritsche LG, et al. Hypothetical LOC387715 is a second major susceptibility gene for age-related macular degeneration, contributing independently of complement factor H to disease risk. *Hum Mol Genet* 2005;14:3227-3236.
26. Fritsche LG, Chen W, Schu M, et al. Seven new loci associated with age-related macular degeneration. *Nat Genet* 2013;45:433-439, 439e431-432.
27. Raychaudhuri S, Iartchouk O, Chin K, et al. A rare penetrant mutation in CFH confers high risk of age-related macular degeneration. *Nat Genet* 2011;43:1232-1236.
28. van de Ven JP, Boon CJ, Fauser S, et al. Clinical evaluation of 3 families with basal laminar drusen caused by novel mutations in the complement factor H gene. *Arch Ophthalmol* 2012;130:1038-1047.
29. van de Ven JP, Nilsson SC, Tan PL, et al. A functional variant in the CFI gene confers a high risk of age-related macular degeneration. *Nat Genet* 2013;45:813-817.
30. Boon CJ, Klevering BJ, Hoyng CB, et al. Basal laminar drusen caused by compound heterozygous variants in the CFH gene. *Am J Hum Genet* 2008;82:516-523.
31. Buitendijk GH, Rohtchina E, Myers C, et al. Prediction of Age-related Macular Degeneration in the General Population: The Three Continent AMD Consortium. *Ophthalmology*.
32. Buitendijk GH, Rohtchina E, Myers C, et al. Prediction of Age-related Macular Degeneration in the General Population: The Three Continent AMD Consortium. *Ophthalmology* 2013.
33. Marano F, Deutman AF, Leys A, Aandekerck AL. Hereditary retinal dystrophies and choroidal neovascularization. *Graefe's Archive for Clinical and Experimental Ophthalmology* 2000;238:760-764.
34. Wang L, Clark ME, Crossman DK, et al. Abundant lipid and protein components of drusen. *PLoS One* 2010;5:e10329.
35. Green WR, Enger C. Age-related macular degeneration histopathologic studies. The 1992 Lorenz E. Zimmerman Lecture. *Ophthalmology* 1993;100:1519-1535.
36. Sarks SH. Council Lecture. Drusen and their relationship to senile macular degeneration. *Aust J Ophthalmol* 1980;8:117-130.
37. Mullins RF, Russell SR, Anderson DH, Hageman GS. Drusen associated with aging and age-related macular degeneration contain proteins common to extracellular deposits associated with atherosclerosis, elastosis, amyloidosis, and dense deposit disease. *Faseb J* 2000;14:835-846.



38. Mullins RF, Hageman GS. Human ocular drusen possess novel core domains with a distinct carbohydrate composition. *J Histochem Cytochem* 1999;47:1533-1540.
39. Anderson DH, Ozaki S, Nealon M, et al. Local cellular sources of apolipoprotein E in the human retina and retinal pigmented epithelium: implications for the process of drusen formation. *Am J Ophthalmol* 2001;131:767-781.
40. Crabb JW, Miyagi M, Gu X, et al. Drusen proteome analysis: an approach to the etiology of age-related macular degeneration. *Proc Natl Acad Sci U S A* 2002;99:14682-14687.
41. Malek G, Li CM, Guidry C, Medeiros NE, Curcio CA. Apolipoprotein B in cholesterol-containing drusen and basal deposits of human eyes with age-related maculopathy. *Am J Pathol* 2003;162:413-425.
42. Li CM, Chung BH, Presley JB, et al. Lipoprotein-like particles and cholesteryl esters in human Bruch's membrane: initial characterization. *Invest Ophthalmol Vis Sci* 2005;46:2576-2586.
43. Lengyel I, Flinn JM, Peto T, et al. High concentration of zinc in sub-retinal pigment epithelial deposits. *Exp Eye Res* 2007;84:772-780.
44. Bird AC, Bressler NM, Bressler SB, et al. An international classification and grading system for age-related maculopathy and age-related macular degeneration. The International ARM Epidemiological Study Group. *Surv Ophthalmol* 1995;39:367-374.
45. Seddon JM, Sharma S, Adelman RA. Evaluation of the clinical age-related maculopathy staging system. *Ophthalmology* 2006;113:260-266.
46. Ferris FL, Davis MD, Clemons TE, et al. A simplified severity scale for age-related macular degeneration: AREDS Report No. 18. *Arch Ophthalmol* 2005;123:1570-1574.
47. Sarks JP, Sarks SH, Killingsworth MC. Evolution of soft drusen in age-related macular degeneration. *Eye (Lond)* 1994;8 (Pt 3):269-283.
48. Khanifar AA, Koreishi AF, Izatt JA, Toth CA. Drusen ultrastructure imaging with spectral domain optical coherence tomography in age-related macular degeneration. *Ophthalmology* 2008;115:1883-1890.
49. Agarwal A. *Gass' Atlas of Macular Diseases*. fifth ed. Nashville: Elsevier; 2012.
50. Querques G, Guigui B, Leveziel N, et al. Insights into pathology of cuticular drusen from integrated confocal scanning laser ophthalmoscopy imaging and corresponding spectral domain optical coherence tomography. *Graefes Arch Clin Exp Ophthalmol* 2011;249:1617-1625.
51. Meyerle CB, Smith RT, Barbazetto IA, Yannuzzi LA. Autofluorescence of basal laminar drusen. *Retina* 2007;27:1101-1106.
52. Spaide RF, Curcio CA. Drusen characterization with multimodal imaging. *Retina* 2010;30:1441-1454.
53. van de Ven JP, Smailhodzic D, Boon CJ, et al. Association analysis of genetic and environmental risk factors in the cuticular drusen subtype of age-related macular degeneration. *Mol Vis* 2012;18:2271-2278.
54. Reynolds R, Hartnett ME, Atkinson JP, Giclas PC, Rosner B, Seddon JM. Plasma complement components and activation fragments: associations with age-related macular degeneration genotypes and phenotypes. *Invest Ophthalmol Vis Sci* 2009;50:5818-5827.
55. Scholl HP, Charbel Issa P, Walier M, et al. Systemic complement activation in age-related macular degeneration. *PLoS One* 2008;3:e2593.
56. Mimoun G, Soubrane G, Coscas G. Macular drusen. *J Fr Ophthalmol* 1990;13:511-530.
57. Klein R, Davis MD, Magli YL, Segal P, Klein BE, Hubbard L. The Wisconsin age-related maculopathy grading system. *Ophthalmology* 1991;98:1128-1134.
58. Knudtson MD, Klein R, Klein BE, Lee KE, Meuer SM, Tomany SC. Location of lesions associated with age-related maculopathy over a 10-year period: the Beaver Dam Eye Study. *Invest Ophthalmol Vis Sci* 2004;45:2135-2142.

59. Klein R, Meuer SM, Knudtson MD, Iyengar SK, Klein BE. The epidemiology of retinal reticular drusen. *Am J Ophthalmol* 2008;145:317-326.
60. Fleckenstein M, Charbel Issa P, Helb HM, et al. High-resolution spectral domain-OCT imaging in geographic atrophy associated with age-related macular degeneration. *Invest Ophthalmol Vis Sci* 2008;49:4137-4144.
61. Schmitz-Valckenberg S, Steinberg JS, Fleckenstein M, Visvalingam S, Brinkmann CK, Holz FG. Combined Confocal Scanning Laser Ophthalmoscopy and Spectral-Domain Optical Coherence Tomography Imaging of Reticular Drusen Associated with Age-Related Macular Degeneration. *Ophthalmology* 2010;117:1169-1176.
62. Zweifel SA, Spaide RF, Curcio CA, Malek G, Imamura Y. Reticular pseudodrusen are subretinal drusenoid deposits. *Ophthalmology* 2010;117:303-312 e301.
63. Guigui B, Leveziel N, Martinet V, et al. Angiography features of early onset drusen. *Br J Ophthalmol* 2011;95:238-244.
64. Wabbels B, Demmler A, Paunescu K, Wegscheider E, Preising MN, Lorenz B. Fundus autofluorescence in children and teenagers with hereditary retinal diseases. *Graefes Arch Clin Exp Ophthalmol* 2006;244:36-45.
65. Boon CJ, Theelen T, Hoefsloot EH, et al. Clinical and molecular genetic analysis of best vitelliform macular dystrophy. *Retina (Philadelphia, Pa)* 2009;29:835-847.
66. Spaide RF, Noble K, Morgan A, Freund KB. Vitelliform macular dystrophy. *Ophthalmology* 2006;113:1392-1400.
67. Boon CJ, Klevering BJ, Leroy BP, Hoyng CB, Keunen JE, den Hollander AI. The spectrum of ocular phenotypes caused by mutations in the BEST1 gene. *Progress in Retinal and Eye Research* 2009;28:187-205.
68. Freund KB, Laud K, Lima LH, Spaide RF, Zweifel S, Yannuzzi LA. Acquired Vitelliform Lesions: correlation of clinical findings and multiple imaging analyses. *Retina (Philadelphia, Pa)* 2011;31:13-25.
69. Wang JJ, Foran S, Smith W, Mitchell P. Risk of age-related macular degeneration in eyes with macular drusen or hyperpigmentation: the Blue Mountains Eye Study cohort. *Arch Ophthalmol* 2003;121:658-663.
70. Folgar FA, Chow JH, Farsiu S, et al. Spatial correlation between hyperpigmentary changes on color fundus photography and hyperreflective foci on SDOCT in intermediate AMD. *Invest Ophthalmol Vis Sci* 2012;53:4626-4633.
71. Fleckenstein M, Schmitz-Valckenberg S, Adrion C, et al. Tracking progression with spectral-domain optical coherence tomography in geographic atrophy caused by age-related macular degeneration. *Invest Ophthalmol Vis Sci* 2010;51:3846-3852.
72. Ho J, Witkin AJ, Liu J, et al. Documentation of Intraretinal Retinal Pigment Epithelium Migration via High-Speed Ultrahigh-Resolution Optical Coherence Tomography. *Ophthalmology* 2011;118:687-693.
73. Sarks JP, Sarks SH, Killingsworth MC. Evolution of geographic atrophy of the retinal pigment epithelium. *Eye (Lond)* 1988;2 (Pt 5):552-577.
74. Green WR, Key SN, 3rd. Senile macular degeneration: a histopathologic study. *Trans Am Ophthalmol Soc* 1977;75:180-254.
75. Holz FG, Bindewald-Wittich A, Fleckenstein M, Dreyhaupt J, Scholl HP, Schmitz-Valckenberg S. Progression of geographic atrophy and impact of fundus autofluorescence patterns in age-related macular degeneration. *Am J Ophthalmol* 2007;143:463-472.
76. Bindewald A, Schmitz-Valckenberg S, Jorzik JJ, et al. Classification of abnormal fundus autofluorescence patterns in the junctional zone of geographic atrophy in patients with age related macular degeneration. *Br J Ophthalmol* 2005;89:874-878.



77. Yannuzzi LA, Negrao S, Iida T, et al. Retinal angiomatous proliferation in age-related macular degeneration. *Retina* 2001;21:416-434.
78. Yannuzzi LA, Wong DW, Sforzolini BS, et al. Polypoidal choroidal vasculopathy and neovascularized age-related macular degeneration. *Arch Ophthalmol* 1999;117:1503-1510.
79. Dandekar SS, Jenkins SA, Peto T, et al. Autofluorescence imaging of choroidal neovascularization due to age-related macular degeneration. *Arch Ophthalmol* 2005;123:1507-1513.
80. Framme C, Bunse A, Sofroni R, et al. Fundus autofluorescence before and after photodynamic therapy for choroidal neovascularization secondary to age-related macular degeneration. *Ophthalmic Surg Lasers Imaging* 2006;37:406-414.
81. Yamagishi T, Koizumi H, Yamazaki T, Kinoshita S. Fundus autofluorescence in polypoidal choroidal vasculopathy. *Ophthalmology* 2012;119:1650-1657.
82. Suzuki M, Gomi F, Sawa M, Ueno C, Nishida K. Changes in fundus autofluorescence in polypoidal choroidal vasculopathy during 3 years of follow-up. *Graefes Arch Clin Exp Ophthalmol* 2013.
83. McBain VA, Kumari R, Townend J, Lois N. Geographic atrophy in retinal angiomatous proliferation. *Retina* 2011;31:1043-1052.
84. McBain VA, Townend J, Lois N. Fundus autofluorescence in exudative age-related macular degeneration. *Br J Ophthalmol* 2007;91:491-496.
85. Subfoveal neovascular lesions in age-related macular degeneration. Guidelines for evaluation and treatment in the macular photocoagulation study. Macular Photocoagulation Study Group. *Arch Ophthalmol* 1991;109:1242-1257.
86. Grossniklaus HE, Miskala PH, Green WR, et al. Histopathologic and ultrastructural features of surgically excised subfoveal choroidal neovascular lesions: submacular surgery trials report no. 7. *Arch Ophthalmol* 2005;123:914-921.
87. Jackson GR, Owsley C, McGwin G, Jr. Aging and dark adaptation. *Vision Res* 1999;39:3975-3982.
88. Westeneng-van Haften SC, Boon CJ, Cremers FP, Hoefsloot LH, den Hollander AI, Hoyng CB. Clinical and genetic characteristics of late-onset Stargardt's disease. *Ophthalmology* 2012;119:1199-1210.
89. Boon CJ, van Schooneveld MJ, den Hollander AI, et al. Mutations in the peripherin/RDS gene are an important cause of multifocal pattern dystrophy simulating STGD1/fundus flavimaculatus. *British Journal of Ophthalmology* 2007;91:1504-1511.
90. Isashiki Y, Tabata Y, Kamimura K, Ohba N. Sorsby's fundus dystrophy in two Japanese families with unusual clinical features. *Japanese Journal of Ophthalmology* 1999;43:472-480.
91. Peters AL, Young MJ, Miller JK. Optical coherence tomography for assessing disease progression in sorsby fundus dystrophy. *Retina (Philadelphia, Pa)* 2006;26:1082-1084.
92. Querques G, Guigui B, Leveziel N, Querques L, Bandello F, Souied EH. Multimodal morphological and functional characterization of Malattia Leventinese. *Graefes Arch Clin Exp Ophthalmol* 2012;251:705-714.
93. Puche N, Querques G, Benhamou N, et al. High-resolution spectral domain optical coherence tomography features in adult onset foveomacular vitelliform dystrophy. *British Journal of Ophthalmology* 2010;94:1190-1196.
94. Renner AB, Tillack H, Kraus H, et al. Morphology and functional characteristics in adult vitelliform macular dystrophy. *Retina* 2004;24:929-939.
95. Seddon JM, Ajani UA, Mitchell BD. Familial aggregation of age-related maculopathy. *Am J Ophthalmol* 1997;123:199-206.
96. Sobrin L, Maller JB, Neale BM, et al. Genetic profile for five common variants associated with age-related macular degeneration in densely affected families: a novel analytic approach. *Eur J Hum Genet* 2010;18:496-501.

97. Klevering BJ, Deutman AF, Maueri A, Cremers FP, Hoyng CB. The spectrum of retinal phenotypes caused by mutations in the ABCA4 gene. *Graefes Archive for Clinical and Experimental Ophthalmology* 2005;243:90-100.
98. Allikmets R. Stargardt disease: from gene discovery to therapy. In: Tombran-Tink BC, eds. (ed), *Retinal degeneration: Biology, Diagnostics and Therapeutics*. Totowa, NJ: Humana Press; 2007:105-118.
99. Burke TR, Tsang SH. Allelic and phenotypic heterogeneity in ABCA4 mutations. *Ophthalmic Genetics* 2011;32:165-174.
100. Boon CJ, den Hollander AI, Hoyng CB, Cremers FP, Klevering BJ, Keunen JE. The spectrum of retinal dystrophies caused by mutations in the peripherin/RDS gene. *Progress in Retinal and Eye Research* 2008;27:213-235.
101. Doyne R. Peculiar condition of choroiditis occurring in several members of the same family. *Trans Ophthalmol Soc UK* 1899;19:71.
102. Evans K, Gregory CY, Wijesuriya SD, et al. Assessment of the phenotypic range seen in Doyne honeycomb retinal dystrophy. *Arch Ophthalmol* 1997;115:904-910.
103. Piguet B, Haimovici R, Bird AC. Dominantly inherited drusen represent more than one disorder: a historical review. *Eye (Lond)* 1995;9 (Pt 1):34-41.
104. Souied EH, Leveziel N, Querques G, Darmon J, Coscas G, Soubrane G. Indocyanine green angiography features of Malattia leventinese. *Br J Ophthalmol* 2006;90:296-300.
105. Haimovici R, Wroblewski J, Piguet B, et al. Symptomatic abnormalities of dark adaptation in patients with EFEMP1 retinal dystrophy (Malattia Leventinese/Doyne honeycomb retinal dystrophy). *Eye (Lond)* 2002;16:7-15.
106. Michaelides M, Jenkins SA, Brantley MA, Jr., et al. Maculopathy due to the R345W substitution in fibulin-3: distinct clinical features, disease variability, and extent of retinal dysfunction. *Invest Ophthalmol Vis Sci* 2006;47:3085-3097.
107. Takeuchi T, Hayashi T, Bedell M, Zhang K, Yamada H, Tsuneoka H. A novel haplotype with the R345W mutation in the EFEMP1 gene associated with autosomal dominant drusen in a Japanese family. *Invest Ophthalmol Vis Sci* 2010;51:1643-1650.
108. Marmorstein L. Association of EFEMP1 with malattia leventinese and age-related macular degeneration: a mini-review. *Ophthalmic Genet* 2004;25:219-226.
109. Schmitz-Valckenberg S, Fleckenstein M, Scholl HP, Holz FG. Fundus autofluorescence and progression of age-related macular degeneration. *Survey of Ophthalmology* 2009;54:96-117.
110. von Ruckmann A, Schmidt KG, Fitzke FW, Bird AC, Jacobi KW. Fundus autofluorescence in patients with hereditary macular dystrophies, malattia leventinese, familial dominant and aged-related drusen. *Klin Monbl Augenheilkd* 1998;213:81-86.
111. Souied EH, Leveziel N, Letien V, Darmon J, Coscas G, Soubrane G. Optical coherent tomography features of malattia leventinese. *Am J Ophthalmol* 2006;141:404-407.
112. Gerber DM, Niemeyer G. Ganzfeld and multifocal electroretinography in Malattia Leventinese and Zermatt Macular Dystrophy. *Klinische Monatsblätter für Augenheilkunde* 2002;219:206-210.
113. Stone EM, Lotery AJ, Munier FL, et al. A single EFEMP1 mutation associated with both Malattia Leventinese and Doyne honeycomb retinal dystrophy. *Nat Genet* 1999;22:199-202.
114. Dusek J, Streicher T, Schmidt K. Hereditary drusen of Bruch's membrane. II: Studies of semi-thin sections and electron microscopy results. *Klinische Monatsblätter für Augenheilkunde* 1982;181:79-83.
115. Collins ET. A pathological report upon a case of Doyne's choroiditis ('Honeycomb' or 'family' choroiditis). *The ophthalmoscope* 1913;11:2.

116. Zhang Y, Marmorstein LY. Focus on molecules: fibulin-3 (EFEMP1). *Experimental Eye Research* 2010;90:374-375.
117. Marmorstein LY, Munier FL, Arsenijevic Y, et al. Aberrant accumulation of EFEMP1 underlies drusen formation in Malattia Leventinese and age-related macular degeneration. *Proceedings of the National Academy of Sciences of the United States of America* 2002;99:13067-13072.
118. Fu L, Garland D, Yang Z, et al. The R345W mutation in EFEMP1 is pathogenic and causes AMD-like deposits in mice. *Human Molecular Genetics* 2007;16:2411-2422.
119. Marmorstein LY, McLaughlin PJ, Peachey NS, Sasaki T, Marmorstein AD. Formation and progression of sub-retinal pigment epithelium deposits in Efemp1 mutation knock-in mice: a model for the early pathogenic course of macular degeneration. *Human Molecular Genetics* 2007;16:2423-2432.
120. Saihan Z, Li Z, Rice J, et al. Clinical and biochemical effects of the E139K missense mutation in the TIMP3 gene, associated with Sorsby fundus dystrophy. *Molecular Vision* 2009;15:1218-1230.
121. Sivaprasad S, Webster AR, Egan CA, Bird AC, Tufail A. Clinical course and treatment outcomes of Sorsby fundus dystrophy. *American Journal of Ophthalmology* 2008;146:228-234.
122. Szental JA, Harper CA, Baird PN, Michalova K, Guymer RH. Sorsby's Fundus Dystrophy: a case report to raise awareness of the disease and potential future treatments. *Clinical & Experimental Ophthalmology* 2009;37:325-327.
123. Hoskin A, Sehmi K, Bird AC. Sorsby's pseudoinflammatory macular dystrophy. *British Journal of Ophthalmology* 1981;65:859-865.
124. Polkinghorne PJ, Capon MR, Berninger T, Lyness AL, Sehmi K, Bird AC. Sorsby's fundus dystrophy. A clinical study. *Ophthalmology* 1989;96:1763-1768.
125. Lin RJ, Blumenkranz MS, Binkley J, Wu K, Vollrath D. A novel His158Arg mutation in TIMP3 causes a late-onset form of Sorsby fundus dystrophy. *American Journal of Ophthalmology* 2006;142:839-848.
126. Felbor U, Benkwitz C, Klein ML, Greenberg J, Gregory CY, Weber BH. Sorsby fundus dystrophy: reevaluation of variable expressivity in patients carrying a TIMP3 founder mutation. *Archives of Ophthalmology* 1997;115:1569-1571.
127. Capon MR, Marshall J, Krafft JI, Alexander RA, Hiscott PS, Bird AC. Sorsby's fundus dystrophy. A light and electron microscopic study. *Ophthalmology* 1989;96:1769-1777.
128. Capon MR, Polkinghorne PJ, Fitzke FW, Bird AC. Sorsby's pseudoinflammatory macula dystrophy-Sorsby's fundus dystrophies. *Eye (London, England)* 1988;2 (Pt 1):114-122.
129. Schoenberger SD, Agarwal A. A Novel Mutation at the N-Terminal Domain of the Timp3 Gene in Sorsby Fundus Dystrophy. *Retina (Philadelphia, Pa)* 2013;33:429-435.
130. Boon CJ, Jeroen Klevering B, Keunen JE, Hoyng CB, Theelen T. Fundus autofluorescence imaging of retinal dystrophies. *Vision Research* 2008;48:2569-2577.
131. Lip PL, Good PA, Gibson JM. Sorsby's fundus dystrophy: a case report of 24 years follow-up with electrodiagnostic tests and indocyanine green angiography. *Eye (London, England)* 1999;13 (Pt 1):16-25.
132. Assink JJ, de Backer E, ten Brink JB, et al. Sorsby fundus dystrophy without a mutation in the TIMP-3 gene. *British Journal of Ophthalmology* 2000;84:682-686.
133. Hamilton WK, Ewing CC, Ives EJ, Carruthers JD. Sorsby's fundus dystrophy. *Ophthalmology* 1989;96:1755-1762.
134. Stohr H, Anand-Apte B. A review and update on the molecular basis of pathogenesis of Sorsby fundus dystrophy. *Advances in Experimental Medicine and Biology* 2012;723:261-267.
135. Weber BH, Vogt G, Pruett RC, Stohr H, Felbor U. Mutations in the tissue inhibitor of metalloproteinases-3 (TIMP3) in patients with Sorsby's fundus dystrophy. *Nat Genet* 1994;8:352-356.

136. Della NG, Campochiaro PA, Zack DJ. Localization of TIMP-3 mRNA expression to the retinal pigment epithelium. *Investigative Ophthalmology & Visual Science* 1996;37:1921-1924.
137. Qi JH, Ebrahem Q, Moore N, et al. A novel function for tissue inhibitor of metalloproteinases-3 (TIMP3): inhibition of angiogenesis by blockage of VEGF binding to VEGF receptor-2. *Nature Medicine* 2003;9:407-415.
138. Langton KP, McKie N, Curtis A, et al. A novel tissue inhibitor of metalloproteinases-3 mutation reveals a common molecular phenotype in Sorsby's fundus dystrophy. *Journal of Biological Chemistry* 2000;275:27027-27031.
139. Langton KP, McKie N, Smith BM, Brown NJ, Barker MD. Sorsby's fundus dystrophy mutations impair turnover of TIMP-3 by retinal pigment epithelial cells. *Human Molecular Genetics* 2005;14:3579-3586.
140. Fariss RN, Apte SS, Luthert PJ, Bird AC, Milam AH. Accumulation of tissue inhibitor of metalloproteinases-3 in human eyes with Sorsby's fundus dystrophy or retinitis pigmentosa. *British Journal of Ophthalmology* 1998;82:1329-1334.
141. Lefler WH, Wadsworth JA, Sidbury JB, Jr. Hereditary macular degeneration and amino-aciduria. *American Journal of Ophthalmology* 1971;71:224-230.
142. Small KW, Killian J, McLean WC. North Carolina's dominant progressive foveal dystrophy: how progressive is it? *British Journal of Ophthalmology* 1991;75:401-406.
143. Schworm HD, Ulbig MW, Hoops J, et al. North Carolina macular dystrophy. Hereditary macular disease with good functional prognosis. *Der Ophthalmologe* 1998;95:13-18.
144. Szlyk JP, Paliga J, Seiple W, Rabb MF. Comprehensive functional vision assessment of patients with North Carolina macular dystrophy (MCDR1). *Retina (Philadelphia, Pa)* 2005;25:489-497.
145. Small KW. North Carolina macular dystrophy, revisited. *Ophthalmology* 1989;96:1747-1754.
146. Kiernan DF, Shah RJ, Hariprasad SM, et al. Thirty-Year follow-up of an African American family with macular dystrophy of the retina, locus 1 (North Carolina macular dystrophy). *Ophthalmology* 2011;118:1435-1443.
147. Rosenberg T, Roos B, Johnsen T, et al. Clinical and genetic characterization of a Danish family with North Carolina macular dystrophy. *Molecular Vision* 2010;16:2659-2668.
148. Small KW. North Carolina macular dystrophy: clinical features, genealogy, and genetic linkage analysis. *Transactions of the American Ophthalmological Society* 1998;96:925-961.
149. Reichel MB, Kelsell RE, Fan J, et al. Phenotype of a British North Carolina macular dystrophy family linked to chromosome 6q. *British Journal of Ophthalmology* 1998;82:1162-1168.
150. Khurana RN, Sun X, Pearson E, et al. A reappraisal of the clinical spectrum of North Carolina macular dystrophy. *Ophthalmology* 2009;116:1976-1983.
151. Yang Z, Tong Z, Chorich LJ, et al. Clinical characterization and genetic mapping of North Carolina macular dystrophy. *Vision Research* 2008;48:470-477.
152. Small KW, Weber JL, Roses A, Lennon F, Vance JM, Pericak-Vance MA. North Carolina macular dystrophy is assigned to chromosome 6. *Genomics* 1992;13:681-685.
153. Michaelides M, Johnson S, Tekriwal AK, et al. An early-onset autosomal dominant macular dystrophy (MCDR3) resembling North Carolina macular dystrophy maps to chromosome 5. *Invest Ophthalmol Vis Sci* 2003;44:2178-2183.
154. Voo I, Glasgow BJ, Flannery J, Udar N, Small KW. North Carolina macular dystrophy: clinicopathologic correlation. *American Journal of Ophthalmology* 2001;132:933-935.
155. Small KW, Voo I, Flannery J, Udar N, Glasgow BJ. North Carolina macular dystrophy: clinicopathologic correlation. *Transactions of the American Ophthalmological Society* 2001;99:233-237; discussion 237-238.
156. Borooh S, Collins C, Wright A, Dhillon B. Late-onset retinal macular degeneration: clinical insights into an inherited retinal degeneration. *British Journal of Ophthalmology* 2009;93:284-289.

157. Kuntz CA, Jacobson SG, Cideciyan AV, et al. Sub-retinal pigment epithelial deposits in a dominant late-onset retinal degeneration. *Investigative Ophthalmology & Visual Science* 1996;37:1772-1782.
158. Milam AH, Curcio CA, Cideciyan AV, et al. Dominant late-onset retinal degeneration with regional variation of sub-retinal pigment epithelium deposits, retinal function, and photoreceptor degeneration. *Ophthalmology* 2000;107:2256-2266.
159. Soumpelis V, Sergouniotis PI, Robson AG, et al. Phenotypic findings in C1QTNF5 retinopathy (late-onset retinal degeneration). *Acta Ophthalmologica* 2013;91:e191-195.
160. Vincent A, Munier FL, Vandenhoven CC, Wright T, Westall CA, Heon E. The characterization of retinal phenotype in a family with C1QTNF5-related late-onset retinal degeneration. *Retina (Philadelphia, Pa)* 2012;32:1643-1651.
161. Hayward C, Shu X, Cideciyan AV, et al. Mutation in a short-chain collagen gene, CTRP5, results in extracellular deposit formation in late-onset retinal degeneration: a genetic model for age-related macular degeneration. *Human Molecular Genetics* 2003;12:2657-2667.
162. Chavali VR, Khan NW, Cukras CA, Bartsch DU, Jablonski MM, Ayyagari R. A CTRP5 gene S163R mutation knock-in mouse model for late-onset retinal degeneration. *Human Molecular Genetics* 2011;20:2000-2014.
163. Shu X, Tulloch B, Lennon A, et al. Disease mechanisms in late-onset retinal macular degeneration associated with mutation in C1QTNF5. *Human Molecular Genetics* 2006;15:1680-1689.
164. Stargardt K. Über familiäre, progressive Degeneration in der Maculagegend des Auges. *Graefes Arch Clin Exp Ophthalmol* 1909;71:534-550.
165. Maugeri A, van Driel MA, van de Pol DJ, et al. The 2588G-->C mutation in the ABCR gene is a mild frequent founder mutation in the Western European population and allows the classification of ABCR mutations in patients with Stargardt disease. *American Journal of Human Genetics* 1999;64:1024-1035.
166. Jaakson K, Zernant J, Kulm M, et al. Genotyping microarray (gene chip) for the ABCR (ABCA4) gene. *Human Mutation* 2003;22:395-403.
167. Armstrong JD, Meyer D, Xu S, Elfervig JL. Long-term follow-up of Stargardt's disease and fundus flavimaculatus. *Ophthalmology* 1998;105:448-457; discussion 457-448.
168. Pawlak D, Souied E, Mimoun G, Papp-Pawlak M, Coscas G, Soubrane G. Fundus flavimaculatus and choroidal neovascularization. *J Fr Ophtalmol* 2006;29:188-194.
169. Souied EH, Pawlak D, Algan M, Sayag D, Coscas G, Soubrane G. Photodynamic therapy for choroidal neovascularization on late-onset fundus flavimaculatus. *American Journal of Ophthalmology* 2005;140:312-314.
170. Allikmets R, Shroyer NF, Singh N, et al. Mutation of the Stargardt disease gene (ABCR) in age-related macular degeneration. *Science* 1997;277:1805-1807.
171. Holz FG, Bellman C, Staudt S, Schutt F, Volcker HE. Fundus autofluorescence and development of geographic atrophy in age-related macular degeneration. *Invest Ophthalmol Vis Sci* 2001;42:1051-1056.
172. Radu RA, Mata NL, Bagla A, Travis GH. Light exposure stimulates formation of A2E oxiranes in a mouse model of Stargardt's macular degeneration. *Proceedings of the National Academy of Sciences of the United States of America* 2004;101:5928-5933.
173. Quazi F, Lenevich S, Molday RS. ABCA4 is an N-retinylidene-phosphatidylethanolamine and phosphatidylethanolamine importer. *Nature Communications* 2012;3:925.
174. Sparrow JR, Vollmer-Snarr HR, Zhou J, et al. A2E-epoxides damage DNA in retinal pigment epithelial cells. Vitamin E and other antioxidants inhibit A2E-epoxide formation. *Journal of Biological Chemistry* 2003;278:18207-18213.

175. Mata NL, Tzekov RT, Liu X, Weng J, Birch DG, Travis GH. Delayed dark-adaptation and lipofuscin accumulation in abcr+/- mice: implications for involvement of ABCR in age-related macular degeneration. *Invest Ophthalmol Vis Sci* 2001;42:1685-1690.
176. Radu RA, Hu J, Yuan Q, et al. Complement system dysregulation and inflammation in the retinal pigment epithelium of a mouse model for Stargardt macular degeneration. *Journal of Biological Chemistry* 2011;286:18593-18601.
177. Age-Related Eye Disease Study Research G. A randomized, placebo-controlled, clinical trial of high-dose supplementation with vitamins C and E, beta carotene, and zinc for age-related macular degeneration and vision loss: AREDS report no. 8. *Archives of Ophthalmology* 2001;119:1417-1436.
178. Radu RA, Yuan Q, Hu J, et al. Accelerated accumulation of lipofuscin pigments in the RPE of a mouse model for ABCA4-mediated retinal dystrophies following Vitamin A supplementation. *Investigative Ophthalmology & Visual Science* 2008;49:3821-3829.
179. Alkuraya H, Zhang K. Pattern Dystrophy of the Retinal Pigment Epithelium. *Retinal Physician* 2010.
180. Kim RY, Dollfus H, Keen TJ, et al. Autosomal dominant pattern dystrophy of the retina associated with a 4-base pair insertion at codon 140 in the peripherin/RDS gene. *Arch Ophthalmol* 1995;113:451-455.
181. Yang Z, Li Y, Jiang L, et al. A novel RDS/peripherin gene mutation associated with diverse macular phenotypes. *Ophthalmic Genet* 2004;25:133-145.
182. Sohn EH, Mullins RF, Stone EM. Macular dystrophies. In: Ryan JR (ed), *Retina*. London, New York, Oxford, St. Louis, Sydney, Toronto: Elsevier; 2013.
183. Deutman AF, van Blommestein JD, Henkes HE, Waardenburg PJ, Solleveld-van Driest E. Butterfly-shaped pigment dystrophy of the fovea. *Arch Ophthalmol* 1970;83:558-569.
184. Sjogren H. Dystrophia reticularis laminae pigmentosae retinae, an earlier not described hereditary eye disease. *Acta Ophthalmol (Copenh)* 1950;28:279-295.
185. Slezak H, Hommer K. Fundus pulverulentus. *Albrecht Von Graefes Arch Klin Exp Ophthalmol* 1969;178:176-182.
186. Agarwal A, Patel P, Adkins T, Gass JD. Spectrum of pattern dystrophy in pseudoxanthoma elasticum. *Archives of Ophthalmology* 2005;123:923-928.
187. Vaclavik V, Tran HV, Gaillard MC, Schorderet DF, Munier FL. Pattern dystrophy with high intrafamilial variability associated with Y141C mutation in the peripherin/RDS gene and successful treatment of subfoveal CNV related to multifocal pattern type with anti-VEGF (ranibizumab) intravitreal injections. *Retina (Philadelphia, Pa)* 2012;32:1942-1949.
188. Tuppurainen K, Mantyjarvi M. The importance of fluorescein angiography in diagnosing pattern dystrophies of the retinal pigment epithelium. *Doc Ophthalmol* 1994;87:233-243.
189. Hannan SR, de Salvo G, Stinghe A, Shawkat F, Lotery AJ. Common spectral domain OCT and electrophysiological findings in different pattern dystrophies. *Br J Ophthalmol* 2013;97:605-610.
190. Fishman GA, Birch DG, Holder GE, al. e. Electrophysiologic testing in disorders of the retina, optic nerve, and visual pathway. *Ophthalmology Monograph*. San Francisco: Foundation of the American Academy of Ophthalmology; 2001.
191. Jaouni T, Averbukh E, Burstyn-Cohen T, et al. Association of pattern dystrophy with an HTRA1 single-nucleotide polymorphism. *Arch Ophthalmol* 2012;130:987-991.
192. Arikawa K, Molday LL, Molday RS, Williams DS. Localization of peripherin/rds in the disk membranes of cone and rod photoreceptors: relationship to disk membrane morphogenesis and retinal degeneration. *J Cell Biol* 1992;116:659-667.



193. Connell G, Bascom R, Molday L, Reid D, McInnes RR, Molday RS. Photoreceptor peripherin is the normal product of the gene responsible for retinal degeneration in the rds mouse. *Proc Natl Acad Sci U S A* 1991;88:723-726.
194. Travis GH, Sutcliffe JG, Bok D. The retinal degeneration slow (rds) gene product is a photoreceptor disc membrane-associated glycoprotein. *Neuron* 1991;6:61-70.
195. Zhang K, Garibaldi DC, Li Y, Green WR, Zack DJ. Butterfly-shaped pattern dystrophy: a genetic, clinical, and histopathological report. *Arch Ophthalmol* 2002;120:485-490.
196. Arnold JJ, Sarks JP, Killingsworth MC, Kettle EK, Sarks SH. Adult vitelliform macular degeneration: a clinicopathological study. *Eye (Lond)* 2003;17:717-726.
197. Wickham L, Chen FK, Lewis GP, et al. Clinicopathological case series of four patients with inherited macular disease. *Invest Ophthalmol Vis Sci* 2009;50:3553-3561.
198. Querques G, Forte R, Querques L, Massamba N, Souied EH. Natural course of adult-onset foveomacular vitelliform dystrophy: a spectral-domain optical coherence tomography analysis. *American Journal of Ophthalmology* 2011;152:304-313.
199. Boon CJ, Klevering BJ, den Hollander AI, et al. Clinical and genetic heterogeneity in multifocal vitelliform dystrophy. *Archives of Ophthalmology* 2007;125:1100-1106.
200. Mimoun G, Caillaux V, Querques G, Rothschild PR, Puche N, Souied EH. Ranibizumab for choroidal neovascularization associated with adult-onset foveomacular vitelliform dystrophy: one-year results. *Retina (Philadelphia, Pa)* 2013;33:513-521.
201. Querques G, Regenbogen M, Quijano C, Delphin N, Soubrane G, Souied EH. High-definition optical coherence tomography features in vitelliform macular dystrophy. *Am J Ophthalmol* 2008;146:501-507.
202. Zhuk SA, Edwards AO. Peripherin/RDS and VMD2 mutations in macular dystrophies with adult-onset vitelliform lesion. *Molecular Vision* 2006;12:811-815.
203. Brecher R, Bird AC. Adult vitelliform macular dystrophy. *Eye (London, England)* 1990;4 (Pt 1):210-215.
204. Kramer F, White K, Pauleikhoff D, et al. Mutations in the VMD2 gene are associated with juvenile-onset vitelliform macular dystrophy (Best disease) and adult vitelliform macular dystrophy but not age-related macular degeneration. *Eur J Hum Genet* 2000;8:286-292.
205. Seddon JM, Afshari MA, Sharma S, et al. Assessment of mutations in the Best macular dystrophy (VMD2) gene in patients with adult-onset foveomacular vitelliform dystrophy, age-related maculopathy, and bull's-eye maculopathy. *Ophthalmology* 2001;108:2060-2067.
206. Dubovy SR, Hairston RJ, Schatz H, et al. Adult-onset foveomacular pigment epithelial dystrophy: clinicopathologic correlation of three cases. *Retina (Philadelphia, Pa)* 2000;20:638-649.
207. Gass JD. A clinicopathologic study of a peculiar foveomacular dystrophy. *Trans Am Ophthalmol Soc* 1974;72:139-156.
208. Patrinely JR, Lewis RA, Font RL. Foveomacular vitelliform dystrophy, adult type. A clinicopathologic study including electron microscopic observations. *Ophthalmology* 1985;92:1712-1718.
209. Clemett R. Vitelliform dystrophy: long-term observations on New Zealand pedigrees. *Australian and New Zealand Journal of Ophthalmology* 1991;19:221-227.
210. Mohler CW, Fine SL. Long-term evaluation of patients with Best's vitelliform dystrophy. *Ophthalmology* 1981;88:688-692.
211. Wabbels B, Preising MN, Kretschmann U, Demmler A, Lorenz B. Genotype-phenotype correlation and longitudinal course in ten families with Best vitelliform macular dystrophy. *Graefe's Archive for Clinical and Experimental Ophthalmology* 2006;244:1453-1466.
212. Deutman AF. *Vitelliform dystrophy of the fovea. The hereditary dystrophies of the posterior pole of the eye*. Assen: Van gorcum & Comp. N.V.; 1971.

213. Chung MM, Oh KT, Streb LM, Kimura AE, Stone EM. Visual outcome following subretinal hemorrhage in Best disease. *Retina (Philadelphia, Pa)* 2001;21:575-580.
214. Leu J, Schrage NF, Degenring RF. Choroidal neovascularisation secondary to Best's disease in a 13-year-old boy treated by intravitreal bevacizumab. *Graefe's Archive for Clinical and Experimental Ophthalmology* 2007;245:1723-1725.
215. Deutman AF. Electro-oculography in families with vitelliform dystrophy of the fovea. Detection of the carrier state. *Archives of Ophthalmology* 1969;81:305-316.
216. Petrukhin K, Koisti MJ, Bakall B, et al. Identification of the gene responsible for Best macular dystrophy. *Nat Genet* 1998;19:241-247.
217. Boon CJ, van den Born LI, Visser L, et al. Autosomal recessive bestrophinopathy: differential diagnosis and treatment options. *Ophthalmology* 2013;120:809-820.
218. Boon CJ, Klevering BJ, Cremers FP, et al. Central areolar choroidal dystrophy. *Ophthalmology* 2009;116:771-782, 782 e771.
219. Piguet B, Heon E, Munier FL, et al. Full characterization of the maculopathy associated with an Arg-172-Trp mutation in the RDS/peripherin gene. *Ophthalmic Genetics* 1996;17:175-186.
220. Hoyng CB, Deutman AF. The development of central areolar choroidal dystrophy. *Graefe's Archive for Clinical and Experimental Ophthalmology* 1996;234:87-93.
221. Smailhodzic D, Fleckenstein M, Theelen T, et al. Central areolar choroidal dystrophy (CACD) and age-related macular degeneration (AMD): differentiating characteristics in multimodal imaging. *Investigative Ophthalmology & Visual Science* 2011;52:8908-8918.
222. Renner AB, Fiebig BS, Weber BH, et al. Phenotypic variability and long-term follow-up of patients with known and novel PRPH2/RDS gene mutations. *American Journal of Ophthalmology* 2009;147:518-530.
223. Michaelides M, Holder GE, Bradshaw K, Hunt DM, Moore AT. Cone-rod dystrophy, intrafamilial variability, and incomplete penetrance associated with the R172W mutation in the peripherin/RDS gene. *Ophthalmology* 2005;112:1592-1598.
224. Nakazawa M, Wada Y, Tamai M. Macular dystrophy associated with monogenic Arg172Trp mutation of the peripherin/RDS gene in a Japanese family. *Retina (Philadelphia, Pa)* 1995;15:518-523.
225. Klevering BJ, van Driel M, van Hogerwou AJ, et al. Central areolar choroidal dystrophy associated with dominantly inherited drusen. *British Journal of Ophthalmology* 2002;86:91-96.
226. Ferry AP, Llovera I, Shafer DM. Central areolar choroidal dystrophy. *Archives of Ophthalmology* 1972;88:39-43.
227. Deutman AF, Jansen LM. Dominantly inherited drusen of Bruch's membrane. *British Journal of Ophthalmology* 1970;54:373-382.
228. Gundogan FC, Dinc UA, Erdem U, Ozge G, Sobaci G. Multifocal electroretinogram and central visual field testing in central areolar choroidal dystrophy. *European Journal of Ophthalmology* 2010;20:919-924.
229. Ashton N. Central areolar choroidal sclerosis; a histo-pathological study. *British Journal of Ophthalmology* 1953;37:140-147.
230. Krill AE, Deutman AF, Fishman M. The cone degenerations. *Doc Ophthalmol* 1973;35:1-80.
231. Rowe SE, Trobe JD, Sieving PA. Idiopathic photoreceptor dysfunction causes unexplained visual acuity loss in later adulthood. *Ophthalmology* 1990;97:1632-1637.
232. Francois J, de Rouck A, Verriest G, de Laey JJ, Cambie E. Progressive generalized cone dysfunction. *Ophthalmologica* 1974;169:255-284.
233. Ladewig M, Kraus H, Foerster MH, Kellner U. Cone dysfunction in patients with late-onset cone dystrophy and age-related macular degeneration. *Arch Ophthalmol* 2003;121:1557-1561.



234. Langwinska-Wosko E, Szulborski K, Broniek-Kowalik K. Late onset cone dystrophy. *Doc Ophthalmol* 2010;120:215-218.
235. Kellner U, Kellner S. Clinical findings and diagnostics of cone dystrophy. *Ophthalmologie* 2009;106:99-108.
236. Gilbert CM, Owens SL, Smith PD, Fine SL. Long-term follow-up of central serous chorioretinopathy. *British Journal of Ophthalmology* 1984;68:815-820.
237. Nicholson B, Noble J, Forooghian F, Meyerle C. Central serous chorioretinopathy: update on pathophysiology and treatment. *Survey of Ophthalmology* 2013;58:103-126.
238. Oosterhuis JA. Familial central serous retinopathy. *Graefe's Archive for Clinical and Experimental Ophthalmology* 1996;234:337-341.
239. Yannuzzi LA, Shakin JL, Fisher YL, Altomonte MA. Peripheral retinal detachments and retinal pigment epithelial atrophic tracts secondary to central serous pigment epitheliopathy. *Ophthalmology* 1984;91:1554-1572.
240. Wang M, Munch IC, Hasler PW, Prunte C, Larsen M. Central serous chorioretinopathy. *Acta Ophthalmologica* 2008;86:126-145.
241. Wang MS, Sander B, Larsen M. Retinal atrophy in idiopathic central serous chorioretinopathy. *American Journal of Ophthalmology* 2002;133:787-793.
242. Spaide RF, Klancnik JM, Jr. Fundus autofluorescence and central serous chorioretinopathy. *Ophthalmology* 2005;112:825-833.
243. Giovannini A, Scassellati-Sforzolini B, D'Altobrando E, Mariotti C, Rutili T, Tittarelli R. Choroidal findings in the course of idiopathic serous pigment epithelium detachment detected by indocyanine green videoangiography. *Retina (Philadelphia, Pa)* 1997;17:286-293.
244. Song IS, Shin YU, Lee BR. Time-periodic characteristics in the morphology of idiopathic central serous chorioretinopathy evaluated by volume scan using spectral-domain optical coherence tomography. *American Journal of Ophthalmology* 2012;154:366-375 e364.
245. Inhoffen W, Ziemssen F, Bartz-Schmidt KU. Chronic central serous chorioretinopathy (cCSC): differential diagnosis to choroidal neovascularisation (CNV) secondary to age-related macular degeneration (AMD). *Klinische Monatsblätter für Augenheilkunde* 2012;229:889-896.
246. Castro-Correia J, Coutinho MF, Rosas V, Maia J. Long-term follow-up of central serous retinopathy in 150 patients. *Documenta Ophthalmologica Advances in Ophthalmology* 1992;81:379-386.
247. Chen H, Wu D, Huang S, Guan T, Liu C. Microperimetry evaluation in central serous chorioretinopathy. *Yan Ke Xue Bao* 2006;22:149-153.
248. Weenink AC, Borsje RA, Oosterhuis JA. Familial chronic central serous chorioretinopathy. *Ophthalmologica* 2001;215:183-187.
249. Zhao M, Celerier I, Bousquet E, et al. Mineralocorticoid receptor is involved in rat and human ocular chorioretinopathy. *Journal of Clinical Investigation* 2012;122:2672-2679.
250. Gass JD, Blodi BA. Idiopathic juxtafoveolar retinal telangiectasis. Update of classification and follow-up study. *Ophthalmology* 1993;100:1536-1546.
251. Issa PC, Gillies MC, Chew EY, et al. Macular telangiectasia type 2. *Prog Retin Eye Res* 2013;34:49-77.
252. Schmitz-Valckenberg S, Ong EE, Rubin GS, et al. Structural and functional changes over time in MacTel patients. *Retina* 2009;29:1314-1320.
253. Helb HM, Charbel Issa P, RL VDV, Berendschot TT, Scholl HP, Holz FG. Abnormal Macular Pigment Distribution in Type 2 Idiopathic Macular Telangiectasia. *Retina* 2008;28:808-816.
254. Theelen T, Berendschot TT, Boon CJ, Hoyng CB, Klevering BJ. Analysis of visual pigment by fundus autofluorescence. *Experimental Eye Research* 2008;86:296-304.

255. Charbel Issa P, Berendschot TT, Staurengi G, Holz FG, Scholl HP. Confocal blue reflectance imaging in type 2 idiopathic macular telangiectasia. *Invest Ophthalmol Vis Sci* 2008;49:1172-1177.
256. Powner MB, Gillies MC, Zhu M, Vevis K, Hunyor AP, Fruttiger M. Loss of Muller's Cells and Photoreceptors in Macular Telangiectasia Type 2. *Ophthalmology* 2013; 2013; 120:2344-2352.
257. Gass JD, Oyakawa RT. Idiopathic juxtafoveal retinal telangiectasis. *Arch Ophthalmol* 1982;100:769-780.
258. Gillies MC, Zhu M, Chew E, et al. Familial asymptomatic macular telangiectasia type 2. *Ophthalmology* 2009;116:2422-2429.
259. Issa PC, Helb HM, Rohrschneider K, Holz FG, Scholl HP. Microperimetric assessment of patients with type 2 idiopathic macular telangiectasia. *Invest Ophthalmol Vis Sci* 2007;48:3788-3795.
260. Barbazetto IA, Room M, Yannuzzi NA, et al. ATM gene variants in patients with idiopathic perifoveal telangiectasia. *Investigative Ophthalmology & Visual Science* 2008;49:3806-3811.
261. Parmalee NL, Schubert C, Figueroa M, et al. Identification of a potential susceptibility locus for macular telangiectasia type 2. *Plos One* 2012;7:e24268.
262. Sallo FB, Leung I, Chung M, et al. Retinal crystals in type 2 idiopathic macular telangiectasia. *Ophthalmology* 2011;118:2461-2467.
263. Baumuller S, Charbel Issa P, Scholl HP, Schmitz-Valckenberg S, Holz FG. Outer retinal hyperreflective spots on spectral-domain optical coherence tomography in macular telangiectasia type 2. *Ophthalmology* 2010;117:2162-2168.
264. Powner MB, Gillies MC, Tretiach M, et al. Perifoveal muller cell depletion in a case of macular telangiectasia type 2. *Ophthalmology* 2010;117:2407-2416.
265. Cherepanoff S, Killingsworth MC, Zhu M, et al. Ultrastructural and clinical evidence of subretinal debris accumulation in type 2 macular telangiectasia. *Br J Ophthalmol* 96:1404-1409.
266. Zhu M, Krilis M, Gillies MC. The relationship between inner retinal cavitation, photoreceptor disruption, and the integrity of the outer limiting membrane in macular telangiectasia type 2. *Retina* 2013;33:1547-1550.
267. Goto Y, Nonaka I, Horai S. A mutation in the tRNA(Leu)(UUR) gene associated with the MELAS subgroup of mitochondrial encephalomyopathies. *Nature* 1990;348:651-653.
268. Kobayashi Y, Momoi MY, Tominaga K, et al. A point mutation in the mitochondrial tRNA(Leu)(UUR) gene in MELAS (mitochondrial myopathy, encephalopathy, lactic acidosis and stroke-like episodes). *Biochem Biophys Res Commun* 1990;173:816-822.
269. Massin P, Virally-Monod M, Vialettes B, et al. Prevalence of macular pattern dystrophy in maternally inherited diabetes and deafness. GEDIAM Group. *Ophthalmology* 1999;106:1821-1827.
270. de Laat P, Smeitink JA, Janssen MC, Keunen JE, Boon CJ. Mitochondrial Retinal Dystrophy Associated with the m.3243A>G Mutation. *Ophthalmology* 2013; 2013;120:2684-2696.
271. van den Ouweland JM, Lemkes HH, Ruitenbeek W, et al. Mutation in mitochondrial tRNA(Leu)(UUR) gene in a large pedigree with maternally transmitted type II diabetes mellitus and deafness. *Nat Genet* 1992;1:368-371.
272. de Laat P, Koene S, van den Heuvel LP, Rodenburg RJ, Janssen MC, Smeitink JA. Clinical features and heteroplasmy in blood, urine and saliva in 34 Dutch families carrying the m.3243A > G mutation. *Journal of Inherited Metabolic Disease* 2012;35:1059-1069.
273. Reardon W, Ross RJ, Sweeney MG, et al. Diabetes mellitus associated with a pathogenic point mutation in mitochondrial DNA. *Lancet* 1992;340:1376-1379.
274. Manouvrier S, Rotig A, Hannebique G, et al. Point mutation of the mitochondrial tRNA(Leu) gene (A 3243 G) in maternally inherited hypertrophic cardiomyopathy, diabetes mellitus, renal failure, and sensorineural deafness. *J Med Genet* 1995;32:654-656.

275. Chinnery PF, Howell N, Andrews RM, Turnbull DM. Clinical mitochondrial genetics. *J Med Genet* 1999;36:425-436.
276. Rath PP, Jenkins S, Michaelides M, et al. Characterisation of the macular dystrophy in patients with the A3243G mitochondrial DNA point mutation with fundus autofluorescence. *Br J Ophthalmol* 2008;92:623-629.
277. Michaelides M, Jenkins SA, Bamiou DE, et al. Macular dystrophy associated with the A3243G mitochondrial DNA mutation. Distinct retinal and associated features, disease variability, and characterization of asymptomatic family members. *Arch Ophthalmol* 2008;126:320-328.
278. Bellmann C, Neveu MM, Scholl HP, et al. Localized retinal electrophysiological and fundus autofluorescence imaging abnormalities in maternal inherited diabetes and deafness. *Invest Ophthalmol Vis Sci* 2004;45:2355-2360.
279. de Laat P, Koene S, Heuvel LP, Rodenburg RJ, Janssen MC, Smeitink JA. Inheritance of the m.3243A>G mutation. *JIMD Rep* 2013;8:47-50.
280. Koopman WJ, Willems PH, Smeitink JA. Monogenic mitochondrial disorders. *N Engl J Med* 2012;366:1132-1141.
281. Klein BA. Angioid streaks: a clinical and histopathologic study. *Am J Ophthalmol* 1947;30:955-968.
282. Lam LA. Angioid Streaks. In: Ryan JR (ed), *Retina*. London, New York, Oxford, St. Louis, Sydney, Toronto: Elsevier; 2013:1267-1273.
283. Conner PJ, Juergens JL. Pseudoxanthoma elasticum and angioid streaks. A review of 106 cases. *Am J Med* 1961;30:537-543.
284. Finger RP, Charbel Issa P, Ladewig MS, et al. Pseudoxanthoma elasticum: genetics, clinical manifestations and therapeutic approaches. *Surv Ophthalmol* 2009;54:272-285.
285. Clarkson JG, Altman RD. Angioid streaks. *Surv Ophthalmol* 1982;26:235-246.
286. Georgalas I, Papaconstantinou D, Koutsandrea C, et al. Angioid streaks, clinical course, complications, and current therapeutic management. *Ther Clin Risk Manag* 2009;5:81-89.
287. Mansour AM, Ansari NH, Shields JA, Annesley WH, Jr., Cronin CM, Stock EL. Evolution of angioid streaks. *Ophthalmologica* 1993;207:57-61.
288. Groenblad E. Color photographs of angioid streaks in the late stages. *Acta Ophthalmol* 1958;36:472-474.
289. Hu X, Plomp AS, van Soest S, Wijnholds J, de Jong PT, Bergen AA. Pseudoxanthoma elasticum: a clinical, histopathological, and molecular update. *Surv Ophthalmol* 2003;48:424-438.
290. Krill AE, Klien BA, Archer DB. Precursors of angioid streaks. *Am J Ophthalmol* 1973;76:875-879.
291. Gass JD. "Comet" lesion: an ocular sign of pseudoxanthoma elasticum. *Retina* 2003;23:729-730.
292. Sawa M, Ober MD, Freund KB, Spaide RF. Fundus autofluorescence in patients with pseudoxanthoma elasticum. *Ophthalmology* 2006;113:814-820 e812.
293. Shiraki K, Kohno T, Moriwaki M, Yanagihara N. Fundus autofluorescence in patients with pseudoxanthoma elasticum. *Int Ophthalmol* 2001;24:243-248.
294. Lafaut BA, Leys AM, Scassellati-Sforzolini B, Priem H, De Laey JJ. Comparison of fluorescein and indocyanine green angiography in angioid streaks. *Graefes Arch Clin Exp Ophthalmol* 1998;36:346-353.
295. Pece A, Avanza P, Introini U, Brancato R. Indocyanine green angiography in angioid streaks. *Acta Ophthalmol Scand* 1997;75:261-265.
296. Quaranta M, Cohen SY, Krott R, Sterkers M, Soubrane G, Coscas GJ. Indocyanine green videoangiography of angioid streaks. *Am J Ophthalmol* 1995;119:136-142.
297. Charbel Issa P, Finger RP, Holz FG, Scholl HP. Multimodal imaging including spectral domain OCT and confocal near infrared reflectance for characterization of outer retinal pathology in pseudoxanthoma elasticum. *Invest Ophthalmol Vis Sci* 2009;50:5913-5918.

298. Francois J, de Rouck A. Electrophysiological Studies in Groenblad-strandberg Syndrome. *Doc Ophthalmol Proc Ser* 1980;23:19-25.
299. Audo I, Vanakker OM, Smith A, et al. Pseudoxanthoma elasticum with generalized retinal dysfunction, a common finding? *Invest Ophthalmol Vis Sci* 2007;48:4250-4256.
300. Ringpfeil F, Pulkkinen L, Uitto J. Molecular genetics of pseudoxanthoma elasticum. *Exp Dermatol* 2001;10:221-228.
301. Chassaing N, Martin L, Calvas P, Le Bert M, Hovnanian A. Pseudoxanthoma elasticum: a clinical, pathophysiological and genetic update including 11 novel ABCC6 mutations. *J Med Genet* 2005;42:881-892.
302. Dreyer R, Green WR. The pathology of angioid streaks: a study of twenty-one cases. *Trans Pa Acad Ophthalmol Otolaryngol* 1978;31:158-167.
303. Appel GB, Cook HT, Hageman G, et al. Membranoproliferative glomerulonephritis type II (dense deposit disease): an update. *J Am Soc Nephrol* 2005;16:1392-1403.
304. McAvoy CE, Silvestri G. Retinal changes associated with type 2 glomerulonephritis. *Eye (Lond)* 2005;19:985-989.
305. Leys A, Proesmans W, Van Damme-Lombaerts R, Van Damme B. Specific eye fundus lesions in type II membranoproliferative glomerulonephritis. *Pediatr Nephrol* 1991;5:189-192.
306. Leys A, Vanrenterghem Y, Van Damme B, Snyers B, Pirson Y, Leys M. Fundus changes in membranoproliferative glomerulonephritis type II. A fluorescein angiographic study of 23 patients. *Graefes Arch Clin Exp Ophthalmol* 1991;29:406-410.
307. Ulbig MR, Riordan-Eva P, Holz FG, Rees HC, Hamilton PA. Membranoproliferative glomerulonephritis type II associated with central serous retinopathy. *Am J Ophthalmol* 1993;116:410-413.
308. Kim RY, Faktorovich EG, Kuo CY, Olson JL. Retinal function abnormalities in membranoproliferative glomerulonephritis type II. *Am J Ophthalmol* 1997;123:619-628.
309. O'Brien C, Duvall-Young J, Brown M, Short C, Bone M. Electrophysiology of type II mesangiocapillary glomerulonephritis with associated fundus abnormalities. *Br J Ophthalmol* 1993;77:778-780.
310. Boon CJ, van de Kar NC, Klevering BJ, et al. The spectrum of phenotypes caused by variants in the CFH gene. *Mol Immunol* 2009;46:1573-1594.
311. Berger SP, Daha MR. Complement in glomerular injury. *Semin Immunopathol* 2007;29:375-384.
312. Williams DG. C3 nephritic factor and mesangiocapillary glomerulonephritis. *Pediatr Nephrol* 1997;11:96-98.
313. Alchi B, Jayne D. Membranoproliferative glomerulonephritis. *Pediatr Nephrol* 2010;25:1409-1418.
314. Mullins RF, Aptsiauri N, Hageman GS. Structure and composition of drusen associated with glomerulonephritis: implications for the role of complement activation in drusen biogenesis. *Eye (Lond)* 2001;15:390-395.
315. Duvall-Young J, MacDonald MK, McKechnie NM. Fundus changes in (type II) mesangiocapillary glomerulonephritis simulating drusen: a histopathological report. *Br J Ophthalmol* 1989;73:297-302.
316. Steinert H. Myopathologische Beitrage 1: Uber das klinischeund anatomische Bild des Muskelschwunds der Myotoniker. *Dtsch Z Nervenheilkd* 1909;37:58-104.
317. Batten F, Gibb H. Myotonia atrophica. *Brain* 1909;32:187-205.
318. Ranum LP, Day JW. Myotonic dystrophy: RNA pathogenesis comes into focus. *Am J Hum Genet* 2004;74:793-804.
319. Schara U, Schoser BG. Myotonic dystrophies type 1 and 2: a summary on current aspects. *Semin Pediatr Neurol* 2006;13:71-79.



320. Harper PS. *Myotonic dystrophy*. London: Saunders; 2001.
321. Burian HM, Burns CA. Ocular changes in myotonic dystrophy. *Am J Ophthalmol* 1967;63:22-34.
322. Kimizuka Y, Kiyosawa M, Tamai M, Takase S. Retinal changes in myotonic dystrophy. Clinical and follow-up evaluation. *Retina* 1993;13:129-135.
323. Kim US, Kim JS, Hwang JM. A case of myotonic dystrophy with pigmentary retinal changes. *Korean J Ophthalmol* 2009;23:121-123.
324. Brook JD, McCurrach ME, Harley HG, et al. Molecular basis of myotonic dystrophy: expansion of a trinucleotide (CTG) repeat at the 3' end of a transcript encoding a protein kinase family member. *Cell* 1992;69:385.
325. Liquori CL, Ricker K, Moseley ML, et al. Myotonic dystrophy type 2 caused by a CCTG expansion in intron 1 of ZNF9. *Science* 2001;293:864-867.
326. Lueck JD, Lungu C, Mankodi A, et al. Chloride channelopathy in myotonic dystrophy resulting from loss of posttranscriptional regulation for CLCN1. *Am J Physiol Cell Physiol* 2007;292:C1291-1297.
327. Gomes-Pereira M, Cooper TA, Gourdon G. Myotonic dystrophy mouse models: towards rational therapy development. *Trends Mol Med* 2011;17:506-517.
328. Ranum LP, Cooper TA. RNA-mediated neuromuscular disorders. *Annu Rev Neurosci* 2006;29:259-277.
329. Sicot G, Gourdon G, Gomes-Pereira M. Myotonic dystrophy, when simple repeats reveal complex pathogenic entities: new findings and future challenges. *Hum Mol Genet* 2011;20:R116-123.
330. McBain VA, Townend J, Lois N. Progression of retinal pigment epithelial atrophy in stargardt disease. *American Journal of Ophthalmology* 2012;154:146-154.
331. Mauschitz MM, Fonseca S, Chang P, et al. Topography of geographic atrophy in age-related macular degeneration. *Invest Ophthalmol Vis Sci* 2012;53:4932-4939.
332. Balaskas K, Hovan M, Mahmood S, Bishop P. Ranibizumab for the management of Sorsby fundus dystrophy. *Eye (London, England)* 2013;27:101-102.



Chapter 3

Age-related macular degeneration

3.1

Clinical characteristics of familial and sporadic age-related macular degeneration: differences and similarities

N.T.M. Saksens, E. Kersten, J.M. Groenewoud, M.J. van Grinsven, J.P.H. van de Ven, C.I. S'anchez, T. Schick, S. Fauser, A.I. den Hollander, C.B. Hoyng, C.J.F. Boon

Published in: Investigative Ophthalmology & Visual Science 2014;55:7085-7092



PURPOSE. We describe the differences and similarities in clinical characteristics and phenotype of familial and sporadic patients with age-related macular degeneration (AMD).

METHODS. We evaluated data of 1828 AMD patients and 1715 controls enrolled in the European Genetic Database. All subjects underwent ophthalmologic examination, including visual acuity testing and fundus photography. Images were graded and fundus photographs were used for automatic drusen quantification by a machine learning algorithm. Data on disease characteristics, family history, medical history and lifestyle habits were obtained by a questionnaire.

RESULTS. The age at first symptoms was significantly lower in AMD patients with a positive family history (68.5 years) than in AMD patients with no family history (71.6 years; $P = 1.9 \times 10^{-5}$). Risk factors identified in sporadic and familial subjects were increasing age (OR 1.08 per year; $P = 3.0 \times 10^{-51}$ and OR 1.15; $P = 5.3 \times 10^{-36}$, respectively) and smoking (OR 1.01 per pack year; $P = 1.1 \times 10^{-6}$ and OR 1.02; $P = 0.005$). Physical activity and daily red meat consumption were significantly associated with AMD in sporadic subjects only (OR 0.49; $P = 3.7 \times 10^{-10}$ and OR 1.81; $P = 0.001$). With regard to the phenotype, geographic atrophy and cuticular drusen were significantly more prevalent in familial AMD (17.5% and 21.7%, respectively) as compared to sporadic AMD (9.8% and 12.1%).

CONCLUSIONS. Familial AMD patients become symptomatic at a younger age. The higher prevalence of geographic atrophy and cuticular drusen in the familial AMD cases may be explained by the contribution of additional genetic factors segregating within families.

INTRODUCTION

Age-related macular degeneration (AMD) is a multifactorial retinal disease leading to severe vision loss among the elderly. Advanced age, female sex, smoking, and obesity (body mass index (BMI) >30) are most commonly reported as important demographic and environmental risk factors for the development of AMD.¹⁻⁶ In addition, several important genetic variants have been found to be associated with AMD, either as a risk factor or as a protective factor. The strongest associations have been reported for the single-nucleotide polymorphisms (SNPs) in the complement factor H gene (CFH Y402H; rs1061170), and in the age-related maculopathy susceptibility 2 gene (ARMS2 A69S; rs10490924), which strongly increase the risk of developing AMD.⁷⁻¹¹

Previous studies have demonstrated aggregation of AMD in families.^{12, 13} A family history of AMD has been reported as a significant risk factor for AMD.¹⁴ Individuals are at a higher risk of developing AMD when a first-degree relative is affected. Moreover, having an affected parent is associated with a higher risk than having an affected sibling.^{13, 14} Shahid et al. showed an odds ratio (OR) for AMD of 27.8 in people with an affected parent and an OR of 12.0 for people with an affected sibling. Likewise, Luo et al. reported a relative risk for the development of AMD of 5.66 for people with an affected parent, and a relative risk of 2.95 for people with an affected sibling.

A lower age at onset has been reported in familial AMD patients and heritability of AMD subtypes has been suggested.^{14, 15} Even though environmental and genetic risk factors can cluster in families, the number of affected family members in large densely affected families cannot be fully explained by clustering of known risk factors.¹² Several recent studies have shown that rare, highly penetrant genetic variants can strongly increase the risk of developing AMD in families with AMD, as well as in the AMD population in general.¹⁶⁻²⁰

Little is known about clinical differences and similarities between patients with and without a family history of AMD. The purpose of this study is to gain more insight into the clinical and phenotypic characteristics of familial and sporadic AMD patients, and to analyze if there are distinct clinical differences between these subgroups.

METHODS

Study population

The European Genetic Database (EUGENDA, www.eugenda.org) is a multicenter database for clinical and molecular analysis of AMD founded by the Radboud University Medical Center (Nijmegen, the Netherlands) and the Department of Ophthalmology of the University Hospital of Cologne (Cologne, Germany). This database contains data of AMD patients and control individuals, including family history, environmental risk factors and ophthalmologic examination. For this retrospective study we evaluated data of 1828 Caucasian patients

with AMD and 1715 Caucasian controls enrolled in EUGENDA of whom family history of AMD, smoking status, BMI, age and sex data were available.

This study was performed in accordance with the tenets of the Declaration of Helsinki and was approved by the local ethical committees at the Radboud University Medical Center (Nijmegen) and the University of Cologne. Written informed consent was obtained from all participants before enrolling in EUGENDA.

Questionnaire, clinical evaluation and grading

Before enrollment in the EUGENDA database, all subjects were interviewed with a detailed questionnaire about disease characteristics (e.g. age at first symptoms), family history, medical history and lifestyle habits, such as smoking status, diet and physical activity. For each subject, BMI was calculated using body height and body weight as reported in the questionnaire. Based on years of smoking and number of cigarettes smoked per day we calculated the number of pack years. Each subject underwent an ophthalmologic examination, including Early Treatment Diabetic Retinopathy Study (ETDRS) visual acuity testing, dilated fundus examination and color fundus photography. The best corrected visual acuity (BCVA) was converted to Logarithm of the Minimal Angle of Resolution (logMAR) visual acuity for the purpose of statistical analysis. Two independent certified reading center graders evaluated color fundus photographs of both eyes of all subjects according to the standard protocol of the Cologne Image Reading Center and Laboratory (CIRCL).²¹ Digital non-stereoscopic 30° color fundus photographs centered on the fovea were performed with a Topcon TRC 50IX camera (Topcon Corporation, Tokyo, Japan). The diagnosis and grading of AMD was based on a classification and grading scheme as described previously.²² For all analyses in this study we used the grading of the worst affected eye, and subjects with only one gradable color fundus photograph were excluded. Additionally, in 1184 AMD subjects spectral-domain optical coherence tomography (SD-OCT) (SPECTRALIS, Heidelberg Engineering, Heidelberg, Germany) was available and evaluated for the presence of reticular pseudodrusen. In 677 subjects the presence of cuticular drusen was evaluated based on available fluorescein angiography, performed using the Spectralis HRA system (Heidelberg Engineering, Heidelberg, Germany).²³ The SD-OCT volume scans consisting of 19 or 37 parallel OCT B-scans were used for analysis, covering 6 x 4 mm of the macula. For each OCT B-scan, 20 images were averaged using the automated real-time function.²¹ Evaluation of the presence of reticular pseudodrusen on SD-OCT and cuticular drusen on fluorescein angiography were done by one senior grader.

Based on diagnosis and family history, the participants in this study were divided into four groups: sporadic AMD, sporadic control, familial AMD and familial control. We classified subjects as familial in case of confirmed or possible AMD in at least one close relative, defined as a parent, sibling or child. Sporadic subjects were defined as individuals who did not have a close relative with AMD.

Automatic drusen quantification

In addition to the human grading of AMD based on photographs, a machine learning algorithm for computer-aided diagnosis of AMD was used for detection and quantification of drusen number and area (measured in pixels). This was previously described as accurate in detecting and quantifying drusen number and area on color fundus photographs of patients with non-advanced AMD and control subjects,²⁴. Patients with advanced AMD in the worst affected eye have been excluded for this specific analysis, because the automatic system was not designed to deal with images containing signs of advanced stage AMD. A quality score ranging from 0 to 1 was calculated with 0 being the worst quality and 1 best quality. Only color fundus photographs were selected with a quality score of 0.3 or more, which corresponds to sufficient quality for human grading.

Statistical analysis

All statistical analyses were performed using IBM SPSS Statistics software, version 20.0 (IBM Corp. Released 2011, Armonk, NY). Each potential risk factor for the development of AMD obtained from the questionnaire was included separately in a logistic regression analysis adjusted for age, sex, smoking and BMI. The ORs were calculated for familial subjects (familial AMD versus familial controls) and sporadic subjects (sporadic AMD versus sporadic controls). Significant differences between ORs for sporadic and familial subjects were identified by interaction analysis using binary logistic regressions. All continuous variables were analyzed using an independent sample t-test or 1-way ANOVA. An univariate general linear model was used when continuous variables were analyzed with correction for other variables. Categorical variables were analyzed using a Chi squared test. Differences with a *P*-values less than 0.05 were considered statistically significant. Because multiple possible risk factors were analyzed and many tests of significance were performed in our study, Bonferroni correction was performed for the risk and interaction analysis of environmental factors.

RESULTS

Demographic characteristics of the cohort are shown in **Table 3.1.1**. All four groups were comparable for sex, smoking and BMI. The mean age of the familial subjects was slightly lower than in sporadic subjects (69.6 and 73.0 years, respectively; $P = 4.7 \times 10^{-16}$), mainly due to younger familial control individuals. In 309 subjects who reported in the questionnaire to have a close relative with (possible) AMD, the ophthalmologically examined AMD status of close relatives was available. To determine the degree of misclassification of subjects into familial or sporadic based on the questionnaire, we compared the family history with these examined data. Only in 3 out of 309 cases (1.0%) who reported in the questionnaire to have at least one close relative with AMD, no family members seemed to be affected



upon ophthalmological examination. Therefore, these cases were incorrectly classified as familial. No ophthalmological information was available of relatives of sporadic subjects included in this study.

Table 3.1.1 Demographic characteristics

	Sporadic		Total	Familial		Total
	AMD	Control		AMD	Control	
Cases, n	1330	1405	2735	498	310	808
Sex, n(%)						
Male	536 (40.3)	587 (41.8)	1123 (41.1)	181 (36.3)	132 (42.6)	313 (38.7)
Female	794 (59.7)	818 (58.2)	1612 (58.9)	317 (63.7)	178 (57.4)	495 (61.3)
Age, mean±SD *	75.6±9.1	70.5±7.3	73.0±8.6	74.0±8.4	62.6±10.2	69.6±10.7
Smoking, mean±SD †	14.6±20.1	11.6±16.6	13.1±18.4	14.5±17.9	12.2±15.9	13.6±17.2
BMI, n(%)						
< 25	600 (45.1)	638 (45.4)	1238 (45.2)	233 (46.8)	139 (44.8)	372 (46.0)
25-30	558 (42.0)	599 (42.6)	1157 (42.3)	208 (41.8)	124 (40.0)	332 (41.1)
> 30	172 (12.9)	168 (12.0)	340 (12.4)	57 (11.4)	47 (15.2)	104 (12.9)
Examined family history, n(%)						
Familial				165 (100)	144 (100)	309 (100)
Sporadic				164 (99.4)	142 (98.6)	306 (99.0)
				1 (0.6)	2 (1.4)	3 (1.0)

The study included 498 familial AMD patients deriving from 393 families (393 probands and 105 family members) and 310 controls deriving from 216 families (216 probands and 94 family members). In 309 familial cases information about ophthalmologic examination in their close relatives (parents, sibling, and/or children) was available and was compared to family history based on the questionnaire to determine the degree of misclassification. Familial = positive family history of AMD (confirmed or possible AMD in at least one close relative [parent, sibling or child]); Sporadic = no positive family history.

* Age of participation in years.

† Smoking in pack years.

Familial and sporadic AMD: clinical differences and similarities

Information about the age at first symptoms was available in 703 AMD patients (469 sporadic subjects, 234 familial subjects, **Table 3.1.2**). The age at first symptoms was significantly lower ($P = 1.9 \times 10^{-5}$) in familial AMD patients (mean 68.5 years; SD 9.8) than in sporadic AMD patients (mean 71.6 years; SD 8.7) with a mean difference of 3.1 years (95% CI 1.7-4.5). When subdividing AMD in the presence or absence of the reticular pseudodrusen subtype, the age at first symptoms was also lower in familial AMD patients. In addition, AMD patients with reticular pseudodrusen have a significantly higher age at first symptoms than patients without reticular pseudodrusen, in both sporadic and familial patients ($P = 4.4 \times 10^{-10}$ and $P = 0.002$, respectively). In contrast, in AMD patients with the cuticular drusen

subtype, the age at first symptoms was lower than in patients without cuticular drusen, in both sporadic and familial patients ($P = 1.26 \times 10^{-6}$ and $P = 0.074$, respectively). However, no significant difference in age at first symptoms was observed between familial and sporadic patients with the cuticular drusen subtype ($P = 0.740$).

Despite a younger age at first symptoms, BCVA of both eyes did not differ significantly between familial and sporadic AMD patients when subdivided in three age categories (data shown in **Table 3.1.2**). Also, if young patients (< 60 years) were analyzed separately, no difference in BCVA was observed between familial and sporadic patients (data not shown). After distinguishing between advanced and non-advanced AMD subjects, BCVA also was comparable between sporadic and familial patients.

Table 3.1.2 Clinical features and staging of sporadic and familial AMD patients

	Sporadic AMD Mean±SD	Familial AMD Mean±SD	P-value
Age at first symptoms, years			
AMD (Total*)	71.6±8.7	68.5±9.8	1.9×10 ⁻⁵
AMD (Reticular pseudodrusen†)	76.2±7.2	72.5±7.3	0.008
AMD (Cuticular drusen‡)	65.8±9.2	64.5±17.7	0.740
Visual acuity per age category§			
< 70	0.12±0.27	0.09±0.25	0.293
70-80	0.19±0.29	0.26±0.36	0.107
> 80	0.40±0.40	0.38±0.46	0.814
Visual acuity per stages			
Non-advanced	0.05±0.14	0.03±0.13	0.367
Advanced	0.33±0.37	0.37±0.42	0.314
Grading, n (%)			
Early	301 (22.6)	94 (18.9)	0.158
Intermediate	250 (18.8)	90 (18.1)	
Advanced	779 (58.6)	314 (63.1)	
GA	76 (9.8)	55 (17.5)	3.0×10 ⁻⁴
CNV	660 (84.7)	234 (74.5)	
Mixed	43 (5.5)	25 (8.0)	

* Data on age of first symptoms were available in 469 sporadic and 234 familial AMD patients

† Data on age of first symptoms were available in 75 sporadic and 45 familial AMD patients with reticular pseudodrusen

‡ Data on age of first symptoms were available in 32 sporadic and 19 familial AMD patients with cuticular drusen

§ Visual acuity defined as best-corrected logMAR visual acuity

AMD = Age-related macular degeneration, SD = standard deviation, GA = Geographic atrophy, CNV = Choroidal neovascularization

P-values < 0.05 indicate significant associations

Table 3.1.3 Risk and interaction analysis for demographic and environmental factors in sporadic and familial subjects

	Sporadic [n(%)]		Sporadic AMD vs. control		Familial [n(%)]		Familial AMD vs. control		Familial AMD vs. sporadic AMD	
	AMD	Control	OR (95% CI)*	P-value	AMD	Control	OR (95% CI)*	P-value	P-value	P-value
Age †	1330 (100)	1405 (100)	1.08 (1.07-1.09)	3.0x10 ⁻⁵¹ #	498 (100)	310 (100)	1.15 (1.13-1.18)	5.3x10 ⁻³⁶ #	9.4x10 ⁻⁷ #	
Sex										
- Male	536 (40.3)	587 (41.8)	reference		181 (36.3)	132 (42.6)	reference			0.811
- Female	794 (59.7)	818 (58.2)	1.27 (1.07-1.51)	0.007	317 (63.7)	178 (57.4)	1.33 (0.93-1.91)	0.120	0.120	0.811
Smoking ‡	1330 (100)	1405 (100)	1.01 (1.01-1.02)	1.1x10 ⁻⁶ #	498 (100)	310 (100)	1.02 (1.01-1.03)	0.005	0.005	0.914
BMI										
- < 25	600 (45.1)	638 (45.4)	reference		233 (46.8)	139 (44.8)	reference			0.314
- 25-30	558 (42.0)	599 (42.6)	1.04 (0.88-1.24)	0.635	208 (41.8)	124 (40.0)	0.80 (0.56-1.16)	0.244	0.244	0.314
- > 30	172 (12.9)	168 (12.0)	1.21 (0.94-1.56)	0.149	57 (11.4)	47 (15.2)	0.70 (0.41-1.17)	0.172	0.172	0.051
Comorbidity										
Cardiovascular disease§	519 (43.0)	545 (42.2)	0.84 (0.71-1.00)	0.053	200 (41.7)	83 (27.9)	1.31 (0.90-1.90)	0.163	0.163	0.019
Diabetes	157 (11.8)	113 (8.0)	1.34 (1.02-1.75)	0.035	41 (8.3)	17 (5.5)	0.88 (0.46-1.70)	0.704	0.704	0.365
Renal disease	72 (5.4)	60 (4.3)	1.15 (0.79-1.66)	0.480	28 (5.7)	11 (3.5)	0.98 (0.43-2.24)	0.959	0.959	0.954
Autoimmune disease	101 (7.6)	93 (6.6)	1.11 (0.81-1.51)	0.520	54 (10.9)	16 (5.2)	1.82 (0.91-3.64)	0.091	0.091	0.150
Allergy	239 (18.0)	371 (26.4)	0.74 (0.61-0.89)	0.002#	88 (17.8)	92 (29.7)	0.63 (0.43-0.94)	0.024	0.024	0.294
Diet										
Use of butter/oil										
- Butter/margarine	101 (15.8)	105 (14.3)	reference		53 (17.6)	30 (13.5)	reference			0.225
- Low-fat margarine	58 (9.1)	45 (6.1)	1.40 (0.84-2.33)	0.195	49 (16.3)	50 (22.5)	0.92 (0.44-1.95)	0.836	0.836	0.225
- Vegetable oil	255 (40.0)	411 (56.1)	0.77 (0.55-1.08)	0.127	78 (25.9)	84 (37.8)	0.74 (0.38-1.44)	0.373	0.373	0.795
- Other	226 (35.3)	172 (23.5)	1.34 (0.94-1.93)	0.110	121 (40.2)	58 (26.1)	1.35 (0.69-2.66)	0.384	0.384	0.999
Fish										
- Once a week or less	871 (73.9)	1015 (74.2)	reference		357 (77.4)	244 (78.7)	reference			0.765
- Few times a week	300 (25.4)	346 (25.3)	0.99 (0.82-1.20)	0.941	103 (22.3)	65 (21.0)	0.84 (0.56-1.27)	0.412	0.412	0.765
- Every day	8 (0.7)	7 (0.5)	0.80 (0.27-2.38)	0.684	1 (0.2)	1 (0.3)	0.26 (0.01-10.37)	0.470	0.470	0.677
Red meat										
- Once a week or less	434 (36.7)	602 (44.3)	reference		118 (25.7)	75 (24.3)	reference			0.142
- Few times a week	638 (53.9)	680 (50.1)	1.24 (1.05-1.48)	0.013	273 (59.3)	188 (60.8)	0.92 (0.62-1.39)	0.702	0.702	0.142
- Every day	112 (9.5)	76 (5.6)	1.81 (1.30-2.54)	0.001#	69 (15.0)	46 (14.9)	1.16 (0.66-2.05)	0.605	0.605	0.074
Fruit										
- Once a week or less	84 (7.1)	75 (5.5)	reference		36 (7.8)	26 (8.4)	reference			0.370
- Few times a week	138 (11.7)	207 (15.1)	0.60 (0.40-0.90)	0.013	73 (15.8)	70 (22.6)	0.85 (0.40-1.79)	0.661	0.661	0.370
- Every day	962 (81.3)	1093 (79.5)	0.74 (0.52-1.04)	0.085	352 (76.4)	214 (69.0)	0.73 (0.37-1.44)	0.361	0.361	0.542

Vegetables							
- Not every day	189 (16.0)	244 (17.7)	reference	61 (13.3)	54 (17.4)	reference	0.922
- Every day	995 (84.0)	1131 (82.3)	1.11 (0.89-1.39)	399 (86.7)	256 (82.6)	0.92 (0.56-1.52)	0.741
Physical activity							
- (Almost) never	566 (44.1)	377 (27.2)	reference	177 (37.0)	84 (27.2)	reference	0.942
- 1-2 times a week	509 (32.1)	629 (45.4)	0.67 (0.56-0.81)	227 (47.5)	174 (56.3)	0.62 (0.42-0.94)	0.022
- 3 times a week or more	209 (16.3)	378 (27.3)	0.49 (0.39-0.61)	74 (15.5)	51 (16.5)	0.75 (0.44-1.27)	0.281

* The ORs were adjusted for age, sex, smoking and BMI

† Age of participation in years

‡ Smoking in pack years

§ Cardiovascular disease defined as presence or history of hypertension, angina pectoris, myocardial infarction, congestive heart failure and/or stroke/transient ischemic attack

|| Autoimmune disease defined as presence or history of rheumatoid arthritis or systemic lupus erythematosus

P-values < 0.05 indicate significant associations

Significant after Bonferroni correction

AMD = Age-related macular degeneration, OR = Odds ratio, CI = Confidence interval

To identify risk factors in our cohort, we analyzed several demographic and environmental factors (**Table 3.1.3**). Risk factors identified in both sporadic and familial AMD patients were increasing age ($P = 3.0 \times 10^{-51}$ and $P = 5.3 \times 10^{-36}$) and smoking ($P = 1.1 \times 10^{-6}$ and $P = 0.005$). Interaction analysis showed a significant difference between sporadic and familial subjects for increasing age ($P = 9.4 \times 10^{-7}$).

In terms of comorbidity (**Table 3.1.3**), allergy was significantly associated with a decreased risk of AMD for both sporadic and familial subjects ($P = 0.002$ and $P = 0.024$, respectively). Diabetes mellitus was a risk factor for the development of AMD in sporadic patients (OR 1.34; 95% CI 1.02-1.75; $P = 0.035$), but not in familial cases ($P = 0.704$). No significant interaction between family history and allergy or diabetes was present. Cardiovascular disease, renal disease and auto-immune disease were no significant risk factors for AMD in our cohort.

With regard to dietary factors, we observed that eating red meat a few times per week or daily is a significant risk factor in sporadic AMD patients (OR 1.24; 95% CI 1.05-1.48; $P = 0.013$ and OR 1.81; 95% CI 1.30-2.54; $P = 0.001$, respectively), but not in familial subjects. A protective factor for AMD in sporadic patients was eating fruit a few times per week (OR 0.60; 95% CI 0.40-0.90; $P = 0.013$). Intake of fruit every day did not seem to further decrease the risk of AMD (OR 0.74; 95% CI 0.52-1.04; $P = 0.085$). However, consumption of fruit was not significantly associated with a decreased risk of AMD in familial subjects.

Regular physical activity, 1 or 2 times a week, was significantly associated with a decreased risk for AMD in the sporadic AMD subgroup (OR 0.67; 95% CI 0.56-0.81; $P = 2.6 \times 10^{-6}$) and the familial AMD subgroup (OR 0.62; 95% CI 0.42-0.94; $P = 0.022$).

After Bonferroni correction of the demographic and environmental risk factors for AMD, the association of increasing age with AMD in familial and sporadic subjects remained significant, as well as the association of female sex, smoking, allergy, daily red meat consumption and physical activity in sporadic patients only.

Familial and sporadic AMD: phenotypic differences and similarities

The prevalence of early, intermediate and advanced stage AMD was similar in the familial and sporadic AMD patient group (**Table 3.1.2**). After differentiation of advanced AMD into geographic atrophy (GA), choroidal neovascularization (CNV) and mixed (both GA and CNV in one patient), we found that GA was more prevalent in familial AMD patients (17.5%) than in sporadic AMD patients (9.8%; $P = 3.0 \times 10^{-4}$), despite a comparable SNP load of CFH Y402H and ARMS2 A69S between familial ($n=51$) and sporadic patients ($n=58$) with GA (data not shown). In 829 sporadic subjects and 355 familial subjects data on reticular pseudodrusen were available and data on cuticular drusen were available in 520 sporadic subjects and 157 familial subjects. The prevalence of reticular pseudodrusen was comparable between familial (18.0%) and sporadic subjects (18.8%; $P = 0.749$), whereas the prevalence of cuticular drusen was significantly higher in familial AMD (21.7%) compared to sporadic AMD (12.1%; $P = 0.003$).

Data on the number of drusen and area of drusen within the macular area were available for 689 sporadic subjects and 203 familial subjects (Table 3.1.4). Familial subjects showed a trend towards a higher number of drusen and a larger area of drusen in the macula as compared to sporadic patients, although this was only significant for the area of drusen in subjects with intermediate AMD ($P = 0.043$). After correction for age, sex, BMI and smoking, the mean area of drusen in sporadic subjects with intermediate AMD was 1114.49 and 1415.63 in familial subjects, which were no longer significantly different ($P = 0.160$).

Table 3.1.4 Number and area of drusen in sporadic and familial control individuals and non-advanced AMD patients

		Sporadic		Familial		P-value
		n	Mean±SD	n	Mean±SD	
Control	Number of drusen	159	2.25±6.0	24	2.85±3.4	0.633
	Area of drusen*	159	81.65±149.6	24	128.86±129.5	0.145
Early	Number of drusen	291	8.69±20.0	93	11.69±27.37	0.254
	Area of drusen*	291	219.17±353.4	93	249.67±416.6	0.489
Intermediate	Number of drusen	239	40.25±62.4	86	46.37±48.9	0.411
	Area of drusen*	239	1167.90±1735.4	86	1598.70±1555.4	0.043

* Area of drusen in pixels

SD = standard deviation

P-values < 0.05 indicate significant associations

DISCUSSION

Familial and sporadic AMD: clinical differences and similarities

Familial AMD patients have a lower age at first symptoms as compared to sporadic AMD patients. The phenomenon of a lower age at onset in patients with familial occurrence has been shown in other complex diseases with a significant genetic component, such as schizophrenia and Alzheimer's disease.^{25, 26} A lower age at onset in familial AMD patients has previously been reported by Shahid et al. (70.4 years in familial patients and 73.2 years in sporadic patients),¹⁴ and is in accordance with the mean difference of 3.1 years in our study. A significant difference in age of onset between familial and sporadic subjects was also observed in AMD patients with reticular pseudodrusen, but not in patients with cuticular drusen. However, as a result of a positive family history, familial subjects may have an increased awareness of visual symptoms which can lead to an earlier visit at a physician for evaluation. Therefore, it should be noted that the lower age at first symptoms in familial AMD patients may be partially attributed to an ascertainment bias.

In our study, BCVA per age category did not differ between familial and sporadic AMD patients, suggesting that visual acuity does not decrease earlier or at a faster rate in familial

patients, despite the lower age at first symptoms in familial AMD patients. Heightened awareness in familial patients may explain why no actual difference in BCVA was observed.

Similar to other studies,^{1-3, 6} smoking and advanced age were associated with the development of AMD in the current study, in both sporadic and familial subjects. Furthermore, age was a more important risk factor for AMD in familial subjects as age shows a significant interaction with family history, resulting in a younger age at onset in familial subjects.

Ristau et al.²² have recently reported that allergy is associated with a reduced risk of AMD. We did not find a significant difference for the association of allergy with AMD between familial and sporadic subjects, so the protective effect of allergy does not seem to be influenced by family history.

The pathogenesis of AMD as well as cardiovascular disease and diabetes have been linked to oxidative stress, inflammation and a vascular origin. Moreover, diabetes, cardiovascular disease, and its risk factors have been associated with the development of AMD, although this was not consistent among studies.^{1, 27-30} In the current study we observed that sporadic subjects with diabetes have an increased risk for AMD. However, diabetes was no risk factor for familial AMD, which may be explained by the larger genetic component in the pathophysiology of familial AMD, while sporadic AMD may be associated with a larger contribution of environmental or lifestyle factors such as diabetes (and associated factors).

Several studies reported an increased risk of AMD for patients with chronic renal disease.^{31, 32} It has been shown that AMD and renal diseases, such as membranoproliferative glomerulonephritis type 2 and atypical hemolytic uremic syndrome, are related to the same genetic variants of the complement pathway, including the complement factor H gene.³³⁻³⁵ Therefore, we evaluated whether renal disease might be correlated with AMD in familial subjects. However, we did not find a clear association between familial AMD and renal disease in our study population, possibly due to the low number of patients with renal disease.

We also compared dietary factors between familial and sporadic subjects. It is interesting to investigate these dietary factors since these are modifiable. The consumption of red meat at least a few times a week increased the risk of AMD in our sporadic patient cohort. This is supported by findings of Chong et al.,³⁶ demonstrating that higher red meat intake was associated with the development of AMD. In our study consumption of fruit a few times a week was associated with a decreased risk for the development of AMD, but we did not observe such an association with frequent consumption of vegetables. In agreement with this finding, Cho et al. and Zerbib et al. described a protective effect of frequent consumption of fruits for exudative AMD, but no association with the consumption of vegetables.^{37, 38} A study by Seddon et al.³⁹ showed that intake of foods rich in carotenoids, in particular green leafy vegetables, decreased the risk of exudative AMD. Our study might be limited because we did not discriminate between different kinds of vegetables and no risk calculation was performed for the progression to advanced AMD. This may explain why

we did not observe a protective effect for the consumption of vegetables. Also, it must be considered that fruit consumption can be related to a more healthy lifestyle in general, and therefore, these results may be confounded by other factors, other than smoking and BMI, related to a healthy lifestyle.

In cuticular drusen, a clinical subtype of AMD which tends to cluster in families, differences in environmental and genetic risk factors have been reported as compared to the AMD group as a whole.^{23, 40} We previously reported that the association with smoking was significantly lower in patients with cuticular drusen compared to AMD patients without cuticular drusen.²³ In this study we observed no significant difference in environmental risk factors, such as smoking, between familial and sporadic AMD. However, several factors such as the consumption of red meat and frequent physical activity, tended to play a less important role in familial AMD than in sporadic AMD, supporting a stronger genetic component in the pathophysiology of AMD in families.

Familial and sporadic AMD: phenotypic differences and similarities

In our study population, GA was more prevalent in familial AMD patients than in sporadic patients. This cannot be explained by selection bias of familial patients, because if only the probands of the familial group (n = 262) were included in the analysis, GA was still significantly more prevalent in the familial AMD group than in the sporadic group (17.6% and 9.8%, respectively, $P = 0.001$). This finding may be explained by the stronger influence of genetic factors in the pathogenesis of familial AMD in certain phenotypic subtypes such as GA. Previously Shahid et al.¹⁴ suggested heritability of AMD subtypes, but these authors were not able to confirm this hypothesis due to low numbers of subjects. Sobrin et al.¹⁵ showed that siblings are more likely to develop the same advanced subtype as their proband. This may suggest the contribution of genetic variants in these familial patients,^{16, 35, 41} which may increase the risk for developing GA rather than CNV. Affected members of densely affected families have been reported to bear a lower SNP load than expected based on five common known AMD risk variants; *CFH* (rs1061170 and rs1410996), *ARMS2* (rs10490924), *C2-CFB* (rs641153 and rs9332739).¹⁰ This supports the hypothesis that rare genetic variants in these families may explain the high prevalence of AMD.

In this study, we reported a higher prevalence of cuticular drusen in familial AMD compared to sporadic AMD, which is in agreement with previous reports.^{40, 42, 43} However, in our cohort the prevalence of cuticular drusen was higher and 32% of the patients with cuticular drusen had a positive family history of AMD compared to 44% of the patients in a study of Grassi et al.⁴⁰ Previously, our group demonstrated that heterozygous loss-of-function mutations in the *CFH* gene are found among family members with cuticular drusen.^{35, 41} In addition, rare, highly penetrant variants in the *CFI* gene have been identified in patients with cuticular drusen.^{16, 44} Therefore, the higher prevalence of cuticular drusen in families may be explained by segregation of rare, highly penetrant variants within these families.



In addition to a possible ascertainment bias, caused by an increased awareness of disease-associated visual symptoms in familial subjects, another limitation of this study is the classification of subjects into familial or sporadic based on the family history in the questionnaire, which may lead to misclassification. However, in a subset of the familial cases ophthalmologic examination data of their close relatives were available and compared with our classification based on the family history of the questionnaire. The degree of misclassification of the family history was very low in the familial subjects, as in only 3 cases (1.0%) no close relative with AMD was found by ophthalmologic examination. Unfortunately, no clinical data of family members of sporadic cases were available. The rate of misclassification may be higher in sporadic individuals, as these subjects may not have been informed of the eye disease of close relatives or the relatives were asymptomatic and therefore, not yet diagnosed with AMD.

In conclusion, this study demonstrates that familial AMD patients have a lower age at first symptoms compared to sporadic patients. Our findings also indicate that familial AMD patients differ from sporadic patients in terms of risk factors and clinical features. The higher prevalence of GA and cuticular drusen in familial AMD patients may be explained by the contribution of additional genetic factors segregating within these families.

REFERENCES

1. Chakravarthy U, Wong TY, Fletcher A, et al. Clinical risk factors for age-related macular degeneration: a systematic review and meta-analysis. *BMC Ophthalmol* 2010;10:31.
2. Age-Related Eye Disease Study Research G. Risk factors associated with age-related macular degeneration. A case-control study in the age-related eye disease study: Age-Related Eye Disease Study Report Number 3. *Ophthalmology* 2000;107:2224-2232.
3. Evans JR. Risk factors for age-related macular degeneration. *Prog Retin Eye Res* 2001;20:227-253.
4. Clemons TE, Milton RC, Klein R, Seddon JM, Ferris FL, 3rd, Age-Related Eye Disease Study Research G. Risk factors for the incidence of Advanced Age-Related Macular Degeneration in the Age-Related Eye Disease Study (AREDS) AREDS report no. 19. *Ophthalmology* 2005;112:533-539.
5. Seddon JM, Cote J, Davis N, Rosner B. Progression of age-related macular degeneration: association with body mass index, waist circumference, and waist-hip ratio. *Arch Ophthalmol* 2003;121:785-792.
6. Erke MG, Bertelsen G, Peto T, Sjolie AK, Lindekleiv H, Njolstad I. Cardiovascular risk factors associated with age-related macular degeneration: the Tromso Study. *Acta ophthalmologica* 2014;92:662-669.
7. Edwards AO, Ritter R, 3rd, Abel KJ, Manning A, Panhuysen C, Farrer LA. Complement factor H polymorphism and age-related macular degeneration. *Science* 2005;308:421-424.
8. Klein RJ, Zeiss C, Chew EY, et al. Complement factor H polymorphism in age-related macular degeneration. *Science* 2005;308:385-389.
9. Rivera A, Fisher SA, Fritsche LG, et al. Hypothetical LOC387715 is a second major susceptibility gene for age-related macular degeneration, contributing independently of complement factor H to disease risk. *Hum Mol Genet* 2005;14:3227-3236.
10. Sobrin L, Maller JB, Neale BM, et al. Genetic profile for five common variants associated with age-related macular degeneration in densely affected families: a novel analytic approach. *Eur J Hum Genet* 2010;18:496-501.
11. Shastry BS. Assessment of the contribution of the LOC387715 gene polymorphism in a family with exudative age-related macular degeneration and heterozygous CFH variant (Y402H). *J Hum Genet* 2007;52:384-387.
12. Klaver CC, Wolfs RC, Assink JJ, van Duijn CM, Hofman A, de Jong PT. Genetic risk of age-related maculopathy. Population-based familial aggregation study. *Arch Ophthalmol* 1998;116:1646-1651.
13. Luo L, Harmon J, Yang X, et al. Familial aggregation of age-related macular degeneration in the Utah population. *Vision Res* 2008;48:494-500.
14. Shahid H, Khan JC, Cipriani V, et al. Age-related macular degeneration: the importance of family history as a risk factor. *Br J Ophthalmol* 2012;96:427-431.
15. Sobrin L, Ripke S, Yu Y, et al. Heritability and genome-wide association study to assess genetic differences between advanced age-related macular degeneration subtypes. *Ophthalmology* 2012;119:1874-1885.
16. van de Ven JP, Nilsson SC, Tan PL, et al. A functional variant in the CFI gene confers a high risk of age-related macular degeneration. *Nat Genet* 2013;45:813-817.
17. Helgason H, Sulem P, Duvvari MR, et al. A rare nonsynonymous sequence variant in C3 is associated with high risk of age-related macular degeneration. *Nat Genet* 2013;45:1371-1374.
18. Raychaudhuri S, Iartchouk O, Chin K, et al. A rare penetrant mutation in CFH confers high risk of age-related macular degeneration. *Nat Genet* 2011;43:1232-1236.



19. Seddon JM, Yu Y, Miller EC, et al. Rare variants in CFI, C3 and C9 are associated with high risk of advanced age-related macular degeneration. *Nat Genet* 2013;45:1366-1370.
20. Zhan X, Larson DE, Wang C, et al. Identification of a rare coding variant in complement 3 associated with age-related macular degeneration. *Nat Genet* 2013;45:1375-1379.
21. Mokwa NF, Ristau T, Keane PA, Kirchhof B, Sadda SR, Liakopoulos S. Grading of Age-Related Macular Degeneration: Comparison between Color Fundus Photography, Fluorescein Angiography, and Spectral Domain Optical Coherence Tomography. *J Ophthalmol* 2013;2013:385915.
22. Ristau T, Ersoy L, Lechanteur Y, et al. Allergy is a protective factor against age-related macular degeneration. *Invest Ophthalmol Vis Sci* 2014;55:210-214.
23. van de Ven JP, Smailhodzic D, Boon CJ, et al. Association analysis of genetic and environmental risk factors in the cuticular drusen subtype of age-related macular degeneration. *Mol Vis* 2012;18:2271-2278.
24. van Grinsven MJ, Lechanteur YT, van de Ven JP, et al. Automatic drusen quantification and risk assessment of age-related macular degeneration on color fundus images. *Invest Ophthalmol Vis Sci* 2013;54:3019-3027.
25. Suvisaari JM, Haukka J, Tanskanen A, Lonnqvist JK. Age at onset and outcome in schizophrenia are related to the degree of familial loading. *Br J Psychiatry* 1998;173:494-500.
26. Duara R, Lopez-Alberola RF, Barker WW, et al. A comparison of familial and sporadic Alzheimer's disease. *Neurology* 1993;43:1377-1384.
27. Tan JS, Mitchell P, Smith W, Wang JJ. Cardiovascular risk factors and the long-term incidence of age-related macular degeneration: the Blue Mountains Eye Study. *Ophthalmology* 2007;114:1143-1150.
28. Klein R, Klein BE, Tomany SC, Cruickshanks KJ. The association of cardiovascular disease with the long-term incidence of age-related maculopathy: the Beaver Dam eye study. *Ophthalmology* 2003;110:636-643.
29. Mitchell P, Wang JJ. Diabetes, fasting blood glucose and age-related maculopathy: The Blue Mountains Eye Study. *Aust N Z J Ophthalmol* 1999;27:197-199.
30. Klein R, Klein BE, Moss SE. Diabetes, hyperglycemia, and age-related maculopathy. The Beaver Dam Eye Study. *Ophthalmology* 1992;99:1527-1534.
31. Liew G, Mitchell P, Wong TY, Iyengar SK, Wang JJ. CKD increases the risk of age-related macular degeneration. *J Am Soc Nephrol* 2008;19:806-811.
32. Klein R, Knudtson MD, Lee KE, Klein BE. Serum cystatin C level, kidney disease markers, and incidence of age-related macular degeneration: the Beaver Dam Eye Study. *Arch Ophthalmol* 2009;127:193-199.
33. Nitsch D, Douglas I, Smeeth L, Fletcher A. Age-related macular degeneration and complement activation-related diseases: a population-based case-control study. *Ophthalmology* 2008;115:1904-1910.
34. Boon CJ, van de Kar NC, Klevering BJ, et al. The spectrum of phenotypes caused by variants in the CFH gene. *Mol Immunol* 2009;46:1573-1594.
35. van de Ven JP, Boon CJ, Fauser S, et al. Clinical evaluation of 3 families with basal laminar drusen caused by novel mutations in the complement factor H gene. *Arch Ophthalmol* 2012;130:1038-1047.
36. Chong EW, Simpson JA, Robman LD, et al. Red meat and chicken consumption and its association with age-related macular degeneration. *Am J Epidemiol* 2009;169:867-876.
37. Cho E, Seddon JM, Rosner B, Willett WC, Hankinson SE. Prospective study of intake of fruits, vegetables, vitamins, and carotenoids and risk of age-related maculopathy. *Arch Ophthalmol* 2004;122:883-892.

38. Zerbib J, Delcourt C, Puche N, et al. Risk factors for exudative age-related macular degeneration in a large French case-control study. *Graefes Arch Clin Exp Ophthalmol* 2013.
39. Seddon JM, Ajani UA, Sperduto RD, et al. Dietary carotenoids, vitamins A, C, and E, and advanced age-related macular degeneration. Eye Disease Case-Control Study Group. *JAMA* 1994;272:1413-1420.
40. Grassi MA, Folk JC, Scheetz TE, Taylor CM, Sheffield VC, Stone EM. Complement factor H polymorphism p.Tyr402His and cuticular Drusen. *Arch Ophthalmol* 2007;125:93-97.
41. Boon CJ, Klevering BJ, Hoyng CB, et al. Basal laminar drusen caused by compound heterozygous variants in the CFH gene. *Am J Hum Genet* 2008;82:516-523.
42. Lerche W. Pigment epithelium changes in drusen of the macular region. *Ber Zusammenkunft Dtsch Ophthalmol Ges* 1975;439-446.
43. Barbazetto IA, Yannuzzi NA, Klais CM, et al. Pseudo-vitelliform macular detachment and cuticular drusen: exclusion of 6 candidate genes. *Ophthalmic Genet* 2007;28:192-197.
44. Boon CJ, van de Ven JP, Hoyng CB, den Hollander AI, Klevering BJ. Cuticular drusen: stars in the sky. *Prog Retin Eye Res* 2013;37:90-113.



3.2

Predictive value of family history versus genetic risk variants in age-related macular degeneration

N.T.M. Saksens, S.K. Verbakel, C.J.F. Boon, J.M.M. Groenewoud,
T. Schick, S. Fauser, A.I. den Hollander, C.C.W. Klaver, C.B. Hoyng

Manuscript in preparation



PURPOSE. To compare the predictive value of family history and genetic risk variants for age-related macular degeneration (AMD)

METHODS. Retrospective case-control study including 1915 AMD patients and 1555 non-affected controls aged 50+ years from ophthalmologic clinical centers in the Netherlands and Germany. All study participants underwent an extensive ophthalmic examination and a blood draw for DNA analysis. Information regarding family size and number of affected first degree family members was obtained by means of a questionnaire. Genotyping was performed for 23 single nucleotide polymorphisms (SNPs) known to be associated with AMD. The risk of AMD for number of affected parents and siblings was analysed by logistic regression, corrected for age and sex. Prediction models were generated using receiver-operating-characteristics (ROC) curve.

RESULTS. The risk of AMD increased significantly with increasing number of affected parents (1 parent OR 2.038, (95%CI: 0.1361-2.59); two parents OR 8.174; (95%CI: 1.79-37.37) and with increasing number of affected siblings. In large families consisting of at least 5 siblings the OR of at least 3 affected siblings was 3.12 ((95%CI: 1.19-8.17)). The predictive value of developing AMD was 0.724 (95%CI: 0.693-0.756) for family history, and 0.810 (95%CI: 0.784-0.837) for common genetic variants. For probands with at least 2 affected siblings the predictive value was 0.784 (95%CI: 0.639-0.928) in small families and 0.809 (95%CI: 0.677-0.940) in large families; for probands with 2 affected parents the predictive value was 1.000 ((95%CI: 1.000-1.000).

CONCLUSIONS. Common AMD SNPs perform better than family history in the prediction of AMD. However, when a large number of first degree relatives is affected, the prediction of family history exceeds the prediction of SNPs. Our results imply that determination of genetic AMD variants has particular merit in small families with many non-affecteds.

INTRODUCTION

Age-related macular degeneration (AMD) is the leading cause of blindness among the elderly in developed countries¹ and a growing health problem.² The etiology of AMD is complex, and multiple genetic risk variants, smoking, BMI, and various nutrients appear to play a role.³⁻⁸ The importance of AMD risk prediction is increasing, since high-risk groups may benefit from lifestyle advice and nutritional supplements. Moreover, these groups may be particularly suitable for future therapeutic agents like complement inhibitors.

For years it has been known that a positive family history is a risk factor for AMD. Siblings of patients with late AMD have a 4-5 times increased risk of developing AMD,^{1,9} and children of affected parents appear to have an even higher risk.¹⁰ Remarkably, family history has rarely been used as a variable in prediction models. In contrast, the recently identified genetic variants for AMD have frequently been incorporated in prediction models, and their ability to predict AMD is high.¹¹⁻¹³ Nevertheless, current genetic testing is mostly performed for risk analyses in research settings, and is not yet available in most clinics. Family history is easily obtained in the clinic, and may be a good alternative.

The purpose of this study is to compare family history and genetic risk variants in their ability to predict AMD. We investigated family history in a crude as well as in a detailed manner, and compared them to the predictive value of a large set of currently known risk variants.

METHODS

Study population

In this study, we evaluated subjects aged 50+ years from the European Genetic Database (EUGENDA) from whom complete ophthalmic and family history data were available. Details of this study are described elsewhere.¹⁴ In brief, all persons underwent digital colour fundus photography (Topcon TRC 50IX camera, Tokyo, Japan) after pharmacologic mydriasis, and spectral-domain optical coherence tomography (SD-OCT, SPECTRALIS, Heidelberg Engineering, Heidelberg, Germany). Features of AMD were determined by grading of all retinal images by two independent certified reading center graders according to the standard protocol of the Cologne Image Reading Center (CIRCL).¹⁴ Early AMD was classified by the presence of pigmentary changes with at least 10 small drusen (<63µm) or the presence of intermediate (63-124 µm) or large drusen (≥125 µm diameter) in the Early Treatment Diabetic Retinopathy Study (ETDRS) grid. Advanced AMD was defined as either GA and/or CNV in the macula of at least one eye. Persons with early or advanced AMD were diagnosed as cases; persons with no retinal abnormalities or only small drusen or isolated pigmentary abnormalities were diagnosed as controls.



Data on presence of AMD in parents were collected by questionnaire from the start of Eugenda, and were available in 3470 individuals (1915 cases and 1555 controls). Questions on presence of AMD in siblings were added to the questionnaire at a later phase (2011); therefore, data on AMD in siblings were only available in a subset of 944 cases and 512 controls. With respect to families incorporated in Eugenda, the first family member who attended the examination center was included in the current analysis as the proband. EUGENDA was approved by the local ethics committee on Research Involving Human Subjects from RadboudUMC, met the criteria of the Declaration of Helsinki, and all subjects provided written informed consent.

Family history

Information on family history was obtained by detailed, interviewer-administered questionnaire which included questions such as ‘Is AMD present in your family? If so, are your parents affected? Are your siblings affected, how many are affected and how many siblings are in your family?’ Family history was regarded positive when the proband reported the presence of AMD in either parents or siblings; persons with negative family history were considered sporadic. We identified two subgroups in persons with data on siblings: probands with 1-5 siblings, and probands with > 5 siblings, based on inclusion of the upper quartile of individuals in the latter group. Missing data of the number of (affected) siblings were due to being an only child, no contact with siblings or as a consequence of an incomplete questionnaire.

Genotyping

Venous blood was obtained for genetic analysis of 23 single nucleotide polymorphisms (SNPs) known to be associated with AMD in the three continent AMD consortium^{11, 15}; *ADAMTS9* (rs6795735), *APOE* (rs4420638), *ARMS2* (rs10490924), *C3* (rs433594 and rs2230199), *CETP* (rs3764261), *CFB* (rs4151667 and rs641153), *CFH* (rs1061170, rs800292, and rs12144939), and *CFI* (rs10033900), *COL10A1* (rs3812111), *COL8A1* (rs13081855), *HSPH1* (rs9542236), *IER3DDR* (rs3130783), *MYRIP* (rs2679798), *RAD51B* (rs8017304), *SKIV2L* (rs429608), *SLC16A8* (rs8135665), *TGFBR1* (rs334353), *VEGFA* (rs943080), *TNFRSF10A* (rs13278062). Genomic DNA was extracted from peripheral blood samples using standard procedures and genotyping of the 23 SNPs was performed with KASP™ genotyping assays (LGC Genomics) according to the manufacturer’s instructions. Genotype frequencies in the control individuals were tested for Hardy-Weinberg equilibrium. Genotypes of SNPs were coded as 0 for carriers of non-risk variants, 1 for carriers of only 1 risk variant, and 2 for carriers of 2 risk variants.

Covariates

The questionnaire also included questions regarding weight and height, allowing calculation of body mass index (BMI, subdivided in three groups: <25, 25-30 and >30). Smoking behavior was questioned as never, past, current smoking; educational level was ascertained as primary school, high school, and higher professional education or university.

Statistical analysis

Standard descriptive statistics were used to describe baseline and clinical characteristics. Primary outcome was presence of early and advanced AMD versus absence of AMD. The association between single risk variants and AMD were investigated univariately and multivariately using logistic regression analysis, and a genetic risk score was calculated by summation of the beta coefficients of the multivariate analysis. We investigated the association between parental family history and AMD with logistic regression analysis, adjusting for age and gender. Next, we repeated this analysis for family history in siblings.

Finally, we constructed prediction models based on age, gender, family history, genotypes, and other AMD covariates.^{11, 16-18} Models included increasing levels of informativeness of family history, and were based on a receiver-operating curve (ROC) with calculation of the area under the curve (AUC) as a measure of discriminative accuracy. Data were analyzed using SPSS Software version 20.0 (SPSS Inc., Chicago, IL); two-sided *P*-values less than 0.05 were considered statistically significant.



RESULTS

Demographic characteristics of the probands, are depicted in **Table 3.2.1**. A positive family history for first degree relatives was reported in 22.4% of the AMD patients and in 12.0% of the controls, resulting in a significant risk of AMD (OR 2.56; 95% CI 2.10-3.12), adjusted for age and sex. An affected parent was reported by 12.7% AMD patients and 8.5% controls (*P* <0.001). In the subset of 512 controls and 944 AMD patients who had data on family history of siblings, at least one affected sibling was reported by 28.0% of patients versus 15.4% of controls (*P* <0.001). Additionally to a positive family history, an increasing age, current smoking behaviour, and no university education were significantly associated with AMD. We calculated a genetic risk score based on the beta coefficients from the multivariate regression analyses of 23 SNPs. The mean genetic risk score was significantly higher in AMD patients than in controls in the parental as well as the sibling cohort (both *P* < 0.001).

Table 3.2.1 Demographic characteristics of the probands

	Controls		AMD	
	Parental cohort (N=1555)	Sibling cohort (N=512)	Parental cohort (N=1915)	Sibling cohort (N=944)
Mean age, yrs (SD)	70.6 (7.4)	69.8 (6.6)	75.6 (9.0)**	75.1 (8.1)**
Gender, % Female	55.9	59.6	60.1*	60.1
Positive family history, N (%)	186 (12.0)	163 (31.8)	429 (22.4)**	383 (40.6)**
Affected parents, N (%)				
- 0	1423 (92)	403 (78.7)	1671 (87)	746 (79.0)
- 1	130 (8)	107 (20.9)	230 (12)**	185 (19.6)*
- 2	2 (0)	2 (0.4)	14 (1)*	13 (1.4)*
BMI, %				
- <25 kg/m ²	44.7	43.5	46.2	44.3
- 25-30 kg/m ²	43.2	44.6	41.2	41.3
- >30 kg/m ²	12.1	11.9	12.6	14.4
Smoking, %				
- Never	44.1	40.5	41.3	38.7
- Past	48.9	52.2	48.3*	50.1
- Current	6.9	7.3	10.4**	11.2**
Education, %				
- University	54.8	65.2	43.8	46.6
- No-university	45.2	34.8	56.2**	53.4**
Mean Genetic Risk Score (SD)	1.5 (1.8)	1.5 (1.9)	2.3 (1.4)**	2.5 (1.0)**

N = number of patients; OR = odds ratio; CI = confidence interval; SD = standard deviation; Age = age at participation; BMI = body mass index; genetic risk score = sum of beta coefficients of 23 SNPs; Parental cohort is total with available parental family history. Sibling cohort is part of the total cohort with available family history data of siblings. Analyses of differences between AMD patients and controls in the parental and sibling cohort are adjusted for age and gender.

* *P*-value < 0.05; ** *P*-value < 0.001

The risk of AMD for a positive parental family history, adjusted for age and gender (Table 3.2.2) increased with the number of affected parents and was OR 8.17 (95% CI 1.79-37.37, *P* = 0.007) when both parents were affected. A positive parental family history corresponded to a higher proportion of affected siblings: 20% and 22% for subjects with one or two affected parents versus only 11% for patients without affected parents (*P* < 0.001 and *P* = 0.129, respectively)

Table 3.2.2 Family history: Risk of AMD as a function of number of affected parents

Number parents AMD	Controls Total N=1555 N (%)	AMD Total N=1915 N (%)	OR (95% CI) *	P-value *
0 parents AMD	1423 (91.5)	1671 (87.3)	Ref.	
1 parent AMD	130 (8.4)	230 (12.0)	2.04 (1.61-2.59)	<0.001
2 parents AMD	2 (0.1)	14 (0.7)	8.17 (1.79-37.37)	0.007

AMD = age-related macular degeneration; OR = Odds ratio; CI = confidence interval; Ref = reference; % siblings = mean percentage siblings with AMD. * Adjusted for age and gender. P-values < 0.05 indicate significant associations.

Table 3.2.3 shows the ORs of AMD for the number of affected siblings adjusted for age and sex. In the families consisting of 1-5 siblings, having a positive sibling history significantly increased the OR for AMD (OR 2.02; 95% CI 1.40-2.91), but the OR did not increase by the number of affected siblings. In the large families (>5 siblings), having an affected sibling was a significant risk factor for AMD (OR 2.53; 95% CI 1.29-4.99), and the risk increased with the number of affected siblings resulting in an OR of 3.12 (95% CI 1.19-8.16) for having at least 3 affected siblings.

Table 3.2.3 Family history: Risk of AMD as a function of number of affected siblings in small and large families

Small families (≤5 siblings)				Large families (>5 siblings)			
Number affected siblings	N=1078	OR (95%CI)*	P-value *	Number affected siblings	N=378	OR (95%CI)*	P-value *
0	863	Ref.		0	250	Ref.	
≥1	215	2.02 (1.40-2.91)	<0.001	1-2	96	2.41 (1.38-4.23)	0.002
				≥3	32	3.12 (1.19-8.16)	0.021

N = number; OR = odds ratio; CI = confidence interval; Ref = reference; * adjusted for age and gender. P-values < 0.05 indicate significant associations

We created prediction models for AMD using different sets of risk factors (**Table 3.2.4**). Prediction model 1 was based on 23 SNPs (**Table 3.2.5**), age and sex and showed an AUC of 0.810 (95% CI 0.784-0.837). Prediction model 2 was based on age, sex and family history, by which family history was defined as at least one first-degree relative with AMD. The AUC of this model was 0.724 (95% CI 0.693-0.756), which is significantly lower than genetic model 1 ($P < 0.001$).



Table 3.2.4 Predictive value for family history

Variables in Model	AUC (95% CI)	SE	Controls/ AMD (N)
1. 23 SNPs, age, sex	0.810 (0.784-0.837)	0.014	390/596
2. Family history (yes/no), age, sex	0.724 (0.693-0.756)	0.016	390/596
3. Parental history, age, sex	0.724 (0.692-0.755)	0.016	390/596
- 0 affected parents	0.702 (0.665-0.738)	0.019	305/481
- 1 affected parent	0.789 (0.727-0.852)	0.032	83/108
- 2 affected parents	1.000 (1.000-1.000)	0.000	2/7
4. Sibling history, age, sex	0.720 (0.688-0.752)	0.016	390/596
Small families: 0 affected sibs	0.720 (0.678-0.762)	0.021	240/340
1 affected sib	0.745 (0.636-0.853)	0.055	22/72
≥ 2 affected sibs	0.784 (0.639-0.928)	0.074	16/24
Large families: 0 affected sibs	0.683 (0.606-0.760)	0.039	88/96
1 affected sib	0.740 (0.565-0.915)	0.089	10/25
≥ 2 affected sibs	0.809 (0.677-0.940)	0.067	14/39
5. Parental and sibling history, age, sex	0.724 (0.692-0.755)	0.016	390/596
0 affected parents: 0 affected sibs	0.686 (0.645-0.727)	0.021	262/373
1 affected sib	0.754 (0.646-0.863)	0.055	21/68
≥ 2 affected sibs	0.801 (0.687-0.915)	0.058	22/40
1 affected parents: 0 affected sibs	0.790 (0.711-0.869)	0.040	64/60
1 affected sib	0.717 (0.538-0.895)	0.091	11/26
≥ 2 affected sibs	0.827 (0.679-0.974)	0.075	8/22
6. Parental and sibling history, age, sex, smoking, BMI, education level	0.736 (0.703-0.769)	0.017	353/512
0 affected parents: 0 affected sibs	0.701 (0.658-0.744)	0.022	234/317
1 affected sib	0.744 (0.636-0.852)	0.055	19/62
≥ 2 affected sibs	0.854 (0.747-0.961)	0.054	21/31
1 affected parents: 0 affected sibs	0.792 (0.708-0.875)	0.043	61/52
1 affected sib	0.798 (0.627-0.969)	0.087	9/22
≥ 2 affected sibs	0.864 (0.726-1.000)	0.071	7/21
7. Parental and sibling history, age, sex, smoking, BMI, education level, 23 SNPs	0.822 (0.794-0.850)	0.014	353/512
0 affected parents: 0 affected sibs	0.809 (0.773-0.845)	0.019	234/317
1 affected sib	0.849 (0.766-0.932)	0.042	19/62
≥ 2 affected sibs	0.825 (0.696-0.954)	0.066	21/31
1 affected parents: 0 affected sibs	0.839 (0.765-0.913)	0.038	61/52
1 affected sib	0.899 (0.788-1.000)	0.057	9/22
≥ 2 affected sibs	0.884 (0.758-1.000)	0.065	7/21

In addition to age and sex, model 1 includes 23 AMD associated SNPs, model 2 the family history for AMD, model 3 the parental history, model 4 the history of AMD in siblings, model 5 the parental and sibling history, model 6 parental and sibling history and the environmental factors smoking behaviour, BMI and education, and the full model 7 includes parental and sibling history, environmental factors and 23 SNPs.

23 SNPs include: ADAMTS9 (rs6795735), APOE (rs4420638), ARMS2 (rs10490924), C3 (rs433594 and rs2230199), CETP (rs3764261), CFB (rs4151667 and rs641153), CFH (rs1061170, rs800292, and rs12144939), and CFI (rs10033900), COL10A1 (rs3812111), COL8A1 (rs13081855), HSPH1 (rs9542236), IER3DDR (rs3130783), MYRIP (rs2679798), RAD51B (rs8017304), SKIV2L (rs429608), SLC16A8 (rs8135665), TGFBR1 (rs334353), VEGFA (rs943080), TNFRSF10A (rs13278062). Small families consist of 1-5 siblings. Large families consist of > 5 siblings.

AUC = area under the curve, CI = confidence interval; SE = standard error; AMD = age-related macular degeneration; BMI = body mass index; sibs = siblings

Model 3 included the number of affected parents in addition to age and sex. The predictive value of this model increased with the number of affected parents. In case of 2 affected parents the AUC was 1.000, although this was only based on 7 AMD patients and 2 controls. The family history concerning siblings is included in model 4 together with age and sex. The AUC increased with an increasing number of affected siblings. In case of at least 2 affected siblings, the AUC of model 4 is comparable to genetic model 1 in small families ($P = 0.730$) and in large families consisting of >5 siblings ($P = 0.988$). Both parental and sibling history are included in model 5 in addition to age and sex. The AUC of this model also increased with the number of affected siblings and parents. In case of 1 affected parent and at least 2 affected siblings the AUC curve even exceeded the AUC of genetic model number 1, although this was not significant ($P = 0.824$). Addition of the environmental factors BMI, smoking behaviour, and education level to model 5 led to model 6, which resulted in higher AUCs than model 5. Model 7 included age, sex, parental and sibling history, environmental factors and 23 SNPs, and this full model resulted in higher AUCs than model 6 without genetic factors. However, in case of at least 2 affected siblings or 2 affected parents the AUC did not increase or only slightly increased (AUC increase of 0.020; $P = 0.835$) by the addition of 23 SNPs.

The ROC curves with the corresponding AUCs of prediction model 1 and 2 for AMD are displayed in **Figure 1**. Additionally, the curves of at least 2 affected siblings with 0 or 1 affected parent (model 5) and the curve of 2 affected parents (model 3) are presented in **Figure 1**, demonstrating clinical settings in which the predictive value of the familial models are comparable to the genetic model 1.

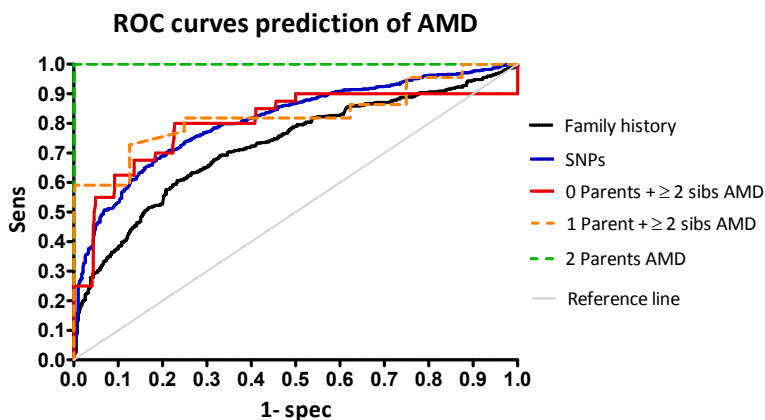


Figure 3.2.1 ROC curves prediction of AMD. Prediction model 2 includes family history, age and sex and has an AUC of 0.724. Genetic model 1 includes 23 SNPs, age and sex and has an AUC of 0.810. Detailed information of the number of affected parents and siblings in combination with age and sex in model 5 resulted in an AUC of 0.801 when 2 or more siblings are affected and an AUC of 0.827 when at least 2 siblings and 1 parent are affected. In case both parents have AMD the AUC is 1.000. Abbreviations= Sens: sensitivity; spec: specificity; SNPs, 23 single nucleotide polymorphisms; AMD: age-related macular degeneration.



Table 3.2.5 Univariate analyses for the 23 SNPs included in this study

	Controls (N=1555) N (%)	AMD (N=1915) N (%)	OR (95% CI)	P-value
ADAMT59 rs6795735				
-CC	491 (36)	495 (33)	Ref.	
-CT	669 (48)	714 (47)	1.06 (0.90-1.25)	0.494
-TT	225 (16)	313 (21)	1.38 (1.12-1.71)	0.003
APOE rs420638				
-AA	942 (69)	1104 (73)	Ref.	
-AG	393 (29)	385 (25)	0.84 (0.71-0.99)	0.034
-GG	41 (3)	29 (2)	0.60 (0.37-0.98)	0.041
ARMS2 rs10490924				
-GG	840 (60)	665 (39)	Ref.	
-GT	488 (35)	763 (44)	1.98 (1.70-2.30)	<0.001
-TT	70 (5)	300 (17)	5.41 (4.09-7.16)	<0.001
C3 rs433594				
-CC	538 (39)	586 (39)	Ref.	
-CT	662 (48)	716 (47)	0.99 (0.85-1.16)	0.930
-TT	186 (13)	220 (14)	1.09 (0.87-1.36)	0.478
C3 rs2230199				
-CC	697 (63)	793 (57)	Ref.	
-CG	369 (33)	486 (35)	1.16 (0.98-1.37)	0.090
-GG	40 (4)	104 (8)	2.29 (1.57-3.34)	<0.001
CEFP rs3764261				
-GG	677 (48)	743 (43)	Ref.	
-GT	577 (41)	778 (45)	1.23 (1.06-1.43)	0.007
-TT	145 (10)	203 (12)	1.28 (1.01-1.62)	0.044
CFB rs4151667				
-TT	1269 (93)	1616 (95)	Ref.	
-TA	98 (7)	86 (5)	0.69 (0.51-0.93)	0.015
-AA	1 (0)	1 (0)	0.79 (0.05-12.57)	0.864
CFB rs641153				
-GG	1159 (84)	1357 (71)	Ref.	
-GA	217 (16)	165 (11)	0.65 (0.52-0.81)	<0.001
-AA	8 (1)	3 (0)	0.32 (0.09-1.21)	0.093
CFH rs1061170				
-TT	544 (39)	412 (24)	Ref.	
-TC	678 (49)	801 (46)	1.56 (1.32-1.84)	<0.001
-CC	173 (12)	515 (30)	3.93 (3.17-4.87)	<0.001
CFH rs800292				
-GG	778 (56)	1044 (69)	Ref.	
-GA	530 (38)	419 (28)	0.59 (0.50-0.69)	<0.001
-AA	73 (5)	60 (4)	0.61 (0.43-0.87)	0.007
CFH rs12144939				
-GG	881 (64)	1173 (77)	Ref.	
-GT	446 (32)	311 (20)	0.52 (0.44-0.62)	<0.001
-TT	58 (4)	37 (2)	0.48 (0.31-0.73)	0.001
CFH rs10033900				
-CC	371 (27)	426 (25)	Ref.	
-CT	717 (51)	854 (50)	1.04 (0.87-1.23)	0.675
-TT	312 (22)	429 (25)	1.20 (0.98-1.47)	0.080



COL10A1 rs3812111									
-AA	180 (13)	212 (14)	Ref.						
-AT	653 (47)	717 (47)	0.93 (0.74-1.17)						0.542
-TT	551 (40)	591 (39)	0.91 (0.72-1.15)						0.425
COL8A1 rs13081855									
-GG	1130 (81)	1245 (82)	Ref.						
-GT	245 (18)	263 (17)	0.97 (0.80-1.18)						0.790
-TT	13 (1)	16 (1)	1.12 (0.54-2.33)						0.768
HSPH1 rs9542236									
-TT	440 (32)	422 (28)	Ref.						
-TC	685 (49)	754 (50)	1.15 (0.97-1.36)						0.110
-CC	262 (19)	347 (23)	1.38 (1.12-1.70)						0.002
IER3DDR rs3130783									
-AA	913 (66)	1033 (68)	Ref.						
-AG	421 (30)	443 (29)	0.93 (0.79-1.09)						0.375
-GG	52 (4)	47 (3)	0.80 (0.53-1.20)						0.276
MYRIP rs2679798									
-AA	445 (32)	480 (32)	Ref.						
-AG	649 (47)	727 (48)	1.04 (0.88-1.23)						0.657
-GG	289 (21)	316 (21)	1.01 (0.83-1.25)						0.897
RAD51B rs8017304									
-AA	544 (39)	628 (41)	Ref.						
-AG	622 (45)	703 (46)	0.98 (0.84-1.15)						0.792
-GG	216 (16)	192 (13)	0.77 (0.61-0.97)						0.023
SKIV2L rs429608									
-GG	1028 (74)	1228 (81)	Ref.						
-GA	326 (24)	276 (18)	0.71 (0.59-0.85)						<0.001
-AA	26 (2)	16 (1)	0.52 (0.28-0.97)						0.039
SLC16A8 rs8135665									
-CC	869 (63)	908 (60)	Ref.						
-CT	451 (33)	520 (34)	1.10 (0.94-1.29)						0.218
-TT	55 (4)	88 (6)	1.53 (1.08-2.17)						0.017
TGFBR1 rs334353									
-TT	785 (57)	883 (58)	Ref.						
-TG	507 (37)	556 (37)	0.98 (0.84-1.14)						0.747
-GG	95 (7)	84 (6)	0.79 (0.58-1.07)						0.127
VEGFA rs943080									
-CC	329 (24)	330 (22)	Ref.						
-CT	707 (51)	770 (51)	1.09 (0.90-1.31)						0.380
-TT	352 (25)	424 (28)	1.20 (0.98-1.48)						0.085
TNFRSF10A rs13278062									
-GG	345 (25)	304 (20)	Ref.						
-GT	687 (50)	764 (50)	1.26 (1.05-1.52)						0.014
-TT	355 (26)	446 (30)	1.43 (1.16-1.76)						0.001

N= number of patients; OR= odds ratio; CI = confidence interval; SD = standard deviation; Ref = reference



DISCUSSION

While risk effects of many demographic, environmental, and genetic risk factors are well established, little is known about the risk of a positive family history for developing AMD. Knowledge of these risks is important for ophthalmologists, because they are regularly confronted with questions about risk of AMD, particularly by persons with affected family members. Therefore, we investigated the risk of a positive family history for AMD and compared the performance of a positive family history to common genetic variants with respect to prediction of AMD.

In the total cohort, the model including family history is less predictive than the genetic model of 23 common genetic variants. Extensive information of the number of affected parents and siblings increases the predictive value in densely affected families. In case of 2 affected parents or at least 2 affected siblings the AUC of the model including family history was comparable or exceeded the AUC of the genetic model. This demonstrates the importance of detailed questioning about familial occurrence of AMD in predicting this disease. The ROC curves of the full model including age, gender, parental and sibling history, environmental and genetic factors resulted in the highest AUC values in general.

A positive family history of AMD is an established risk factor for AMD.^{9, 10, 19-22} Earlier reports have demonstrated that incorporation of family size and the proportion affected helps to discriminate high- and low-risk families.²³ Nevertheless, current AMD prediction models are based on positive family history as a dichotomous variable,^{16, 22, 24} although some sub-stratify for parental and sibling family history.^{9, 10, 25-27} Our results show that, the prediction of AMD risk improved with inclusion of family size. In large families, the number of affected appears to reflect the magnitude of the genetic risk better than currently known risk variants. As Sobrin et al showed that the genotypic load determined by common SNPs in densely affected families is significantly lower than expected from simulation, these families may harbour rare, more penetrant variants for AMD.²⁸

AMD can aggregate in families,^{9, 27} and an affected first-degree relative increases someone's risk on AMD.¹⁰ Several studies have shown that having an affected parent is associated with a higher risk than having an affected sibling.^{10, 27} Our results show a comparable OR between an affected parent and affected sibling. However, the risk of AMD for individuals with two affected parents was significantly higher than for those with many affected siblings. Even in large families with a high proportion of affected siblings, family history of 2 affected parents was more detrimental than family history of many affected siblings.

We found that assessment of 23 AMD associated SNPs does not add any value in the prediction in individuals with large, densely affected families. Therefore, analyses of the 23 common genetic variants to predict personalized risk for developing AMD can be omitted if the family history suggests a densely affected large family.

Since the referral area of the Department of Ophthalmology in Nijmegen includes the Catholic South and the 'Bible belt', where around the 1940s having large families was not uncommon, our cohort has a high frequency of these large, densely affected families.^{9, 21, 23, 25} In 1456 participants of which the family size was available, 26% have more than 5 siblings. Nowadays, families with more than 5 siblings are less common, making it more challenging to estimate the risk of AMD based on family history.

There are several limitations to our study. Unfortunately, we do not have follow-up data of our cohort, which seems to be important phenotypic predicting information in literature.^{11, 16, 29-31} Because of this, we do not aim to create an ideal model, but we want to clarify the role of a positive family history and common genetic variants in predicting AMD.

The questionnaire was completed by the proband of the family, which may have led to inaccuracies or bias in several ways. We used self-reported information of the family history, BMI and smoking status. It has been reported that this may lead to underestimation.^{32, 33} However, this is expected to be parallel for cases and controls, so we do not think this has affected our results. We are aware that a positive family history is generally underestimated.³⁴⁻³⁹ AMD is a late-onset, often asymptomatic disease and therefore patients with non-advanced AMD are not always aware of their own diagnosis, let alone the diagnosis of their family members.³⁵ Previously, we found that the self-reported family history following our definition was correct in 93% of 68 familial subjects of whom we had ophthalmologically examined the siblings and parents. (Saksens et al. submitted to PLoS One). This is in accordance to findings of Shahid et al.¹⁰ However, the uncertainty of AMD diagnosis in family members still exists.^{9, 40}

In conclusion, common AMD SNP analysis has no additional value in a risk model containing detailed family history, demographic and environmental data, in predicting AMD in large, densely affected families. Our results can help clinicians in their decision to perform molecular testing for AMD. However, when prediction tests include more rare, high-risk alleles in the future, this may change.



REFERENCES

1. Coleman HR, Chan CC, Ferris FLr, Chew EY. Age-related macular degeneration. *Lancet* 2008;372:1835-1845.
2. Lechanteur YT, van de Ven JP, Smailhodzic D, et al. Genetic, behavioral, and sociodemographic risk factors for second eye progression in age-related macular degeneration. *Invest Ophthalmol Vis Sci* 2012;53:5846-5852.
3. Age-Related Eye Disease Study Research G. Risk factors associated with age-related macular degeneration. A case-control study in the age-related eye disease study: Age-Related Eye Disease Study Report Number 3. *Ophthalmology* 2000;107:2224-2232.
4. Evans JR. Risk factors for age-related macular degeneration. *Prog Retin Eye Res* 2001;20:227-253.
5. Seddon JM, Cote J, Davis N, Rosner B. Progression of age-related macular degeneration: association with body mass index, waist circumference, and waist-hip ratio. *Arch Ophthalmol* 2003;121:785-792.
6. Klein RJ, Zeiss C, Chew EY, et al. Complement factor H polymorphism in age-related macular degeneration. *Science* 2005;308:385-389.
7. Rivera A, Fisher SA, Fritsche LG, et al. Hypothetical LOC387715 is a second major susceptibility gene for age-related macular degeneration, contributing independently of complement factor H to disease risk. *Hum Mol Genet* 2005;14:3227-3236.
8. Clemons TE, Milton RC, Klein R, Seddon JM, Ferris FL, 3rd, Age-Related Eye Disease Study Research G. Risk factors for the incidence of Advanced Age-Related Macular Degeneration in the Age-Related Eye Disease Study (AREDS) AREDS report no. 19. *Ophthalmology* 2005;112:533-539.
9. Klaver CC, Wolfs RC, Assink JJ, van Duijn CM, Hofman A, de Jong PT. Genetic risk of age-related maculopathy. Population-based familial aggregation study. *Arch Ophthalmol* 1998;116:1646-1651.
10. Shahid H, Khan JC, Cipriani V, et al. Age-related macular degeneration: the importance of family history as a risk factor. *Br J Ophthalmol* 2012;96:427-431.
11. Buitendijk GH, Rochtchina E, Myers C, et al. Prediction of age-related macular degeneration in the general population: the Three Continent AMD Consortium. *Ophthalmology* 2013;120:2644-2655.
12. Grassmann F, Fritsche LG, Keilhauer CN, Heid IM, Weber BH. Modelling the genetic risk in age-related macular degeneration. *PLoS One* 2012;7:e37979.
13. Hageman GS, Gehrs K, Lejnine S, et al. Clinical validation of a genetic model to estimate the risk of developing choroidal neovascular age-related macular degeneration. *Hum Genomics* 2011;5:420-440.
14. Ristau T, Ersoy L, Lechanteur Y, et al. Allergy is a protective factor against age-related macular degeneration. *Invest Ophthalmol Vis Sci* 2014;55:210-214.
15. Klein R, Myers CE, Buitendijk GH, et al. Lipids, lipid genes, and incident age-related macular degeneration: the three continent age-related macular degeneration consortium. *Am J Ophthalmol* 2014;158:513-524 e513.
16. Klein ML, Francis PJ, Ferris FL, 3rd, Hamon SC, Clemons TE. Risk assessment model for development of advanced age-related macular degeneration. *Arch Ophthalmol* 2011;129:1543-1550.
17. Seddon JM, Reynolds R, Maller J, Fagerness JA, Daly MJ, Rosner B. Prediction model for prevalence and incidence of advanced age-related macular degeneration based on genetic, demographic, and environmental variables. *Invest Ophthalmol Vis Sci* 2009;50:2044-2053.

18. Spencer KL, Olson LM, Schnetz-Boutaud N, et al. Using genetic variation and environmental risk factor data to identify individuals at high risk for age-related macular degeneration. *PLoS One* 2011;6:e17784.
19. Klein ML, Mauldin WM, Stoumbos VD. Heredity and age-related macular degeneration. Observations in monozygotic twins. *Arch Ophthalmol* 1994;112:932-937.
20. Meyers SM, Greene T, Gutman FA. A twin study of age-related macular degeneration. *Am J Ophthalmol* 1995;120:757-766.
21. Seddon JM, Ajani UA, Mitchell BD. Familial aggregation of age-related maculopathy. *Am J Ophthalmol* 1997;123:199-206.
22. Smith W, Mitchell P. Family history and age-related maculopathy: the Blue Mountains Eye Study. *Aust N Z J Ophthalmol* 1998;26:203-206.
23. Assink JJ, Klaver CC, Houwing-Duistermaat JJ, et al. Heterogeneity of the genetic risk in age-related macular disease: a population-based familial risk study. *Ophthalmology* 2005;112:482-487.
24. Hyman LG, Liliensfeld AM, Ferris FL, 3rd, Fine SL. Senile macular degeneration: a case-control study. *Am J Epidemiol* 1983;118:213-227.
25. Silvestri G, Johnston PB, Hughes AE. Is genetic predisposition an important risk factor in age-related macular degeneration? *Eye (Lond)* 1994;8:564-568.
26. Hemminki K, Forsti A, Li X, Sundquist K, Sundquist J. Familial risks of age-related macular degeneration. *Am J Ophthalmol* 2011;151:561-562.
27. Luo L, Harmon J, Yang X, et al. Familial aggregation of age-related macular degeneration in the Utah population. *Vision Res* 2008;48:494-500.
28. Sobrin L, Maller JB, Neale BM, et al. Genetic profile for five common variants associated with age-related macular degeneration in densely affected families: a novel analytic approach. *Eur J Hum Genet* 2010;18:496-501.
29. Chiu CJ, Mitchell P, Klein R, et al. A risk score for the prediction of advanced age-related macular degeneration: development and validation in 2 prospective cohorts. *Ophthalmology* 2014;121:1421-1427.
30. Perlee LT, Bansal AT, Gehrs K, et al. Inclusion of genotype with fundus phenotype improves accuracy of predicting choroidal neovascularization and geographic atrophy. *Ophthalmology* 2013;120:1880-1892.
31. Seddon JM, Reynolds R, Yu Y, Daly MJ, Rosner B. Risk models for progression to advanced age-related macular degeneration using demographic, environmental, genetic, and ocular factors. *Ophthalmology* 2011;118:2203-2211.
32. Gorber SC, Tremblay M, Moher D, Gorber B. A comparison of direct vs. self-report measures for assessing height, weight and body mass index: a systematic review. *Obes Rev* 2007;8:307-326.
33. Gorber SC, Schofield-Hurwitz S, Hardt J, Levasseur G, Tremblay M. The accuracy of self-reported smoking: a systematic review of the relationship between self-reported and cotinine-assessed smoking status. *Nicotine Tob Res* 2009;11:12-24.
34. Janssens AC, Henneman L, Detmar SB, et al. Accuracy of self-reported family history is strongly influenced by the accuracy of self-reported personal health status of relatives. *J Clin Epidemiol* 2012;65:82-89.
35. MacLennan PA, McGwin G, Jr., Searcey K, Owsley C. Medical record validation of self-reported eye diseases and eye care utilization among older adults. *Curr Eye Res* 2012;38:1-8.
36. Glanz K, Grove J, Le Marchand L, Gotay C. Underreporting of family history of colon cancer: correlates and implications. *Cancer Epidemiol Biomarkers Prev* 1999;8:635-639.
37. Soegaard M, Jensen A, Frederiksen K, et al. Accuracy of self-reported family history of cancer in a large case-control study of ovarian cancer. *Cancer Causes Control* 2008;19:469-479.



38. Chang ET, Smedby KE, Hjalgrim H, Glimelius B, Adami HO. Reliability of self-reported family history of cancer in a large case-control study of lymphoma. *J Natl Cancer Inst* 2006;98:61-68.
39. Kerber RA, Slattery ML. Comparison of self-reported and database-linked family history of cancer data in a case-control study. *Am J Epidemiol* 1997;146:244-248.
40. Klein R, Klein BE, Knudtson MD, Meuer SM, Swift M, Gangnon RE. Fifteen-year cumulative incidence of age-related macular degeneration: the Beaver Dam Eye Study. *Ophthalmology* 2007;114:253-262.

3.3

Analysis of risk alleles and complement activation levels in familial and non-familial age-related macular degeneration

N.T.M. Saksens, Y.T.E. Lechanteur, S. Verbakel, J.M.M. Groenewoud, M.R. Daha, T. Schick, S. Fauser, C.J.F. Boon, C.B. Hoyng, A.I. den Hollander

PLoS One; Under review



PURPOSE. Age-related macular degeneration (AMD) is a multifactorial disease, in which complement-mediated inflammation plays a pivotal role. A positive family history is an important risk factor for developing AMD. Certain lifestyle factors are shown to be significantly associated with AMD in non-familial cases, but not in familial cases. This study aimed to investigate whether the contribution of common genetic variants and complement activation levels differs between familial and sporadic cases with AMD.

METHODS. 1216 AMD patients (281 familial and 935 sporadic) and 1043 controls (143 unaffected members with a family history of AMD and 900 unrelated controls without a family history of AMD) were included in this study. Ophthalmic examinations were performed, and lifestyle and family history were documented with a questionnaire. Nine single nucleotide polymorphisms (SNPs) known to be associated with AMD were genotyped, and serum concentrations of complement components C3 and C3d were measured. Associations were assessed in familial and sporadic individuals.

RESULTS. The association with risk alleles of the age-related maculopathy susceptibility 2 (*ARMS2*) gene was significantly stronger in sporadic AMD patients compared to familial cases ($P = 0.017$ for all AMD stages and $P = 0.003$ for advanced AMD, respectively). *ARMS2* risk alleles had the largest effect in sporadic cases but were not significantly associated with AMD in densely affected families. The C3d/C3 ratio was a significant risk factor for advanced AMD in familial cases, especially in patients with a densely affected family, and the association was significantly stronger than in sporadic patients ($P = 0.038$).

CONCLUSIONS. This study suggests that in familial AMD patients, the common genetic risk variant in *ARMS2* is less important compared to sporadic AMD. In contrast, factors leading to increased complement activation appear to play a larger role in patients with a positive family history compared to sporadic patients. A better understanding of the different contributions of risk factors in familial compared to non-familial AMD will aid the development of reliable prediction models for AMD, and may provide individuals with more accurate information regarding their individual risk for AMD. This information is especially important for individuals who have a positive family history for AMD.

INTRODUCTION

Age-related macular degeneration (AMD) is a multifactorial disease and the leading cause of blindness among the elderly in developed countries.¹ With an aging population, AMD is considered a major and growing health problem.² The disease, in its early stages, is characterized by drusen deposits and pigmentary abnormalities. Vision loss mainly occurs when the disease progresses to late AMD, which can be subdivided into geographic atrophy (GA) and choroidal neovascularization (CNV).³

Both environmental and genetic risk factors have been associated with the development and progression of AMD. The most consistently reported demographic and environmental risk factors are advanced age, high body mass index (BMI) and current cigarette smoking.⁴⁻⁸

Population-based analysis and twin studies have shown a strong genetic contribution to the development of AMD.^{2,9-12} Major associations were reported for genetic variants in the complement factor H (*CFH*) and age-related maculopathy susceptibility 2 (*ARMS2*) genes.^{3,13-17} Several pathways have been described to be implicated in the development of AMD, including the alternative complement pathway.^{18,19} Genetic variants in several complement genes have been associated with AMD, including the *CFH*,^{13-15,20} complement factor 3 (*C3*),²¹⁻²⁵ complement factor B (*CFB*),^{24,26,27} and complement factor I (*CFI*) genes.²⁸ Besides genetic variants in the complement genes, also systemic levels of complement components have been associated with AMD.^{24,29,30}

Approximately 20% of AMD patients have a positive family history,^{9-11,31} and first-degree relatives of AMD patients have an increased risk of developing AMD.^{9,10,32} It has been suggested that the familial component of AMD may be explained by shared genetic or environmental factors.¹⁰ However, the contribution of such factors in familial compared to non-familial AMD patients has not yet been studied comprehensively. We recently demonstrated that certain lifestyle factors, such as physical activity and red meat consumption, are significantly associated with AMD in sporadic cases but not in families.³³ A recent study showed that the mean genotypic load of common AMD risk alleles in AMD families did not deviate significantly from genotypic loads predicted by simulation models.³⁴ However, the mean genotypic load in densely affected families was significantly lower than expected, suggesting that such families may carry rare, highly penetrant genetic variants.³⁴ The purpose of this study is to investigate whether the contribution of common genetic variants differs between familial and non-familial AMD cases by interaction analyses. This will support the development of reliable prediction models for AMD, and may provide more accurate information regarding the individual risk for AMD, in particular for individuals who have family members with AMD and for whom this question is most urgent.



METHODS

Subjects

In this study, we evaluated 2259 subjects, including 1216 AMD patients and 1043 control individuals from the Netherlands and Germany. All participants were derived from the European Genetic Database (EUGENDA, www.eugenda.org), an international database for molecular and clinical analysis of AMD. Subjects 50 years of age or older were included when information about gender, BMI, smoking behavior, and family history was available. In case subjects were related, only the first derived AMD patient and control subject of the family were included. Clinical data of their relatives were available in 68 families and were only used to determine the degree of reliability of the self-reported questionnaire. This study was approved by a local ethics committee on Research Involving Human Subjects and met the criteria of the Declaration of Helsinki.

Before enrollment in the EUGENDA database, all subjects provided written informed consent and completed a detailed questionnaire on their medical history, family history of AMD, BMI, and lifestyle factors, such as smoking behavior. The study cohort was split in familial and sporadic subjects, based on the self-reported family history. A positive family history was defined as at least two first-degree relatives (parents and/or siblings) with AMD or possible AMD in a family. Participants with a positive family history were labeled as familial and participants without a positive family history were labeled as sporadic. Based on diagnosis and family history, the participants in this retrospective study were divided into four groups: unaffected individuals with a family history of AMD (referred to as familial controls) (n=143), familial AMD cases (n=281), unaffected individuals without a family history of AMD (referred to as sporadic controls) (n=900), and sporadic AMD cases (n=935). Familial cases were subdivided in patients with a mild (n=184) or dense (n=97) positive family history, in which the latter group meets one of next 3 criteria: (1) both parents have (possible) AMD, or (2) one affected parent and at least 25% of the siblings are affected, or (3) at least 50% of the siblings are affected. Subjects with a mild positive family history do not meet any of these criteria. The BMI was subdivided in three groups: <25, 25-30 and >30 and smoking behavior was categorized into never, past and current smoking.

Each participant underwent digital color fundus photography performed after pupillary dilatation with topical 1.0% tropicamide and 2.5% phenylephrine. Both patients and controls also received spectral-domain optical coherence tomography (SD-OCT). Color fundus photographs and OCT scans of both eyes of all individuals were evaluated by two independent certified reading center graders according to the standard protocol of the Cologne Image Reading Center and Laboratory (CIRCL).³⁵ The diagnosis of AMD was defined as described previously,³⁶ based on the grading of the worst affected eye. AMD was classified by the presence of pigmentary changes together with at least 10 small drusen (<63µm) or the presence of intermediate (63-124 µm) or large drusen (≥125 µm diameter) in the Early Treatment Diabetic Retinopathy Study (ETDRS) grid. The subgroup of advanced

AMD was defined as either AMD with subfoveal GA and/or CNV in at least one eye. Controls were classified as no abnormalities or only small drusen or pigmentary abnormalities.

Genotyping

Venous blood was obtained for genetic analysis and the measurement of the complement components C3 and C3d. Complement component C3 and the activation fragment C3d were measured in serum samples as described previously.²⁹ The C3d/C3 ratio was calculated as a measure of complement activation. Genomic DNA was extracted from peripheral blood samples using standard procedures. Genotyping of nine single nucleotide polymorphisms (SNPs) known to be associated with AMD, in the *ARMS2* (rs10490924), *CFH* (rs1061170, rs800292, and rs12144939), *C3* (rs2230199 and rs1047286), *CFB* (rs4151667 and rs641153), and *CFI* (rs10033900) genes was performed in at least 85% of the included subjects with KASP™ genotyping assays (LGC Genomics) according to the manufacturer's instructions. Genotype frequencies in the control individuals were tested for Hardy-Weinberg equilibrium.

Statistical analysis

Standard descriptive statistics were used to describe baseline and clinical characteristics. To study differences in age (at participation), gender, BMI, smoking status, risk allele frequencies for AMD-associated SNPs, and complement levels between AMD patients and controls, multivariable logistic regression analyses were performed adjusted for the covariates age, gender, BMI and smoking status, if possible.

Differences in association of AMD-associated SNPs and complement levels in familial compared to sporadic AMD were analyzed with a multivariable logistic regression analysis, with correction for the covariates age, gender, BMI and smoking status. Statistical analyses were also performed with subdivision into mildly and densely affected families for factors which were significantly associated with familial AMD, to study the effect of AMD-associated SNPs and complement levels on the density of AMD in affected families. Two-sided *P*-values of less than 0.05 were considered statistically significant

RESULTS

Baseline demographic data are depicted in **Table 3.3.1**. Increased age was a significant risk factor for AMD, in sporadic (Odds ratio (OR) 1.10; 95% Confidence Interval (CI) 1.09-1.11; *P* < 0.001) and familial patients (OR 1.17; 95% CI 1.13-1.21; *P* < 0.001). Female gender was not significantly associated with AMD in sporadic nor in familial cases. In sporadic patients the risk for AMD increased with increasing BMI (OR 1.45; 95% CI 1.05-1.99; *P* = 0.023), while BMI was not associated with AMD in familial patients. Current smoking was a significant risk factor for developing AMD in sporadic patients (OR 2.12; 95% CI 1.44-3.12; *P* < 0.001) but was not significantly associated with AMD in familial patients.



In a subset of 68 families, clinical examination data of the siblings and parents were available. The self-reported family history of the probands was correct in 93%. Only in 1 out of 68 subjects (1.5%) who reported in the questionnaire to have close relatives with (possible) AMD, none of the examined family members seemed to be affected on ophthalmological examination and therefore he was incorrectly classified as familial. In addition, 4 out of 68 subjects (6%) were incorrectly classified as sporadic. 56 probands reported a positive family history. Of those, 30 reported a densely positive family history, which was correct in 29 probands (97%). Only in one proband who reported AMD in one parent and in 1 out of 4 sibs, the densely positive family history was incorrect since no siblings had AMD at ophthalmic examination. The number of affected family members was correct in 66%, and an underestimation or overestimation of the number affected family members was reported in 27% and 7%, respectively.

The allele frequencies of AMD-associated SNPs and the differences in association with AMD (all stages) between familial and sporadic subjects are shown in **Table 3.3.2**. The *ARMS2* risk allele was a significant risk factor for AMD in sporadic cases (OR 2.49; 95% CI 2.12-2.93; $P < 0.001$). In familial cases this effect was also observed, albeit with a weaker effect (OR 1.60; 95% CI 1.16-2.22; $P = 0.005$). This difference in association was significant ($P = 0.017$). The *CFH* Y402H allele was significantly associated with AMD in both sporadic and familial cases (OR 1.81; 95% CI 1.57-2.09; and OR 2.20; 95% CI 1.58-3.06, respectively ($P < 0.001$)), and contrary to the *ARMS2* SNP, this association did not significantly differ between familial and sporadic patients. Other genetic variants in the *CFH*, *C3* and *CFB* genes were significantly associated with AMD in sporadic cases, but not in familial cases. However, the association of these SNPs did not significantly differ between familial and non-familial cases. A variant in the *CFI* gene (rs10033900) was not significantly associated with sporadic or familial AMD. The serum C3d/C3 ratio, as a measure of the systemic activity of the complement system, was a significant risk factor for AMD in familial patients (OR 1.12; 95% CI 1.00-1.25; $P = 0.042$) but not in sporadic patients. The difference in serum C3d/C3 levels between familial and sporadic subjects was not significant, but showed a trend towards association ($P = 0.096$).



Table 3.3.2 Risk estimates and risk differences of allele frequencies of AMD-associated SNPs and serum complement activation levels for all AMD grades based on family history

SNP / risk allele	Total (N=2259)	Familial / sporadic		Familial		Sporadic				
		N (%)	P-value [†]	AMD (N=281)	Controls (N=143)	P-value [†]	OR (95% CI) [†]	AMD (N=935)	Controls (N=900)	P-value [†]
ARMS2 / rs10490924/ T (%)	2259 (100)	0.017	46.6	33.2	0.005	1.60 (1.16-2.22)	39.4	21.0	<0.001	2.49 (2.12-2.93)
CFH Y402H / rs1061170/ C (%)	2259 (100)	0.288	60	40.9	<0.001	2.20 (1.58-3.06)	50.6	35.4	<0.001	1.81 (1.57-2.09)
CFH / rs800292 / A (%)	1936 (85.7)	0.478	16.9	19.0	0.385	0.82 (0.53-1.28)	18.8	25.5	<0.001	0.70 (0.58-0.83)
CFH / rs12144939/ T (%)	1947 (86.2)	0.896	9.2	16.4	0.052	0.62 (0.38-1.01)	13.9	20.3	<0.001	0.60 (0.49-0.73)
C3 / rs2230199/ G (%)	2254 (99.8)	0.848	28.1	23.5	0.148	1.31 (0.91-1.88)	23.5	20.4	0.007	1.26 (1.06-1.49)
C3 / rs1047286/ A (%)	1952 (86.4)	0.556	28.6	21.1	0.052	1.48 (1.00-2.21)	22.8	19.6	0.005	1.30 (1.08-1.56)
CFB / rs4151667/ A (%)	2241 (99.2)	0.574	3.1	3.2	0.781	0.88 (0.36-2.15)	3.5	4.9	0.027	0.67 (0.47-0.96)
CFB / rs641153 / A(%)	1944 (86.1)	0.728	5.3	8.2	0.210	0.64 (0.32-1.28)	6.4	8.2	0.044	0.74 (0.55-0.99)
CFI / rs10033900/ T (%)	2227 (98.6)	0.260	49.1	44.7	0.193	1.25 (0.90-1.73)	50.7	49.2	0.851	1.01 (0.88-1.16)
C3d/C3 ratio	1844 (81.6)	0.096	5.10 (2.65)*	4.64 (2.80)*	0.042	1.12 (1.00-1.24)	5.01 (3.61)*	4.56 (5.05)*	0.251	1.02 (0.99-1.05)

AMD = age-related macular degeneration; Familial = positive family history of AMD; Sporadic = negative family history of AMD; OR = odds ratio; CI = confidence interval; N = number of patients

* Mean (standard deviation); [†] Adjusted for age, gender, body mass index and smoking status; Missing genotypes were <15%. P-values and ORs printed in bold indicate significant associations.

Table 3.3.3 Risk estimates and risk differences of AMD-associated SNPs and serum complement activation levels for advanced AMD based on family history

SNP / risk allele	Total (N=1815) N (%)	Familial / sporadic		Familial			Sporadic			
		P-value [†]	AMD (N=201)	Controls (N=143)	P-value [†]	OR (95% CI) [†]	AMD (N=571)	Controls (N=900)	P-value [†]	OR (95% CI) [†]
ARMS2 / rs10490924 / T (%)	1815 (100)	0.003	50.3	33.3	0.001	1.92 (1.33-2.79)	46.6	21.0	< 0.001	3.63 (2.98-4.42)
CFH Y402H / rs1061170 / C (%)	1815 (100)	0.875	64.2	40.9	< 0.001	2.66 (1.79-3.95)	58.3	35.4	< 0.001	2.75 (2.30-3.30)
CFH / rs800292 / A (%)	1522 (83.9)	0.373	12.8	19.0	0.089	0.60 (0.34-1.08)	13.9	25.5	< 0.001	0.45 (0.35-0.59)
CFH / rs12144939 / T (%)	1532 (84.4)	0.824	7.2	16.4	0.011	0.44 (0.23-0.83)	11.6	20.3	< 0.001	0.40 (0.30-0.54)
C3 / rs2230199 / G (%)	1810 (99.7)	0.928	28.3	23.5	0.185	1.32 (0.87-2.00)	23.8	20.4	0.012	1.30 (1.06-1.59)
C3 / rs1047286 / A (%)	1537 (84.7)	0.882	27.7	21.1	0.261	1.32 (0.82-2.12)	23.1	19.6	0.008	1.37 (1.09-1.73)
CFB / rs4151667 / A (%)	1799 (99.1)	0.466	3.1	3.2	0.690	0.81 (0.29-2.26)	3.1	4.9	0.008	0.53 (0.34-0.85)
CFB / rs641153 / A (%)	1529 (84.2)	0.949	5.2	8.2	0.294	0.64 (0.27-1.48)	5.5	8.2	0.022	0.62 (0.41-0.93)
CFI / rs10033900 / T (%)	1791 (98.7)	0.578	48.0	44.7	0.463	1.15 (0.79-1.66)	51.6	49.2	0.784	1.02 (0.87-1.21)
C3d/C3 ratio	1481 (81.6)	0.038	5.13 (2.92)*	4.64 (2.80)*	0.021	1.14 (1.02-1.27)	4.91 (2.73)*	4.56 (5.05)*	0.458	1.01 (0.98-1.04)

AMD = age-related macular degeneration; Familial = positive family history of AMD; Sporadic = negative family history of AMD; OR = odds ratio; CI = confidence interval; N = number of patients;

* Mean (standard deviation); † Adjusted for age, gender, body mass index and smoking status; Missing genotypes were <17%. P-values and ORs printed in bold indicate significant associations.

The allele frequencies of AMD-associated SNPs and the differences in association with advanced AMD between familial and sporadic subjects are shown in **Table 3.3.3**. The findings for advanced AMD were similar as for all AMD stages, although the ORs of the common variants were stronger than for all AMD stages. Also, the difference in association of the *ARMS2* allele in subjects with a positive family history compared to those with a negative family history was even stronger for the development of advanced AMD ($P = 0.003$). No other SNPs differed in association between familial and sporadic subjects with advanced AMD. The C3d/C3 ratio significantly differed with family history ($P = 0.038$), as it was a significant risk factor for advanced AMD in familial patients (OR 1.14; 95% CI 1.02-1.27; $P = 0.021$) but not in sporadic patients.

97 of the 281 familial AMD patients and 34 of the 143 familial controls reported a densely affected family history. The *ARMS2* SNP was not associated with AMD in patients with a densely affected family, and this was significantly different from the association with sporadic AMD ($P = 0.010$ for all AMD stages and $P = 0.002$ for advanced AMD) (**Table 3.3.4 and Figure 3.3.1**). The association of the *CFH* Y402H allele with familial and sporadic AMD again did not differ. The C3d/C3 ratio showed the largest risk effect in patients with a densely affected family for advanced AMD (OR 1.39; 95% CI 1.08-1.78; $P = 0.010$) and differed significantly ($P = 0.033$) from the association with sporadic AMD. The same was observed for all AMD stages, with an OR of 1.42 (95% CI 1.07-1.87; $P = 0.015$) in patients with a densely affected family, although there was only a trend of difference between the association of the C3d/C3 ratio for subjects with a densely affected family and sporadic subjects ($P = 0.063$).

Table 3.3.4 Risk estimates and risk differences of allele frequencies of ARMS2 and CFH SNPs and serum complement activation levels in mild and densely affected AMD families

	All AMD grades					
	Familial / sporadic		Sporadic		Advanced AMD	
	P-value	OR (95% CI)	P-value	OR (95% CI)	P-value	OR (95% CI)
ARMS2						
<i>Mild familial</i>	0.001	1.95 (1.31-2.92)	<0.001	2.49 (2.12-2.93)	<0.001	2.38 (1.49-3.80)
<i>Dense familial</i>	0.946	1.02 (0.58-1.81)			0.595	1.19 (0.63-2.24)
CFH Y402H						
<i>Mild familial</i>	<0.001	2.18 (1.48-3.22)	<0.001	1.81 (1.57-2.09)	<0.001	2.75 (1.71-4.41)
<i>Dense familial</i>	0.575	2.23 (1.18-4.23)			0.015	2.47 (1.19-5.12)
C3d/C3 ratio						
<i>Mild familial</i>	0.063	1.04 (0.94-1.17)	0.252	1.02 (0.99-1.05)	0.280	1.07 (0.95-1.20)
<i>Dense familial</i>	0.015	1.42 (1.07-1.87)			0.010	1.39 (1.08-1.78)

AMD = age-related macular degeneration; Familial = positive family history of AMD; Sporadic = negative family history of AMD; OR = odds ratio; CI = confidence interval; Dense familial = a positive family history of AMD satisfying 1 out of 3 criteria: (1) both parents have (possible) AMD, or (2) one affected parent and at least 25% of number of the sibs are affected, or (3) at least 50% of the number of sibs is affected; Mild familial = a positive family history of AMD but in a lesser extent, not meeting one of the 3 criteria. All data are adjusted for age, gender, body mass index and smoking status;

P-values and ORs printed in bold indicate significant associations.

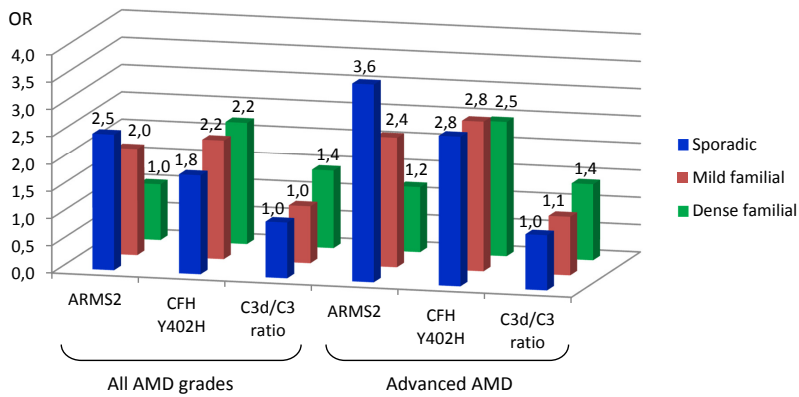


Figure 3.3.1 Odds ratios for risk variants in ARMS2 and CFH and the C3d/C3 ratio for development of AMD split by family history. The risk variant in ARMS2 confers a strong risk for AMD in the sporadic group. In the group with a dense family history there is no effect of this SNP. The CFH Y402H risk allele is associated with AMD in all subgroups, irrespective of family history. In case of a dense family history, the C3d/C3 ratio is associated with AMD development. In the subgroups with no or a mild family history, this effect was not observed.

OR = odds ratio; AMD = age-related macular degeneration; Sporadic = negative family history of AMD; Familial = positive family history of AMD; Dense familial = a positive family history of AMD satisfying 1 out of 3 criteria: (1) both parents have (possible) AMD, or (2) one affected parent and at least 25% of number of the sibs are affected, or (3) at least 50% of the number of sibs is affected; Mild familial = a positive family history of AMD but in a lesser extent, not meeting one of the 3 criteria.

DISCUSSION

In addition to environmental and genetic risk factors, a positive family history of AMD is an important risk factor for the development of AMD.^{9,10,32} For a proper risk assessment it is therefore important to determine an individual’s family history of AMD. In this study we investigated whether the contribution of AMD-associated SNPs and C3d/C3 ratio differs between familial and non-familial AMD cases.

Our results show that the association of the ARMS2 A69S genotype differed between familial and sporadic subjects. Within the group of cases and controls with a dense family history, ARMS2 was not associated with AMD, whereas it was a strong risk factor for sporadic individuals. Another difference was found for the C3d/C3 ratio between familial and sporadic subjects. In case of no or only a mild family history the ratio did not differ between cases and controls. However, in the subgroup with a dense family history, complement activation was significantly associated with the presence of all AMD stages and advanced AMD.

The ARMS2 A69S variant is one of the strongest genetic risk factors for AMD.³⁷ However, in densely affected families this risk variant seems to have less effect, and a high ARMS2 risk allele frequency was found in familial controls. Testing the ARMS2 SNP to estimate an

individual's AMD risk is thus more informative in patients without a positive family history. However, since both family history and SNPs are important factors in the development of AMD, and some discordance exists between risk estimates by genetic testing and by family history analysis,³⁸ they should be used complementary in risk assessment. The fact that the family history for AMD affects the risk of the *ARMS2* genotype, suggests that there are other, unknown factors that increase the risk for AMD in the patients with densely affected families. This supports the theory that densely affected families may harbor rare, more penetrant genetic variants for AMD.^{34,39,40} The difference in the association of the C3d/C3 ratio with advanced AMD between familial and sporadic subjects, can point towards a more important role for systemic complement activation in families with AMD compared to sporadic AMD patients, especially for the development of advanced AMD. Risk alleles of *CFH* and *ARMS2* are independently associated with an increased C3d/C3 ratio,²⁹ and the higher complement level in familial AMD patients may (partly) be explained by the higher number of risk alleles of those SNPs in familial patients compared to sporadic patients. However, after additional adjustment for the *ARMS2* and complement SNPs, we determined that the OR and corresponding CI for the C3d/C3 ratio does not significantly change. This further supports the hypothesis that rare, highly penetrant variants may contribute to the higher complement activation in familial AMD. Interestingly, several rare, highly penetrant AMD alleles have been described in several genes of the complement system,^{39,41-44} and in densely affected families, mutations in the *CFH* gene have been identified.^{40,43}

In this study no difference for the role of the *CFH* Y402H risk variant was observed between familial and sporadic subjects. Unlike *ARMS2*, the *CFH* Y402H risk SNP seems to be of equal importance for the development of AMD in sporadic and familial individuals. This finding further underlines the important role of the complement system in familial AMD, both through common SNPs as well as rare genetic variants.

Eight SNPs in the *ARMS2*, *CFH*, *C3* and *CFB* genes were associated with AMD in sporadic cases in our study, but only the 2 major SNPs, *ARMS2* rs10490924 and *CFH* rs1061170, were also significantly associated with AMD in familial cases. The lack of association with the remaining 6 SNPs in the familial cases is likely due to the limited number of available subjects, since the ORs of these 6 variants were comparable in sporadic and familial subjects and did not differ between familial and sporadic subjects. Stronger associations for advanced AMD compared to all AMD stages in sporadic cases indicate that the risk SNPs play a more important role in the development of advanced stages of AMD than in the development of small and intermediate drusen. In sporadic AMD, an increased BMI and current smoking status showed a significant association with AMD in our study, which is in agreement with previous studies.^{6-8,45} As these factors were not significantly associated with AMD in familial cases, environmental factors like smoking behavior and BMI may play a more important role in the development of AMD in sporadic patients than in familial patients. However, it should be noted that the absence of significant associations with AMD in familial subjects may be due to the limited number of available familial subjects.



The relatively low number of familial cases and controls is the main limitation of our study. This may reduce the power of our analyses. However, after subdividing our familial dataset into mild and densely affected families we observed that the differences in association between familial and sporadic cases were more pronounced, and this further underlines our findings. Nonetheless, our results should be interpreted with care and should be replicated in additional familial AMD cohorts in order to confirm our hypothesis.

In conclusion, this study demonstrates that the association of the *ARMS2* risk allele and complement activation levels in serum with AMD differs between familial and sporadic subjects. Our study suggests that *ARMS2* risk alleles have less effect in familial AMD patients than in sporadic AMD. In contrast, increased complement activation levels seem to play a larger role in patients with a positive family history compared to sporadic patients, which cannot be explained by known, common SNPs in the complement genes. A better understanding of factors that differ between individuals with and without a family history will aid the development of reliable prediction models for AMD, and may provide individuals with more accurate information regarding their individual risk for AMD. This information is especially important for individuals who have a dense positive family history for AMD.

REFERENCES

1. Coleman HR, Chan CC, Ferris FLr, Chew EY. Age-related macular degeneration. *Lancet* 2008;372: 1835-1845.
2. Lim LS, Mitchell P, Seddon JM, Holz FG, Wong TY. Age-related macular degeneration. *Lancet* 2012;379: 1728-1738.
3. Chakravarthy U, McKay GJ, de Jong PT, Rahu M, Seland J, et al. ARMS2 increases the risk of early and late age-related macular degeneration in the european eye study. *Ophthalmology* 2012;120: 342-348.
4. Rudnicka AR, Jarrar Z, Wormald R, Cook DG, Fletcher A, Owen CG. Age and gender variations in age-related macular degeneration prevalence in populations of European ancestry: a meta-analysis. *Ophthalmology* 2012;119: 571-580.
5. Klein BE, Klein R, Lee KE, Jensen SC. Measures of obesity and age-related eye diseases. *Ophthalmic Epidemiol* 2001;8: 251-262.
6. Thornton J, Edwards R, Mitchell P, Harrison RA, Buchan I, Kelly SP. Smoking and age-related macular degeneration: a review of association. *Eye (Lond)* 2005;19: 935-944.
7. van de Ven JP, Smailhodzic D, Boon CJ, Fauser, S, Groenewoud JM, et al. Association analysis of genetic and environmental risk factors in the cuticular drusen subtype of age-related macular degeneration. *Mol Vis* 2012;18: 2271-2278.
8. Khan JC, Thurlby DA, Shahid H, Clayton DG, Yates JR, et al. Smoking and age related macular degeneration: the number of pack years of cigarette smoking is a major determinant of risk for both geographic atrophy and choroidal neovascularisation. *Br J Ophthalmol* 2006;90: 75-80.
9. Klaver CC, Wolfs RC, Assink JJ, van Duijn CM, Hofman A, de Jong PT. Genetic risk of age-related maculopathy. Population-based familial aggregation study. *Arch Ophthalmol* 1998;116: 1646-1651.
10. Seddon JM, Ajani UA, Mitchell BD. Familial aggregation of age-related maculopathy. *Am J Ophthalmol* 1997;123: 199-206.
11. Meyers SM, Greene T, Gutman FA. A twin study of age-related macular degeneration. *Am J Ophthalmol* 1995;120: 757-766.
12. Klein ML, Mauldin WM, Stoumbos VD. Heredity and age-related macular degeneration. Observations in monozygotic twins. *Arch Ophthalmol* 1994;112: 932-937.
13. Edwards AO, Ritter R, 3rd, Abel KJ, Manning A, Panhuysen C, Farrer LA. Complement factor H polymorphism and age-related macular degeneration. *Science* 2005;308: 421-424.
14. Klein RJ, Zeiss C, Chew EY, Tsai JY, Sackler RS, et al. Complement factor H polymorphism in age-related macular degeneration. *Science* 2005;308: 385-389.
15. Haines JL, Hauser MA, Schmidt S, Scott WK, Olson LM, et al. Complement factor H variant increases the risk of age-related macular degeneration. *Science* 2005;308: 419-421.
16. Fritsche LG, Loenhardt T, Janssen A, Fisher SA, Rivera A, et al. Age-related macular degeneration is associated with an unstable ARMS2 (LOC387715) mRNA. *Nat Genet* 2008;40: 892-896.
17. Rivera A, Fisher SA, Fritsche LG, Keilhauer CN, Lichtner P, et al. Hypothetical LOC387715 is a second major susceptibility gene for age-related macular degeneration, contributing independently of complement factor H to disease risk. *Hum Mol Genet* 2005;14: 3227-3236.
18. Johnson LV, Leitner WP, Staples MK, Anderson DH. Complement activation and inflammatory processes in Drusen formation and age related macular degeneration. *Exp Eye Res* 2001;73: 887-896.
19. Zipfel PF, Lauer N, Skerka C. The role of complement in AMD. *Adv Exp Med Biol* 2010;703: 9-24.



20. Hageman GS, Anderson DH, Johnson LV, Hancox LS, Taiber AJ, et al. A common haplotype in the complement regulatory gene factor H (HF1/CFH) predisposes individuals to age-related macular degeneration. *Proc Natl Acad Sci USA* 2005;102: 7227-7232.
21. Park KH, Fridley BL, Ryu E, Tosakulwong N, Edwards AO. Complement component 3 (C3) haplotypes and risk of advanced age-related macular degeneration. *Invest Ophthalmol Vis Sci* 2009;50: 3386-3393.
22. Maller JB, Fagerness JA, Reynolds RC, Neale BM, Daly MJ, Seddon JM. Variation in complement factor 3 is associated with risk of age-related macular degeneration. *Nat Genet* 2007;39: 1200-1201.
23. Yates JR, Sepp T, Matharu BK, Khan JC, Thurlby DA, et al. Complement C3 variant and the risk of age-related macular degeneration. *N Engl J Med* 2007;357: 553-561.
24. Reynolds R, Hartnett ME, Atkinson JP, Giclas PC, Rosner B, Seddon JM. Plasma complement components and activation fragments: associations with age-related macular degeneration genotypes and phenotypes. *Invest Ophthalmol Vis Sci* 2009;50: 5818-5827.
25. Thakkinstian A, McKay GJ, McEvoy M, Chakravarthy U, Chakrabarti S, et al. Systematic review and meta-analysis of the association between complement component 3 and age-related macular degeneration: a HuGE review and meta-analysis. *Am J Epidemiol* 2011;173: 1365-1379.
26. Gold B, Merriam JE, Zernant J, Hancox LS, Taiber AJ, et al. Variation in factor B (BF) and complement component 2 (C2) genes is associated with age-related macular degeneration. *Nat Genet* 2006;38: 458-462.
27. Spencer KL, Hauser MA, Olson LM, Schmidt S, Scott WK, et al. Protective effect of complement factor B and complement component 2 variants in age-related macular degeneration. *Hum Mol Genet* 2007;16: 1986-1992.
28. Fagerness JA, Maller JB, Neale BM, Reynolds RC, Daly MJ, Seddon JM. Variation near complement factor I is associated with risk of advanced AMD. *Eur J Hum Genet* 2009;17: 100-104.
29. Smailhodzic D, Klaver CC, Klevering BJ, Boon CJ, Groenewoud JM, et al. Risk alleles in CFH and ARMS2 are independently associated with systemic complement activation in age-related macular degeneration. *Ophthalmology* 2012;119: 339-346.
30. Nozaki M, Raisler BJ, Sakurai E, Sarma JV, Barnum SR, et al. Drusen complement components C3a and C5a promote choroidal neovascularization. *Proc Natl Acad Sci USA* 2006;103: 2328-2333.
31. Saksens NT, Fleckenstein M, Schmitz-Valckenberg S, Holz, FG, den Hollander AI, et al. Macular dystrophies mimicking age-related macular degeneration. *Prog Retin Eye Res* 2014;39: 23-57.
32. Shahid H, Khan JC, Cipriani V, Sepp T, Matharu BK, et al. Age-related macular degeneration: the importance of family history as a risk factor. *Br J Ophthalmol* 2012;96: 427-431.
33. Saksens NT, Kersten E, Groenewoud JM, van Grinsven MJ, van de Ven JP, et al. Clinical characteristics of familial and sporadic age-related macular degeneration; differences and similarities. *Invest Ophthalmol Vis Sci* 2014;9:7085-7092.
34. Sobrin L, Maller JB, Neale BM, Reynolds RC, Fagerness JA, et al. Genetic profile for five common variants associated with age-related macular degeneration in densely affected families: a novel analytic approach. *Eur J Hum Genet* 2010;18: 496-501.
35. Mokwa NF, Ristau T, Keane PA, Kirchhof B, Sadda SR, Liakopoulos S. Grading of age-related macular degeneration: comparison between color fundus photography, fluorescein angiography, and spectral domain optical coherence tomography. *J Ophthalmol* 2013;385915.
36. Ristau T, Ersoy L, Lechanteur Y, den Hollander AI, Daha MR, et al. Allergy is a protective factor against age-related macular degeneration. *Invest Ophthalmol Vis Sci* 2014;55: 210-214.
37. Fritsche LG, Chen W, Schu M, Yaspan BL, Yu Y, et al. Seven new loci associated with age-related macular degeneration. *Nat Genet* 2014;45: 433-439.

38. Aiyar L, Shuman C, Hayeems R, Dupuis A, Pu S, et al. Risk estimates for complex disorders: comparing personal genome testing and family history. *Genet Med* 2014;16: 231-237.
39. Duvvari MR, Paun CC, Buitendijk GH, Saksens NT, Volokhina EB, et al. Analysis of rare variants in the c3 gene in patients with age-related macular degeneration. *PLoS One* 2014;15:9(4).
40. Yu Y, Triebwasser MP, Wong EK, Schramm EC, Thomas B, et al. Whole -exome sequencing identifies rare, functional CFH variants in families with macular degeneration. *Hum Mol Genet* 2014;23: 5283-5293.
41. van de Ven JP, Boon CJ, Fauser S, Hoefsloot LH, Smailhodzic D, et al. Clinical evaluation of 3 families with basal laminar drusen caused by novel mutations in the complement factor H gene. *Arch Ophthalmol* 2012;130: 1038-1047.
42. Raychaudhuri S, Iartchouk O, Chin K, Tan PL, Tai AK, et al. A rare penetrant mutation in CFH confers high risk of age-related macular degeneration. *Nat Genet* 2011; 43: 1232-1236.
43. Boon CJ, Klevering BJ, Hoyng CB, Zonneveld-Vrieling MN, Nabuurs SB, et al. Basal laminar drusen caused by compound heterozygous variants in the CFH gene. *Am J Hum Genet* 2008; 82: 516-523.
44. van de Ven JP, Nilsson SC, Tan PL, Buitendijk GH, Ristau T, et al. A functional variant in the CFI gene confers a high risk of age-related macular degeneration. *Nat Genet* 2013; 45: 813-817.
45. Howard KP, Klein BE, Lee KE, Klein R. Measures of body shape and adiposity as related to incidence of age-related eye diseases: observations from the Beaver Dam Eye Study. *Invest Ophthalmol Vis Sci* 2014; 55: 2592-2598.



3.4

Rare variants associated with age-related macular degeneration result in a lower age at onset and higher familial occurrence

N.T.M. Saksens, M.J. Geerlings, B. Bakker, T. Schick, M.R. Daha, S. Fauser, C.J.F. Boon, E.K. de Jong, C.B. Hoyng, A.I. den Hollander

JAMA Ophthalmology; Under review



PURPOSE. Recently, rare variants in the complement genes *CFH*, *CFI*, *C9* and *C3* were found to be highly associated with age-related macular degeneration (AMD). The aim of the current study was to determine the contribution of these rare variants in the development of AMD in 22 multiplex families. In addition, we aimed to describe clinical differences in carriers versus non-carriers, in these families and in a large case-control cohort.

METHODS. Retrospective case-control study including 114 affected and 60 unaffected family members of 22 multiplex AMD families, as well as 1589 AMD patients and 1386 control individuals from the European Genetic Database (EUGENDA). All individuals underwent an extensive ophthalmic examination and completed a questionnaire on family history for AMD and age at first symptoms. Venous blood was obtained for genetic analysis and measurement of complement activation levels. Main outcome measures are differences in age at first symptoms, family history for AMD, complement activation levels (C3d/C3 ratio), presence of reticular pseudodrusen, and AMD phenotype between carriers and non-carriers of rare variants.

RESULTS. Rare variants *CFI* Gly119Arg, *C9* Pro167Ser and *C3* Lys155Gln were confirmed in five out of 22 multiplex AMD families, but did not completely segregate with the disease. In our case-control cohort affected carriers of these variants had a significantly lower age at first symptoms (67.4 vs 71.3 years; $P = 0.010$), and more often had a positive family history for AMD (44.9% vs 30.6%; $P = 0.008$) compared to non-carriers. Patients with advanced atrophic AMD carried these rare variants more frequently than patients with neovascular AMD (11.8% vs 4.8%; $P = 0.044$).

CONCLUSIONS. Previously reported rare variants do not completely segregate within AMD families. However, patients carrying these rare variants differ clinically from non-carriers by a lower age at first symptoms, a higher prevalence of a positive family history, and by AMD phenotype. Genetic tests for AMD should therefore be designed to detect common and rare genetic variants, especially in families, since rare variants significantly contribute to the age at onset and progression of the disease.

INTRODUCTION

Age-related macular degeneration (AMD) is the leading cause of irreversible, central vision loss in the elderly population in developed countries.¹ A combination of genetic and non-genetic factors plays a role in the development and progression of this multifactorial disease.^{2,3} Genome-wide association studies have identified common genetic risk variants that are strongly associated with AMD, such as single nucleotide variant Tyr402His (rs1061170) in the *CFH* gene, and Ala69Ser (rs10490924) in the *ARMS2* gene.^{2,4,5}

Previous family- and twin-studies have demonstrated a strong genetic component and aggregation of AMD within families.⁶⁻⁹ Approximately 20-30% of the patients have a positive family history for AMD,^{7,10-12} which has been reported as a significant risk factor for AMD. A positive family history has also been associated with an earlier age at onset of disease.¹³⁻¹⁷ Clustering of known common genetic risk factors does not fully explain the number of affected family members in large, densely affected families.⁷ Several recent studies have identified rare genetic variants, which strongly increase the risk of AMD, including *CFH* Arg1210Cys, *CFI* Gly119Arg, *C9* Pro167Ser, and *C3* Lys155Gln.^{15,18-21} These rare variants are located in genes of the complement system, which plays a major role in the pathogenesis of AMD.^{2,22} Due to their strong effect size, these rare, highly penetrant genetic variants may account for clustering of AMD in families, and might lead to a more severe disease. Recently, highly penetrant variants have been identified in AMD families confirming the hypothesis that rare variants can cluster in families.¹⁵⁻¹⁷

The aim of the current study was to determine the contribution of known rare genetic variants in the development of AMD in large, multiplex AMD families. In addition, we aimed to describe differences in clinical characteristics in carriers versus non-carriers of these rare genetic variants, in multiplex families and in a large case-control cohort.

METHODS

Subjects

In this retrospective study, we evaluated 114 affected and 60 unaffected family members of 22 multiplex AMD families, and 1589 AMD patients and 1386 control individuals from the European Genetic Database (EUGENDA). This study was approved by the local ethics committees on Research Involving Human Subjects and met the criteria of the Declaration of Helsinki.

Before enrolment in the EUGENDA database, all subjects provided written informed consent and completed a detailed questionnaire on their medical history, age at onset of first symptoms, family history of AMD, and lifestyle factors. A positive family history of AMD was defined as at least two first-degree relatives (parents and/or siblings) with AMD or possible AMD in a family.



Each participant underwent digital color fundus photography and spectral-domain optical coherence tomography (SD-OCT, Spectralis; Heidelberg Engineering, Heidelberg, Germany) after pupillary dilatation with topical 1.0% tropicamide and 2.5% phenylephrine. Digital non-stereoscopic 30° color fundus photography centered on the fovea was performed with a Topcon TRC 50IX camera (Topcon Corporation, Tokyo, Japan). SD-OCT volume scans consisting of 19 or 37 parallel OCT B-scans were used for analysis, covering 6x4 mm of the macula. For each OCT B-scan, 20 images were averaged using the automated real-time function.²³ Color fundus photographs and OCT scans of both eyes of all individuals were evaluated by two independent certified reading center graders according to the standard protocol of the Cologne Image Reading Center and Laboratory (CIRCL).²³ AMD was classified by the presence of pigmentary changes together with at least 10 small drusen (<63µm) or the presence of intermediate (63-124 µm) or large drusen (≥125 µm diameter) in the Early Treatment Diabetic Retinopathy Study (ETDRS) grid. Advanced AMD was defined as either AMD with subfoveal geographic atrophy (GA) or choroidal neovascularization (CNV) in at least one eye. Age at onset of AMD was defined as the age at which first visual complaints occurred. Controls were classified as having no abnormalities or only small drusen or pigmentary abnormalities, and were 60 years of age or older. Additionally, in 303 AMD patients infrared images and SD-OCTs were evaluated for the presence of reticular pseudodrusen by one senior grader.

Genotyping

Whole exome sequencing was used to genotype 85 affected members of 22 multiplex AMD families. The samples were sequenced at the Erasmus Medical Center (Rotterdam, the Netherlands) using DNA obtained from venous blood, extracted using standard procedures. The DNA was fragmented using Covaris Adaptive Focused Acoustics shearing according to the manufacturer's instructions (Covaris, Inc., Woburn, MA), and Kapa Library preparation (Kapa Biosystems, Inc., Wilmington, MA) was performed on a Caliper Sciclone NGS workstation (Caliper Life Sciences, Hopkinton, MA). Exome capture was achieved using the Nimblegen SeqCap EZ V2 kit (Roche Nimblegen, Inc., Madison, WI), designed to capture over 44 Mb of exonic regions. Paired-end 2 ×100 sequencing was done on an Illumina HiSeq2000 sequencer using Illumina TruSeq V3 chemistry (Illumina, Inc., San Diego, CA). Downstream analyses included demultiplexing (CASAVA software, Illumina) and alignment to the hg19 reference genome (Genome Reference Consortium Human Reference 37) by the Burrows-Wheeler alignment tool.²⁴ Alignments were sorted by Picard (<http://broadinstitute.github.io/picard>) and subsequently processed by GATK (Indel Realignment and Base-Quality Score Recalibration).²⁵ Finally, PCR duplicates were marked by Picard, Mean Depth of Coverage was determined using GATK, and Freemix values were estimated through verifyBAMid.²⁶ Samples that passed technical QC metrics were genotyped to gVCF level through GATKs HaplotypeCaller. Insertions and deletions (Indels) and single nucleotide variants (SNVs) were filtered separately using GATKs Variant-Quality Score Recalibration, and both the SNV

and indel sets were annotated using ANNOVAR.²⁷ We used simple filtering steps to select the previously associated variants in *CFH* (Arg1210Cys; rs121913059), *CFI* (Gly119Arg; rs141853578), *C9* (Pro167Ser; rs34882957) and *C3* (Lys155Gln; rs147859257) from the exome files of the 85 affected family members. The annotation of the identified variants were confirmed manually using Alamut Visual (Interactive Biosoftware, Rouen, France) by uploading the BAM alignments obtained by exome sequencing into the reference genome. In addition, the variants were confirmed by Sanger sequencing using primers designed with Primer3 software. The variants were also analyzed in all collected affected and unaffected family members using Sanger sequencing (**Table 3.4.1**).

Table 3.4.1 Primer sets used to amplify and Sanger sequence the rare variants in five AMD families

Primer	Primer sequence	Melting temp (°C)	Product length (in basepairs)
<i>CFI</i> Gly119Arg forward	CGTAAATGATTGCTTACTACTTCTTG	57.1	431
<i>CFI</i> Gly119Arg reverse	TGATGCACATAGTTAATTTCTTAGG	58.0	
<i>C3</i> Lys155Gln forward	AGATCCGGAAGCTGGACC	60.2	444
<i>C3</i> Lys155Gln reverse	TTGCCTCTCCTAAGCCTGTG	60.5	
<i>C9</i> Pro167Ser forward	ACGGTGACATGAACTGAAGC	58.7	388
<i>C9</i> Pro167Ser reverse	CCAAACTACATCGCCTCTTC	57.4	

Genotyping of the rare genetic variants *CFH* Arg1210Cys, *CFI* Gly119Arg, *C9* Pro167Ser, and *C3* Lys155Gln was performed in all included subjects of the EUGENDA case-control cohort. Genotyping of *CFI* Gly119Arg was performed using a custom-made TaqMan assay (Life Technologies), as described previously.¹⁸ Genotyping of *CFH* Arg1210Cys, *C9* Pro167Ser and *C3* Lys155Gln were performed by competitive allele-specific PCR assays (KASP SNP Genotyping System, LGC). *CFH* as previously described²⁸ and *C9*, *C3*, according to the manufacturers' recommendations (**Table 3.4.2**).

Table 3.4.2 KASPAR assays used for genotyping the rare variants in EUGENDA case-control cohort

ID	C9_rs34882957	C3_rs147859257
Primer_AlleleFAM	CATTGTCAAAAGGTGTGCTTAGGGA	GGATCTTCACCGTCAACCACC
Primer_AlleleHEX	GTCAAAAGGTGTGCTTAGGGG	CGGATCTTCACCGTCAACCACA
Primer_Common	TTCTCAGGATCAACATTTTAGGGATGGAT	ACCGTCCGGCCACGGGTA

Complement measurements

Complement component C3 and the activation fragment C3d were measured in serum samples as described previously.²⁹ The C3d/C3 ratio was calculated as a measure of complement activation,³⁰ and is a strong marker for AMD.²⁹ For the statistical analysis the C3d/C3 ratio was log transformed to normalize the data.

Statistical analysis

The odds ratio (OR) of the presence of a rare variant for AMD was calculated by binary logistic regression analysis. Statistical analyses were performed to study differences in age at first symptoms, complement activation levels, family history for AMD and AMD subtype between carrier and non-carrier patients of the rare variants *CFI* Gly119Arg, *C9* Pro167Ser or *C3* Lys155Gln. We analyzed mean values of the continuous traits, complement activation levels, and age at first symptoms using independent sample t-tests and compared the mean value using Pearson's chi-square for the other variables. Data were analyzed using SPSS Software version 20.0 (SPSS Inc., Chicago, IL), and two-sided *P*-values of less than 0.05 were considered statistically significant.

RESULTS

The rare variants *CFI* Gly119Arg, *C9* Pro167Ser and *C3* Lys155Gln were observed in five of the 22 multiplex AMD families. Although these variants aggregated within these families, they did not segregate completely with the disease (**Figure 3.4.1**). The *CFH* Arg1210Cys variant was not observed in any of the 22 families.

The *CFI* Gly119Arg variant was detected in one family (**Figure 3.4.1, family A**). Of the four affected individuals, three were carrier of the *CFI* Gly119Arg variant. Affected individual II:4, lacking the *CFI* Gly119Arg, carried the *CFH* Tyr402His risk allele homozygously. The youngest unaffected individual (64 years of age) carried the risk conferring *CFI* variant. In a second family (**Figure 3.4.1, family B**), two rare variants, *C9* Pro167Ser and *C3* Lys155Gln, were identified heterozygously. While both variants were only found in affected individuals, neither variant segregated fully with the disease phenotype. The *C3* Lys155Gln variant was found to cluster in two additional families (**Figure 3.4.1, families C and D**). In family C, the *C3* Lys155Gln variant was detected in two affected individuals (II:2 and II:4), who also carried the *ARMS2* Ala69Ser and *CFH* Tyr402His risk alleles homozygously. Individuals II:1 and II:3 were both affected by intermediate AMD without carrying the rare variant in *C3*, and were heterozygous for the common *ARMS2* Ala69Ser and *CFH* Tyr402His risk alleles. In family D, five individuals carried the *C3* Lys155Gln variant, of which four were affected by AMD and one was unaffected (II:8). Individuals II:6 and II:7 carried the *C3* variant and were diagnosed with intermediate AMD. Their older siblings II:4 and II:5 who did not carry the rare variant did not develop AMD, although they had a higher genotypic load of the two common variants. Additionally to family B, the *C9* Pro167Ser variant was also identified in family E (**Figure 3.4.1**). Two affected individuals carrying the variant had a more advanced AMD stage than the affected non-carrying family members.

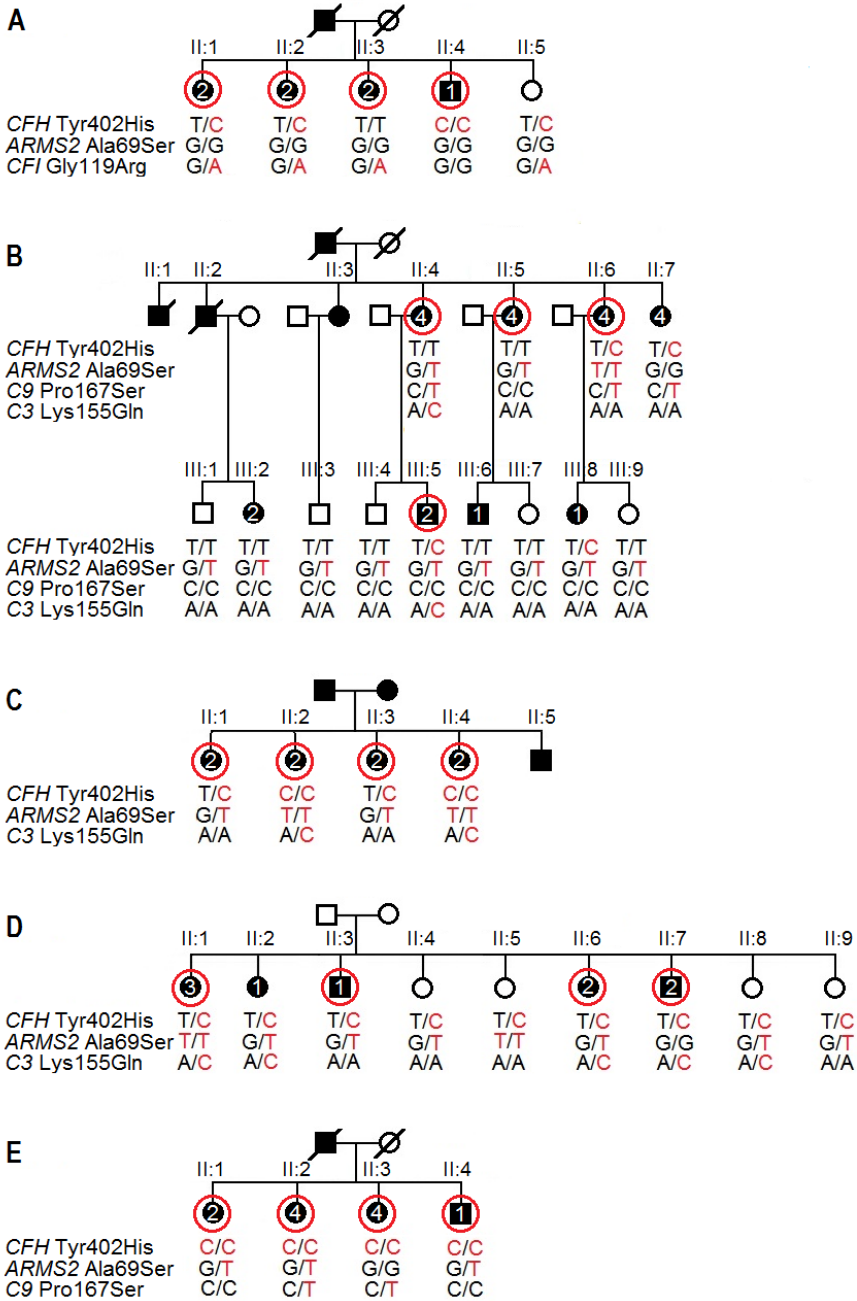


Figure 3.4.1. Pedigrees of five AMD families carrying rare variants in CFI, C9 and C3. Segregation analysis of the rare variants, and common variants CFH Tyr402His and ARMS2 Ala69Ser. Risk alleles are indicated in red. Affected individuals are numbered to represent the stage of AMD (1 early; 2 intermediate; 3 advanced geographic atrophy; 4 advanced choroidal neovascularization). The circles mark the individuals analyzed by whole-exome sequencing.

Within the five families, rare variants were detected in 16 affected individuals and 2 unaffected individuals (**Table 3.4.3**). Carrying one of the variants in *CFI*, *C9* or *C3* resulted in an OR of 7.11 for AMD (95% CI 1.23-40.98; $P = 0.028$).

The age at first symptoms was lower in affected family members who carried the rare variants *CFI* Gly119Arg, *C9* Pro167Ser, or *C3* Lys155Gln, as compared to affected individuals who did not, although this difference was not statistically significant (63.9 vs 69.4 years; $P = 0.254$)(**Figure 3.4.2**). The complement activation level (log C3d/C3 ratio) was slightly higher in affected family members who carried a rare variant in a complement gene compared to non-carriers, although this difference was also not statistically significant ($P = 0.141$)(**Figure 3.4.2**). Most patients graded as advanced AMD carried a rare variant. This holds true for the single patient affected by GA and five out of the six patients affected by CNV ($P = 0.167$) (**Figure 3.4.1**).

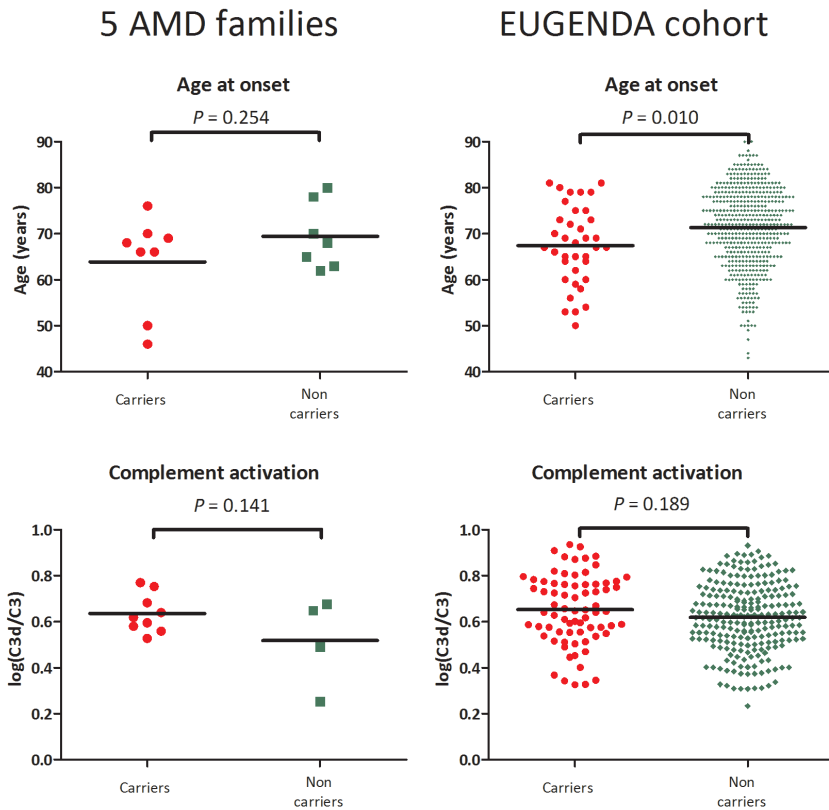


Figure 3.4.2 Age at onset and complement activation in carriers versus non-carriers in the five AMD families and EUGENDA cohort. There is a possible trend ($P = 0.254$) in the families and a significant association ($P = 0.010$) in the cohort for an earlier age at onset for rare variant carriers. Complement activation levels (Log C3d/C3 ratio) do not differ significantly in the cohorts. Lines indicate mean values.

Table 3.4.3. Clinical characteristics of carriers and non-carriers of the rare variants in the 5 AMD families

Carrier and disease status	Gender Female %	Age at participation to EUGENDA*	Age at first symptoms*	Complement activation Mean Log C3d/C3 ratio (SD)	Patient graded with GA and CNV Number	Individuals with reticular drusen Number (%)
Affected carriers (n = 16)	87.5%	74.9	63.9	0.636 (0.084)	1 and 5	5 (31.3%)
Affected non-carriers (n = 9)	55.6%	71.4	69.4	0.518 (0.194)	0 and 1	0 (0.0%)
Unaffected carriers (n = 2)	100.0%	66.0	-	0.547 (0.202)	-	0 (0.0%)
Unaffected non-carriers (n = 8)	50.0%	66.9	-	0.508 (0.097)	-	0 (0.0%)

* Mean age in years; SD = standard deviation; GA = geographic atrophy; CNV = choroidal neovascularization; carrier = carrying a rare variant CFI Gly119Arg, C9 Pro167Ser or C3 Lys155Gln

Table 3.4.4. Clinical characteristics of carriers and non-carriers of the rare variants in the EUGENDA case-control cohort

Carrier and disease status	Gender Female %	Age at participation to EUGENDA*	Age at first symptoms*	Complement activation Mean Log C3d/C3 ratio (SD)	Patient graded with GA and CNV Number	Individuals with reticular drusen Number (%)
Affected carriers (n = 91)	56.0%	73.7	67.4	0.656 (0.153)	11 and 40	3 (3.3%)
Affected non-carriers (n = 1498)	56.1%	75.5	71.3	0.633 (0.149)	82 and 795	56 (3.7%)
Unaffected carriers (n = 43)	67.4%	70.2	-	0.545 (0.161)	-	0 (0.0%)
Unaffected non-carriers (n = 1343)	56.9%	70.4	-	0.596 (0.157)	-	0 (0.0%)

* Mean age in years; SD = standard deviation; GA = geographic atrophy; CNV = choroidal neovascularization; carrier = carrying a rare variant CFI Gly119Arg, C9 Pro167Ser or C3 Lys155Gln

Five of 25 affected family members showed an AMD phenotype with reticular pseudodrusen, and all of these patients carried the rare variant *CFI* Gly119Arg, *C9* Pro167Ser, or *C3* Lys155Gln (Table 3.4.3). Carrying one of these variants was associated with developing reticular pseudodrusen ($P = 0.019$). The Pro167Ser variant in the *C9* gene appeared to segregate with the reticular pseudodrusen phenotype in the family E, since II:2 and II:3, who carried the rare variant, showed reticular pseudodrusen while II:1 and II:4 did not. However, the rare variants in the *CFI* and *C3* gene did not segregate with the reticular drusen phenotype. Individual II:1 of family A, and individuals II:2 and II:6 of family D, showed the reticular pseudodrusen phenotype, but this phenotype was not observed in their siblings who carried the same rare variant.

To verify the findings observed in the five families, the analyses were replicated in a large case-control cohort from the EUGENDA database, which was genotyped for the rare variants *CFH* Arg1210Cys, *CFI* Gly119Arg, *C9* Pro167Ser, and *C3* Lys155Gln. Out of the 1589 patients and 1386 control individuals we identified 91 (5.7%) carriers in the AMD cohort and 43 (3.1%) carriers in the cohort of the controls (Table 3.4.4). The *CFH* Arg1210Cys variant was not present in our case-control cohort. The presence of a rare genetic variant was significantly associated with AMD and conferred an OR of 1.90 (95% CI 1.31-2.75; $P = 0.001$). This was comparable with the OR for advanced AMD (OR 1.90; 95% CI 1.27-2.85; $P = 0.002$). Separate analyses for each rare variant showed large effect sizes for the *CFI* Gly119Arg variant (OR 11.38; 95% CI 1.49-87.06; $P = 0.003$), while the effect size of the *C9* Pro167Ser variant (OR 1.54; 95% CI 0.96-2.45 $P = 0.070$) and the *C3* Lys155Gln variant (OR 1.81; 95% CI 0.96-3.44; $P = 0.064$) were smaller (Table 3.4.5). AMD patients who carried rare variant *CFI* Gly119Arg, *C9* Pro167Ser or *C3* Lys155Gln reported a positive family history for AMD significantly more often than AMD patients without these rare variants (44.9% and 30.6%, respectively $P = 0.008$). This difference in positive family history was the largest for carriers of the *CFI* Gly119Arg variant (58.3% vs 30.6%, $P = 0.038$), followed by variant Pro167Ser in *C9* (44.7% vs 30.6%, $P = 0.040$)(Table 3.4.6).

Table 3.4.5. Frequencies and effect sizes of the rare variants in the EUGENDA case-control cohort

Rare variant	Carrier patients	Carrier controls	OR	95% CI	P-value
<i>CFI</i> Gly119Arg	13 (0.008%)	1 (<0.001%)	11.38	(1.49 - 87.06)	0.003
<i>C9</i> Pro167Ser	49 (0.031%)	28 (0.020%)	1.54	(0.96 - 2.45)	0.070
<i>C3</i> Lys155Gln	29 (0.018%)	14 (0.010%)	1.81	(0.96 - 3.44)	0.064
<i>CFH</i> Arg1210Cys	0 (0%)	0 (0%)	-	-	-

P-value and OR printed in bold indicate a significant association.

Table 3.4.6. Quantitative traits for each of the rare variants in the EUGENDA case-control cohort

Rare variant	Mean age at onset in carriers vs non-carriers (years)	<i>P</i> -value	Familial occurrence in affected carriers vs non-carriers (%)	<i>P</i> -value	Mean log C3d/C3 ratio in affected carriers vs non-carriers	<i>P</i> -value
<i>CFI</i> Gly119Arg	58.75 vs 71.3	0.005	58.3 vs 30.6	0.038	0.705 vs 0.633	0.198
<i>C9</i> Pro167Ser	69.12 vs 71.3	0.225	44.7 vs 30.6	0.040	0.645 vs 0.633	0.599
<i>C3</i> Lys155Gln	66.5 vs 71.3	0.127	36.6 vs 30.6	0.556	0.663 vs 0.633	0.332

P-values printed in bold indicate significant associations.

Additionally, a lower age at first symptoms was found in AMD patients with rare variant *CFI* Gly119Arg, *C9* Pro167Ser, or *C3* Lys155Gln than in patients who did not carry these rare variants (67.4 and 71.3 years, respectively; $P = 0.010$)(**Figure 3.4.2**). In individuals carrying a rare variant, the mean complement activation level (log C3d/C3 ratio) was significantly higher in cases compared to controls ($P = 0.001$). In contrast, the mean log C3d/C3 ratio in AMD patients carrying one of the rare variants was not different from non-carriers of these variants ($P = 0.189$)(**Figure 3.4.2**). In advanced AMD patients, rare variants *CFI* Gly119Arg, *C9* Pro167Ser, or *C3* Lys155Gln were present significantly more often in patients with GA (11.8%) than patients with CNV (4.8%; $P = 0.044$)(**Table 3.4.4**). A reticular pseudodrusen phenotype was present in 59 of 202 AMD patients and none of the 183 controls (**Table 3.4.4**). No association was found between the presence of reticular pseudodrusen and the presence of one of these rare variants in the large AMD cohort ($P = 0.804$).

DISCUSSION

The development of AMD in densely affected families can be influenced by rare genetic variants, of which four (*CFH* Arg1210Cys, *CFI* Gly119Arg, *C9* Pro167Ser, and *C3* Lys155Gln) were previously associated to AMD.^{15,18-21} In our EUGENDA case-control cohort, the presence of a variant resulted in an OR of 1.90 for AMD, which is comparable with previously reported effect sizes for the *C9* Pro167Ser and *C3* Lys155Gln variants.^{15,18-21} However, the effect size of the Gly119Arg variant in the *CFI* gene was much stronger, with an OR of 11.38, which is in line with previous reports (OR 8.5 and 22.2).^{18,31} The *CFH* Arg1210Cys variant was previously associated to AMD in North-American cohorts,^{15,20} but not in Icelandic and Han Chinese cohorts.^{19,32} The absence of this variant in our AMD case-control cohort may reflect the different distribution of low-frequency alleles among populations.²⁸

Almost half of the patients who carried one of the rare genetic variants *CFI* Gly119Arg, *C9* Pro167Ser or *C3* Lys155Gln reported a positive family history for AMD, which has important implications for counseling of these patients and their family members, and underlines the importance of including these rare variants in genetic tests for AMD. Despite their strong association with AMD in case-control cohorts,¹⁸⁻²¹ variants *CFI* Gly119Arg, *C9* Pro167Ser and

C3 Lys155Gln do not segregate with the disease in the five families in this study. This could point to the contribution of other genetic risk alleles and environmental factors in such multiplex families. Further research is warranted to determine whether additional rare variants aggregate in the remaining 17 multiplex AMD families in this study.

Patients carrying a known rare genetic variant differ clinically from patients that do not. We demonstrated that carriers of rare variants *CFI* Gly119Arg, *C9* Pro167Ser or *C3* Lys155Gln have a 4-year-earlier onset of first symptoms, of which *CFI* Gly119Arg shows the strongest effect. This is comparable to the earlier onset previously described in patients carrying the rare Arg1210Cys variant in the *CFH* gene,¹⁵ and is in line with the lower age at first symptoms in familial AMD patients.¹⁴

Many of the common genetic variants associated with AMD reside in genes encoding components of the complement cascade,^{2,4,34-36} some of which have been associated with increased systemic levels of complement activation and complement components.^{29,37,38} Additionally, nearly all the recently identified rare variants are located in complement genes,^{15,17-21,33,39,40} emphasizing the important role of the complement system in the pathophysiology of AMD. Mean complement activation levels were slightly higher in AMD patients carrying rare variants in *CFI*, *C9*, or *C3* compared to non-carriers, but this difference was not significant. This suggests that the difference in complement activation levels cannot be explained by the presence of the rare variants evaluated in this study. Preventive and therapeutic options inhibiting the complement cascade have been suggested to be effective in treating AMD,⁴¹ but our current results do not support the hypothesis that subjects who carry a rare variant in a complement gene will benefit more from such treatments than non-carriers.

In this study rare variants were more frequently identified in advanced AMD patients with GA than in patients with CNV. This is in line with a recent study, which observed a higher prevalence of GA among patients carrying the *CFH* Arg1210Cys variant.⁴² We previously suggested that additional genetic factors may contribute to the development of GA in familial patients, because we found a higher prevalence of GA in familial AMD cases than in sporadic patients,¹⁴ and it had been shown that siblings are more likely to develop the same advanced AMD subtype as the proband of the family.³⁰ The findings of the current study are thus consistent with our suggestion that additional genetic factors play a role in GA development.¹⁴

In conclusion, we observed a higher familial occurrence and a lower age at onset in carriers of rare variants *CFI* Gly119Arg, *C9* Pro167Ser or *C3* Lys155Gln. This emphasizes the importance of counseling of patients and family members to increase awareness and enable early detection of the disease. Genetic tests for AMD should therefore be designed to detect common and rare genetic variants, especially in families, since these rare variants significantly contribute to the age at onset and progression of the disease.

REFERENCES

1. Friedman DS, O'Colmain BJ, Munoz B, et al. Prevalence of age-related macular degeneration in the United States. *Arch Ophthalmol*. 2004;122:564-572.
2. Fritsche LG, Chen W, Schu M, et al. Seven new loci associated with age-related macular degeneration. *Nat genet*. 2013;45:433-439.
3. Risk factors associated with age-related macular degeneration. A case-control study in the age-related eye disease study: Age-Related Eye Disease Study Report Number 3. *Ophthalmology*. 2000;107:2224-2232.
4. Klein RJ, Zeiss C, Chew EY, et al. Complement factor H polymorphism in age-related macular degeneration. *Science*. 2005;308:385-389.
5. Chen W, Stambolian D, Edwards AO, et al. Genetic variants near TIMP3 and high-density lipoprotein-associated loci influence susceptibility to age-related macular degeneration. *Proc Natl Acad Sci U S A*. 2010;107:7401-7406.
6. Heiba IM, Elston RC, Klein BE, Klein R. Sibling correlations and segregation analysis of age-related maculopathy: the Beaver Dam Eye Study. *Genetic Epidemiology*. 1994;11:51-67.
7. Klaver CC, Wolfs RC, Assink JJ, van Duijn CM, Hofman A, de Jong PT. Genetic risk of age-related maculopathy. Population-based familial aggregation study. *Arch Ophthalmol*. 1998;116:1646-1651.
8. Klein ML, Mauldin WM, Stoumbos VD. Heredity and age-related macular degeneration. Observations in monozygotic twins. *Archives of Ophthalmology*. 1994;112:932-937.
9. Luo L, Harmon J, Yang X, et al. Familial aggregation of age-related macular degeneration in the Utah population. *Vision Res*. 2008;48:494-500.
10. Seddon JM, Ajani UA, Mitchell BD. Familial aggregation of age-related maculopathy. *Am J Ophthalmol*. 1997;123:199-206.
11. Meyers SM, Greene T, Gutman FA. A twin study of age-related macular degeneration. *American Journal of Ophthalmology*. 1995;120:757-766.
12. Saksens NT, Fleckenstein M, Schmitz-Valckenberg S, et al. Macular dystrophies mimicking age-related macular degeneration. *Prog Retin Eye Res*. 2014;39:23-57.
13. Shahid H, Khan JC, Cipriani V, et al. Age-related macular degeneration: the importance of family history as a risk factor. *Br J Ophthalmol*. 2012;96:427-431.
14. Saksens N, Kersten E, Groenewoud JM, et al. Clinical characteristics of familial and sporadic age-related macular degeneration: differences and similarities. *Invest ophthalmol vis sci*. 2014;9:14-14659.
15. Raychaudhuri S, Iartchouk O, Chin K, et al. A rare penetrant mutation in CFH confers high risk of age-related macular degeneration. *Nat genet*. 2011;43:1232-1236.
16. Ratnapriya R, Zhan X, Fariss RN, et al. Rare and common variants in extracellular matrix gene Fibrillin 2 (FBN2) are associated with macular degeneration. *Hum Mol Genet*. 2014;23:5827-5837.
17. Yu Y, Triebwasser MP, Wong EK, et al. Whole-exome sequencing identifies rare, functional CFH variants in families with macular degeneration. *Hum Mol Genet*. 2014;23:5283-5293.
18. van de Ven JP, Nilsson SC, Tan PL, et al. A functional variant in the CFI gene confers a high risk of age-related macular degeneration. *Nat genet*. 2013;45:813-817.
19. Helgason H, Sulem P, Duvvari MR, et al. A rare nonsynonymous sequence variant in C3 is associated with high risk of age-related macular degeneration. *Nat genet*. 2013;45:1371-1374.
20. Zhan X, Larson DE, Wang C, et al. Identification of a rare coding variant in complement 3 associated with age-related macular degeneration. *Nat genet*. 2013;45:1375-1379.

21. Seddon JM, Yu Y, Miller EC, et al. Rare variants in CFI, C3 and C9 are associated with high risk of advanced age-related macular degeneration. *Nat genet.* 2013;45:1366-1370.
22. Schramm EC, Clark SJ, Triebwasser MP, Raychaudhuri S, Seddon JM, Atkinson JP. Genetic variants in the complement system predisposing to age-related macular degeneration: a review. *Mol Immunol.* 2014;61:118-125.
23. Mokwa NF, Ristau T, Keane PA, Kirchhof B, Sadda SR, Liakopoulos S. Grading of Age-Related Macular Degeneration: Comparison between Color Fundus Photography, Fluorescein Angiography, and Spectral Domain Optical Coherence Tomography. *Journal of ophthalmology.* 2013;385915.
24. Li H, Durbin R. Fast and accurate short read alignment with Burrows-Wheeler transform. *Bioinformatics.* 2009;25:1754-1760.
25. McKenna A, Hanna M, Banks E, et al. The Genome Analysis Toolkit: a MapReduce framework for analyzing next-generation DNA sequencing data. *Genome Res.* 2010;20:1297-1303.
26. Jun G, Flickinger M, Hetrick KN, et al. Detecting and estimating contamination of human DNA samples in sequencing and array-based genotype data. *Am J Hum Genet.* 2012;91:839-848.
27. Wang K, Li M, Hakonarson H. ANNOVAR: functional annotation of genetic variants from high-throughput sequencing data. *Nucleic Acids Res.* 2010;38:3.
28. Duvvari MR SN, van de Ven JPH, de Jong-Hesse Y, Schick T, Nillesen WM, Fauser S, Hoefsloot LH, Hoyng CB, de Jong EK, den Hollander AI. Analysis of Rare Variants in the CFH Gene in Patients with the Cuticular Drusen Subtype of Age-related Macular Degeneration. *Submitted.* 2014.
29. Smailhodzic D, Klaver CC, Klevering BJ, et al. Risk alleles in CFH and ARMS2 are independently associated with systemic complement activation in age-related macular degeneration. *Ophthalmology.* 2012;119:339-346.
30. Rother E, Lang B, Coldewey R, Hartung K, Peter HH. Complement split product C3d as an indicator of disease activity in systemic lupus erythematosus. *Clin Rheumatol.* 1993;12:31-35.
31. Alexander P, Gibson J, Cree AJ, Ennis S, Lotery AJ. Complement factor I and age-related macular degeneration. *Mol Vis.* 2014;20:1253-1257.
32. Shen SK, Liu XQ, Lu F, Yang ZL, Shi Y. Association study between age-related macular degeneration and R1210C mutation of CFH gene in Chinese population. *Chinese journal of medical genetics.* 2012;29:570-572.
33. Hoffman JD, Cooke Bailey JN, D'Aoust L, et al. Rare complement factor H variant associated with age-related macular degeneration in the Amish. *Invest ophthalmol vis sci.* 2014;55:4455-4460.
34. Maller J, George S, Purcell S, et al. Common variation in three genes, including a noncoding variant in CFH, strongly influences risk of age-related macular degeneration. *Nat genet.* 2006;38:1055-1059.
35. Hughes AE, Orr N, Esfandiary H, Diaz-Torres M, Goodship T, Chakravarthy U. A common CFH haplotype, with deletion of CFHR1 and CFHR3, is associated with lower risk of age-related macular degeneration. *Nat genet.* 2006;38:1173-1177.
36. Maller JB, Fagerness JA, Reynolds RC, Neale BM, Daly MJ, Seddon JM. Variation in complement factor 3 is associated with risk of age-related macular degeneration. *Nat genet.* 2007;39:1200-1201.
37. Reynolds R, Hartnett ME, Atkinson JP, Giclas PC, Rosner B, Seddon JM. Plasma complement components and activation fragments: associations with age-related macular degeneration genotypes and phenotypes. *Invest ophthalmol vis sci.* 2009;50:5818-5827.
38. Hecker LA, Edwards AO, Ryu E, et al. Genetic control of the alternative pathway of complement in humans and age-related macular degeneration. *Hum Mol Genet.* 2010;19:209-215.
39. Duvvari MR, Paun CC, Buitendijk GH, et al. Analysis of rare variants in the C3 gene in patients with age-related macular degeneration. *Plos One.* 2014;9.

40. Boon CJ, Klevering BJ, Hoyng CB, et al. Basal laminar drusen caused by compound heterozygous variants in the CFH gene. *Am J Hum Genet.* 2008;82:516-523.
41. Volz C, Pauly D. Antibody therapies and their challenges in the treatment of age-related macular degeneration. *European journal of pharmaceutics and biopharmaceutics:* 2015.
42. Ferrara D, Seddon JM. Phenotypic characterization of Complement Factor H R1210C rare genetic variant in age-related macular degeneration. *JAMA ophthalmology.* 2015;133:785-791.



3.5

Analysis of rare variants in the *CFH* gene in patients with the cuticular drusen subtype of age-related macular degeneration

M.R. Duvvari, N.T.M. Saksens, J.P.H. van de Ven, Y. de Jong-Hesse, T. Schick, W.M. Nillesen, S. Fauser, L.H. Hoefsloot, C.B. Hoyng, E.K. de Jong, A.I. den Hollander

Published in: Molecular Vision 2015; 21:285-292



PURPOSE. Age-related macular degeneration (AMD) and cuticular drusen (CD), a clinical subtype of AMD, have both been linked to genetic variants in the complement factor H (*CFH*) gene. In this study we aimed to investigate the frequency of rare variants in the *CFH* gene in 180 cases with CD. In addition, we aimed to determine the frequency of a previously reported rare, highly penetrant *CFH* variant (p.Arg1210Cys) in a Dutch-German non-CD type AMD case-control cohort, and to describe the phenotype of patients carrying the p.Arg1210Cys variant.

METHODS. Study subjects were selected from the European Genetic Database (EUGENDA), a joint AMD database of the Radboud University Medical Centre and the University Hospital of Cologne, and graded at the Cologne Image Reading Centre and Laboratory (CIRCL). Additionally, two CD cases were recruited from the VU Medical Centre in Amsterdam. The *CFH* gene was analyzed in 180 CD cases by Sanger sequencing. All identified variants were analyzed for potential damaging effects by prediction software tools SIFT and PolyPhen. In addition, we genotyped the p.Arg1210Cys variant in 813 non-CD type AMD cases and 1175 controls.

RESULTS. Sequencing identified 11 rare, heterozygous missense variants, one frameshift variant, and one splice acceptor site variant in 16 CD cases. The p.Arg1210Cys variant was identified in two CD cases, but was not identified in our Dutch-German non-CD type AMD case-control cohort.

CONCLUSIONS. The present study identified the presence of rare variants in the *CFH* gene in 16 (8.8%) of 180 patients with the CD subtype of AMD. The carriers of rare *CFH* variants displayed a significantly earlier age at onset than non-carriers ($P = 0.016$). The rare missense variant p.Arg1210Cys was identified in two CD cases, but was not detected in 813 non-CD type AMD cases nor 1175 controls of our Dutch-German cohort. The current study suggests that the p.Arg1210Cys variant may be restricted to a subset of AMD patients with CD. Detailed clinical phenotyping, including fluorescein angiography, of AMD patients carrying the p.Arg1210Cys variant in other cohorts is required to confirm this finding.

INTRODUCTION

Age-related macular degeneration (AMD, MIM 603075) is the most common cause of vision loss and irreversible blindness in the Western world among the elderly.¹ A major hallmark of AMD is the appearance of drusen in the macula accompanied with loss of sharp and central vision with advancing disease.² Cuticular drusen (CD, MIM 126700), also termed ‘basal laminar drusen’ or ‘early adult-onset, grouped drusen’, is a clinical subtype of AMD, characterized by the fundoscopic findings of innumerable, small (25-75µm), slightly raised, round drusen, scattered throughout the central and peripheral retina.³ CD commonly appear in early adulthood, and are readily visualized by fluorescein angiography (FA). In more advanced stages the large number of CD present as a typical ‘stars-in-the-sky’ appearance in the early phases of the angiogram.⁴ Approximately 10% of AMD cases display the CD phenotype.⁵

The early age of onset and the clustering of the CD phenotype in families implies a large genetic contribution to the development of CD.⁵⁻⁸ This is supported by the observation that heterozygous mutations in the complement factor H (*CFH*) gene segregate with the CD phenotype in multiplex families.^{5, 8} Common variants in and near the *CFH* gene have been associated with CD and with AMD.^{6, 7} In addition, a rare, highly penetrant variant (p.Arg1210Cys) in the *CFH* gene has been associated with AMD.^{9, 10} However, the p.Arg1210Cys variant was not detected in an Icelandic cohort nor in the Han Chinese population.^{11, 12} This suggests that the rare p.Arg1210Cys variant does not consistently associate with AMD among different populations.

In this study we aimed to investigate the frequency of rare variants in the *CFH* gene in 180 cases with CD. In addition, we aimed to determine the frequency of the rare, highly penetrant p.Arg1210Cys variant in a Dutch-German non-CD type AMD case-control cohort, and to describe the phenotype of patients carrying the p.Arg1210Cys variant.

METHODS

EUGENDA Study

The study participants were recruited from the European Genetic Database (EUGENDA), a multicenter database consisting of subjects from the Nijmegen area, the Netherlands and Cologne area, Germany (**Table 3.5.1**). In addition, two CD cases were recruited at the VU Medical Centre in Amsterdam. All subjects analyzed in this study are Dutch and German and are of Caucasian descent. All subjects underwent ophthalmological examinations, and AMD staging was performed by the Cologne Image Reading Centre and Laboratory (CIRCL). CD was classified as a symmetric distributed pattern in both eyes of at least 50 scattered, uniformly-sized, small (25-75µm) and hyperfluorescent drusen on FA in each eye, with a minimum of 20 drusen located outside the Wisconsin age-related maculopathy



grading template.^{6, 13} AMD was classified by the presence of at least 15 intermediate (63-124µm) drusen or at least one large (≥125µm) druse in the Early Treatment Diabetic Retinopathy Study (ETDRS) grid (intermediate AMD) or geographic atrophy or choroidal neovascularization secondary to AMD (advanced AMD). Control subjects were ≥65 years of age and did not display AMD, which includes cases without drusen, with only small drusen (<63µm) or with pigmentary abnormalities alone or combined with less than 10 small drusen. Early AMD cases with ≥10 small drusen and pigmentary abnormalities or 1-14 intermediate drusen were excluded. The age at onset of subjects was noted as the age at which first visual complaints were experienced.

The EUGENDA study was approved by the local research ethics committees (Commissie Mensgebonden Onderzoek Regio Arnhem-Nijmegen, the Netherlands, and the Ethics Committee of the University Hospital Cologne, Germany). Written informed consent was obtained from all participants, and the study was performed in accordance with the tenets of the Declaration of Helsinki.

Table 3.5.1 Demographics of studied subjects of the EUGENDA cohort

Variables	CD	Intermediate AMD	Advanced AMD	Controls
Number (Total)	180	207	606	1175
Mean age (±SD)	70 ± 13.7	74 ± 6.8	77 ± 7.7	70 ± 5.9
Gender				
Male	59 (32.8%)	80 (38.6%)	251 (41.4%)	504 (42.9%)
Female	121 (67.2%)	127 (61.4%)	355 (58.6%)	671 (57.1%)

CD: Cuticular drusen; AMD: Age-related macular degeneration; SD: Standard deviation

Sequencing

Sanger sequencing of the *CFH* (NM_000186) gene was performed in 178 CD cases from the EUGENDA database and two CD cases from Amsterdam. Primers were designed to amplify all 22 exons and flanking intron-exon junctions by Primer3 software (Table 3.5.2). Polymerase chain reactions (PCR) were performed, and amplification products were sequenced using an automated sequencer (BigDye Terminator, version 3, 3730 DNA analyzer; Applied Biosystems). All sequencing chromatograms were compared to the reference sequence using ContigExpress (Vector NTI Advance, Version 11.0, Life Technologies). Each newly identified variant was confirmed by a second independent PCR and bidirectional Sanger sequencing. All identified variants were annotated based on the Human Genome Variation Society (HGVS) nomenclature. Variants with a minor allele frequency <1% (MAF<1%) were considered as rare variants. The number of carriers of rare variants discovered in the CD cohort (n = 180) was compared to the general population (n = 4300) using data from Exome Variant Server (EVS). Rare coding (missense, frameshift, and nonsense) and splice site variants in the *CFH* gene, were utilized in the analysis.

Table 3.5.2 List of *CFH* gene sequencing primers

Primers	Sequence (5'- 3')	Product (bp)
Exon 1F	tgtaaaacgacggccagtttggcttggttgatt	409
Exon 1R	caggaaacagctatgacctcaaagccactcaattgtca	
Exon 2F	tgtaaaacgacggccagctctgtgactgtctaggcattttt	519
Exon 2R	caggaaacagctatgacctctcaaattgcgccactg	
Exon 3F	tgtaaaacgacggccagcttgttccccactcctaca	462
Exon 3R	caggaaacagctatgacctgtttccccactctccataa	
Exon 4F	tgtaaaacgacggccagttggacactcagaatggcatc	395
Exon 4R	caggaaacagctatgaccagatcaggctgcattcgttt	
Exon 5F	tgtaaaacgacggccagctcctccatagaaaagaatcagg	586
Exon 5R	caggaaacagctatgaccgaacttagctcaattacaggcaga	
Exon 6F	tgtaaaacgacggccagctctgatggaacaacatttctg	527
Exon 6R	caggaaacagctatgacctgaacttttctggccctgtt	
Exon 7F	tgtaaaacgacggccagtaagggattaagaccaggga	585
Exon 7R	caggaaacagctatgaccttctggcaactcgaaaaact	
Exon 8F	tgtaaaacgacggccagtgcatcatgtgatccacaagacat	592
Exon 8R	caggaaacagctatgacctggtcactttgcttgaaaaact	
Exon 9F	tgtaaaacgacggccagttcttttggcaaacctttgttag	505
Exon 9R	caggaaacagctatgacccattggtaaaacaaggtgaca	
Exon 10F	tgtaaaacgacggccagtcagggaactctctgtttgg	517
Exon 10R	caggaaacagctatgaccgcagtgagtaaatgcctcaa	
Exon 11F	tgtaaaacgacggccagtgcttatggttatccaggtttcag	424
Exon 11R	caggaaacagctatgacccagccccacaaaaagacta	
Exon 12F	tgtaaaacgacggccagtttggggcttaagcaatgaaa	591
Exon 12R	caggaaacagctatgaccaaactccctcttttccagtt	
Exon 13F	tgtaaaacgacggccagttctgatgccctctgtatga	413
Exon 13R	caggaaacagctatgacctgggagcccaacaaaaatta	
Exon 14F	tgtaaaacgacggccagtcattcttgattgttaggatgc	516
Exon 14R	caggaaacagctatgacccagccatgttcaagttcagg	
Exon 15F	tgtaaaacgacggccagttgttgatggagagtgagaca	482
Exon 15R	caggaaacagctatgacctgaagactggaaatgttgagg	
Exon 16F	tgtaaaacgacggccagttgatgcaatgtgatcaggaa	491
Exon 16R	caggaaacagctatgacccctgccttattcagtagcatttg	
Exon 17F	tgtaaaacgacggccagttctatgagaatacaagccaaaagttc	612
Exon 17R	caggaaacagctatgaccagtggtgattgattaatgtgccta	
Exon 18F	tgtaaaacgacggccagtgaggagaatatactttgcgagtt	458
Exon 18R	caggaaacagctatgacccctcactttgataacaagagattat	
Exon 19F	tgtaaaacgacggccagtttggtagactcagatagaca	535
Exon 19R	caggaaacagctatgaccaattcccacagcagtcag	
Exon 20F	tgtaaaacgacggccagttctcaattgctacggctacca	735
Exon 20R	caggaaacagctatgacctggccccacttcaatcttcat	
Exon 21F	tgtaaaacgacggccagttcagttctagcgaaggatg	660
Exon 21R	caggaaacagctatgaccccaactctcaatttggtcgaa	
Exon 22F	tgtaaaacgacggccagtcagtgtctgtttgcgttt	435
Exon 22R	caggaaacagctatgaccagaaatatttgtaggcaagc	
Exon 23F	tgtaaaacgacggccagtcagcaggatcctaaaatga	838
Exon 23R	caggaaacagctatgaccgcttccatttctgtaaacagtg	



The average age at onset of CD patients were compared in carriers of rare *CFH* variants ($n = 16$; age at onset known = 13) versus non-carriers of rare *CFH* variants ($n = 164$; age at onset known = 64). The predicted effects of identified missense variants were examined using Polymorphism Phenotyping (PolyPhen) and Sorting Intolerant from Tolerant (SIFT).^{14, 15}

Genotyping

The *CFH* p.Arg1210Cys variant was genotyped in 813 non-CD type AMD cases and 1175 controls from the EUGENDA database using a competitive allele-specific PCR assay (KASPar SNP Genotyping System, KBiosciences). KASPar genotyping was performed according to the manufacturer's protocol in a volume of 4 μ l containing 10ng of genomic DNA, 2.5 μ l of 2X reaction mix, and 0.069 μ l of assay (Table 3.5.3). Thermal cycling conditions included a pre-incubation step at 94°C for 15min, 20 cycles of 94°C for 10s, 57°C for 5s, 72°C for 10s, followed by 23 cycles of 94°C for 10s, 57°C for 20s, 72°C for 40s. Plates were analyzed on a 7900 Fast Real-Time PCR system (Applied Biosystems).

RESULTS

Through sequencing of the exons and flanking intron-exon boundaries of the *CFH* gene in 180 unrelated CD cases 13 heterozygous rare variants in 16 cases (8.8%) were identified (Table 3.5.4). Of these 13 variants, 11 were missense variants, one was a frameshift variant (p.Ala301Asnfs*25), and one was a splice acceptor site variant (c.428-2A>G). Seven variants (c.428-2A>G, p.Ala161Ser, p.Ala173Gly, p.Arg175Gln, p.Ser193Leu, p.Ala301Asnfs*25, and p.Trp379Arg) were not present in public genetic variant databases (dbSNP, ESP6500/EVS) and therefore represent rare, unique variants. Six variants (p.Leu3Val / rs139254423, p.Ile216Thr / rs183474263, p.Gln400Lys / rs201671665, p.Gln950His/rs149474608, p.Thr956Met / rs145975787, and p.Arg1210Cys / rs121913059) had very low reported minor allele frequencies (MAF) in these databases (MAF<0.001). The total number of carriers of rare *CFH* variants in CD patients (16 (8.8%) of 180) is significantly higher than the total number of carriers of rare *CFH* variants in the general population (185 (4.3%) of 4300) ($P = 0.008$, Fisher's test). The mean age at onset in carriers of rare *CFH* variants (57.2 ± 16.8 years) is significantly earlier than non-carriers of rare *CFH* variants (66.1 ± 10.8 years) ($P = 0.016$, Student's *t*-test). Using online prediction algorithms SIFT and PolyPhen, potential damaging effects of the missense variants were assessed. Three missense variants (p.Ser193Leu, p.Trp379Arg and p.Gln950His) showed a consistent deleterious and damaging score by both PolyPhen and SIFT, while three variants were predicted deleterious or damaging by one of the prediction algorithms. Five missense variants were not predicted to be deleterious or damaging by either algorithm, including the p.Arg1210Cys variant.

Table 3.5.3 Arg1210Cys variant KASPar primers

Variant	Allele X Primer	Allele Y Primer	Common Primer	Allele X	Allele Y
Arg1210Cys/rs121913059	AAACGGKGGATATCGTCTTTTCATCAC	GTA AACGGKGGATATCGTCTTTTCATCAT	CCCATCCCAACATGTTGTWCGCAAT	C	T

Table 3.5.4 Rare sequence variants identified in the CFH gene in 180 cuticular drusen cases

Number of cases	Nucleotide change	Protein change	SNP Id	MAF (%)	CD cases	EVS/dbsNP	Previous disease associations	Prediction algorithms	PolyPhen2
1	c.7C>G	p.Leu3Val	rs139254423	0.27	0.02	0	Novel	Tolerated (0.06)	Damaging (0.91)
1	c.428-2A>G	Splice-acceptor site	NA	0.27	0	0	Novel	NA	NA
1	c.481G>T	p.Ala161Ser	NA	0.27	0	0	Novel	Tolerated (0.17)	Benign (0.09)
1	c.518C>G	p.Ala173Gly	NA	0.27	0	0	Novel	Deleterious (0.03)	Benign (0.08)
1	c.524G>A	p.Arg175Gln	NA	0.27	0	0	Novel	Tolerated (0.17)	Benign (0.00)
1	c.578C>T	p.Ser193Leu	NA	0.27	0	0	Novel	Deleterious (0.0)	Damaging (0.99)
1	c.647T>C	p.Ile216Thr	rs183474263	0.27	0.001	0	Novel	Tolerated (0.19)	Benign (0.003)
1	c.901_902del	p.Ala301Asnfs*25	NA	0.27	0	0	Novel	NA	NA
1	c.1135T>C	p.Trp379Arg	NA	0.27	0	0	Novel	Deleterious (0.0)	Damaging (1.0)
2	c.1198C>A	p.Gln400Lys	rs201671665	0.55	0.01	0	aHUS [29]	Tolerated (0.94)	Benign (0.01)
2	c.2850G>C	p.Gln950His	rs149474608	0.55	0.61	0	aHUS [28]	Deleterious (0.0)	Damaging (0.80)
1	c.2867C>T	p.Thr956Met	rs145975787	0.27	0.16	0	aHUS [30]	Tolerated (0.38)	Damaging (0.96)
2	c.3628C>T	p.Arg1210Cys	rs121913059	0.55	0.02	0	aHUS/AMD [10, 24]	Tolerated (0.05)	Benign (0.02)

MAF: Minor Allele Frequency

SIFT: Sorting Intolerant from Tolerant (Intolerance ≤ 0.05)

PolyPhen2: Polymorphism Phenotyping (score 0 \rightarrow 1)



3.5

The p.Arg1210Cys variant was identified in two unrelated individuals with CD. To test for a possible association of the p.Arg1210Cys variant in our Dutch-German non-CD type AMD case-control cohort, we genotyped this variant in 813 cases and 1175 controls from the EUGENDA database (**Table 3.5.1**). The p.Arg1210Cys variant was not found in our genotyped cohort, besides the two CD patients in which the p.Arg1210Cys variant was identified by sequence analysis of the *CFH* gene.

Both individuals carrying the p.Arg1210Cys variant presented with hyperfluorescent drusen on FA, typical for the CD subtype of AMD (**Figure 3.5.1**). In case 1 drusen were first noted at 50 years, with both eyes displaying numerous small drusen in the posterior pole and peripheral retina (**Figure 3.5.1A-D**). Case 2 had an age of onset of visual impairment at 64 years and presented with numerous small drusen in the posterior pole in both eyes. Furthermore, case 2 displayed a large fibrotic scar in the right eye (**Figure 3.5.1E and G**), pigmentary changes and an occult choroidal neovascularization in the left eye (**Figure 3.5.1F and H**).

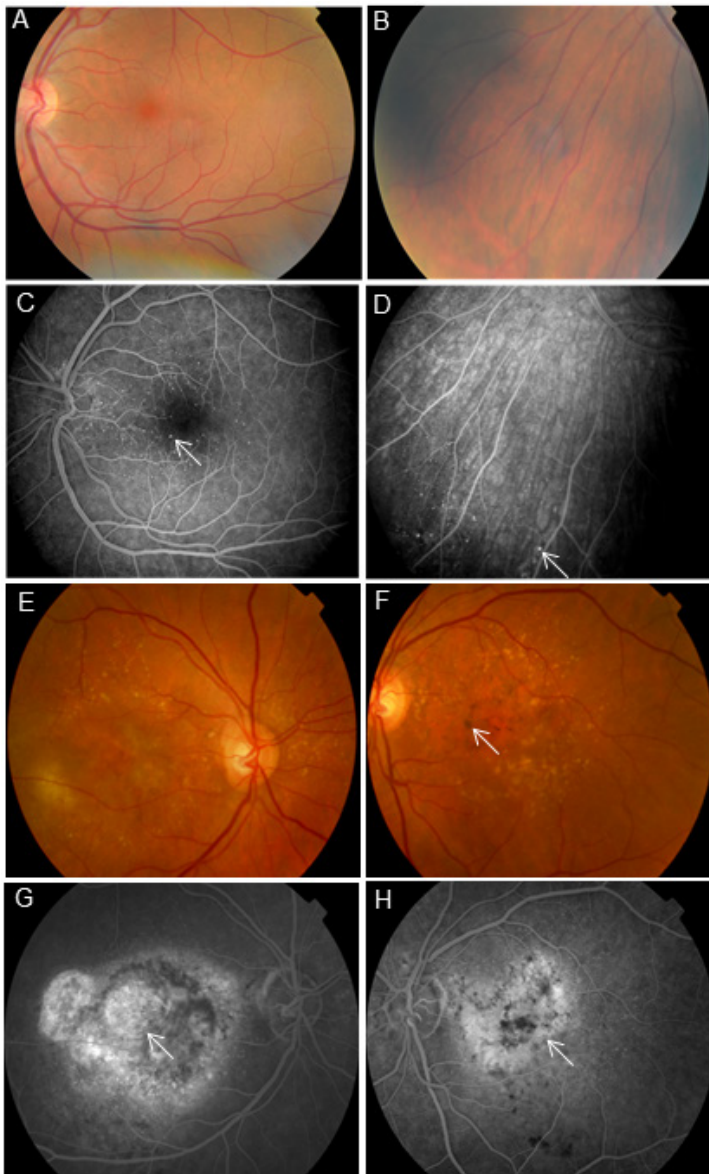


Figure 3.5.1 Fundus photographs and fluorescein angiographs of two cases carrying the Arg1210Cys variation. Case 1, displayed numerous small drusen (arrow) in the posterior pole and in peripheral retina in both eyes (A and B represent color fundus photographs of the posterior pole and the periphery of the left eye respectively, whereas C and D represent fluorescein angiographs of the posterior pole and the periphery of the left eye respectively). Case 2, showed small drusen of the posterior pole in both eyes (E and F represent color fundus photographs of right and left eye respectively, whereas G and H represent fluorescein angiographs of right and left eye respectively). In addition, case 2 displayed a large fibrotic scar (G, arrow) in the right eye. In the left eye pigmentary changes (F, arrow) and an occult choroidal neovascularization (H, arrow) were observed.

DISCUSSION

The present study identified the presence of rare variants (MAF<1%) in the *CFH* gene in 16 (8.8%) of 180 patients diagnosed with the CD subtype of AMD. This number is significantly higher than the number of carriers of rare *CFH* variants in the general population (4.3%, $P = 0.008$). This study evidenced that carriers of rare *CFH* variants display an earlier age at onset than non-carriers of rare *CFH* variants ($P = 0.016$). The rare missense variant p.Arg1210Cys was identified in two CD cases, but was not detected in 813 non-CD type AMD cases and 1175 controls of our Dutch-German cohort. The p.Arg1210Cys variant was previously found to be highly associated with AMD in North American cohorts, with a frequency in AMD patients of 40/2423 (1.65%)¹⁰ and 23/2335 (0.99%),⁹ respectively. However, the p.Arg1210Cys variant was not detected in an Icelandic cohort (consisting of 1143 AMD patients) nor in a Han Chinese cohort (consisting of 258 AMD patients).^{11, 12}

The current study suggests that the p.Arg1210Cys variant may be restricted to a subset of AMD patients with CD. Since the cohort of CD patients analyzed in our study was too small to reliably test for an association, this finding would need to be confirmed in additional cohorts of patients with CD, and/or by detailed clinical phenotyping of AMD patients carrying the p.Arg1210Cys variant using FA. An under or overrepresentation of AMD patients with CD-like characteristics between cohorts might explain the observed discrepancy of the p.Arg1210Cys association between the North American,¹⁰ Icelandic,¹¹ Han Chinese,¹² and the Dutch-German cohorts. On the other hand it is well-known that the distribution of low-frequency alleles varies among populations, since they tend to be the result of recent mutation and are expected to geographically cluster around the location at which the mutation first arose.¹⁶ Indeed, the frequency of disease-causing variants can significantly differ among populations,¹⁷ or can even be restricted to a geographical region.¹⁸

The CFH protein is an important regulator of the alternative pathway of the complement cascade that plays a key role in clearance of pathogens and immune complexes, and modulates adaptive immunity.¹⁹ CFH is composed of 20 sequential complement control protein (CCP) domains (**Figure 3.5.2**). Five of the identified rare variants (p.Ala161Ser, p.Ala173Gly, p.Arg175Gln, p.Ser193Leu and p.Ile216Thr) are clustered within the N-terminal domains CCPs 1-4. This region has been demonstrated to be involved in cofactor activity,²⁰ suggesting that these variants potentially have an impact on CFH cofactor activity. Two variants, p.Trp379Arg and p.Gln400Lys, are located within the CCP6 and CCP7 domains respectively, close to the common p.Tyr402His²¹ AMD risk variant which is known to cause defective heparin binding properties.²⁰ This raises the possibility that these variants may exert a similar effect. Three variants (p.Gln950His, p.Thr956Met and p.Arg1210Cys) are clustered in the C-terminal CCP domains 16-20. Functional studies have demonstrated that these four C-terminal CCP domains are necessary for host cell recognition or discrimination properties of CFH.²² In addition, we identified one frameshift (p.Ala301Asnfs*25) variant and one splice-acceptor site (428-2A>G) variant, which are both predicted to abolish CFH function.



Figure 3.5.2 Schematic representation of factor H and its functional domains. Factor H is composed of 20CCP domains, and the approximate locations of missense variations are indicated on top of the diagram. The location of binding sites for C3b in black, cofactor activity in purple, heparin in orange, sialic acid in green, and self-surface recognition in blue bars, are mentioned below.

Notably, not all missense variants identified in this study were predicted to be pathogenic by SIFT and PolyPhen. In particular this is the case for the p.Arg1210Cys variant, which was not predicted to be deleterious or damaging by either algorithm. However, functional studies demonstrate that the p.Arg1210Cys variant compromises CFH function, as the mutant protein exhibits defective binding to C3d, C3b, heparin, and endothelial cells, and forms a covalent interaction with human serum albumin.^{10, 23-26} Therefore it should be noted that although prediction software tools like SIFT and PolyPhen may assist in the assessment of potential damaging rare variants, functional validation of CFH mutant proteins is needed in order to properly assess the functional consequence of these genetic variations.

The majority of identified variants were not present in public databases, nor have they previously been linked to other diseases, demonstrating that many *CFH* variants are novel and unique for individual patients. The number of carriers of rare variants is significantly higher in CD patients than the number of carriers in the general population (EVS) ($P = 0.008$). The carriers of rare *CFH* variants displayed an earlier age at onset than non-carriers ($P = 0.016$). This underlines the importance of sequence analysis of the entire *CFH* coding region and splice junction of the *CFH* gene to identify the causative allele, in particular in individuals with the CD subtype of AMD. The p.Arg1210Cys variant has previously been demonstrated to confer a high risk of developing AMD,¹⁰ underscoring its pathogenicity. However, two *CFH* variants were recently identified in a large scale sequencing study, and were found not to be associated with the disease: p.Glu950His was identified in 9/3343 AMD patients and 10/1480 controls ($P = 0.98$), p.Thr956Met was identified in 4/3348 AMD patients and 6/1484 controls ($P = 0.99$).²⁷ This implies that these alleles may not be causative for AMD. Interestingly, four of the identified variants (p.Gln400Lys, p.Gln950His, p.Thr956Met and p.Arg1210Cys) were previously reported in patients with atypical haemolytic uremic syndrome (aHUS), a devastating renal disease, supporting a previously proposed theory that an allelic overlap exists between two distinct pathologies, AMD and aHUS.²⁸⁻³⁰ CD patients carrying aHUS mutations did not have renal complaints at the time of recruitment (**Table 3.5.5**). This suggests that additional genetic variants and/or external triggers determine the disease outcome in individuals carrying these alleles.

Table 3.5.5 Clinical description of Cuticular drusen patients with rare variants in the CFH gene

Number	Gender	Age	Age at onset	Variants		Protein level	Family history		Visual acuity		Retinal phenotype
				DNA level	DNA level		history	OD	OS		
1	F	48	45	c.7C>G		p.Leu3Val	NO	NO	0.3+	0.1+	ODS: Confluent large drusen in macula and numerous small drusen in posterior pole. OS: Small geographic atrophic lesion
2	F	57	51	c.428-2A>G		NA	NO	NO	0.5/60	1.0	OD: Central fibrotic scar. OS: Confluent large drusen in macula. ODS: Small drusen and punched out lesions in peripheral retina
3	F	48	47	c.481G>T		p.Ala161Ser	YES	YES	1.0	0.8+	ODS: Confluent large drusen in macula and some small drusen in posterior pole
4	M	74	69	c.518C>G		p.Ala173Gly	NO	NO	0.8	0.32-	ODS: Extensive small and large drusen in macula and mid-peripheral retina. OS: Large occult subfoveal CNV
5	M	77	75	c.524G>A		p.Arg175Gln	YES	YES	0.6++	0.25	ODS: Extensive hard macular drusen and temporal to the macula small areas of chorioretinal atrophy
6	M	73	No visual loss	c.647T>C		p.Ile216Thr	YES	YES	1.25=	0.8=	ODS: Some small drusen in posterior pole and numerous small drusen in peripheral retina
7	F	56	44	c.901_902del		p.Ala301AsnfsX25	YES	YES	NA	NA	ODS: Innumerable small drusen in posterior pole. OD: Hard exudates, fluid pocket and CNV. OS: Juxta foveal confluent soft drusen
8	F	86	81	c.1198C>A		p.Gln400Lys	NA	NA	0.4+	2/30	OD: Pigmentary changes, numerous reticular drusen in posterior pole and occult CNV. OS: Central fibrotic scar
9	M	44	NA	c.1198C>A		p.Gln400Lys	NA	NA	NA	NA	ODS: Extensive soft confluent and small hard drusen in posterior pole
10	F	46	20	c.2850G>C		p.Gln950His	NA	NA	1.25=	1.0+	ODS: Numerous hard drusen, especially from the border of the macula to the vascular arcade; fundoscopic changes at the age of 20 years
11	M	80	73	c.2850G>C		p.Gln950His	NO	NO	2/60	0.1-	ODS: Para macular drusen. OD: Large fibrotic scar in macula. OS: Macular pigmentary changes, occult CNV

12	F	77	71	c.2867C>T	p.Thr956Met	NO	0.8++	0.6	ODS: Extensive small drusen in posterior pole and peripheral retina
13	F	55	54	c.1135C>T	p.Trp379Arg	YES	0.9	0.5+	ODS: Extensive small drusen in posterior pole and mid-peripheral retina OD: Soft large drusen in macula. OS: Classic exudative CNV in macula
14	F	54	50	c.3628C>T	p.Arg1210Cys	YES	0.6	0.4	ODS: Numerous small drusen in posterior pole and some drusen in peripheral retina
15	F	76	64	c.3628C>T	p.Arg1210Cys	NA	1/60	0.5	ODS: Innumerable small drusen in posterior pole. OD: Large fibrotic scar and hard exudates; OS: Pigmentary changes and occult CNV

Abbreviations: Age = age at moment of examination in years; OD = oculus dexter; OS = oculus sinister; ODS = oculo dexter and sinister; F = female; M = male; NA = not available; CNV = choroidal neovascularization; Visual acuity in Snellen decimals.



In conclusion, the present study identified the presence of rare variants in the *CFH* gene in 16 (8.8%) of 180 patients with the CD subtype of AMD. The carriers of rare *CFH* variants displayed an earlier age at onset than non-carriers ($P = 0.016$). A previously reported rare missense variant, p.Arg1210Cys, was identified in two CD cases, but was not detected in 813 non-CD type AMD cases and 1175 controls of our Dutch-German cohort. The current study suggests that the p.Arg1210Cys variant may be restricted to a subset of AMD patients with CD. Detailed clinical phenotyping, including fluorescein angiography, of AMD patients carrying the p.Arg1210Cys variant in other cohorts is required to confirm this finding.

REFERENCES

1. Klaver CC, Wolfs RC, Vingerling JR, Hofman A, de Jong PT. Age-specific prevalence and causes of blindness and visual impairment in an older population: the Rotterdam Study. *Arch Ophthalmol* 1998;116:653-658.
2. de Jong PT. Age-related macular degeneration. *N Engl J Med* 2006;355:1474-1485.
3. Boon CJ, van de Ven JP, Hoyng CB, den Hollander AI, Klevering BJ. Cuticular drusen: stars in the sky. *Prog retin eye res* 2013;37:90-113.
4. Guigui B, Leveziel N, Martinet V, et al. Angiography features of early onset drusen. *Br j of ophthalmol* 2011;95:238-244.
5. van de Ven, Boon CJ, Fauser S, et al. Clinical evaluation of 3 families with basal laminar drusen caused by novel mutations in the complement factor H gene. *Arch Ophthalmol* 2012;130:1038-1047.
6. van de Ven, Smailhodzic D, Boon CJ, et al. Association analysis of genetic and environmental risk factors in the cuticular drusen subtype of age-related macular degeneration. *Mol Vis* 2012;18:2271-2278.
7. Grassi MA, Folk JC, Scheetz TE, Taylor CM, Sheffield VC, Stone EM. Complement factor H polymorphism p.Tyr402His and cuticular Drusen. *Arch of ophthalmol* 2007;125:93-97.
8. Boon CJ, Klevering BJ, Hoyng CB, et al. Basal laminar drusen caused by compound heterozygous variants in the CFH gene. *Am J Hum Genet* 2008;82:516-523.
9. Zhan X, Larson DE, Wang C, et al. Identification of a rare coding variant in complement 3 associated with age-related macular degeneration. *Nat genet* 2013;45:1375-1379.
10. Raychaudhuri S, Iartchouk O, Chin K, et al. A rare penetrant mutation in CFH confers high risk of age-related macular degeneration. *Nat Genet* 2011;43:1232-1236.
11. Helgason H, Sulem P, Duvvari MR, et al. A rare nonsynonymous sequence variant in C3 is associated with high risk of age-related macular degeneration. *Nat genet* 2013;45:1371-1374.
12. Shen SK, Liu XQ, Lu F, Yang ZL, Shi Y. Association study between age-related macular degeneration and R1210C mutation of CFH gene in Chinese population. *Chin j of med genet* 2012;29:570-572.
13. Klein R, Davis MD, Magli YL, Segal P, Klein BE, Hubbard L. The Wisconsin age-related maculopathy grading system. *Ophthalmology* 1991;98:1128-1134.
14. Adzhubei I, Jordan DM, Sunyaev SR. Predicting functional effect of human missense mutations using PolyPhen-2. *Curr Protoc Hum Genet* 2013; Chapter 7:Unit7.20.
15. Kumar P, Henikoff S, Ng PC. Predicting the effects of coding non-synonymous variants on protein function using the SIFT algorithm. *Nat Protoc* 2009;4:1073-1081.
16. Novembre J, Johnson T, Bryc K, et al. Genes mirror geography within Europe. *Nature* 2008;456:98-101.
17. Maugeri A, Flothmann K, Hemmrich N, et al. The ABCA4 2588G>C Stargardt mutation: single origin and increasing frequency from South-West to North-East Europe. *Eur J Hum Genet* 2002;10:197-203.
18. Mukhopadhyay A, Nikopoulos K, Maugeri A, et al. Erosive vitreoretinopathy and wagner disease are caused by intronic mutations in CSPG2/Versican that result in an imbalance of splice variants. *Invest Ophthalmol Vis Sci* 2006;47:3565-3572.
19. Walport MJ. Complement. First of two parts. *N Engl J Med* 2001;344:1058-1066.
20. Clark SJ, Higman VA, Mulloy B, et al. His-384 allotypic variant of factor H associated with age-related macular degeneration has different heparin binding properties from the non-disease-associated form. *J Biol Chem* 2006;281:24713-24720.



21. Haines JL, Hauser MA, Schmidt S, et al. Complement factor H variant increases the risk of age-related macular degeneration. *Science* 2005;308:419-421.
22. Pickering MC, de Jorge EG, Martinez-Barricarte R, et al. Spontaneous hemolytic uremic syndrome triggered by complement factor H lacking surface recognition domains. *J Exp Med* 2007;204:1249-1256.
23. Sanchez-Corral P, Perez-Caballero D, Huarte O, et al. Structural and functional characterization of factor H mutations associated with atypical hemolytic uremic syndrome. *Am j of hum geneti*2002;71:1285-1295.
24. Manuelian T, Hellwege J, Meri S, et al. Mutations in factor H reduce binding affinity to C3b and heparin and surface attachment to endothelial cells in hemolytic uremic syndrome. *J Clin Invest* 2003;111:1181-1190.
25. Jozsi M, Heinen S, Hartmann A, et al. Factor H and atypical hemolytic uremic syndrome: mutations in the C-terminus cause structural changes and defective recognition functions. *J Am Soc of Nephrol: JASN* 2006;17:170-177.
26. Ferreira VP, Herbert AP, Cortes C, et al. The binding of factor H to a complex of physiological polyanions and C3b on cells is impaired in atypical hemolytic uremic syndrome. *J immunol* 2009;182:7009-7018.
27. Seddon JM, Yu Y, Miller EC, et al. Rare variants in CFI, C3 and C9 are associated with high risk of advanced age-related macular degeneration. *Nat genet* 2013;45:1366-1370.
28. Caprioli J, Castelletti F, Bucchioni S, et al. Complement factor H mutations and gene polymorphisms in haemolytic uraemic syndrome: the C-257T, the A2089G and the G2881T polymorphisms are strongly associated with the disease. *Hum Mol Genet* 2003;12:3385-3395.
29. Dragon-Durey MA, Fremeaux-Bacchi V, Loirat C, et al. Heterozygous and homozygous factor h deficiencies associated with hemolytic uremic syndrome or membranoproliferative glomerulonephritis: report and genetic analysis of 16 cases. *J Am Soc Nephrol* 2004;15:787-795.
30. Perez-Caballero D, Gonzalez-Rubio C, Gallardo ME, et al. Clustering of missense mutations in the C-terminal region of factor H in atypical hemolytic uremic syndrome. *Am J Hum Genet* 2001;68:478-484.



Chapter 4

Dominant cystoid macular dystrophy

Dominant cystoid macular dystrophy

N.T.M. Saksens, R.A.C. van Huet, J.J. van Lith-Verhoeven,
A.I. den Hollander, C.B. Hoyng, C.J.F. Boon

Published in: Ophthalmology 2015;122:180-191



PURPOSE. Retrospective case series to describe the clinical characteristics and long-term follow-up in patients with autosomal dominant cystoid macular dystrophy (DCMD).

METHODS. Extensive ophthalmic examination, including visual acuity (VA), fundus photography, fluorescein angiography (FA), fundus autofluorescence (FAF) imaging, optical coherence tomography (OCT), color vision testing, dark adaptation testing, full-field electroretinography (ERG), and electro-oculography (EOG) in ninety-seven patients with DCMD. Blood samples were obtained for DNA extraction and subsequent haplotype analysis. Main outcome measures are age at onset, VA, fundus appearance, and characteristics on FA, FAF, OCT, ERG, and EOG.

RESULTS. Cystoid fluid collections (CFCs) were the first retinal abnormalities detectable in DCMD, developing during childhood. At long-term follow-up, the CFCs decreased in size and number, and eventually disappeared with concurrent development of progressive chorioretinal atrophy and hyperpigmented deposits in the posterior pole. Dominant cystoid macular dystrophy could be classified into 3 stages, based on characteristics on ophthalmoscopy, FAF, FA, and OCT, as well as on results of electrophysiologic analysis. The staging system correlated with age and VA. In stage 1 DCMD (20 patients; 22%), patients generally were younger than 20 years and had CFCs with fine folding of the internal limiting membrane and mild pigment changes. In stage 2 DCMD (48 patients; 52%), the CFCs tended to decrease in size, and moderate macular chorioretinal atrophy developed. Patients with stage 3 DCMD (24 patients; 26%) generally were older than 50 years and showed profound chorioretinal atrophy, as well as coarse hyperpigmented deposits in the posterior pole. Most patients were (highly) hyperopic (72 patients; 92%). All DCMD patients shared the disease haplotype at the DCMD locus at 7p15.3.

CONCLUSIONS. Dominant cystoid macular dystrophy is a progressive retinal dystrophy, characterized primarily by early-onset cystoid fluid collections in the neuroretina, which distinguishes this disorder from other retinal dystrophies. The phenotypic range of DCMD can be classified into 3 stages. The genetic locus for this retinal dystrophy has been mapped to 7p15.3, but the involved gene is currently unknown.

INTRODUCTION

Dominant cystoid macular dystrophy (DCMD) is an autosomal-dominantly inherited retinal disorder that primarily affects the macula.^{1,2} A hallmark feature and presenting symptom of DCMD is the appearance of cystoid intraretinal fluid collections (CFCs) in the macula that resemble cystoid macular edema before any other visible retinal abnormalities appear. The onset of these CFCs is generally in the first or second decade of life. Most patients with DCMD have moderate to high axial hyperopia.³⁻⁵ As the disease progresses, the CFCs diminish, and progressive central vision loss develops between 20 and 50 years of age as a result of progressive chorioretinal atrophy.^{1,5}

DCMD has been linked to a genetic interval on chromosome 7p15-p21,⁶ but the causative gene has not been identified to date. DCMD has also been abbreviated as CYMD (OMIM 153880). In the Netherlands, one large family with DCMD is known and extensive genealogical studies revealed a common Dutch ancestor, who supposedly lived in the early 18th century.⁴ In addition to this large Dutch family, one unrelated American family of Greek ancestry,⁷ and an American and a Spanish patient,⁸ have been described with presumed DCMD.^{7,9}

Little is known about the spectrum and variability of fundus abnormalities in DCMD, as well as the visual outcome. We report the clinical characteristics and follow-up data of the large Dutch DCMD family with 97 affected family members. Based on multimodal imaging and electrophysiological studies, we propose a clinical classification system for DCMD in 3 stages. In addition, we evaluate the therapeutic options and discuss a possible pathophysiologic disease sequence.

METHODS

Clinical Assessment

This study included 97 patients with DCMD, who were all examined at the Institute of Ophthalmology of the Radboud University Medical Center (Nijmegen, the Netherlands) between October 1958 and August 2013. All patients belong to one large pedigree, descending from one common Dutch ancestor (**Figure 4.1**).⁴ Most patients originated from the southeast region of the Netherlands. Patients received the diagnosis of DCMD based on the aspect of the lesions on ophthalmoscopy, fluorescein angiography (FA) and optical coherence tomography (OCT).⁴ In addition, genealogical research and haplotype analysis confirmed the diagnosis DCMD.



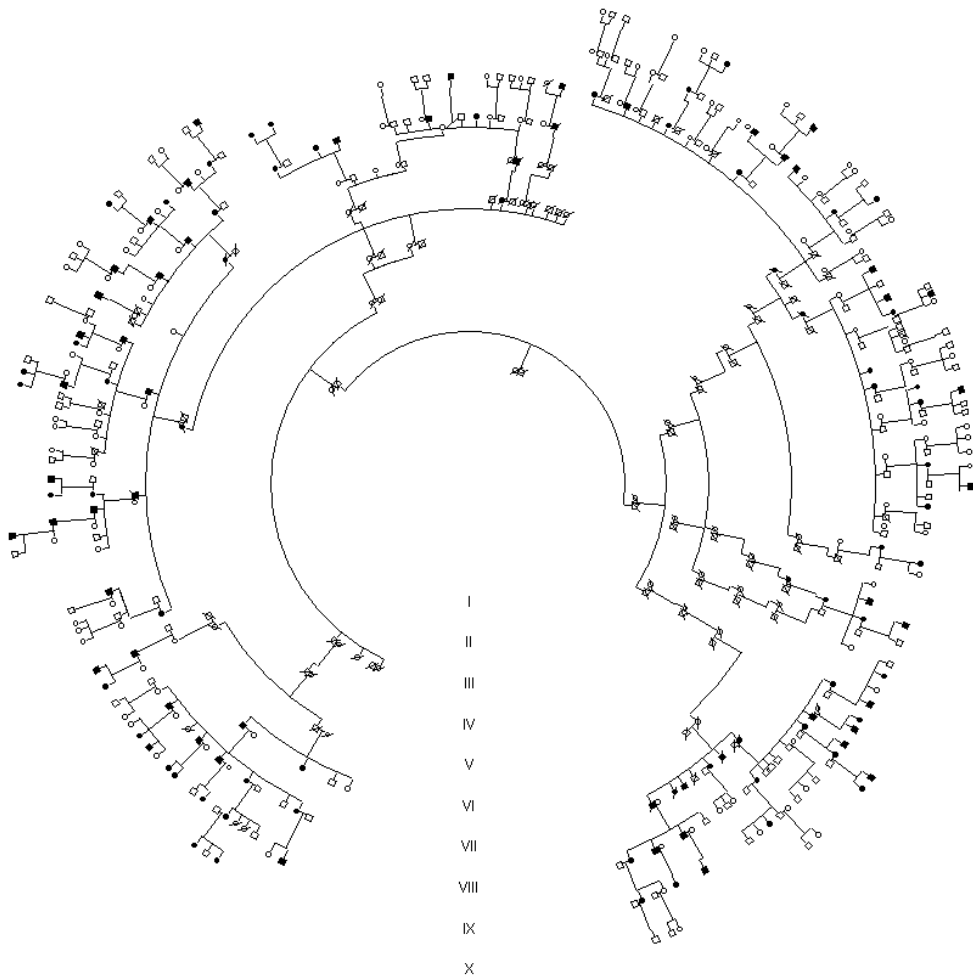


Figure 4.1 Diagram showing that all dominant cystoid macular dystrophy patients in the Netherlands belong to one large pedigree with a common ancestor.

The medical history, age at onset, (best-corrected) Snellen visual acuity (VA), fundus appearance, including slit-lamp examination, fundus examination by indirect ophthalmoscopy, and fundus photography, as well as results of electrophysiological testing were retrieved from medical records. To analyze the course of the VA over time, we recorded the age at which the decrease in VA exceeded 20/40, 20/60, and $\leq 20/200$ for survival analyses. Fundus autofluorescence (FAF) imaging was performed with a confocal scanning laser ophthalmoscope (Spectralis; Heidelberg Engineering, Heidelberg, Germany; excitation light 488 nm). FAF follow-up images were available in 9 patients. Based on ophthalmoscopy, autofluorescence, or both, mild atrophy of the retinal pigment epithelium (RPE) was defined as indistinct granular hypopigmented RPE changes, and profound atrophy was defined as

sharply demarcated areas of chorioretinal atrophy in the macula, corresponding with a decrease and absence of autofluorescence. Spectral-domain OCT (Spectralis™, Heidelberg Engineering, Heidelberg, Germany) was performed using the ‘Macular Thickness Map’ protocol provided by the manufacturer (Heidelberg Eye Explorer Software, version 1.6.4.0; Heidelberg Engineering, Heidelberg, Germany). Follow-up OCT scans were available in 14 patients to detect progression of retinal changes. Follow-up FA data were available in 29 of them. In addition electro-oculography (EOG), full-field electroretinography (ERG), visual field analysis by means of Goldmann perimetry (stimuli V4e-III4e-I4e-I3e-I2e-I1e), dark adaptation, and color vision testing were performed in selected patients as described previously (**Table 4.1**).¹⁰ Altogether, follow-up data were available in 71 DCMD patients. Furthermore, 10 DCMD patients were invited for an additional, extensive clinical examination to complete the follow-up data, resulting in a better appreciation of the disease course and characteristics. EOG and full-field ERG recordings were performed according to the standards of the International Society for Clinical Electrophysiology of Vision (ISCEV).¹¹⁻¹³ EOG Arden ratios were registered and stratified as normal (≥ 1.8), mildly reduced (< 1.8 , but ≥ 1.5), or severely reduced (< 1.5). Full-field ERG was defined as normal (equal to or above the lower 5% of the range for a normal population: photopic ≥ 78 μV , scotopic ≥ 263 μV), subnormal in case of moderately reduced amplitudes of the B-wave (1-5% of normal range: photopic ≥ 69 μV and < 78 μV , scotopic ≥ 195 μV and < 263 μV) or as abnormal in case of severely reduced amplitudes ($< 1\%$ of normal range: photopic < 69 μV , scotopic < 195 μV). The study adhered to the tenets of the Declaration of Helsinki, and Ethics Committee approval was obtained. Informed consent was received from all examined subjects.

Haplotype Analysis

Peripheral venous blood samples were obtained from 69 patients for analysis of the haplotypes at the previously described DCMD locus.⁶ The haplotypes at the DCMD locus were also determined in 52 unaffected family members. The genomic DNA was isolated as described elsewhere.¹⁴ Haplotype analysis was performed with microsatellite markers (D7S493 and D7S673) surrounding the genetic locus located at 7q15-p21.



Table 4.1 Three stages of dominant cystoid macular dystrophy

Stage	Mean Age [range] (n=92)	Mean VA [range] (n=92)	Funduscopy (n=92)	OCT (n=30)	FAF (n=20)	FA (n=54)	EOG* (n=65)	ERG † (n=61)	Goldmann visual field (n=29)	Dark adaptation ‡ (n=34)	Color vision testing (n=50)
I	12.8 [0-32] (n=20)	20/37 [20/15 – 20/200] (n=20)	- Fine folding of ILM - CFCs - Mild granular pigment changes in the macula (n=20)	- CFCs (n=10)	- Mildly increased FAF in the macula (n=6)	- Hyperfluorescent CFCs - Perifoveal capillary dilation (n=15)	55% Normal 45% Mildly reduced (n=20)	100% Normal (n=13)	100% Normal (n=5)	38% Abnormal (n=8)	35% Diminished red-sensitivity (n=20)
II	37.7 [21-50] (n=48)	20/54 [20/20 – CF] (n=48)	- Mild but visible chorioretinal macular atrophy - CFCs (n=48)	- Mild retinal atrophy - Small CFCs (n=12)	- Moderately decreased FAF in the macula (n=9)	- Hyperfluorescent CFCs (n=26)	32% Normal 68% Mildly-severely reduced (n=34)	86% Normal 14% Subnormal (cone and rod) (n=35)	25% Peripheral visual field constriction (n=16)	33% Abnormal (n=18)	76% Blue-yellow Defect (n=17)
III	59.9 [44-72] (n=24)	20/212 [20/40- HM] (n=24)	- Profound, chorioretinal atrophy in the macula - Coarse hyperpigmentations - Attenuated arterioles (n=24)	- Profound chorioretinal atrophy - No CFCs (n=8)	- Large area of corresponding to profound RPE atrophy (n=5)	- Early hypofluorescence with late staining of atrophic area, surrounded by hyperfluorescence (n=13)	73% Severely reduced (n=11)	23% Subnormal 77% Abnormal (cone and rod) (n=13)	63% Peripheral visual field constriction (n=8)	75% Abnormal (n=8)	100 % Blue-yellow defect 77% Additional red-green defect (n=13)

Abbreviations: Age = age at moment of examination in years; n = number of patients tested; VA = visual acuity; OCT = optical coherence tomography; FAF = fundus autofluorescence; FA = fluorescein angiography; EOG = electro-oculography; ERG = electroretinography; ILM = internal limiting membrane; CFCs = cystoid fluid collections; CF = counting fingers; HM = hand movements; RPE = retinal pigment epithelium; * Expressed in International Society for Clinical Electrophysiology of Vision (ISCEV) Arden ratios: normal (≥ 1.8), mildly reduced (<1.8 , but ≥ 1.5), severely reduced (<1.5).

† Full-field ERG results are defined as normal (photopic: >78 mV, scotopic: >263 mV), subnormal (photopic: ≥ 69 mV and, <78 mV, scotopic: ≥ 195 mV and <263 mV) or abnormal (photopic: <69 mV, scotopic: <195 mV).

‡ Abnormal dark adaptation responses are defined by an absolute threshold at 30 minutes raised at least 1.0 log U above reference values.

RESULTS

Clinical Findings

General characteristics

The study cohort included 97 patients, of which 55 were female (57%) and 42 male (43%), as well as 52 unaffected family members. The age at the first visit of the DCMD patients to our department ranged from 1 month to 72 years (median: 27 years). The mean age at onset of visual symptoms was 12.9 years (range: 2–45 years), and showed a remarkable trend of a lower age at onset in younger generations ($P = 0.02$). At first presentation, the fundus aspect ranged from no abnormalities or only an absence of the foveal reflex and mild pigment changes in the fovea (**Figure 4.2A**) to profound chorioretinal atrophy with extensive hyperpigmentation in the posterior pole (**Figure 4.2M**).

All patients experienced a certain degree of central vision loss, with a progressive decline, but the course of the VA loss was highly variable among patients as shown in **Figure 4.3**. The age at which patients reached the level of legal blindness (VA $\leq 20/200$) in the better eye, despite optimal refractive correction, varied widely from 10 to 65 years (median: 43.5 years). Two patients (2%) became totally blind (no light perception) in 1 eye, at the age of 58 and 73, respectively, due to serous retinal detachment that resulted in phthisis bulbi despite several vitreoretinal procedures. In addition to vision loss, 7 patients (7%) reported difficulties with night vision, and 5 patients (5%) with advanced disease experienced (para) central scotoma. Four female patients (7%) noticed a more rapid and irreversible visual decline during hormonal events, like first menarche, pregnancy, and menopause.

Hyperopia was a frequent finding in DCMD patients. Information about the refractive error of the eye was available in 78 patients, of which 72 had hyperopia at presentation, with a mean hyperopic refraction of +5.78 diopters (D, range of spherical equivalents (SE): +1.00 to +13.00 D), of which 30 patients (38%) were highly hyperopic (SE $\geq +6.00$ D). The axial length measurements were available in 24 eyes of 12 patients, performed with A-scan ultrasound measurement. In all cases, the axial length was significantly below normal (mean: 19.6 mm; range: 18.6–21.0 mm).

Acute angle-closure glaucoma occurred in 6 patients (6%), at a mean age of 48 years (range: 42–58 years). Although normal intraocular pressure could be accomplished by either topical treatment, laser intervention, surgical treatment or a combination, all 6 patients experienced irreversible vision loss. In 1 patient with acute angle-closure glaucoma, laser iridotomy and iridectomy treatment had insufficient effect. Finally, this patient received a Baerveldt tube implant which resulted in hypotonia, causing a serous retinal detachment. This was treated with pars plana vitrectomy with oil tamponade and laser treatment. The retina eventually redetached, resulting in complete blindness with phthisis bulbi leading to evisceration of this eye. The other eye was treated preventively with laser iridotomy resulting in a prolonged normal intra-ocular pressure. One patient with a narrow anterior chamber angle was treated preventively with phaco-emulsification, but nevertheless acute glaucoma developed in 1 eye.



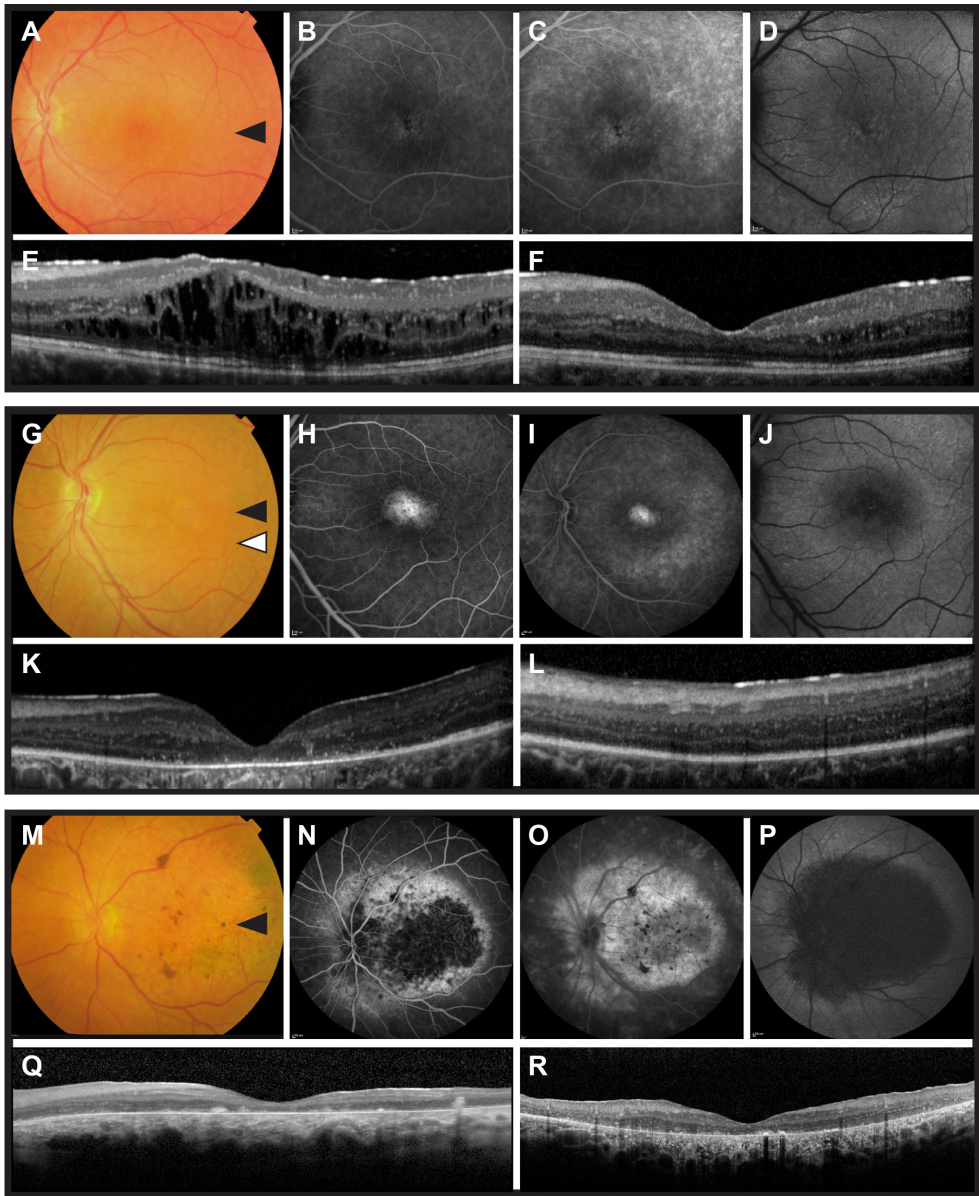


Figure 4.2 Clinical classification of dominant cystoid macular dystrophy (DCMD) into 3 stages. A-F Stage 1 DCMD. G-L Stage 2 DCMD. M-R Stage 3 DCMD. (A) Color fundus photograph of a 15-year-old patient with stage 1 DCMD (visual acuity 20/63; spherical equivalent (SE) +4.00 diopters (D), subjectively fluctuating vision for 4 years), showing cystoid fluid collections (CFCs) and fine pigment changes in the macula. **(B)** Fluorescein angiography (FA, early phase) showing mild hyperfluorescence of the foveal fluid collections. **(C)** FA (late phase) showing hyperfluorescent CFCs located in the fovea and more diffuse hyperfluorescence in the macula. **(D)** Fundus autofluorescence (FAF) showing areas of mildly increased autofluorescence at the cystoid areas and diffuse hyperautofluorescence within the vascular arcades. **(E)** Horizontal optical coherence tomography (OCT) scan through the fovea

(scanning plane indicated by black arrow head in **A**) showing CFCs in the inner and outer nuclear layer. (**F**) Six months before, only some small CFCs were visible on OCT at the same level as in **E**, demonstrating the fluctuating course of the CFCs without any treatment intervention. (**G**) Color fundus photograph of a 32-year-old patient with stage 2 DCMD (visual acuity 20/100, SE +1.50 D), showing pigment changes in the macula and mild residual CFCs. (**H-I**) FA showing a central hyperfluorescent lesion caused by an retinal pigment epithelium (RPE) window defect and residual edema in the early (**H**) and late (**I**) phase, surrounded by mild, indistinct hyperfluorescence. (**J**) FAF showing moderately decreased autofluorescence in the central macula, corresponding with atrophy of the RPE in the fovea on OCT (**K**) at the level of the black arrowhead in **G**. (**L**) A horizontal OCT scan through the scanning plane indicated by the white arrowhead in **G**, showing possible mild thickening of the outer nuclear layer but an RPE layer that seemed largely intact. (**M**) Color fundus photograph of a 67-year-old patient with stage 3 DCMD (visual acuity 20/800; SE +7.00 D), showing profound chorioretinal atrophy in the macula with attenuated arterioles and coarse hyperpigmentations. (**N-O**) Early (**N**) and late (**O**) phase FA showing early hypofluorescence and some late staining in the deeply atrophic central macula, encircled by hyperfluorescence that seems to be diffuse edema, extending beyond the vascular arcade and optic nerve. (**P**) FAF showing a large area of markedly decreased autofluorescence as a result of RPE atrophy in and beyond the macula. (**Q**) Horizontal OCT scan (scanned through plane indicated by black arrowhead in **M**) showing chorioretinal atrophy in the macula, with hyperreflective lesions consistent with the hyperpigmentations on color fundus photograph (**M**). (**R**) Vertical OCT scan through the fovea of the fellow (right) eye showing marked attenuation of the outer photoreceptor and RPE layers, although there appears to be a certain degree of persistent thickening of the inner and outer nuclear layer centrally in the macula.

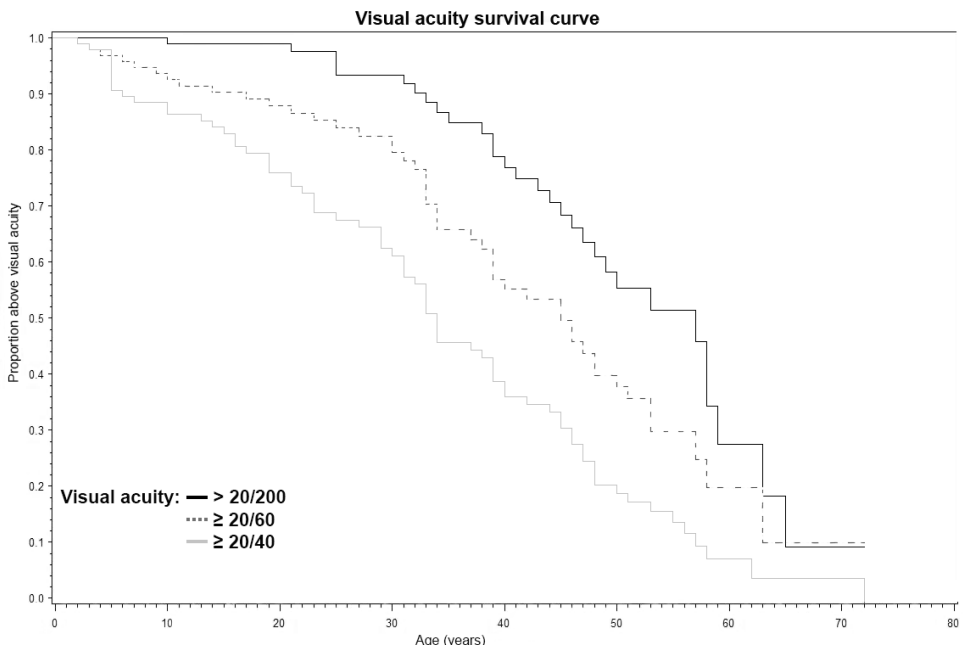


Figure 4.3 Kaplan-Meier survival curves of visual acuity (VA) of >20/40 (a threshold of visual disability, according to the United States definition reflecting the legal inability to drive a car); VA>20/60 (a cutoff point for low vision defined by the World Health Organization criteria associated with increasing difficulties in reading without visual aids); VA≥20/200 (a threshold of legal blindness according to World Health Organization criteria) related to the age. The median age at which the VA in our cohort exceeded 20/40, 20/60, and decreased to 20/200 or less were, 34, 45, and 57 years, respectively.

Disease Spectrum and Clinical Classification

The spectrum of retinal abnormalities in this DCMD cohort could be subdivided generally into 3 stages by an experienced retina specialist (C.J.F.B.) based on ophthalmoscopy and supported by the findings obtained from multimodal imaging (**Table 4.1**). These 3 stages were delineated by analyzing ophthalmoscopic findings in combination with FA, FAF, and SD-OCT, which were available in 92 DCMD patients.

Stage 1 DCMD (20 patients, 22%; **Table 4.1**) was characterized by wrinkling of the internal limiting membrane, CFCs and mild granular pigment changes in the macula (**Figure 4.2A**). The CFCs were visible as mildly hyperautofluorescent areas in the fovea and perimacular area on fundus autofluorescence (**Figure 4.2D**); on OCT the CFCs were located in the inner and outer nuclear layer of the retina (**Figure 4.2E**). FA clearly showed an aspect of hyperfluorescent cystoid macular edema, and in 60% evidence of mild perifoveal capillary dilation was seen (**Figure 4.2B and C**). In 14 patients (70%) the CFCs gradually increased in size, number, and extent during follow-up, affecting the entire posterior pole. However, during this progression the degree of CFCs was highly variable, corresponding with intra-individual variability of the VA (**Figure 4.2E-F and Figure 4.4A-E**).

In addition to the CFCs, in two patients with stage 1 DCMD, the OCT also showed a serous detachment of the neuroretina with a fluctuating course. The mean VA was 20/37 and decreased to less than 20/125 in only 4 patients (20%). In one patient with stage 1 DCMD and large CFCs who had a VA of 20/200, the VA recovered to 20/50 after remission of the cysts by treatment with acetazolamide.

In *stage 2* DCMD (48 patients, 52%; **Table 4.1**), the CFCs tended to become progressively smaller over time (**Figure 4.2K**). Unlike stage 1 DCMD, only 5 cases showed evidence of perifoveal capillary dilatation on FA. Mildly atrophic lesions appeared in the macula, with a corresponding decrease in VA (**Figure 4.2G, J and K**).

In *stage 3* DCMD (24 patients, 26%; **Table 4.1**), the macula was affected by profound chorioretinal atrophy (**Figure 4.2M-R**). In the macula and mid-peripheral retina, multiple coarse hyper-pigmentations were present in all patients, who also showed attenuated arterioles in varying degrees (**Figure 4.2N**). In this advanced disease stage, CFCs were no longer present on OCT (**Figure 4.2Q and R**). A variable degree of small whitish punctate deposits in the vitreous were seen in stage 2 and 3 DCMD.

The VA decreased to the level of legal blindness in 18 patients (75%) with stage 3 DCMD. Most patients (88%) were above the age of 50 years. The majority (77%) of the full-field ERG results were abnormal without selective cone or rod impairment in stage 3 DCMD (**Figure 4.5**). The EOG and full-field ERG results in all stages are depicted in **Table 4.1**.

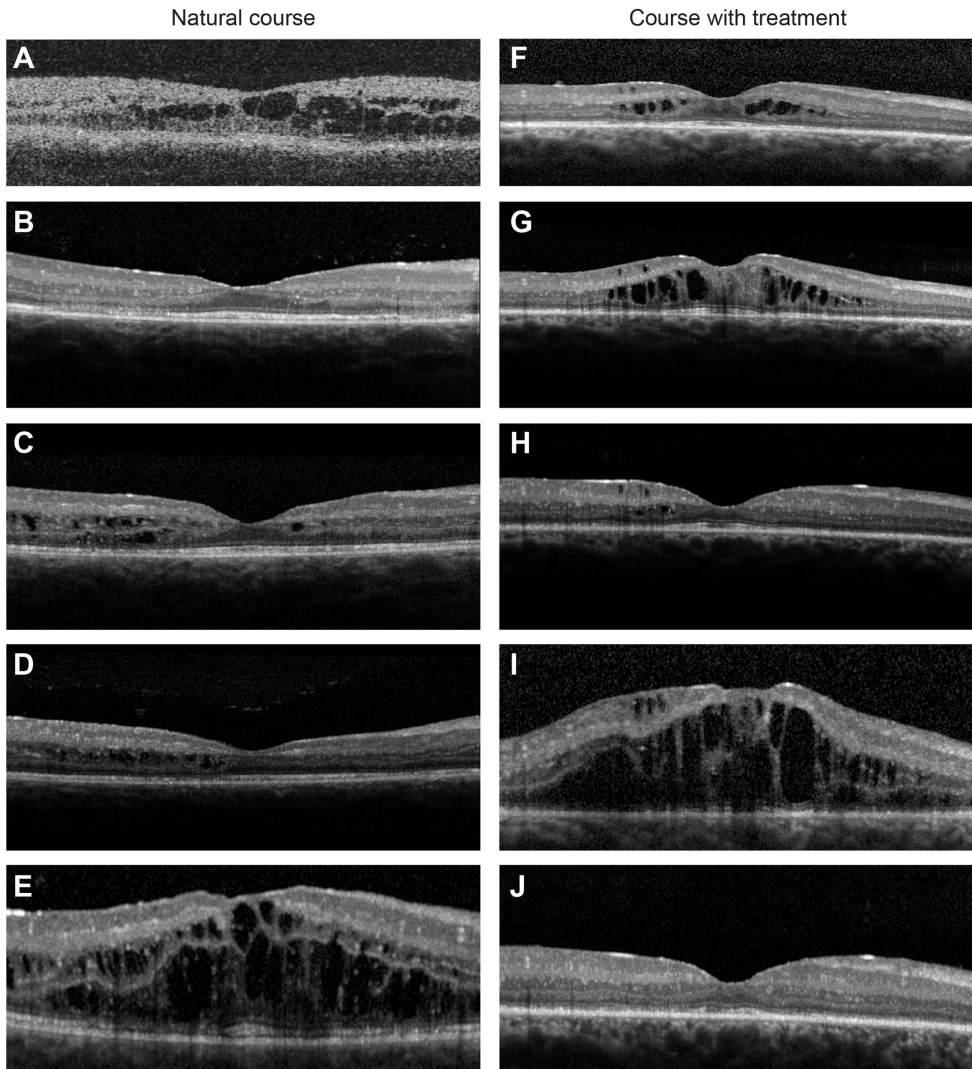


Figure 4.4 Follow-up of 2 dominant cystoid macular dystrophy (DCMD) patients with cystoid fluid collections (CFCs) on time-domain (A) or spectral-domain (B-J) optical coherence tomography (OCT). (A-E) Patient with stage 1 DCMD and fluctuation of CFCs without treatment over 7 years. The OCT follow-up data of the left eye shows the fluctuating natural course of CFCs. (A) At 8 years of age, OCT clearly showed moderate CFCs in the inner and outer nuclear layers without visual symptoms (visual acuity (VA): 20/20; spherical equivalent (SE) +4.00 diopters (D)). During the ensuing years, she experienced vision loss with fluctuating vision. (B) At the age of 11, no fluid collections were present on OCT, but fundoscopy showed fine pigment changes in the fovea with some wrinkling of the internal limiting membrane. The patient experienced fluctuating vision for 1 year (VA in this eye 20/40). (C) Two months after image B was obtained, mild CFCs recurred and her visual complaints increased (VA decreased to 20/63). (D) Three years after image C was obtained, the CFCs and vision symptoms decreased, whereas the VA increased to 20/50. (E) Five months after the image D was obtained, extensive and large CFCs recurred, associated with vision loss (VA: 20/63). (F-J) Stage 1 DCMD patient



treated with octreotide-acetate (20 mg intramuscular monthly) and oral acetazolamide (250 mg 1-4 times a day), reducing the CFCs and showing a possible dose-dependent effect of acetazolamide on OCT follow-up of 1 year. (F) Nineteen-year-old patient with late stage 1 DCMD with mild CFCs causing visual complaints before starting treatment (VA: 20/25; SE +3.25 D). (G) One year later, despite treatment with monthly intramuscular octreotide-acetate injections (20 mg) and oral acetazolamide 125 mg twice daily either separately or combined, CFCs increased with loss of vision (VA: 20/50). (H) Increasing the dose of acetazolamide to 250 mg three times a day, in addition to octreotide-acetate treatment, resulted in a significant decrease of CFCs within 2 weeks, with an increase of the VA to 20/32. (I) The CFCs increased markedly within 2 weeks after lowering the dose of acetazolamide to 250 mg twice a day, with a corresponding vision loss (VA: 20/80). (J) Raising the dose of acetazolamide to 250 mg four times daily resulted in a significant resolution of the CFCs within the next 2 weeks, with an increase in VA to 20/50.

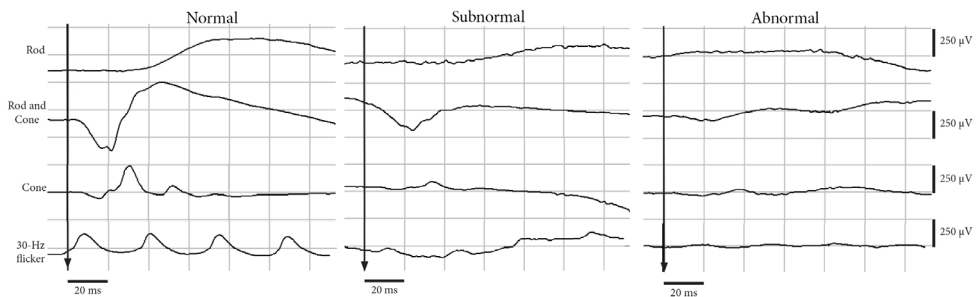


Figure 4.5 Representative full-field electroretinograms (ERGs) of 3 patients with dominant cystoid macular dystrophy (DCMD), showing normal, subnormal and abnormal results of the rod, rod and cone, cone, and 30-hertz flicker ERG. (Left) Normal full-field ERG results in a 15-year-old patient with stage 1 DCMD (visual acuity (VA): 20/50; spherical equivalent (SE) +4.25 diopters (D)). (Middle) Subnormal cone and rod driven responses on full-field ERG in a 67-year-old patient with stage 3 DCMD (VA: 20/800; SE +7.25 D). (Right) Abnormal photopic and scotopic full-field ERG in a 58-year-old patient with stage 3 DCMD (VA: 1/200; SE +4.00 D). Hz = hertz; ms = milliseconds; μV = microvolts.

An atypical phenotype was seen in 4 patients with stage 3 DCMD (17%). In 2 patients (8%) a phenotype reminiscent of Coats' disease developed at the age of 56 and 61, respectively, consisting of an exudative serous retinal detachment with RPE atrophy and coarse hyperpigmentations (**Figure 4.6A and B**). Furthermore, two patients (44 and 57 years) originating from two different branches of the pedigree, showed a retinal phenotype similar to end-stage retinitis pigmentosa, with attenuated arterioles, peripheral pigment changes resembling bone spicules, a waxy-pale optic disc, in addition to advanced chorioretinal atrophy in the posterior pole (**Figure 4.6C and D**). Both patients showed fundoscopic signs of CFCs in their childhood. These two patients had difficulties with night vision, with markedly abnormal dark adaptation and marked constriction of the peripheral visual field on Goldmann perimetry. Full-field ERG showed no scotopic response and a decreased photopic response corresponding to a rod-cone dystrophy dysfunction pattern. Both patients had a subnormal EOG with mildly reduced Arden ratios. Both patients shared the genetic DCMD locus, and their affected parents showed a typical DCMD phenotype without these retinitis pigmentosa-like features.

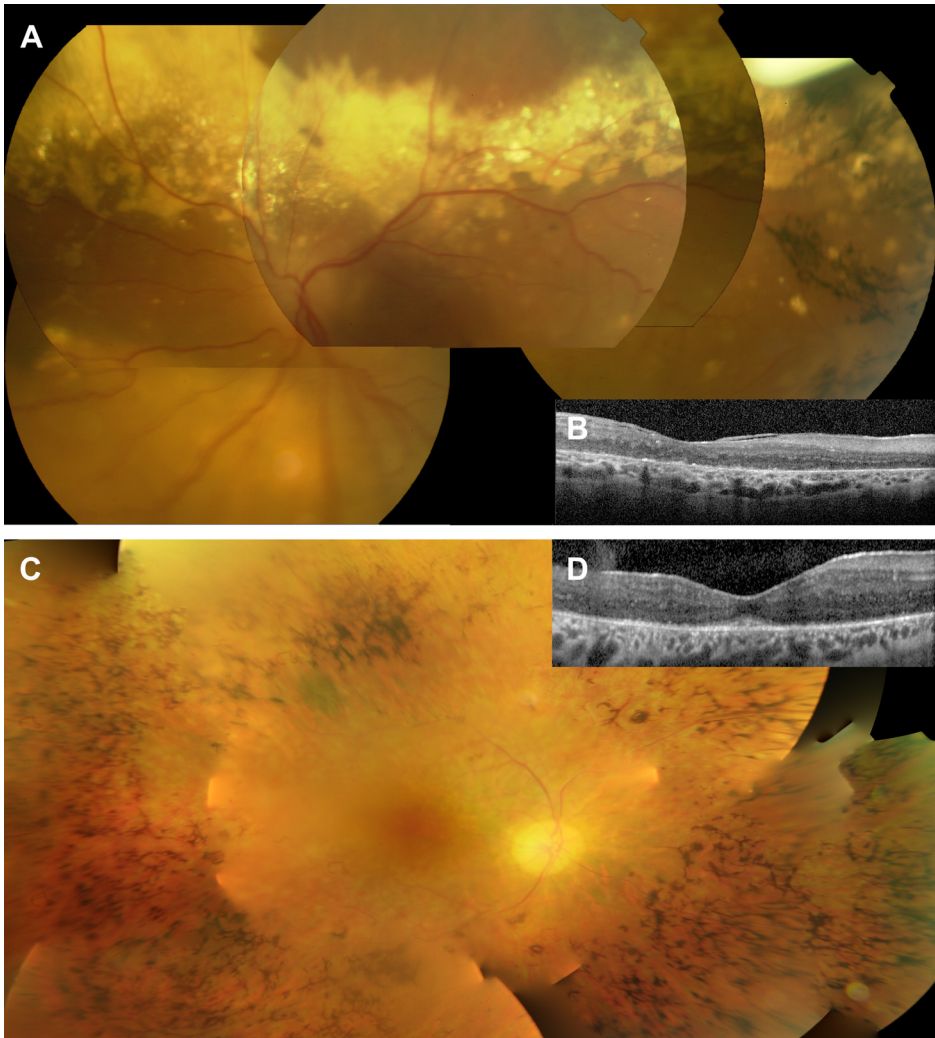


Figure 4.6 Atypical cases of dominant cystoid macular dystrophy (DCMD). (A-B) Coats-like exudative abnormalities in a 62-year-old DCMD patient (visual acuity (VA): light perception; spherical equivalent (SE) +4.25 diopters (D)). (A) Composite color fundus photograph showing a serous retinal detachment with exudates superior to the upper vascular arcade and temporal pigment accumulations mimicking bone spicules. This patient experienced vision loss at the age of 30 years, with cystoid fluid collections (CFCs) in the macula. (B) Horizontal optical coherence tomography (OCT) scan through the scanning plane indicated by the black arrowhead in A, showing retinal atrophy and a mild epiretinal membrane. (C-D) Retinitis pigmentosa-like phenotype in a 44-year-old patient with stage 3 DCMD (VA 20/63; SE +7.00 D), who also experienced night blindness and constriction of the peripheral visual fields. (C) Composite color fundus photograph, showing peripheral bone-spicule-like pigment changes, a waxy-pale optic disc, attenuated arterioles, and chorioretinal atrophy. Vision loss started at the age of 7 with fundoscopic foveal pigment changes and wrinkling of the internal limiting membrane. Because of loss of follow-up, no findings of CFCs are available, but in that period of time he experienced fluctuating vision loss. (D) OCT scan through the fovea (black arrowhead in C) showing retinal pigment epithelium atrophy in the macula with some structural sparing of the fovea.



The different stages of DCMD correlated significantly with age ($r=0.871$; $P < 0.001$), VA ($r=-0.562$; $P < 0.001$), EOG test results ($r=-0.404$; $P < 0.001$) and ERG findings ($r=-0.590$; $P < 0.001$) (**Table 4.1**). During progression of the disease, electrophysiological testing became more abnormal and constriction of the peripheral visual field developed in stage 2 and stage 3 DCMD. Of the 16 patients with stage 2 DCMD, 1 patient (6%) showed no abnormalities, 11 patients (69%) demonstrated small central absolute scotomata / sensitivity loss, and 4 (25%) patients showed sensitivity loss of the central retina with mild constriction of the peripheral visual field (40-50° nasal and 60-80° temporal for the II4e isopter). All stage 3 DCMD patients showed central absolute scotomata (15° for the V4e isopter) of which 5 patients (63%) additionally showed a moderate constricted peripheral visual field in Goldmann perimetry (25-45° nasal and 45-65° temporal for the III4e isopter and 0-25° nasal and 30-35° temporal for the I4e isopter) and 2 (25%) presented with nyctalopia. These were the 2 patients with the retinitis pigmentosa-like phenotype (**Figure 4.4C**).

In all DCMD stages, dark adaptation testing could be normal as well as abnormal, but abnormal test results were most often present in DCMD stage 3 (6/8; 75%). In stage 1 and 2 only 38% (3/8) and 33% (6/18), respectively, has an abnormal dark adaptation. From the 15 patients with abnormal dark adaptation, 8 underwent Goldmann perimetry, which revealed a constricted peripheral visual field in 3 patients (38%), who also had pigment lesions in their peripheral retina. Abnormalities of color vision testing were seen in all DCMD stages, ranging from anomaloscopic diminished red-sensitivity in stage 1 (35%), to an acquired blue-yellow defect in stage 2 (76%) and 3 (100%), with an additional red-green defect when fixation became eccentric in 10/13 stage 3 DCMD patients (77%).

Follow-up

Follow-up data were available for 71 patients, with a mean follow-up time of 17 years (range: 0.5-44 years). Fifteen patients (21%) progressed from stage 1 to stage 2 after a mean follow-up time of 17 years (range: 4-28 years) and 9 patients (13%) progressed from stage 2 to stage 3 after a mean time of 23 years (range: 10-35 years) (**Figure 4.7**). Additionally, a progression from stage 1, via stage 2, to stage 3 was observed in 3 patients (4%) after a mean time of 32 years (range: 29-34 years).

The degree of CFCs was observed to decrease progressively with advancing disease stages, while chorioretinal atrophy and pigmentary abnormalities concurrently became more pronounced. Visual acuity, EOG and full-field ERG data of patients who progressed from one stage of DCMD to the next stage are summarized in **Table 4.2**.

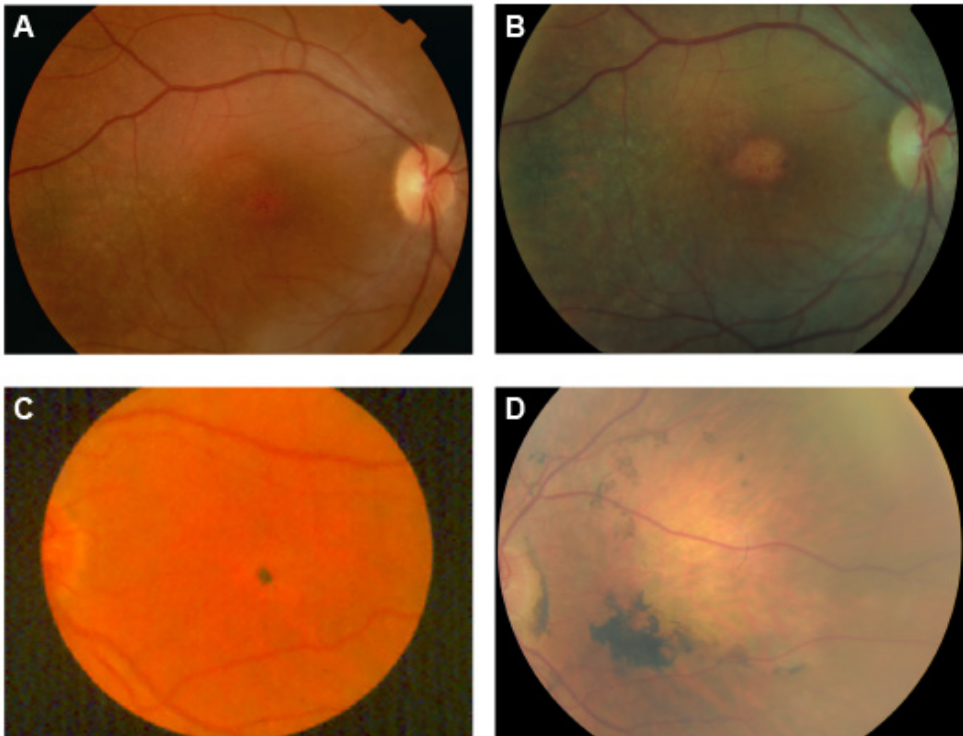


Figure 4.7 Long-term follow-up of dominant cystoid macular dystrophy (DCMD). (A-D) Follow-up images showing (A-B) progression during stage 2 DCMD and (C-D) progression to stage 3 DCMD. (A) Color fundus photograph of a 35-year-old patient with early stage 2 DCMD, (visual acuity (VA) 20/160; spherical equivalent (SE) +7.00 diopters (D)) showing pigmentary changes of the retinal pigment epithelium (RPE) and some small cystoid fluid collections (CFCs). At the age of 7 years, vision loss started and pigmentary changes and CFCs were seen. (B) Ten years later, a central atrophic lesion developed with absence of CFCs. (C-D) Follow-up color fundus photographs showing progression from stage 2 to stage 3 DCMD. (C) Color fundus photograph of a 38-year-old patient with stage 2 DCMD (VA 20/100; SE +5.50 D), showing mild atrophic hypopigmentation and a central spot of hyperpigmentation. (D) Thirty-five years later, a progression to profound chorioretinal atrophy with marked hyperpigmentations and some arteriolar attenuation was seen. The VA at this stage was 20/400.



Table 4.2 Follow-up results of patients who progressed to another stage of dominant cystoid macular dystrophy

Stage progression	Stage	VA Mean	EOG*			Full-field ERG †		
			Normal	Mildly reduced	Severely reduced	Normal	Subnormal	Abnormal
1 → 2	1	20/25	6/8	2/8	0/8	2/2	0/2	0/2
	2		2/8	5/8	1/8	2/2	0/2	0/2
2 → 3	2	20/63	0/9	6/9	3/9	2/5	2/5	1/5
	3	20/300	0/9	3/9	6/9	0/5	0/5	5/5

Abbreviations: EOG = electro-oculography; ERG = electroretinography

* EOG Arden ratios were stratified as normal (≥ 1.8), mildly reduced (< 1.8 , but ≥ 1.5), or severely reduced (< 1.5).

† Full-field ERG was defined as normal in case of normal amplitudes of the B-wave (photopic: > 78 mV, scotopic: > 263 mV), subnormal in case of moderately reduced amplitudes (photopic: ≥ 69 μ V and < 78 μ V, scotopic: ≥ 195 μ V and < 263 μ V) or as abnormal in case of severely reduced amplitudes (photopic: < 69 μ V, scotopic: < 19).

Treatment

During the natural course of DCMD stage 1 and 2, the degree of CFCs varied largely over time in 26 patients (mean follow-up: 18 years; range 4-43 years) (Figure 4.4A-E), but the fluid collections could also be influenced by treatment (Figure 4.4F-J). In an attempt to reduce the CFCs, 16 patients with stage 1 or 2 DCMD used acetazolamide, a carbonic anhydrase inhibitor, generally for several years (mean 40 months; range 2-221 months). In 10 of these patients (63%), oral administration of acetazolamide for several years (mean 56 months; range 2-221 months) seemed to result in a reduction of CFCs on OCT, with an improvement of the VA (mean VA from 20/46 to 20/35). In 2 patients (13%), the treatment resulted in reduction of CFCs without VA improvement. The daily dose in which a significant reduction of CFCs was seen on OCT ranged from 125 mg twice daily to 250 mg four times daily.

Octreotide-acetate, a somatostatin analogue assumed to promote the removal of intraretinal edema across the RPE,¹⁵ was used in 16 patients with stage 1 or 2 DCMD for several years (mean 68 months; range 6-151 months). In 12 patients (75%), octreotide-acetate administered 20 mg intramuscular monthly for several years (mean 84 months; range 14-151 months) seemed effective in reducing CFCs and improving the VA with a mean increase in VA of 20/125, but in two patients (13%) side effects like nausea, diarrhea, fatigue and cholelithiasis were present, resulting in cessation of this treatment in 1 patient. Four patients (25%) treated with octreotide-acetate stopped the treatment because of the lack of effect on VA. In 3 of them, no effect on CFCs was detectable on OCT.

During six years of follow-up, in three patients with stage 1 DCMD who were treated, the mean VA increased from 20/34 to 20/25, whereas in four patients with stage 1 DCMD who were not treated, the mean VA decreased from 20/29 to 20/35. In stage 2 DCMD patients, the mean VA decreased from 20/51 to 20/67 in 12 treated patients with a follow-up of 17 years and in 12 untreated patients, the mean VA decreased from 20/54 to 20/87 during 15 years of follow-up.

Haplotype Analysis

Linkage analysis previously showed that DCMD is linked to the interval D7S493 – D7S526 at 7p15-p21,⁶ but the disease-associated gene and mutation have not yet been identified. In 69 of the 97 clinically affected DCMD patients (71%), the haplotypes at the DCMD locus were analyzed, and all carried the disease-associated haplotype. The genetic DCMD locus seemed to be completely penetrant. Haplotype analysis in the 52 clinically unaffected family members revealed the absence of the DCMD haplotype in all. One DCMD patient with the genetic DCMD locus was also tested for the *BEST1* gene, but he showed no mutations in this gene.

DISCUSSION

Clinical characteristics and staging of dominant cystoid macular dystrophy

Dominant cystoid macular dystrophy is a unique retinal dystrophy, because the appearance of CFCs in the macula is the first and most prominent abnormality at the onset of the disease, resembling cystoid macular edema.¹⁶ The spectrum of severity of DCMD ranges from an absence of the foveal reflex with mild CFCs and some pigment changes in the macula early in the course of the disease, to profound chorioretinal atrophy in the posterior pole in the late stage of DCMD. In this study, we propose a clinical classification system for DCMD into three stages. This classification system is based on ophthalmoscopy and multimodal imaging, and correlates well with age, VA and results on EOG and full-field ERG (**Table 4.1**). We observed an evolution of DCMD through the proposed stages, supporting that DCMD is a progressive disease.

The age at onset of visual symptoms in DCMD is generally in childhood, but seems to vary depending on the generation. The apparently earlier age at onset in more recent generations may be due to an increased awareness and earlier screening of younger family members as a result of their affected father or mother.

All patients show a gradual decrease in VA, and most progress to visual disability at a relatively early age. In advanced DCMD, the VA generally evolves to finger counting (20/800), or even worse when relatively rare complications such as serous retinal detachment or acute angle-closure glaucoma occur. Due to the short axial length of the eye, glaucoma can accompany the retinal abnormalities, and (high) hyperopia is present in most DCMD patients, similar to other retinal dystrophies such as the bestrophinopathies which are caused by mutations in the *BEST1* gene.^{17, 18}

The finding that EOG abnormalities generally preceded photopic and scotopic dysfunction on full-field ERG indicates that impaired RPE function occurs earlier in the course of DCMD, whereas the panretinal photoreceptor function is affected later in the disease.¹ Because half of the stage 1 DCMD patients with macular CFCs had normal EOG results, primary panretinal RPE dysfunction with dysfunctional ionic homeostasis, as observed in *BEST1*-



related dystrophies such as Best vitelliform macular dystrophy and autosomal recessive bestrophinopathy,¹⁷ is presumably not present in DCMD. Presence of primary CFCs without reduced EOG might be explained by primary dysfunction of a cell population other than the RPE and photoreceptors, such as the Müller cells.

In addition to the large DCMD family described in the present study, two cases and one small family with features of DMCD have been described.^{7,9} The clinical findings of a Spanish patient with presumed DCMD are consistent with DCMD stage 2.⁹ In an American DCMD family from Greek ancestry,⁷ the EOG results in affected patients were normal, and none of the examined children of affected family members, 10 to 18 years of age, showed any abnormalities. This does not support an autosomal dominant mode of inheritance, and rather suggests a different disease than the typical DCMD phenotype observed in our large Dutch family.

Differential diagnosis

Several other retinal diseases with early-onset CFCs should be considered in the differential diagnosis of DCMD, such as X-linked juvenile retinoschisis, retinitis pigmentosa, phenotypes associated with mutations in the *BEST1* gene, and uveitis. In the absence of a genetic association with the DCMD locus in a patient with presumed DCMD, one should review the clinical evidence for DCMD carefully, and consider the possibility of one of the following clinical entities associated with early-onset CFCs.

X-linked juvenile retinoschisis, which is inherited in an X-linked pattern in contrast to DCMD, gives rise to vision loss in boys at a young age and progresses to atrophy and alterations of the RPE,¹⁹ like in DCMD. The ‘cystoid’ schisis cavities are mainly situated in the inner and outer nuclear layer,²⁰ like the CFCs in DCMD, but the schisis cavities in X-linked juvenile retinoschisis often become confluent, with only small strands of tissue bordering these spaces on OCT, and without apparent fluorescein leakage into the schisis spaces on FA, in contrast to the CFCs in DCMD.²¹ Also, a typical radial pattern is visible in the fovea on FAF and red-free images in X-linked juvenile retinoschisis cases, which is not observed in DCMD. The full-field ERG in X-linked juvenile retinoschisis characteristically shows an ‘electronegative’ aspect,¹⁹ in contrast to DCMD.

Like stage 3 DCMD, retinitis pigmentosa can present with hyperpigmentation in the (mid) peripheral fundus, and cystoid macular edema.²² However, compared to DCMD, patients with retinitis pigmentosa experience night blindness early in the course of the disease, and retinitis pigmentosa patients characteristically show early arteriolar attenuation and bone-spicule pigmentary changes, with a rod-cone dysfunction on full-field ERG that outweighs EOG abnormalities. In contrast to bone-spicule hyperpigmentation in retinitis pigmentosa, the hyperpigmented abnormalities in DCMD are typically more coarse and mainly located in the posterior pole.

Phenotypes associated with *BEST1* gene mutations – inherited either autosomal dominantly or recessively – can have somewhat similar retinal lesions and abnormalities,

like an abnormal EOG that outweighs full-field ERG abnormalities, hyperopia and CFCs in the macula.¹⁶⁻¹⁸ In contrast to DCMD, all patients with *BEST1*-related dystrophies have a severely abnormal EOG at onset, and *BEST1*-related fundus abnormalities usually include highly autofluorescent yellowish deposits in the macula.¹⁷

Posterior uveitis should also be considered, since DCMD can be accompanied by a variable degree of whitish punctate deposits (although these are not cells) in the vitreous body in stage 2 and 3 disease. Finally, the clinical characteristics of vascular causes of cystoid macular edema such as diabetic retinopathy, retinal venous occlusions, as well as age-related macular degeneration,²³ allow an easy distinction from DCMD.

Genetic Background

Dominant cystoid macular dystrophy is inherited autosomal dominantly, but the associated gene and mutation have not yet been identified.⁶ We show that the genetic defect in DCMD appears to be completely penetrant in the large family in this study. The *KLHL7* gene, causing autosomal dominant retinitis pigmentosa,²⁴ is located within the critical interval of the DCMD locus, which may explain why two DCMD patients in our study exhibited abnormalities and phenotypic characteristics of retinitis pigmentosa (**Figure 4.6C and D**). However, no coding variant in the coding region of the *KLHL7* gene was detected in our DCMD family. This, however, does not exclude the presence of a deep intronic mutation or a mutation affecting a regulatory element of the *KLHL7* gene. Alternatively, due to the distinct disease characteristics between the families described by Friedman et al and our DCMD family, it is plausible that another gene at the DCMD locus can be involved in the disease rather than *KLHL7*. Further analysis of all genes located within the DCMD locus at the genomic and at a transcriptional level using next-generation sequencing technologies may identify the causative mutation of DCMD in the near future. Identification of the associated gene can provide insight into the pathogenesis of the disease, and may improve our understanding on the development of hyperopia and cystoid fluid collections in other rare and common retinal diseases.

Pathophysiology and treatment

Cystoid fluid accumulation in the macula is the first clinically visible abnormality in DCMD. This indicates that the CFCs in DCMD are the direct result of the primary genetic defect and its immediate pathophysiological consequences. Interestingly, a histopathological study on 2 donor eyes of a 78-year-old American patient with presumed DCMD has been published.²⁵ Large intraretinal cystoid spaces were observed in the macula, with mildly attenuated retinal vessels, atrophy and marked disorganization of the inner nuclear layer. The large cyst-like spaces within the inner nuclear layer were surrounded by Müller cell fibers and pigment-laden cells with remnants of photoreceptor segments, and degeneration of Müller cells was seen. Based on these findings, the authors suggested a primary pathologic process affecting Müller cells in DCMD.²⁵ These histopathological findings correlate well with the



clinical findings in our DCMD cohort, which could support primary Müller cell dysfunction in DCMD.⁸ If this is the case, DCMD would be a rare example of retinal dystrophy that results from a genetic defect that primarily affects Müller cell function. The gene defect in DCMD might interfere with capillary permeability, resulting in a disturbance of the inner blood-retinal barrier and early CFCs.

It is also possible that CFCs in DCMD are the result of primary dysfunction of the RPE, as the EOG becomes abnormal early in the course of the disease. It is unlikely that the photoreceptors are primarily affected, at least on the panretinal level, as the full-field ERG remains normal for a long time. Cystoid macular edema in the outer neuroretinal layers, such as in the course of retinitis pigmentosa, is presumed to be caused by a dysfunction of the outer blood-retina barrier.²⁶⁻²⁸ In DCMD, CFCs located in the outer nuclear layer are possibly induced by dysfunction of the RPE layer, comparable to cystoid macular edema that occurs in retinitis pigmentosa.²⁹

Cystoid macular edema in the inner neuroretinal layers, such as in pseudophakic macular edema and diabetic retinopathy, is predominantly caused by a failure of the inner blood-retinal barrier.^{27,30} The CFCs located in the inner nuclear layer in DCMD could also be caused by a dysfunctional macular inner blood-retinal-barrier, which depends on Müller cells, astrocytes, and pericytes.²⁷ This could be supported by the fundoscopic and fluorescein angiographic finding of perifoveal capillary dilation early in the course of the disease.

We suggest that the Müller cells, the RPE, or both, may be the primarily affected cells in DCMD, resulting in CFCs early in the course of the disease.

Previous studies in patients with retinal dystrophies showed that treatment with acetazolamide reduced intraretinal fluid collections,^{18, 22, 31-34} although the effect can be dose-dependent,¹⁸ but the exact mechanism is unclear. Boon et al. suggested that acetazolamide may interact with carbonic anhydrase subtypes XIV and II in the RPE and Müller cells, resulting in intracellular acidification with consequently Cl⁻ transport in the RPE, with water following passively.¹⁸ Treatment with acetazolamide has previously been shown to be ineffective in treating CFCs in most DCMD patients at a daily dose of 250 mg,³⁵ but we now demonstrate that the effect can be dose dependent in DCMD, as treatment with higher doses can indeed be effective in DCMD patients. A possible rebound effect that has been postulated in half of the retinitis pigmentosa patients with cystoid macular edema treated with acetazolamide for 8 to 12 weeks,³¹ was present in only 2 of the 16 DCMD patients after 1.5 and 6 years of treatment with acetazolamide. Treatment seems to be most effective in DCMD patients with stage 1 and has a less strong influence on the long term VA in stage 2 DCMD patients.

In conclusion, we describe the clinical spectrum, which can be subdivided into three clinical stages, in the largest DCMD cohort to date. CFCs are a hallmark feature in earlier disease, but during progression the CFCs diminish and chorioretinal atrophy develops. Haplotype analysis using microsatellite markers at the DCMD locus at 7p15.3 confirmed the diagnosis,

and the disease was fully penetrant in our DCMD cohort. Future studies will be directed towards determining the causative gene by next-generation sequencing at a genomic and transcriptional level. The elucidation of the causative gene and pathogenesis in DCMD will not only give important insight into this intriguing and peculiar retinal dystrophy, but the findings can also shed a light on the pathogenesis of hyperopia and cystoid macular edema in other retinal dystrophies, uveitis, diabetic macular edema or following ophthalmic surgery, and provide a new target for treatment.



REFERENCES

1. Deutman AF, Pinckers AJ, Aan de Kerk AL. Dominantly inherited cystoid macular edema. *Am J Ophthalmol* 1976;82:540-548.
2. Notting JG, Pinckers JL. Dominant cystoid macular dystrophy. *Am J Ophthalmol* 1977;83(2):234-41.
3. Pinckers A, Notting JG, Lion F. [Dominant cystoid macular dystrophy (author's transl)]. *J Fr Ophthalmol* 1978;1:107-110.
4. Pinckers A, Deutman AF, Lion F, Aan de Kerk AL. Dominant cystoid macular dystrophy (DCMD). *Ophthalmic Paediatr Genetics* 1983;3:11.
5. Pinckers A, Deutman AF, Notting JG. Retinal functions in dominant cystoid macular dystrophy (DCMD). *Acta Ophthalmol (Copenh)* 1976;54:579-590.
6. Kremer H, Pinckers A, van den Helm B, et al. Localization of the gene for dominant cystoid macular dystrophy on chromosome 7p. *Hum Mol Genet* 1994;3:299-302.
7. Fishman GA, Goldberg MF, Trautmann JC. Dominantly inherited cystoid macular edema. *Ann Ophthalmol* 1979;11:21-27.
8. Schadlu R, Shah GK, Prasad AG. Optical coherence tomography findings in autosomal dominant macular dystrophy. *Ophthalmic Surg Lasers Imaging* 2008;39:69-72.
9. Mendivil A. Bilateral cystoid macular edema in a 21-year-old woman. *Surv Ophthalmol* 1996;40(5):407-12.
10. Boon CJ, Klevering BJ, Cremers FP, et al. Central areolar choroidal dystrophy. *Ophthalmology* 2009;116:771-82.
11. Brown M, Marmor M, Vaegan, et al. ISCEV Standard for Clinical Electro-oculography (EOG) 2006. *Doc Ophthalmol* 2006;113:205-212.
12. Marmor MF, Holder GE, Seeliger MW, et al. Standard for clinical electroretinography (2004 update). *Doc Ophthalmol* 2004;108:107-114.
13. Marmor MF, Fulton AB, Holder GE, et al. ISCEV Standard for full-field clinical electroretinography (2008 update). *Doc Ophthalmol* 2009;118:69-77.
14. Miller SA, Dykes DD, Polesky HF. A simple salting out procedure for extracting DNA from human nucleated cells. *Nucleic Acids Res* 1988;16:1215.
15. Hogewind BF, Pieters G, Hoyng CB. Octreotide acetate in dominant cystoid macular dystrophy. *Eur J Ophthalmol* 2008;18:99-103.
16. Saksens NT, Fleckenstein M, Schmitz-Valckenberg S, et al. Macular dystrophies mimicking age-related macular degeneration. *Prog Retin Eye Res* 2014;39:23-57.
17. Boon CJ, Klevering BJ, Leroy BP, et al. The spectrum of ocular phenotypes caused by mutations in the *BEST1* gene. *Prog Retin Eye Res* 2009;28:187-205.
18. Boon CJ, van den Born LI, Visser L, et al. Autosomal recessive bestrophinopathy: differential diagnosis and treatment options. *Ophthalmology* 2013;120:809-820.
19. Sieving PA, Bingham EL, Kemp J, et al. Juvenile X-linked retinoschisis from *XLRS1* Arg213Trp mutation with preservation of the electroretinogram scotopic b-wave. *Am J Ophthalmol* 1999;128:179-184.
20. Gregori NZ, Lam BL, Gregori G, et al. Wide-field spectral-domain optical coherence tomography in patients and carriers of X-linked retinoschisis. *Ophthalmology* 2013;120:169-174.
21. Ganesh A, Stroh E, Manayath GJ, et al. Macular cysts in retinal dystrophy. *Curr Opin Ophthalmol* 2011;22:332-339.
22. Thobani A, Fishman GA. The use of carbonic anhydrase inhibitors in the retreatment of cystic macular lesions in retinitis pigmentosa and X-linked retinoschisis. *Retina* 2011;31:312-315.

23. Jittpoonkuson T, Garcia PM, Rosen RB. Correlation between fluorescein angiography and spectral-domain optical coherence tomography in the diagnosis of cystoid macular edema. *Br J Ophthalmol* 2010;94:1197-1200.
24. Friedman JS, Ray JW, Waseem N, et al. Mutations in a BTB-Kelch protein, *KLHL7*, cause autosomal-dominant retinitis pigmentosa. *Am J Hum Genet* 2009;84:792-800.
25. Loeffler KU, Li ZL, Fishman GA, Tso MO. Dominantly inherited cystoid macular edema. A histopathologic study. *Ophthalmology* 1992;99:1385-1392.
26. Bringmann A, Reichenbach A, Wiedemann P. Pathomechanisms of cystoid macular edema. *Ophthalmic Res* 2004;36:241-249.
27. Kaur C, Foulds WS, Ling EA. Blood-retinal barrier in hypoxic ischaemic conditions: basic concepts, clinical features and management. *Prog Retin Eye Res* 2008;27:622-647.
28. Newsome DA. Retinal fluorescein leakage in retinitis pigmentosa. *Am J Ophthalmol* 1986;101:354-360.
29. Scorolli L, Morara M, Meduri A, et al. Treatment of cystoid macular edema in retinitis pigmentosa with intravitreal triamcinolone. *Arch Ophthalmol* 2007;125:759-764.
30. Yannuzzi LA. A perspective on the treatment of aphakic cystoid macular edema. *Surv Ophthalmol* 1984;28 Suppl:540-53.
31. Grover S, Apushkin MA, Fishman GA. Topical dorzolamide for the treatment of cystoid macular edema in patients with retinitis pigmentosa. *Am J Ophthalmol* 2006;141:850-858.
32. Genead MA, McAnany JJ, Fishman GA. Topical dorzolamide for treatment of cystoid macular edema in patients with choroideremia. *Retina* 2012;32:826-833.
33. Ghajarnia M, Gorin MB. Acetazolamide in the treatment of X-linked retinoschisis maculopathy. *Arch Ophthalmol* 2007;125:571-573.
34. Hori K, Ishida S, Inoue M, et al. Treatment of cystoid macular edema with oral acetazolamide in a patient with best vitelliform macular dystrophy. *Retina* 2004;24:481-482.
35. Pinckers A, Cruysberg JR, Kremer H, Aandekerck AL. Acetazolamide in dominant cystoid macular dystrophy. A pilot study. *Ophthalmic Paediatr Genet* 1993;14:95-99.



Chapter 5

Butterfly-shaped pigment dystrophy

Mutations in α -catenin 1 cause Butterfly-shaped pigment dystrophy and perturbed retinal pigment epithelium integrity

N.T.M. Saksens, M.P. Krebs, F.E. Schoenmaker-Koller, W. Hicks, M. Yu, L. Shi,
L. Rowe, S.J. Letteboer, K. Neveling, T.W. van Moorsel, S. Abu-Ltaif, E. de Baere,
S. Walraedt, S. Banfi, F. Simonelli, F.P.M. Cremers, C.J.F. Boon, R. Roepman, B.P. Leroy,
N.S. Peachey, C.B. Hoyng, P.M. Nishina, A.I. den Hollander**

Nature Genetics; accepted.



Butterfly-shaped pigment dystrophy is a macular disease, which in the advanced stage bears similarity to age-related macular degeneration. Here, we report the identification of heterozygous missense mutations in the α -catenin 1 (*CTNNA1*) gene in three families with butterfly-shaped pigment dystrophy. In addition, we identified a *Ctnna1* missense mutation in a chemically-induced mouse mutant, *tvrn5*. Parallel clinical phenotypes were observed in the retinal pigment epithelium (RPE) of individuals with butterfly-shaped pigment dystrophy and in *tvrn5* mice, including pigmentary abnormalities, focal thickening and elevated lesions, and decreased light-activated responses. Morphological studies in *tvrn5* mice revealed increased cell shedding and large multinucleated RPE cells, suggesting defects in intercellular adhesion and cytokinesis. This study identifies *CTNNA1* gene variants as a cause of macular dystrophy, suggests that α -catenin 1 is involved in maintaining RPE integrity, and suggests that other components that participate in intercellular adhesion may be implicated in macular disease.

INTRODUCTION

Butterfly-shaped pigment dystrophy (MIM 608970) belongs to a group of autosomal dominant pattern dystrophies of the retinal pigment epithelium (RPE), and was first described in a large Dutch family (Family A, **Figure 5.1A**) by Deutman et al. in 1970.¹⁻³ The disease is characterized by bilateral accumulation of pigmented and/or yellowish/gray material at the level of the RPE in the macula, which can resemble the wings of a butterfly.³ Affected individuals present from middle age with either normal or slightly diminished best-corrected visual acuity (BCVA) and color vision, and the activity of the RPE measured by electrooculogram (EOG) recordings may be abnormal.⁴⁻⁶ Responses of the retina, recorded by full-field electroretinogram (ERG), and dark adaptation are generally normal.^{4,7,8} The disease is relatively benign, but it can progress to a form resembling age-related macular degeneration (AMD), with chorioretinal atrophy in the (para)foveal and peripapillary regions^{4,6,8} and to subretinal neovascularization,⁹ both resulting in severe vision loss.

Mutations in the *PRPH2* gene (also known as peripherin 2 or *RDS*, MIM 179605) have been identified in individuals with butterfly-shaped pigment dystrophy,^{1,4,7,10-15} but in the majority of individuals the genetic cause is unknown. Genetic heterogeneity for butterfly-shaped pigment dystrophy has been demonstrated through the analysis of a large Dutch family with butterfly-shaped pigment dystrophy (Family A, **Figure 5.1A**), in which the involvement of the *PRPH2* gene as well as several other retinal disease genes were excluded⁸. Subsequently, a genome-wide linkage scan identified a novel disease locus for butterfly-shaped pigment dystrophy in this family, located on chromosome 5q21.2-q33.2.¹⁶

Here we report the identification of mutations in the α -catenin 1 (*CTNNA1*) gene (MIM 116805) in the large Dutch family (Family A, **Figure 5.1A**) and in additional *PRPH2*-negative cases with butterfly-shaped pigment dystrophy. In addition, we describe a *Ctnna1* mutation in a chemically-induced mouse mutant, *tvrms*, and characterize the pathologic events leading to RPE dysmorphology in this model.

METHODS

Clinical Evaluations of Human Subjects

Fourteen affected and twelve unaffected individuals from three BSMD families were included in this study. Participants received the diagnosis of BSMD based on the aspect of the lesions on ophthalmoscopy sometimes combined with fluorescein angiography (FA). The medical histories, age at onset, (best-corrected) Snellen visual acuity (BCVA) and fundus appearance, including slit-lamp examination, fundus examination by indirect ophthalmoscopy and fundus photography were retrieved from medical records of all included subjects. Additionally, FA was available in 11 affected subjects, fundus autofluorescence and near-infra red images were obtained in 6 and spectral-domain optical coherence



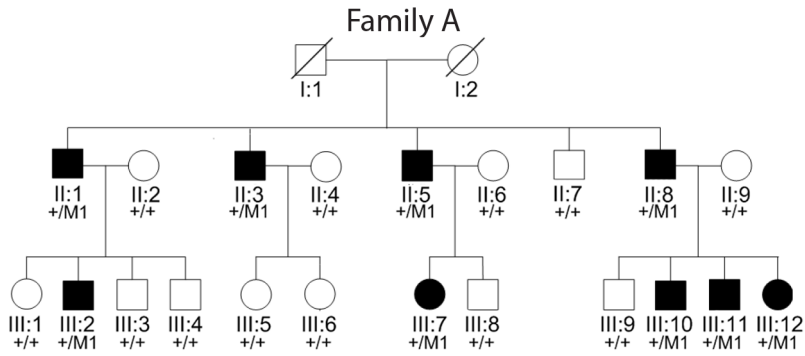
tomography (OCT) in 4 affected participants. Eleven affected subjects underwent electro-oculography (EOG) and electroretinography (ERG) and color vision testing were available in 6 and 7 affected subjects, respectively. ERG and EOG were recorded and interpreted as previously described.⁴⁹ In 6 patients, EOG was performed according to the International Society for Clinical Electrophysiology of Vision (ISCEV) protocol. The study was approved by the local medical ethics committees (Commissie Mensgebonden Onderzoek regio Arnhem-Nijmegen, Ethics Committee of Ghent University Hospital, and Ethical Committee of the Second University of Naples) and adhered to the tenets of the Declaration of Helsinki. All participants provided written informed consent prior to participation in the study.

Whole Exome Sequencing and Mutation Analysis in Human Subjects

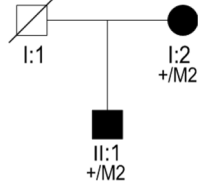
To identify the genetic defect in a large Dutch family with nine individuals affected by butterfly-shaped pigment dystrophy (family A; **Figure 5.1A**), the DNA of two affected individuals (A-III:7 and A-III:11) was analyzed using whole exome sequencing. The exomes were enriched using Agilent's SureSelect Human All Exon v.2 Kit (50Mb), which targets the exonic sequences of approximately 21.000 genes, according to the manufacturer's protocol (Agilent, Santa Clara, CA, USA). Sequencing was performed on a 5500xl SOLiD sequencing platform (Life Technologies, Carlsbad, CA, USA). BioScope software v.1.3 (Life Technologies, Carlsbad, CA, USA) was used to map color space reads along the hg19 reference genome assembly. The high-stringency calling DiBayes algorithm was used for single-nucleotide variant calling, and small insertions and deletions were detected using the small Indel Tool.

All coding exons and intron-exon boundaries of the *CTNNA1* gene were screened for mutations in 93 unrelated probands with butterfly-shaped pigment dystrophy (N=19) or other pattern dystrophies (N=74) by Sanger sequencing. Primers for PCR amplification and sequencing were designed with Primer3 software (**Table 5.1**). Missense variants detected in the *CTNNA1* gene were analyzed in ethnically matched control individuals by restriction enzyme analysis (*TaqI* for c.953T>C; p.[Leu318Ser] and *BclI* for c.1293T>G; p.[Ile431Met]), allele-specific PCR (for c.919G>A; p.[Glu307Lys]), or Sanger sequencing (for c.160C>T; p.[Arg54Cys]).

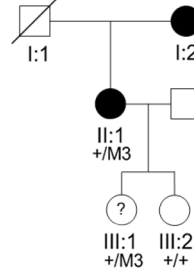
A



Family B



Family C



B

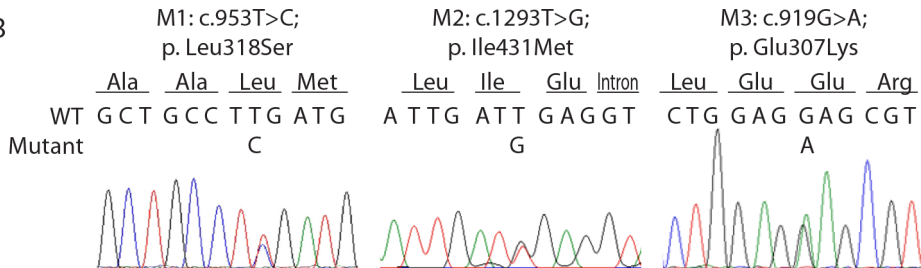


Figure 5.1 CTNNA1 mutations in three families with butterfly-shaped pigment dystrophy. (A) Two affected individuals (A-III:7 and A-III:11) of family A were analyzed by whole exome sequencing and the c.953T>C; p.(Leu318Ser) variant in the CTNNA1 gene segregated in all family members. Two additional variants in the CTNNA1 gene were identified in family B and C with complete segregation in both families. (B) The heterozygous mutation c.953T>C; p.[Leu318Ser] (M1) was found in the large Dutch family A, and mutations c.1293T>G; p.[Ile431Met] (M2) and c.919G>A; p.[Glu307Lys] (M3) were found heterozygously in Dutch family B and Belgian family C, respectively.

Table 5.1 Primer sequences for amplification of coding exons and splice junctions of *CTNNA1*

<i>CTNNA1</i> exon	Forward primer sequence	Reverse primer sequence	Product size (bp)
Exon 2	CCTGATGCAAAAGTCCCAA	CCTTGCTCTTATGGTTGTACCC	277
Exon 3	CATTAAGAAAGCTGAATTATTTTGG	AAGGCCTGCCTCTCTTACC	433
Exon 4	TGAGTTCATTCTTGCTGAGTTTG	GAACTAAGGAAGGCCAGTAGCA	279
Exon 5	GCGCAAAGCTCGAGAGCTAAG	TGGAAGTATATTGGCGAAGG	368
Exon 6	CTTTTCAGCATTACCAGCAA	TGAGCTATCATCAGAAGCCTTG	453
Exon 7	CAGTAGGCCATCTTCTGTGG	CGGACAGCATTACACTCTGC	334
Exon 8	TCAGTGTGACATGAGCACAA	GCACTTCTTGTGAAAATCCATC	298
Exon 9	TGAGGGGTCCTCATGTAAGTG	TGTTAAGCGAGCCCTTACAAAT	392
Exon 10	CAGAATGGTCAGAGGTAGGG	CCCAAGACTTCCATCTAAAATCC	300
Exon 11	GCATGTGGTGTGATGTCTCC	CATAGCAGTGTGGCCATT	335
Exon 12	TTCTTGGGGGTGATAACAGG	CTCCTCCTCCTCACCACAG	486
Exon 13	CCCTTCACACAGGTAGAAGCA	AGAATGACGCATTGCTCAAG	358
Exon 14	AACACTGCACATTAATCCAGAA	TGAAACAAGAAAGGGGACA	300
Exon 15-16	CTTCAGGCGAAATGAAACCT	GCCCATGAAACTTACCCTGA	688
Exon 17	GAGGAAGCATGTGAGTGCCA	CCATCTCCAGGCTCAAGTA	595
Exon 18	GTCAGGCCGGTGCTTCTTAC	CTGGTTCAGTCTGCCATT	456

Mouse Maintenance and Mutagenesis

All procedures used in animal experiments for this study were approved by the Institutional Animal Care and Use Committees of the institutions involved and were in accordance with the ‘Guide for the Care and Use of Experimental Animals’ established by the National Institutes of Health (1996, Revised 2011) and the Association for Research in Vision and Ophthalmology Statement for the Use of Animals in Ophthalmic and Vision Research. Mice were bred and maintained on a 12 hour light-dark cycle in the Research Animal Facility vivarium of The Jackson Laboratory (JAX). Pasteurized JL Mouse and Rat Auto 4F/No Hysil 5K54 diet (fat content, 4%, PMI Nutrition International, Brentwood, MO) and HCl-acidified water (pH 2.8-3.2) were provided *ad libitum*.

The *tvrm5* mutant (The Jackson Laboratory Stock# 021610) was identified among G3 mice from an ethylnitrosourea mutagenesis screen of C57BL/6J (B6J; JAX stock number 000664) mice generated by the Center for New Mouse Models of Heart, Lung, Blood and Sleep Disorders at JAX.⁵⁰ Phenotypic screening of these mice by indirect ophthalmoscopy at ~21 weeks of age was performed by the Translational Vision Research Models (TVRM) program.⁵¹ Once heritability was established, the *tvrm5* strain was backcrossed to B6J for seven generations and thereafter maintained in a homozygous state by intercrossing. B6J mice were also used as wild-type controls and in segregating crosses to generate heterozygous animals from the homozygous inbred mutant stock.

tvrm5 Mapping and Sequence Analysis

To identify the causative locus, a mutant *tvrm5* male was outcrossed with a DBA/2J (+/+) female, the resulting F1 progeny were intercrossed, and 31 F2 generation mice were analyzed for linkage using a pool scan with genome-wide simple sequence length polymorphic (SSLP) markers. The map location was confirmed by testing individual F2 mice that made up the pool and additional SSLP markers were used to refine the map position. For whole exome sequencing, genomic DNA (1 µg) was fragmented to a peak size of 300 bp by sonicating for 30 s power on, 30 s power off on low power for a total of 10 min using a Diagenode Bioruptor UCD-200TM-EX (Denville, NJ, USA). The pre-capture paired end library was constructed using the Illumina (Illumina, San Diego, CA, USA) TruSeq DNA Sample Preparation Kit (part number FC-121-100) with no size selection step and 18 cycles of PCR. The pre-capture library was hybridized to the Roche NimbleGen Mouse Exome (Reference #9999042611) capture probe set (Roche NimbleGen, Madison, WI, USA) according to the manufacturer's instructions. The sequencing library was quantified by QPCR, pooled with two similar libraries, and sequenced on a single lane of an Illumina HiSeq 2000 (Illumina, San Diego, CA, USA) using a 2x100 bases (paired end) sequencing protocol. Genotypes were confirmed by sequencing the PCR product obtained with the primers *Ctnna1F* (5'-TTAGAGCTCTCGAAGCCTGTG) and *Ctnna1R* (5'-GAAAGAAGGAAGGGAAAGCAA) amplified as follows: 97°C, 3 min; 45 cycles of 95°C, 10 s and 50°C, 30 s; 72°C, 30 s; 72°C, 3 min.

Live Imaging and Histology of Mouse Eyes

Fundus images of live mice were obtained with a Micron III Retinal Imaging System (Phoenix Research Laboratories, Pleasanton, CA) and an R2200 ultrahigh resolution spectral domain optical coherence tomography (OCT) system (Bioptigen, Raleigh, NC). Image acquisition and processing were performed as described previously.⁵² For conventional histology, animals were first asphyxiated with carbon dioxide. Eyes were enucleated and treated with a 3:1:4 mixture of methanol:acetic acid:phosphate-buffered saline with subsequent paraffin embedding and staining with hematoxylin and eosin as described.⁵³ Brightfield images were acquired using a DMLB light microscope (Leica Microsystems, Buffalo Grove, IL). For flatmounts, enucleated eyes were placed in 4% w/v paraformaldehyde in 0.75x phosphate-buffered saline, dissected to recover the retina and RPE/choroid/sclera complex, and stained with DAPI and rhodamine phalloidin as described,⁵² except that the RPE was examined instead of the retina. Confocal image stacks were obtained with a 63x objective on an SP5 confocal microscope (Leica). Conventional fluorescence images were obtained with a 10x objective on an Axio Observer Z.1 (Carl Zeiss Microscopy, Peabody, MA). Confocal images were processed in Fiji⁵⁴ by dividing the blue by the green channel after denoising to reduce the contribution of autofluorescence to the DAPI signal, and images were oriented with the Interactive Stack Rotation plugin. A subset of the image stacks was maximally projected to visualize the F-actin circumferential boundary with minimal overlap from apical F-actin.



Conventional fluorescence images were oriented with the Interactive Stack Rotation plugin, and contrast and brightness were adjusted in Fiji.

Mouse Visual Electretinography

Mice were studied using ERG stimulation and recording protocols designed to evaluate outer retinal or RPE function. Each experimental session was conducted following overnight dark adaptation. Mice were anesthetized with ketamine (80 mg/kg) and xylazine (16 mg/kg), and placed on a temperature-regulated heating pad throughout the testing sessions. Pupils were dilated with eye drops (2.5% phenylephrine HCl, 1% cyclopentolate, 1% tropicamide). The corneal surface was anesthetized with 1% proparacaine HCl.

The functional response of the outer retina was examined using a conventional strobe-flash ERG protocol.⁷ ERGs were recorded using a stainless-steel wire active electrode referenced to a needle electrode placed in the cheek. A second needle electrode placed in the tail served as ground lead. Responses were differentially amplified (0.3–1.500 Hz), averaged, and stored using a UTAS E-3000 signal averaging system (LKC Technologies, Gaithersburg, MD). White light strobe flashes were initially presented in darkness within a Ganzfeld bowl. Stimuli were presented in increasing order, from $-3.6 \log \text{ cd s/m}^2$ up to $2.1 \log \text{ cd s/m}^2$. Cone ERGs were isolated by superimposing stimuli (-0.8 to $1.9 \log \text{ cd s/m}^2$) upon a steady adapting field (20 cd/m^2). The amplitude of the a-wave was measured 8 ms after flash onset from the prestimulus baseline. The amplitude of the b-wave was measured from the a-wave trough to the peak of the b-wave or, if no a-wave was present, from the prestimulus baseline.

ERG components generated by the RPE were examined using a dc-ERG protocol.⁵⁵ Responses were obtained from the corneal surface of the left eye using a capillary tube with filament (BF100-50-10; Sutter Instrument, Novato, CA) that was filled with Hank's buffered salt solution to make contact with an Ag/Ag Cl wire electrode. A similar electrode placed in contact with the right eye served as the reference. Responses were differentially amplified (dc-100 Hz), digitized at 20 Hz, and stored using LabScribe Data Recording Software (iWorx; Dover, NH). White light stimuli were derived from an optical channel using a Leica microscope illuminator as the light source and delivered to the test eye with a 1-cm-diameter fiber-optic bundle. The stimulus luminance was $2.4 \log \text{ cd/m}^2$. Stimulus timing and duration was controlled at 7 min by a Uniblitz shutter system (Rochester, NY). The amplitude of the c-wave was measured from the prestimulus baseline to the peak of the c-wave. The amplitude of the fast oscillation (FO) was measured from the c-wave peak to the trough of the FO. The amplitude of the light peak (LP) was measured from the FO trough to the asymptotic value. The off-response amplitude was measured from the LP value just prior to stimulus light offset to the peak of the initial component.

Statistical Analysis

Response functions obtained for a- and b-wave amplitudes were compared across genotypes using a two-way repeated measures ANOVA. The amplitudes of dc-ERG components obtained under a standard stimulus condition were compared using Student's t-test.

Co-immunoprecipitations

Co-immunoprecipitation analyses were performed to test the interaction of wild-type and mutant α -catenin 1 (CTNNA1) with vinculin (VCL [MIM 193065]). Expression constructs to produce 3xHA-CTNNA1 (wild-type and variants c.160C>T; p.[Arg54Cys], c.919G>A; p.[Glu307Lys], c.953T>C; p.[Leu318Ser], c.1293T>G; p.[Ile431Met], and c.1307T>C; p.[Leu436Pro]) and 3xFLAG-VCL proteins were co-transfected in human embryonic kidney 293T (HEK293T) cells. As a negative control, production of the functionally unrelated p63 protein (MIM 603273) was used. As positive controls, the previously described interactions between nephrocystin-4 (MIM 607215) and RPGRIP1 (MIM 605446) were used in this assay.⁵⁶ Following transfection, cells were cultured for 24 hr and subsequently lysed on ice in lysis buffer (50 mM Tris-HCl [pH 7.5], 150 mM NaCl, and 0.5% Triton X-100) supplemented with complete protease inhibitor cocktail (Roche). Lysates were incubated with anti-FLAG M2 agarose from mouse (Sigma-Aldrich) for 2 hr at 4°C. After incubation, beads with bound protein complexes were washed in lysis buffer and subsequently taken up in 4x NuPAGE Sample Buffer and heated for 10 min at 70°C. Beads were precipitated by centrifugation, and supernatant was run on a NuPAGE Novex 4%–12% Bis-Tris SDS-PAGE gel. The interaction between 3xHA-CTNNA1 and 3xFLAG-VCL was assessed by immunoblotting, followed by staining with either polyclonal rabbit anti-HA (1:1.000; Sigma-Aldrich) or monoclonal mouse anti-FLAG (1:1.000; Sigma-Aldrich) as a primary antibody, and goat anti-rabbit IRDye800 (1:20.000; Li-Cor) or goat anti-mouse Alexa Fluor 680 (1:20.000; Molecular Probes) as a secondary antibody. Fluorescence was analyzed on a Li-Cor Odyssey 2.1 infrared scanner.

RESULTS

Identification of *CTNNA1* mutations in families with butterfly-shaped pigment dystrophy

Whole exome sequencing in two affected individuals of family A (**Figure 5.1A**) uncovered 38.153 variants for individual A-III:7 and 40.212 variants for individual A-III:11, of which 23.783 variants were shared by both individuals. Shared variants located within the linkage interval on 5q21.2-q33.2 (between markers D5S433 and D5S487),¹⁶ were filtered for heterozygous (present on $\geq 20\%$ and $\leq 80\%$ variant reads), non-synonymous variants, with a frequency of less than 0.5% in the Exome Variant Server (EVS) database, and a PhyloP score > 2.7 . Only one potential causative variant was identified, residing in the *CTNNA1* gene (c.953T>C; p.[Leu318Ser]; PhyloP score 5.1). Sanger sequencing confirmed the presence of a heterozygous c.953T>C; p.(Leu318Ser) allele in the *CTNNA1* gene [MIM 116805] in



affected relatives but absent in all unaffected family members. The variant was predicted disease-causing by SIFT, affects a residue that is completely conserved among vertebrate species (**Figure 5.2**), and was not found in 162 ethnically matched controls nor in the EVS database.



Figure 5.2 Protein sequence alignment of α -catenin 1 orthologs. The amino acids affected by the mutations identified in three families with butterfly-shaped pigment dystrophy (p.[Glu307Lys], p.[Leu318Ser], p.[Ile431Met]) and in the tvrm5 mouse (p.[Leu436Pro]) are completely conserved among vertebrates. Accession numbers: Homo sapiens α -catenin 1 NP_001894, Macaca mulatta α -catenin 1 NP_001244297, Mus musculus α -catenin 1 NP_033948, Rattus norvegicus α -catenin 1 NP_001007146, Bos taurus α -catenin 1 NP_001030443, Gallus gallus α -catenin 1 XP_414513, Danio rerio α -catenin 1 NP_571531.

Sequencing of all 17 coding exons of the CTNNA1 gene in 93 unrelated probands with butterfly-shaped pigment dystrophy and other pattern dystrophies identified three additional rare missense variants in the CTNNA1 gene (**Table 5.2**).

Table 5.2 Variants identified in the *CTNNA1* gene in 93 individuals with pattern dystrophies

Location	Nucleotide change	Amino acid change	Number of cases	Allele frequency in EVS	PhyloP	Grantham	Polyphen	SIFT
Exon 3	<u>c.160C>I</u>	p.(Arg54Cys)	1	0	6.1	180	0.995 (probably damaging)	Deleterious (0.0)
Exon 3	<u>c.240G>C</u>	p.(=)	1	0	-	-	-	-
Intron 5	<u>c.589-5T>C</u>	p.(?)	2	0.326 rs1059014 rs186236399	-	-	-	-
Exon 7	<u>c.c.919G>A</u>	p.(Glu307Lys)	1	0	6.0	56	0.879 (possibly damaging)	Deleterious (0.0)
Exon 9	<u>c.1293T>G</u>	p.(Ile431Met)	1	0	0.6	10	0.948 (possibly damaging)	Deleterious (0.0)
Intron 13	<u>c.1900-84G>A</u>	p.(?)	2	0	-	-	-	-
Exon 17	<u>c.2409C>I</u>	p.(=)	1	0.012 rs367913042	-	-	-	-
Intron 17	<u>c.2433+11G>T</u>	p.(?)	1	0	-	-	-	-

EVS = Exome Variant Server database

Heterozygous variants c.1293T>G; p.(Ile431Met) and c.919G>A; p.(Glu307Lys) were identified in two probands of Dutch and Belgian ancestry, respectively (**Figure 5.1B**), in whom *PRPH2* mutations had been excluded. Analysis of both variants in members of Family B and C, respectively, confirmed segregation with the disease (**Figure 5.1A**). Both variants were predicted disease-causing by Polyphen and SIFT, affect residues that are completely conserved among vertebrate species (**Figure 5.2**), and were not identified in 162 ethnically matched controls nor in the EVS database. A third missense variant, c.160C>T; p.(Arg54Cys), was identified in an Italian proband who presented fundoscopically with a small area of RPE atrophy, superior to the fovea in the right eye, without classical phenotypical features as seen in pattern dystrophies. The variant was predicted disease-causing by Polyphen and SIFT, affects a residue that is completely conserved among vertebrate species (**Figure 5.2**), was not identified in 200 ethnically matched unrelated control individuals nor in the EVS database, but was present in the unaffected 64-year old father of this individual. Therefore, the pathogenic nature of this variant remains unclear.

Clinical features of butterfly-shaped pigment dystrophy caused by *CTNNA1* mutations

The clinical features of the affected individuals of the three families with butterfly-shaped pigment dystrophy are described in **Table 5.3**. A remarkable homogeneous intrafamilial phenotype was observed in affected individuals of the large Dutch pedigree (family A), but considerable phenotypic heterogeneity was noted in families B and C. Among the three families, the age at first presentation was highly variable, even among members of the same family, ranging from 15 to 55 years. In most cases, the BCVA was relatively well preserved, as only three of 13 affected individuals had a BCVA below 20/40. The BCVA values seemed to correlate with the amount and location of RPE atrophy. Follow-up BCVA data was available in four affected individuals of the second generation of family A, with only individual A-II:8 demonstrating significant progressive visual loss. The EOG was abnormal in nine of 11 affected individuals, and Arden ratios on EOG varied from normal values (ISCEV ≥ 2.0 or non-ISCEV ≥ 1.8)¹⁷ to 1.0 (no light rise on EOG). Full-field ERG results were normal in all six examined affected individuals, and in two of seven examined affected individuals color vision testing identified a red-green defect.

Fundoscopy showed typical butterfly-shaped hyperpigmentation in the center of the macula, surrounded by hypopigmentation in all affected individuals of family A (**Figure 5.3A**). On fluorescein angiography, the central pigmented lesions were hypofluorescent radially branching 'butterfly-shaped' structures with hyperfluorescence of the surrounding hypopigmented retina (**Figure 5.3B**). Additionally, two affected relatives showed spicular retinal hyperpigmentation in the peripheral retina, and in four affected relatives chorioretinal atrophy was present in the macula. The clinical presentation of both affected individuals of family B was comparable, although the macular lesion was less butterfly-shaped than in family A. Individual B-II:1 showed a less pronounced butterfly-shaped pigmented lesion, with atrophy of the RPE and photoreceptors (**Figure 5.3C and D**), while only a mild

phenotype of 'dot and halo' lesions was present in individual B-I:2. These 'dot and halo' lesions may progress to a more classic butterfly-shaped pigment dystrophy phenotype¹⁸. Optical coherence tomography (OCT) imaging showed hyperreflective lesions at the level of the RPE with atrophy of the RPE and photoreceptors at the fovea (**Figure 5.3E**). The proband of family C (C-II:1) showed a pattern dystrophy phenotype with a pattern resembling a starfish, with accumulation of material in the foveal area at the level of the RPE in both eyes (**Figure 5.3 I**). Autofluorescence imaging showed that the deposits were predominantly hyperautofluorescent (**Figure 5.3G**). The mother of the proband (individual C-I:2) showed a milder phenotype with irregular hyperpigmentation radiating from the fovea. At age seven, the daughter of the proband (individual C-III:1) had an entirely normal fundus in both eyes, despite being heterozygous for the c.919G>A; p.(Glu307Lys) variant.

Identification of a *Ctnna1* mutant mouse model

An indirect ophthalmoscopy screen of mice from a B6J mutagenesis program identified a mutant, *tvrm5*, which showed widespread mottling of the fundus and occasional bright spots, often with dark centers (ring spots). Linkage analysis of a *tvrm5* × DBA/2J intercross based on the ring spot phenotype revealed a recessive locus associated with the disease phenotype on chromosome 18 that was narrowed to ~14.5 Mbp by fine mapping (distal to *D18Mit22* and proximal to *D18Mit236*). Examination of whole exome sequences in this region identified coding variants in *Ctnna1* (c.1307T>C; p.[Leu436Pro]; PhyloP score 2.6) and *Pcdhb14* (c.1259C>T; p.[Thr420Ile]; PhyloP score 0.3). The higher PhyloP score, the predicted pathogenicity by SIFT, and the much higher expression of *Ctnna1* compared to *Pcdhb14* in the retina and RPE (biogps.org) strongly supports that the *Ctnna1* mutation is the causative allele. By Sanger sequencing, the *Ctnna1* allele was confirmed to be homozygous in 17 affected progeny of the mapping cross, heterozygous in two unaffected progeny and absent from eight unaffected progeny as well as B6J and DBA/2J mice, indicating cosegregation of the mutant allele with ring spot phenotype. Based on these considerations and the similarity of the human *CTNNA1* disease phenotype to that of *tvrm5* mutants (see below), the mutant allele will be referred to herein as *Ctnna1*^{*tvrm5*}.



Table 5.3 Clinical description of individuals with butterfly-shaped pigment dystrophy carrying genetic variants in the CTNNA1 gene

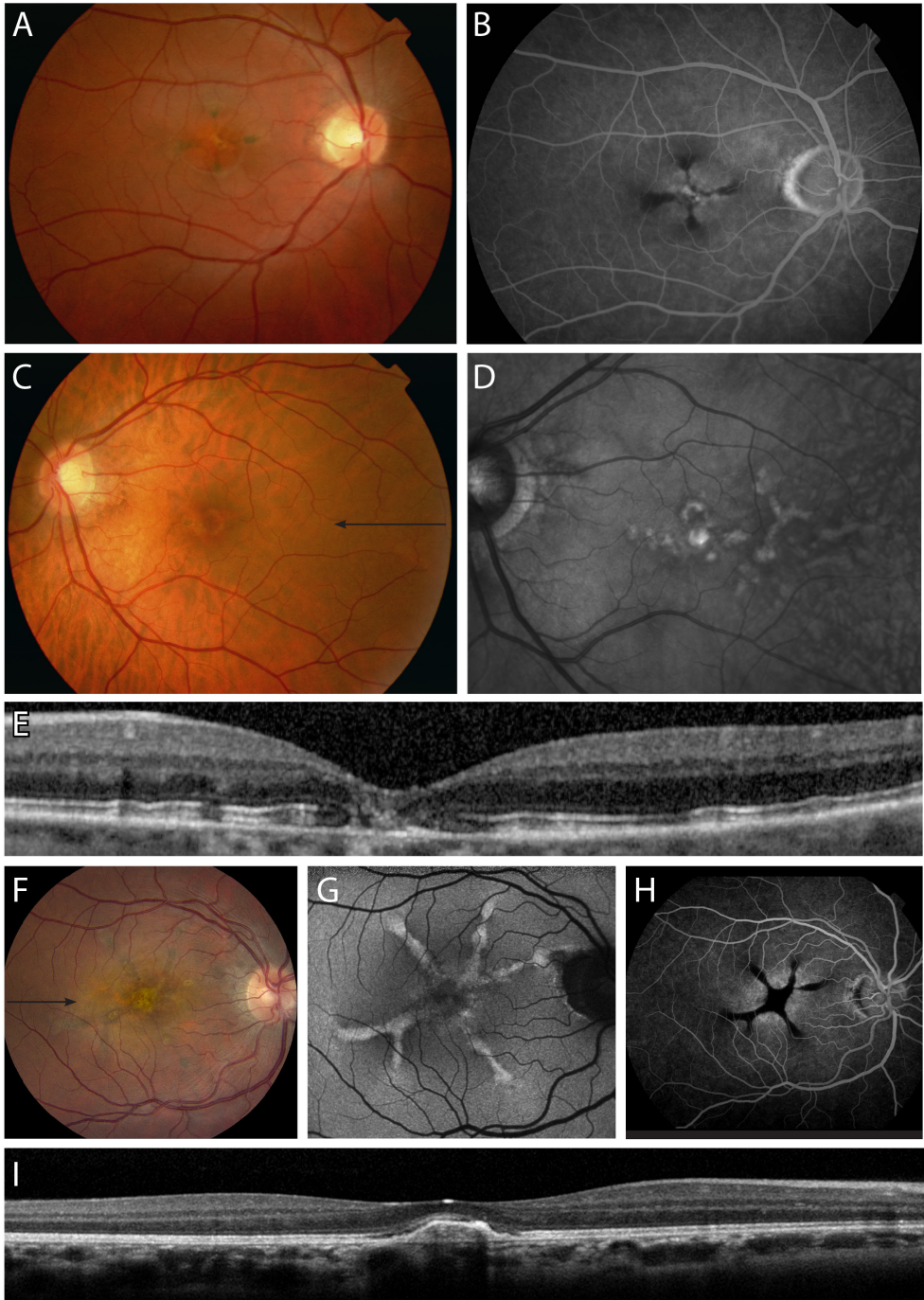
Ancestry	Pedigree	Mutation	Gender	Age at last examination	Age at onset	BCVA		EOG		ERG		Color vision	Fundoscopy
						OD	OS	OD	OS	OD	OS		
Family A													
Dutch	A-II:1	c.953T>C	male	70	43	20/20	20/20	1.6 ^a	1.5 ^a	N	N	-	Parafoveal chorioretinal atrophy ODs and peripheral bone spicule-like structures
Dutch	A-II:3	c.953T>C	male	68	42	20/20	20/25	1.0 ^a	1.0 ^a	N	N	N	ODs typical butterfly retinopathy in center of macula and extensive bone-spicule like peripheral hyperpigmentation.
Dutch	A-II:5	c.953T>C	male	71	45	20/20	20/20	1.3 ^a	1.3 ^a	N	N	N	General hypopigmentation with central IRPE atrophy and bone spicule-like pigmentations in peripheral retina
Dutch	A-II:8	c.953T>C	male	66	51	20/50	20/200	1.9 ^a	2.0 ^a	N	N	Red-green defect	ODs typical butterfly retinopathy in center of macula with central chorioretinal atrophy
Dutch	A-III:2	c.953T>C	male	50	14	20/32	20/40	1.4 ^a	1.5 ^a	N	N	Red-green defect	Butterfly-shaped pigmented lesion macula ODs without peripheral abnormalities
Dutch	A-III:7	c.953T>C	female	40	40	20/40	20/16	1.4 ^b	1.4 ^b	-	-	N	Typical butterfly-shaped hyperpigmentation surrounded by hypopigmentation OD. OS no abnormalities
Dutch	A-III:10	c.953T>C	male	35	Un-known	20/20	20/40	1.4 ^b	1.5 ^b	-	-	-	Butterfly-shaped hyperpigmentation ODs
Dutch	A-III:11	c.953T>C	male	36	36	20/25	20/20	3.0 ^b	2.7 ^b	-	-	-	Typical butterfly-shaped hyperpigmentation surrounded by hypopigmentation OD and a juxtafoveal area of hyperpigmentation surrounded by a small ring of hypopigmentation OS.
Dutch	A-III:12	c.953T>C	female	26	un-known	20/25	20/25	1.8 ^b	1.7 ^b	-	-	-	Typical butterfly-shaped hyperpigmentation surrounded by hypopigmentation OS. OD small pigmentary changes without any pattern



Family B											
Dutch	B-I:2	c.1293T>G	female	71	un-known	20/200	20/63	-	-	-	Mild pattern dystrophy ODS with OS one central lesion and OD several 'dot and halo' lesions in the macula
Dutch	B-II:1	c.1293T>G	male	62	55	20/20	20/25	-	-	-	ODS atrophy of RPE and photoreceptors in the macula, with a less peculiar butterfly-shaped pattern of pigmentary changes OD and focal hyperpigmentation centrally OS.
Family C											
Belgian	C-I:1	c.919G>A	female	33	22	20/100	20/100	1.7 ^b	1.4 ^b	N	Starfish-like pattern dystrophy in ODS with pigmented subretinal deposits radiating outwards from denser deposits in foveal area; small, whitish dots on outline of 6 starfish legs; highlighting of macular luteal pigment, more pronounced in central foveal area
Belgian	C-I:2	c.919G>A	female	59	un-known	20/25	20/20	1.8 ^b	1.7 ^b	-	Fairly mild pattern dystrophy ODS with in OD two and in OS three loosely defined linear tracts containing irregular patches of hyperpigmentation radiating from denser central foveal lesion
Belgian	C-III-1	c.919G>A	female	7	-	20/25	20/20	-	-	-	Normal fundus ODS

Age at onset of individuals with normal BCVA and normal color vision is defined as the age of first fundoscopic features; N = Normal; OD = right eye; OS = left eye; ODS both eyes; BCVA = best-corrected visual acuity (at last visit), ^b = EOG performed according to the International Society for Clinical Electrophysiology of Vision protocol (ISCEV); normal if Arden ratio ≥ 2.0 ; ^a = non-ISCEV Arden ratio





► **Figure 5.3 Retinal images of three families with butterfly-shaped pigment dystrophy.** (A–B) Retinal imaging of the right eye of individual A-III:11 at age 36. (A) Fundus photography showing a peculiar butterfly-shaped pigmented lesion in the center of the macula. (B) Fluorescein angiography (FA) showing hypofluorescence of the hyperpigmentation surrounded by some hyperfluorescence. (C–E) Retinal imaging of the left eye of individual B-II:1 at age 62. (C) Fundus photographs showing mild pigmentary changes in the macula. (D) On near-infrared reflectance images the retinal changes are more pronounced. (E) Spectral-domain optical coherence tomography (SD-OCT) (scan in the plane indicated by black arrow in C) shows that the abnormalities on near-infrared reflectance imaging in D are hyperreflective and located at or just anterior to the retinal pigment epithelium (RPE), and also shows some atrophy of the RPE and outer retina. (F–I) Retinal imaging of the right eye of individual C-II:1 at age 33 (F, G and I) and age 23 (H). (F) Fundus photographs showing pattern dystrophy with a starfish-aspect with thickened fovea and six branches with hyperpigmentation. Relatively pronounced yellowish macular pigment deposition can be seen. (G) Fundus autofluorescence imaging showing hyperautofluorescence of lesions. (H) FA shows blockage of background fluorescence by pigmented lesions. (I) SD-OCT of the central foveal lesion of the right eye (scan in the plane indicated by black arrowhead in A), showing a dome-shaped sub-RPE lesion in the fovea.

RPE lesions and photoreceptor loss in *Ctnna1*^{tvrm5} mutants

To assess the clinical manifestation of the disease, mouse eyes were examined noninvasively. Fundus imaging of homozygous *Ctnna1*^{tvrm5} mice (Figure 5.4A) revealed lesions in the central fundus biased toward the posterior pole, which were correlated with the spots (Figure 5.4C) and ring spots (Figure 5.4D and E) phenotype. Fine pigment mottling was also detected throughout the fundus (Figure 5.4A). Single *en face* slices generated from processed OCT image volumes of the same eyes revealed hyperreflective objects at the same locations as observed by fundus imaging (Figure 5.4B). OCT B-scans of spots (Figure 5.4F) showed localized thickening of hyperreflectivity corresponding to the RPE and a slight distortion of the photoreceptor inner/outer segment junction and external limiting membrane toward the vitreous. B-scans of ring spots showed localized thickening surrounding an elevated hyporeflective core (Figure 5.4G and H). Notably, the B-scan profiles of lesions in homozygous *Ctnna1*^{tvrm5} mice and individuals with butterfly-shaped pigment dystrophy were similar, both for small and large lesions (compare Figures 5.3E and 5.4F and 5.3 I and 5.4H, respectively).

OCT analysis also revealed a slight but significant decrease in outer nuclear layer (ONL) thickness of 9% ($p < 0.001$) in young homozygous *Ctnna1*^{tvrm5} compared to B6J mice (1 month, $51.2 \pm 1.2 \mu\text{m}$ [$n=7$] vs. $56.0 \pm 0.7 \mu\text{m}$ [$n=3$], respectively; 3 months, $50.9 \pm 0.7 \mu\text{m}$ [$n=3$] vs. $55.8 \pm 1.5 \mu\text{m}$ [$n=5$], respectively). With age, ONL thickness was decreased by 16% ($p < 0.004$) in homozygous *Ctnna1*^{tvrm5} compared to B6J mice (12–14 months, $44.1 \pm 1.0 \mu\text{m}$ [$n=3$] vs. $53.0 \pm 1.5 \mu\text{m}$ [$n=5$], respectively). In heterozygotes, lesions were not evident by either fundus imaging or OCT, and ONL thickness was not significantly affected at 1, 3 or 12–14 months of age. Taken together, these findings indicate that pathologic changes occur at the apical surface of the RPE or within the RPE itself and include the outer retina, where progressive photoreceptor loss is observed in homozygous *Ctnna1*^{tvrm5} mice.



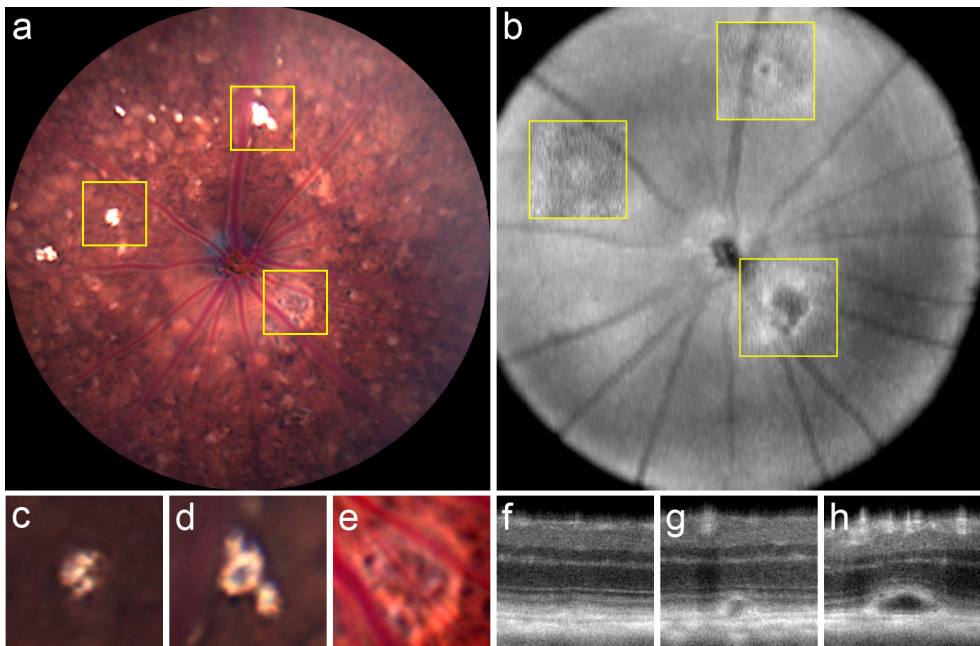


Figure 5.4 Live retinal imaging of homozygous *Cttna1*^{tvm5} mice. (A) Fundus imaging at one year of age revealed bright lesions in the central fundus near the posterior pole and mottling throughout the fundus. (B) Averaged projection of the OCT volume from the inner nuclear layer to the photoreceptor inner/outer segment junction is shown en face, to guide comparison with the fundus image in A. The lesions identified in A are superimposed as single en face slices. (C–E) Detail of lesions shown from left to right in A, respectively, obtained from a less saturated image. (F–G) OCT B-scans corresponding to lesions shown from left to right in B, respectively. Spot lesions (F), show a slight focal thickening of RPE hyperreflectivity and distortion of the overlying retinal layers. Ring lesions (G and H) include an elevated hyperreflective region surrounding a central hyporefective area above the RPE.

Decreased light-activated RPE response in *Cttna1*^{tvm5} mutant mice

To test whether the morphological RPE defects were accompanied by a decrease in RPE function, we examined *Cttna1* mutant mice by dc-ERG electrophysiology. In comparison to wild-type (B6J) mice, dc-ERG responses were reduced in amplitude at one year of age in both heterozygous and homozygous *Cttna1*^{tvm5} mice (Figure 5.5A). When the main components of the response were quantified, significant differences from B6J were noted for the c-wave, fast oscillation (FO) and off-response in both heterozygous and homozygous *Cttna1*^{tvm5} mice (Figure 5.5B); the amplitude reduction of the light peak component, which tends to be variable in amplitude in mice, was not significant. Differences were not noted in responses between heterozygous and homozygous *Cttna1*^{tvm5} mice.

As the dc-ERG signal is generated in response to rod photoreceptor activity¹⁹, it was essential to determine whether the reduced dc-ERGs of *Cttna1* mutant mice resulted from a decrease in RPE function alone or were accompanied by a decline in rod photoreceptor function. Therefore, we also recorded strobe flash ERGs from B6J and *Cttna1*^{tvm5} mutant

mice. While the overall waveform did not differ across genotypes, the amplitudes of both the dark-adapted a- and b-wave were significantly reduced in homozygous *Ctnna1^{tvrm5}* as compared to B6J or heterozygous *Ctnna1^{tvrm5}* mice (**Figure 5.5C**). Thus, the reduction in the dc-ERG responses in homozygous *Ctnna1^{tvrm5}* mice may reflect dysfunction of photoreceptors, RPE cells, or both. By contrast, dark-adapted responses did not differ in heterozygous *Ctnna1^{tvrm5}* and B6J mice (**Figure 5.5C**), indicating that the reduction in dc-ERG response in heterozygous mice occurs without a loss of photoreceptor function. The cone ERG response was significantly reduced in homozygous *Ctnna1^{tvrm5}* mice compared with B6J or heterozygous *Ctnna1^{tvrm5}* mice, which also did not differ (**Figure 5.5D**). Together with the live imaging results, the ERG observations support a pathogenic mechanism in which heterozygous *Ctnna1^{tvrm5}* mice develop RPE dysfunction without significant photoreceptor damage, while homozygous animals develop a more severe RPE functional deficit causing rod and cone photoreceptor cell loss.

Pigmented cells on the RPE apical surface and eosinophilic inclusions in *Ctnna1^{tvrm5}* mice

To assess cellular changes that might provide clues to the underlying cause of RPE lesions and functional defects in *Ctnna1^{tvrm5}* mice, we examined fixed retinal tissues by histology. At one month of age, retinal layers in homozygous *Ctnna1^{tvrm5}* mice (**Figure 5.6B**) were grossly normal compared to those in B6J mice (**Figure 5.6A**), apart from slight ONL thinning. However, distortion of the outer retina was occasionally noted in areas where one of several unusual features was found in the underlying RPE. First, pigmented cells were present on the RPE apical surface in focal lesions appearing as a slightly thickened RPE layer contiguous with the epithelium (**Figure 5.6C**) or as an extensive double layer (**Figure 5.6D**). Single pigmented cells were also observed (**Figure 5.6E**), which may be shed RPE cells. However, the observation of nuclei with no evidence of surrounding pigment (**Figure 5.6F**) suggested the presence of additional cell types in the subretinal space. Second, eosinophilic inclusions were found frequently within the RPE cell layer (**Figure 5.6G**), often with an internal laminar appearance. Serial sections revealed nuclei on the edges of these inclusions and sparse melanin pigment enclosed within a well-defined boundary, compatible with an intracellular location. Finally, pigmented cells on the RPE apical surface and eosinophilic inclusions were both present in larger lesions (**Figure 5.6H-K**), suggesting a common pathogenic basis of these features. In agreement with live imaging results, these features were observed at one month and at 12-14 months in homozygous *Ctnna1^{tvrm5}* mice but were not detected in heterozygous and B6J animals.

These findings provide a histological correlate of the live imaging results. The pigmented cells accumulating on the apical surface of the RPE (**Figure 5.6C and D**) corresponded to the bright spots observed by fundus imaging and *en face* OCT (**Figure 5.4A and B**), and to the localized thickening of the hyperreflective RPE layer in OCT B-scans (**Figure 5.4F-H**). Accumulation of eosinophilic material in the epithelial layer (**Figure 5.6G**) may also contribute to localized thickening observed by OCT. Lesions containing large eosinophilic



inclusions flanked by double layers of pigmented cells corresponded to the ring spots observed by live imaging (**Figure 5.6H-K**).

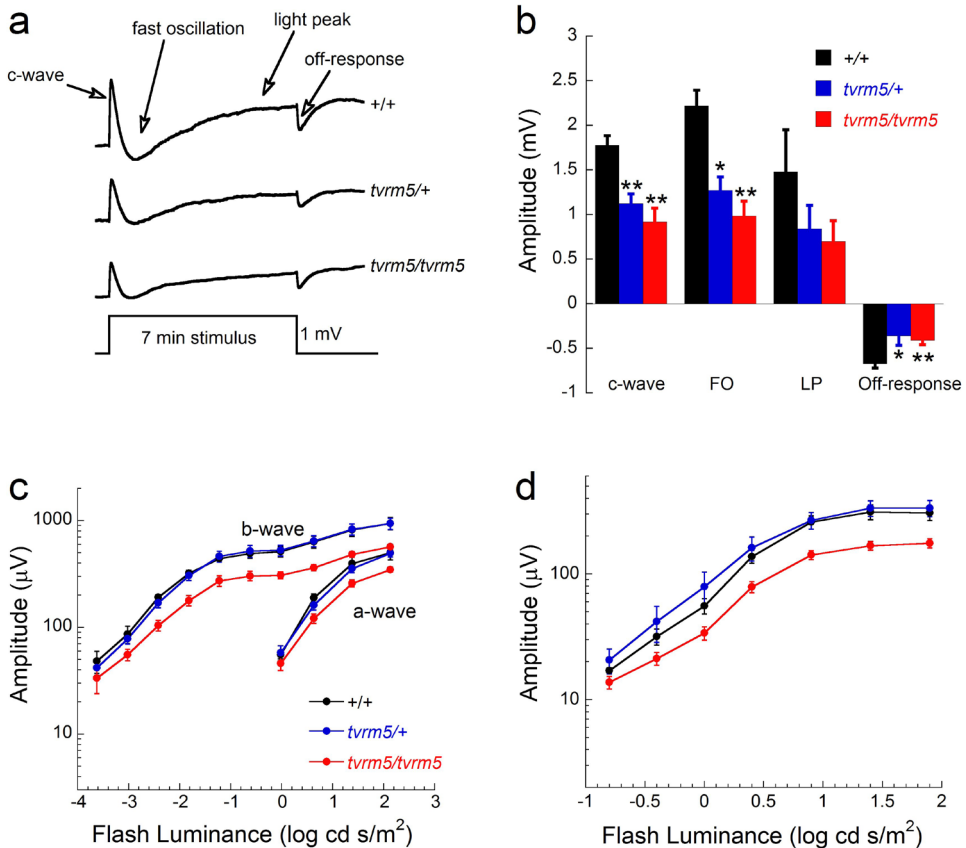


Figure 5.5 ERG recordings of Cttna1^{tvrm5} mice. (A) Waveforms indicate average dc-ERG waveforms obtained from wild-type B6J (+/+, n=11), heterozygous (tvrm5/+, n=5), and homozygous Cttna1^{tvrm5} (tvrm5/tvrm5, n=9) mice. (B) Average (\pm SEM) amplitude of the major dc-ERG components. In comparison to B6J, the amplitudes of the c-wave, fast oscillation (FO) and off response components were significantly reduced in Cttna1 mutant mice (*: $P < 0.015$; **: $P < 0.001$). The reductions of the light peak (LP) component were not significant. There was no significant difference in dc-ERG amplitude between heterozygous and homozygous Cttna1^{tvrm5} mice. (C) Response functions for the amplitude of the a- and b-wave components of the dark-adapted strobe flash ERG. Data points indicate average (\pm SEM) for B6J, heterozygous and homozygous Cttna1^{tvrm5} mice (n=3, 10 and 6, respectively). Responses were significantly reduced ($P < 0.01$) in homozygous as compared to B6J or heterozygous mice, which did not differ. (D) Response function for the amplitude of the cone ERG. Responses were significantly reduced ($P < 0.01$) in homozygous Cttna1^{tvrm5} as compared to B6J or heterozygous mice, which did not differ.

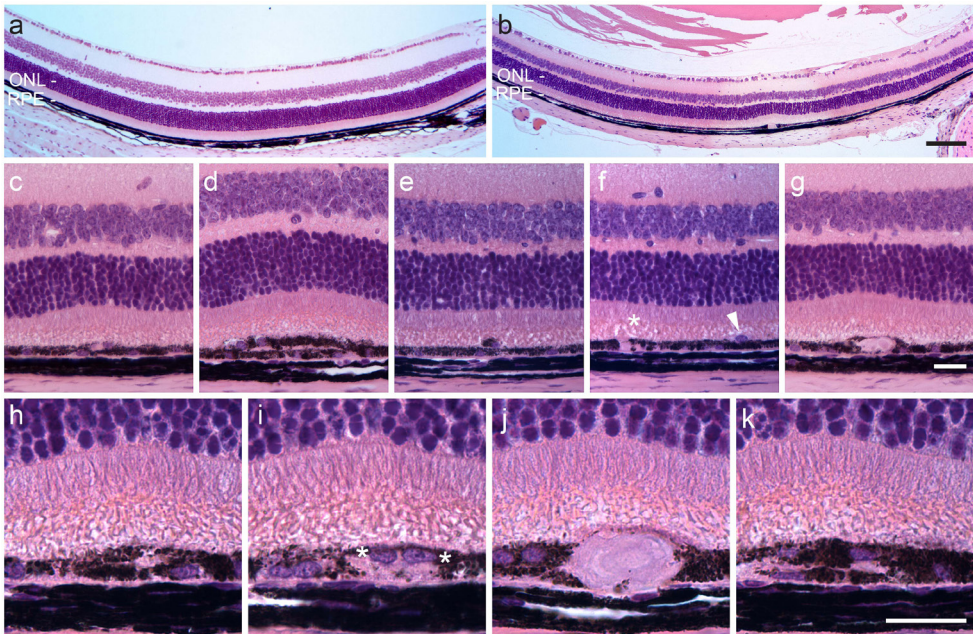


Figure 5.6 Light micrographs of hematoxylin and eosin stained paraffin-embedded ocular sections from *Ctnna1*^{trvm5} mice at one month of age. (A) B6J retina. (B) Homozygous *Ctnna1*^{trvm5} retina showing normal layered organization with occasional outer retinal distortion in an area of abnormal RPE. (C–K) Detail of RPE lesions in eyes of homozygous *Ctnna1*^{trvm5} mice. (C) Slight RPE thickening. (D) A double layer of pigmented cells, possibly RPE. (E) A single pigmented, nucleated cell on the RPE apical surface. (F) A nucleus without surrounding pigment (arrowhead) on the RPE apical surface and a small eosinophilic inclusion (asterisk). (G) An eosinophilic inclusion bounded by melanin pigment. (H–L). Sections 3, 5, 8 and 13 from a series of 14 sections of a large RPE lesion containing both pigmented cells on the RPE surface and an eosinophilic inclusion. Nuclei (asterisks) in I may be in the same cell as the eosinophilic inclusion. Scale bars in panels B, G and K are 100, 20 and 20 μm , respectively, and apply to each row of images. ONL, outer nuclear layer; RPE, retinal pigment epithelium.

RPE dysmorphology and multinucleate cells

As an additional test for RPE structural defects, we stained RPE/choroid/sclera flatmounts at one month of age to detect nuclei and the F-actin cytoskeleton at RPE cell boundaries. Flatmounts from B6J mice revealed mono- and binucleate polygonal RPE cells with vertices shared by three cells (Figure 5.7A). By contrast, homozygous *Ctnna1*^{trvm5} mice exhibited unusual RPE morphology comprising four or more cells surrounding an F-actin circle of variable size (Figure 5.7B–D) or a shared vertex (Figure 5.7E). Orthogonal views of B6J image stacks indicated that RPE nuclei are normally located below F-actin staining at the RPE apical surface (Figure 5.7F, left), which is presumably due to staining of F-actin bundles in the microvilli, and below the circumferential F-actin band that defines the polygonal cell boundary (Figure 5.7F, right). In homozygous *Ctnna1*^{trvm5} mice, nuclei were occasionally observed directly above the circular F-actin motif (Figure 5.7G), consistent with apical shedding of an RPE cell. However, in most of these structures, nuclei were not apparent or



were positioned basally to the circular F-actin motif, possibly indicating that basal shedding also occurs.

RPE dysmorphology was also evident at 12-14 months of age. Compared to normal polygonal cells in B6J mice (**Figure 5.7H**), the RPE cells in heterozygous (**Figure 5.7 I**) and homozygous *Ctnna1^{trms5}* mice (**Figure 5.7J**) were highly variable in size and included extremely large, irregularly-shaped multinucleate cells. In addition to the absence of apical F-actin boundaries in the interior of these abnormal RPE cells, the disordered clustering of nuclei suggested a lack of intercellular barriers. Bright F-actin structures, including tangles and intense staining at the boundaries of rounded cells, were more pronounced in homozygous than in heterozygous *Ctnna1^{trms5}* mice. In summary, a primary consequence of the *Ctnna1^{trms5}* mutation appears to be significant dysmorphology in the form of RPE cell shedding and the accumulation of large multinucleate RPE cells.

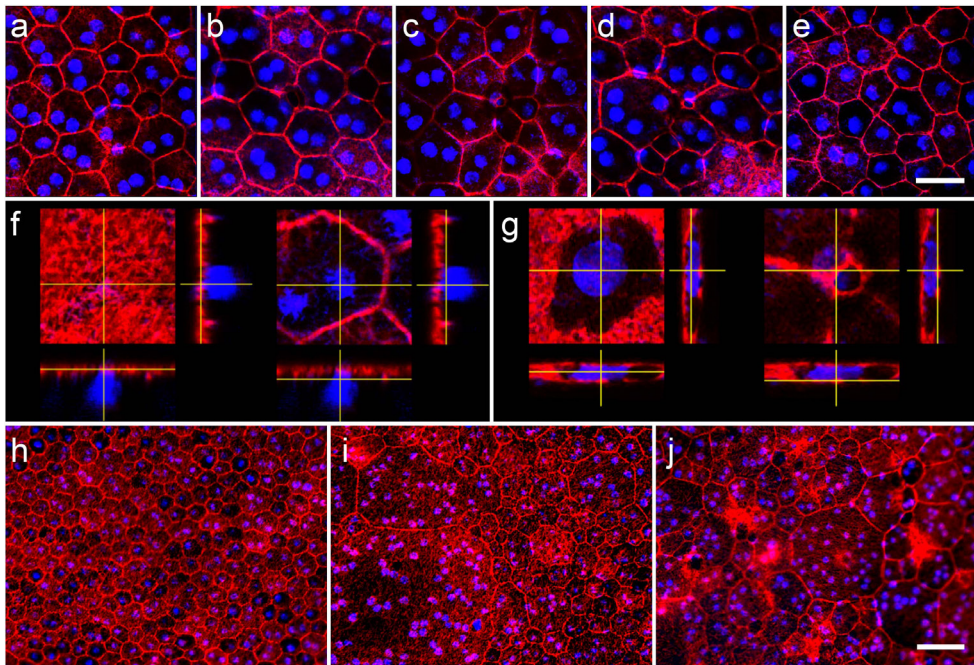


Figure 5.7 RPE cell dysmorphology in RPE/choroid/sclera flatmounts of *Ctnna1^{trms5}* mice stained with rhodamine phalloidin (red) and DAPI (blue) to reveal F-actin and nuclei, respectively. (A) Merged projections of a confocal image stack show normal mono- and binucleate polygonal cells in B6J mice at one month of age. (B-D) Circular F-actin structures or (E) vertices shared by four or more cells were frequent in homozygous *Ctnna1^{trms5}* mice. (F) Orthogonal displays at two z-positions of cells in panel A show that RPE nuclei in B6J mice lie below F-actin on the apical surface (left) and in the circumferential band (right). (G) Orthogonal display of cells from panel C showing a flattened nucleus between apical F-actin and the circular F-actin structure in homozygous *Ctnna1^{trms5}* mice. (H) RPE cells B6J mice at 12-14 months of age remained mostly mono- and binucleate. (I) Heterozygous *Ctnna1^{trms5}* mice at 12-14 months of age showed large multinucleate RPE cells. (J) Homozygous *Ctnna1^{trms5}* mice exhibited multinucleate cells as well bright F-actin tangles and rounded cells with bright F-actin boundaries.

Scale bars in panels E and J are 25 and 50 μm , respectively, and apply to the corresponding rows of images.

Modeling and functionality of variants in α -catenin 1

CTNNA1 encodes α -catenin 1 (also known as α E-catenin or CTNNA1), which stabilizes intercellular adherens junctions as a force-sensing adaptor between cell surface cadherins and the actin cytoskeleton.^{20,21} α -Catenin 1 responds to increased intercellular tension by unfurling binding sites for actin-associated proteins, such as vinculin, afadin, α -actinin, and formin.^{20,21} Given the importance of adherens junctions for RPE integrity,²² we explored possible structural and functional consequences of the α -catenin 1 variants. The *CTNNA1* variants detected in the three families with butterfly-shaped pigment dystrophy (p.[Glu307Lys], p.[Leu318Ser], and p.[Ile431Met]) and the mouse *Ctnna1*^{lvrm5} variant (p.[Leu436Pro]) are predicted to alter residues in α -catenin 1 that are completely conserved among vertebrate species (**Figure 5.2**). As shown in an x-ray crystallographic structural model of the human protein (**Figure 5.8**), four of the five variants affect amino acid residues (p.Glu307, p.Leu318, p.Ile431, p.Leu436) that are clustered in the middle of protein. The variants map to the proposed force-sensing module (domains D3-D4, amino acid residues 260-630) and to protein binding domains within this module that may be sensitive to tension (D3a, residues 260-400; D3b, residues 400-507).²¹ The four variants map in or near the region that has been reported to bind vinculin.^{21,23-25} The fifth variant, which is of uncertain pathogenic significance, affects Arg54 within the N-terminal domain that binds β -catenin, a direct binding partner of cadherin. To test for an effect of the variants on vinculin binding, the wild-type and mutant α -catenin 1 proteins were heterologously co-expressed with vinculin. Although co-immunoprecipitations confirmed interaction of α -catenin 1 with vinculin, the mutations did not affect the interaction of these proteins (**Figure 5.9**).



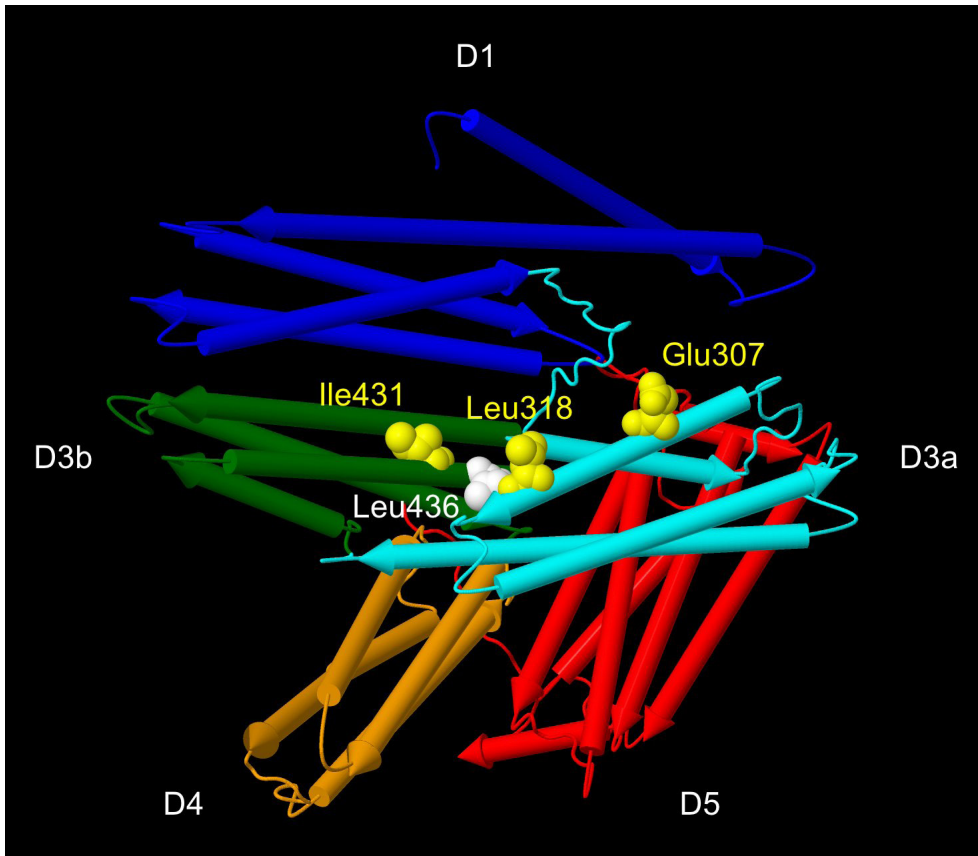


Figure 5.8 Structural model of human α -catenin 1 showing the location of amino acid residues altered by CTNNA1 mutations identified in three families with butterfly-shaped pigment dystrophy and in *Cttna1^{lvrm5}* mice. The model (Protein DataBank entry 4IGG) shows residues 82-635 and 666-861 of polypeptide chain A. The α -helices are depicted as rockets and colored according to domain classification (D1, N-terminal domain; D3a, D3b and D4, middle domains also known as MI, MII and MIII, respectively; D5, C-terminal domain). Affected residues are shown in space-filling representation (yellow, human variants; white, mouse variant). The sequences of human and mouse α -catenin 1 are identical within the affected domains shown.

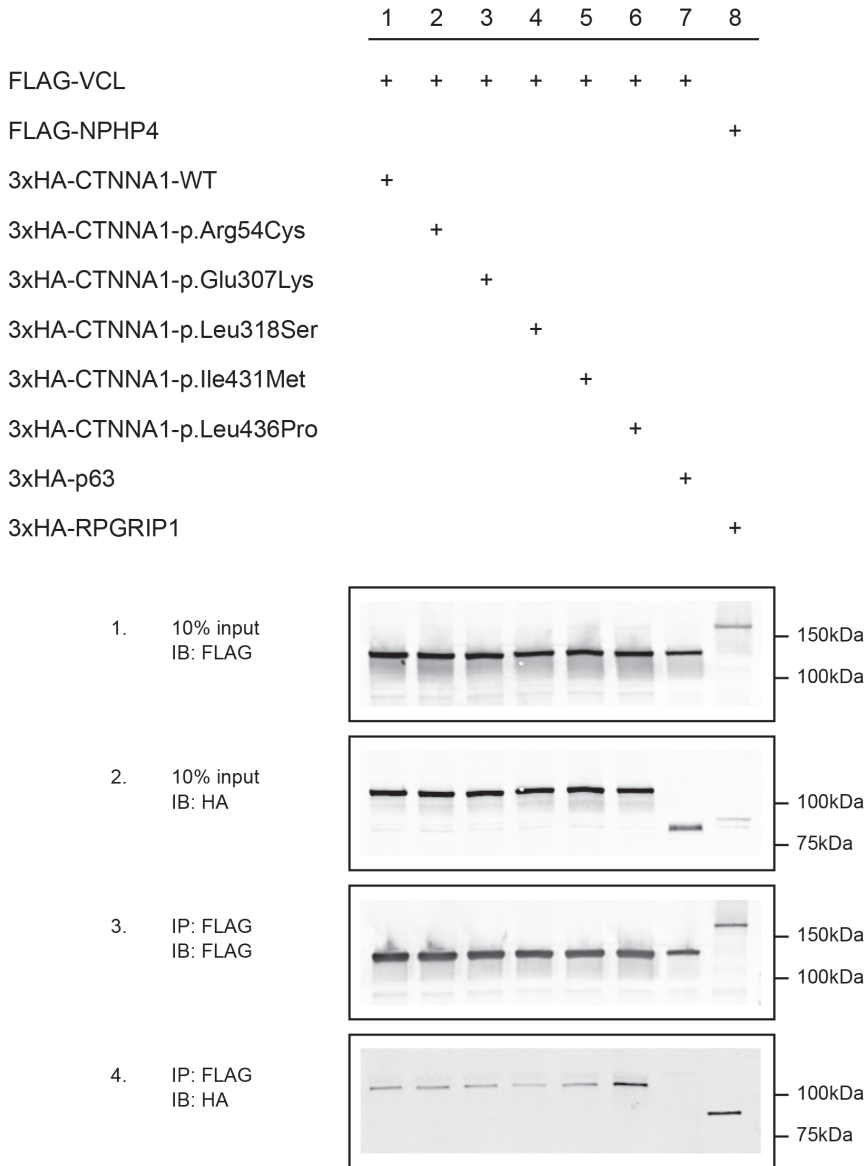


Figure 5.9 Co-immunoprecipitation studies of α -catenin 1 (CTNNA1) and vinculin (VCL). Wild-type 3xHA-CTNNA1 efficiently co-immunoprecipitated with 3xFLAG-VCL (panel 4, lane 1), and introduction of the CTNNA1 variants c.160C>T; p.(Arg54Cys) (lane 2), c.919G>A; p.(Glu307Lys) (lane 3), c.953T>C; p.(Leu318Ser) (lane 4), c.1293T>G; p.(Ile431Met) (lane 5), and c.1307T>C; p.(Leu436Pro) (lane 6) did not significantly affect the binding. Specificity was confirmed by inclusion of the unrelated p63, which failed to co-immunoprecipitate with wild-type vinculin (lane 7). As positive control, RPGRIP1 efficiently co-immunoprecipitated with nephrocystin-4 (NPHP4; lane 8). Immunoblots of the input are shown in panels 1 and 2, and immunoblots of the FLAG immunoprecipitates are shown in panels 3 and 4. Size markers are depicted in kDa.

DISCUSSION

This work for the first time implicates a member of the catenin family in posterior eye disease, namely, mutations in the *CTNNA1* gene as a genetic cause of butterfly-shaped pigment dystrophy. Previously, mutations in peripherin 2 have been associated with this condition, a protein that is thought to function in outer segment disc biogenesis of retinal photoreceptor cells.¹ The finding that the disease is also caused by variants in α -catenin 1, a central component of a complex that links cell surface cadherins to the actin cytoskeleton, broadens our perspective on the cellular and molecular basis of this disease. Intriguingly, a juvenile form of macular dystrophy (MIM 114021) that results in atrophy and pigmentary changes has been linked to variants in *CDH3*, which encodes P-cadherin.²⁶ Thus, cellular components that participate in cadherin-based intercellular adhesion may be implicated in macular dystrophies.

Affected individuals of the families carrying *CTNNA1* mutations show a remarkable interfamilial and intrafamilial heterogenous phenotype, which has also been observed in other families with butterfly-shaped pigment dystrophy due to mutations in *PRPH2*.^{4,27} In advanced cases, the phenotype can progress to chorioretinal atrophy or subretinal neovascularization.^{4,6,8,9} At this stage the disease can be indistinguishable from advanced age-related macular degeneration (AMD), a common cause of visual impairment in the elderly, characterized by yellow deposits called drusen,²⁸ which may progress to geographic atrophy or choroidal neovascularization.²⁹ Genetic testing of the *CTNNA1* and *PRPH2* genes can thus aid in establishing the differential diagnosis between advanced cases of butterfly-shaped pigment dystrophy and AMD.²⁹

Our studies revealed parallel clinical phenotypes in individuals with butterfly-shaped pigment dystrophy carrying a variant allele of *CTNNA1* and in homozygous *Ctnna1*^{trmv5} mice, including pigmentary abnormalities, focal RPE thickening and elevated lesions, and RPE dysfunction in response to light. These observations imply that similar pathogenic mechanisms underlie *CTNNA1/Ctnna1*-associated disease in both species, and suggest that *Ctnna1*^{trmv5} mice accurately model the human disease. Importantly, the dysmorphology of RPE cells observed in *Ctnna1*^{trmv5} mice raises the possibility that RPE defects are a precipitating event in the disease. Although the phenotype is stronger in homozygous *Ctnna1*^{trmv5} mice, we also observed defects in heterozygous *Ctnna1*^{trmv5} mice such as a decrease in RPE function and large multinucleated RPE cells. This indicates that in mice the *Ctnna1* variant also has an effect in heterozygous state, albeit less detrimental than in the homozygous state, suggesting a gene-dosage effect. Although *Ctnna1* is widely expressed, it is likely that the variants affect an RPE-specific function of α -catenin 1, as the human disease affects only the eye, and the mouse *Ctnna1*^{trmv5} mutation is less disruptive than a *Ctnna1* gene-trap allele, which results in embryonic lethality,³⁰ or a conditional knockout allele targeted to retinal progenitor cells, which causes dramatic retinal developmental defects.³¹ Thus, our results point to a causative role of RPE defects in butterfly-shaped pigment dystrophy due to *CTNNA1* variants.

Shed RPE cells in the subretinal space may contribute to the focal thickening of the RPE and melanin pigment abnormalities in patients with butterfly-shaped pigment dystrophy. Consistent with shedding, we observed pigmented cells on the RPE apical surface and aberrant F-actin structures in *Ctnna1^{tvrm5}* mice that were similar to shedding structures in chick embryonic RPE³² and in mouse models of RPE injury.^{33,34} The fate of shed RPE cells is unknown. Some may survive to accumulate and/or proliferate locally at lesions, creating a double layer of pigmented cells as observed in our study. Double RPE layers have been documented in atrophic lesions of geographic atrophy³⁵ and in mouse models that target damage to the RPE.^{33,36} Alternatively, shed RPE cells may die and be phagocytosed by intact RPE or immune cells. Subretinal macrophages containing melanin pigment granules, presumably derived from the RPE, have been observed in mouse models of retinal degeneration.^{37,38} Based on these findings, we propose that RPE shedding is an initial event leading to changes in melanin pigment distribution in *CTNNA1*-associated butterfly-shaped pigment dystrophy.

The large eosinophilic inclusions observed in the RPE of homozygous *Ctnna1^{tvrm5}* mice bear similarities to hard drusen – small (<63 μm diameter) spherical or dome-shaped eosinophilic masses that are located between RPE cells and Bruch's membrane and are associated with AMD when abundant.^{28,39-41} The eosinophilic inclusions possess internal substructure, as is often observed in hard drusen,⁴² and their laminar appearance is reminiscent of the 'onion-skin' feature of drusen associated with Doyme honeycomb retinal dystrophy/Malattia leventinese.⁴³ The inclusions are contiguous with the RPE and appear to be intracellular, although the cell type in which they are localized is unknown. Based on the similar OCT appearance of elevated lesions in affected patients and mice, we suggest that the deep retinal lesions in butterfly-shaped pigment dystrophy derive from aberrant cells in the RPE that accumulate an excess of eosinophilic material.

The presence of abnormally large multinucleate RPE cells in *Ctnna1^{tvrm5}* mutant mice may indicate a defect in RPE cytokinesis. This feature was more apparent in older mice, indicating that these changes accumulate with age in the RPE cell population, which is considered largely postmitotic. RPE hyperproliferation and a cytokinesis defect due to the *Ctnna1^{tvrm5}* mutation may yield this phenotypic feature through repeated rounds of nuclear division without cell division. Alternatively, altered RPE cell adhesion due to the *Ctnna1^{tvrm5}* mutation may lead to syncytia, which are multinucleate cells formed by cell fusion. Large multinucleate cells observed upon conditional deletion of *Ranbp2* in the RPE were interpreted previously as syncytia.⁴⁴

The clustering of the pathogenic human and mouse variants within the α -catenin 1 structure suggests that the variants have a shared effect on the activity of this multifunctional protein. The variants may disrupt the stability of adherens junctions, which are found in RPE cells and are likely critical for maintaining the integrity of the epithelium.²² As our studies do not indicate a decreased affinity of α -catenin 1 variants for vinculin, the mutations may disrupt the binding of other actin-associated proteins or alter the conformational response



to mechanical stress. More recent studies have revealed that α -catenin 1 participates in multiple signal transduction pathways independent of its role in cell adhesion, such as the NF- κ B, Ras-MAPK, Hedgehog and Hippo signaling pathways.^{45,47} Subsequently, the variants may perturb a function of α -catenin 1 in various cellular processes regulated by these pathways, such as cytokinesis, cell differentiation or growth.⁴⁵⁻⁴⁷

In conclusion, this study identified mutations in the human *CTNNA1* and mouse *Ctnna1* genes as a cause of macular dystrophy and RPE dysmorphology with accompanying photoreceptor loss. Our findings have clinical implications, since genetic testing of the *CTNNA1* gene can aid in establishing the differential diagnosis between butterfly-shaped pigment dystrophy and AMD. Additionally, this gene may be used as a target for the development of gene therapy in individuals with butterfly-shaped pigment dystrophy due to *CTNNA1* mutations.⁴⁸ Finally, future studies may focus on identifying other components of the RPE cell adhesion complexes that contribute to macular disease, and on understanding the cellular and molecular mechanisms by which α -catenin 1 dysfunction affects RPE turnover, proliferation, and the pathogenesis of pattern dystrophy.

REFERENCES

1. Boon, C.J. *et al.* The spectrum of retinal dystrophies caused by mutations in the peripherin/RDS gene. *Prog Retin Eye Res* 2008;27, 213-235.
2. Agarwal, A. in *Gass' Atlas of Macular diseases* 2012;254-266 (Elsevier).
3. Deutman, A.F., van Blommestein, J.D., Henkes, H.E., Waardenburg, P.J. & Solleveld-van Driest, E. Butterfly-shaped pigment dystrophy of the fovea. *Arch Ophthalmol* 1970;83, 558-569.
4. Fossarello, M. *et al.* Deletion in the peripherin/RDS gene in two unrelated Sardinian families with autosomal dominant butterfly-shaped macular dystrophy. *Arch Ophthalmol* 1996;114, 448-456.
5. Pinckers, A. Patterned dystrophies of the retinal pigment epithelium. A review. *Ophthalmic Paediatr Genet* 1988;9, 77-114.
6. Prensky, J.G. & Bresnick, G.H. Butterfly-shaped macular dystrophy in four generations. *Arch Ophthalmol* 1983;101, 1198-1203.
7. Nichols, B.E. *et al.* Butterfly-shaped pigment dystrophy of the fovea caused by a point mutation in codon 167 of the RDS gene. *Nat Genet* 1993;3, 202-207.
8. van Lith-Verhoeven, J.J., Cremers, F.P., van den Helm, B., Hoyng, C.B. & Deutman, A.F. Genetic heterogeneity of butterfly-shaped pigment dystrophy of the fovea. *Mol Vis* 2003;9, 138-143.
9. Marano, F., Deutman, A.F. & Aandekerck, A.L. Butterfly-shaped pigment dystrophy of the fovea associated with subretinal neovascularization. *Graefes Arch Clin Exp Ophthalmol* 1996;234, 270-274.
10. Grover, S., Fishman, G.A. & Stone, E.M. Atypical presentation of pattern dystrophy in two families with peripherin/RDS mutations. *Ophthalmology* 2002;109, 1110-1117.
11. Nichols, B.E. *et al.* A 2 base pair deletion in the RDS gene associated with butterfly-shaped pigment dystrophy of the fovea. *Hum Mol Genet* 1993;2, 1347.
12. Richards, S.C. & Creel, D.J. Pattern dystrophy and retinitis pigmentosa caused by a peripherin/RDS mutation. *Retina* 1995;15, 68-72.
13. Vaclavik, V., Tran, H.V., Gaillard, M.C., Schorderet, D.F. & Munier, F.L. Pattern dystrophy with high intrafamilial variability associated with Y141C mutation in the peripherin/RDS gene and successful treatment of subfoveal CNV related to multifocal pattern type with anti-VEGF (ranibizumab) intravitreal injections. *Retina* 2012;32, 1942-1949.
14. Yang, Z. *et al.* A novel RDS/peripherin gene mutation associated with diverse macular phenotypes. *Ophthalmic Genet* 2004;25, 133-145.
15. Zhang, K., Garibaldi, D.C., Li, Y., Green, W.R. & Zack, D.J. Butterfly-shaped pattern dystrophy: a genetic, clinical, and histopathological report. *Arch Ophthalmol* 2002;120, 485-490.
16. den Hollander, A.I. *et al.* Identification of novel locus for autosomal dominant butterfly shaped macular dystrophy on 5q21.2-q33.2. *J Med Genet* 2004;41, 699-702.
17. Marmor, M.F. *et al.* ISCEV standard for clinical electro-oculography (2010 update). *Doc Ophthalmol* 2001;122, 1-7.
18. Boon, C.J. *et al.* Mutations in the peripherin/RDS gene are an important cause of multifocal pattern dystrophy simulating STGD1/fundus flavimaculatus. *Br J Ophthalmol* 2007;91, 1504-1511.
19. Wu, J., Peachey, N.S. & Marmorstein, A.D. Light-evoked responses of the mouse retinal pigment epithelium. *J Neurophysiol* 2004;91, 1134-1142.
20. Kobiela, A. & Fuchs, E. Alpha-catenin: at the junction of intercellular adhesion and actin dynamics. *Nat Rev Mol Cell Biol* 2004;5, 614-625.



21. Leckband, D.E. & de Rooij, J. Cadherin adhesion and mechanotransduction. *Annu Rev Cell Dev Biol* 2014;30, 291-315.
22. Sandig, M. & Kalnins, V.I. Subunits in zonulae adhaerentes and striations in the associated circumferential microfilament bundles in chicken retinal pigment epithelial cells in situ. *Exp Cell Res* 1988;175, 1-14.
23. Provost, E. & Rimm, D.L. Controversies at the cytoplasmic face of the cadherin-based adhesion complex. *Curr Opin Cell Biol* 1999;11, 567-572.
24. Peng, X., Maiers, J.L., Choudhury, D., Craig, S.W. & DeMali, K.A. alpha-Catenin uses a novel mechanism to activate vinculin. *J Biol Chem*. 2012;287, 7728-7737.
25. Huveneers, S. *et al.* Vinculin associates with endothelial VE-cadherin junctions to control force-dependent remodeling. *J Cell Bio*. 2012;196, 641-652.
26. Sprecher, E. *et al.* Hypotrichosis with juvenile macular dystrophy is caused by a mutation in CDH3, encoding P-cadherin. *Nat Genet* 2001;29, 134-136.
27. Francis, P.J. *et al.* Genetic and phenotypic heterogeneity in pattern dystrophy. *Br J Ophthalmol*. 2005;89, 1115-1119.
28. Williams, M.A., Craig, D., Passmore, P. & Silvestri, G. Retinal drusen: harbingers of age, safe havens for trouble. *Ageing*. 2009; 38, 648-654.
29. Saksens, N.T. *et al.* Macular dystrophies mimicking age-related macular degeneration. *Prog Retin Eye Res* 2014;39, 23-57.
30. Torres, M. *et al.* An alpha-E-catenin gene trap mutation defines its function in preimplantation development. *Proc Natl Acad Sci USA* 1997; 94, 901-906.
31. Chen, S., Lewis, B., Moran, A. & Xie, T. Cadherin-mediated cell adhesion is critical for the closing of the mouse optic fissure. *PLoS One* 2012;7, e51705.
32. Nagai, H. & Kalnins, V.I. Normally occurring loss of single cells and repair of resulting defects in retinal pigment epithelium in situ. *Exp Eye Res* 1996;62, 55-61.
33. Longbottom, R. *et al.* Genetic ablation of retinal pigment epithelial cells reveals the adaptive response of the epithelium and impact on photoreceptors. *Proc Natl Acad Sci USA* 2009;106, 18728-18733.
34. Xia, H., Krebs, M.P., Kaushal, S. & Scott, E.W. Enhanced retinal pigment epithelium regeneration after injury in MRL/MpJ mice. *Exp Eye Res* 2011;93, 862-872.
35. Sarks, J.P., Sarks, S.H. & Killingsworth, M.C. Evolution of geographic atrophy of the retinal pigment epithelium. *Eye (Lond)* 1988;2, 552-577.
36. Rakoczy, P.E. *et al.* Progressive age-related changes similar to age-related macular degeneration in a transgenic mouse model. *Am J Pathol* 2002;161, 1515-1524.
37. Hawes, N.L. *et al.* Retinal degeneration 6 (rd6): a new mouse model for human retinitis punctata albescens. *Invest Ophthalmol Vis Sci* 2000;41, 3149-3157.
38. Fogerty, J. & Besharse, J.C. 174delG mutation in mouse MFRP causes photoreceptor degeneration and RPE atrophy. *Invest Ophthalmol Vis Sci* 2011;52, 7256-7266.
39. Hammond, C.J. *et al.* Genetic influence on early age-related maculopathy: a twin study. *Ophthalmology* 2002;109, 730-736.
40. Klein, R. *et al.* Fifteen-year cumulative incidence of age-related macular degeneration: the Beaver Dam Eye Study. *Ophthalmology* 2007;114, 253-262.
41. Klein, R., Klein, B.E., Tomany, S.C., Meuer, S.M. & Huang, G.H. Ten-year incidence and progression of age-related maculopathy: The Beaver Dam eye study. *Ophthalmology* 2002;109, 1767-1779.
42. Rudolf, M. *et al.* Prevalence and morphology of druse types in the macula and periphery of eyes with age-related maculopathy. *Invest Ophthalmol Vis Sci* 2008;49, 1200-1209.

43. Sohn, E.H. *et al.* Comparison of drusen and modifying genes in autosomal dominant radial drusen and age-related macular degeneration. *Retina* 2015;35, 48-57.
44. Patil, H. *et al.* Selective impairment of a subset of Ran-GTP-binding domains of ran-binding protein 2 (Ranbp2) suffices to recapitulate the degeneration of the retinal pigment epithelium (RPE) triggered by Ranbp2 ablation. *J Biol Chem* 2014;289, 29767-29789.
45. Li, J. *et al.* Alpha-catenins control cardiomyocyte proliferation by regulating yap activity. *Circ Res* 2015;116, 70-79.
46. Schlegelmilch, K. *et al.* Yap1 acts downstream of alpha-catenin to control epidermal proliferation. *Cell* 2011;144, 782-795.
47. Stepniak, E., Radice, G.L. & Vasioukhin, V. Adhesive and signaling functions of cadherins and catenins in vertebrate development. *Cold Spring Harb Perspect Biol* 2009; 1, a002949.
48. Conley, S.M. & Naash, M.I. Gene Therapy for PRPH2-Associated Ocular Disease: Challenges and Prospects. *Cold Spring Harb Perspect Med* 2014;4.
49. Saksens, N.T. *et al.* Dominant cystoid macular dystrophy. *Ophthalmology* 2015;122, 180-191.
50. Svenson, K.L., Bogue, M.A. & Peters, L.L. Invited review: Identifying new mouse models of cardiovascular disease: a review of high-throughput screens of mutagenized and inbred strains. *J Appl Physiol* 1985;94, 1650-1659; discussion 2003;1673.
51. Won, J. *et al.* Translational vision research models program. *Adv Exp Med Biol* 2012;723, 391-397.
52. Low, B.E. *et al.* Correction of the Crb1rd8 allele and retinal phenotype in C57BL/6N mice via TALEN-mediated homology-directed repair. *Invest Ophthalmol Vis Sci* 2014;55, 387-395.
53. Sakamoto, K., McCluskey, M., Wensel, T.G., Naggert, J.K. & Nishina, P.M. New mouse models for recessive retinitis pigmentosa caused by mutations in the Pde6a gene. *Hum Mol Genet* 2009;18, 178-192.
54. Schindelin, J. *et al.* Fiji: an open-source platform for biological-image analysis. *Nat Methods* 2012;9, 676-682.
55. Yu, M. *et al.* Age-related changes in visual function in cystathionine-beta-synthase mutant mice, a model of hyperhomocysteinemia. *Exp Eye Res* 2012;96, 124-131.
56. Roepman, R. *et al.* Interaction of nephrocystin-4 and RPGRIP1 is disrupted by nephronophthisis or Leber congenital amaurosis-associated mutations. *Proc Natl Acad Sci USA* 2005;102, 18520-18525.



Chapter 6

General discussion



“Doctor, my father and three of my sisters became blind from macular degeneration; what is my risk of getting the same disease?” Ophthalmologists are confronted frequently with this type of question, which can be answered with confidence in the case of some retinal dystrophies with known genetic causes. On the other hand, this question is notoriously difficult to answer in the case of complex retinal diseases such as age-related macular degeneration (AMD), despite the fact that risk assessment is particularly important to—and desired by—patients with affected relatives. Little is known regarding the risk of AMD among individuals with a positive family history of AMD, and little is known regarding the differences in risk factors between familial and sporadic AMD. This thesis addresses both the clinical and genetic differences between familial AMD and sporadic AMD, and it explores the risk assessment of AMD in subjects with a positive family history of AMD. To facilitate the development of personalized medicine for the macular disorders described in this thesis, preventive and therapeutic decision-making should be tailored to the clinical and genetic characteristics of both the individual patient and the patient’s family history. This chapter elaborates on the primary findings of this thesis, placing them in a broader perspective and discussing their clinical relevance, with particular emphasis on the importance of establishing a strong collaboration between the ophthalmologist and geneticist for providing appropriate medical care and pursuing scientific research regarding familial macular diseases.

6.1 Primary findings and clinical implications

6.1.1 Differential diagnosis in familial macular diseases

Given the phenotypic heterogeneity of AMD, several other macular disorders have characteristics similar to AMD and can therefore be confused with the diagnosis AMD (**Chapter 2**). This overlap in clinical presentation may suggest related underlying molecular mechanisms and can therefore aid in the understanding of the pathogenesis of AMD. On the other hand, because macular dystrophies and AMD differ in several important aspects, including age at onset, visual prognosis, and inheritance pattern, the ability to reliably distinguish between these entities is extremely important. Monogenic macular dystrophies are caused by the inheritance of rare, highly penetrant genetic variants (often referred to as mutations); these macular dystrophies generally present at an earlier age than multifactorial diseases such as AMD. On the other hand, because AMD is a multifactorial disease, its onset is associated with non-genetic (i.e., environmental) factors and a combination of several common genetic variants. However, some AMD patients carry rare, highly penetrant genetic variants, and these patients differ clinically from AMD patients who do not carry such rare genetic variants (see **Chapter 3.1**), as they have a significantly earlier age at onset (**Figure 6.1**).^{1,2}



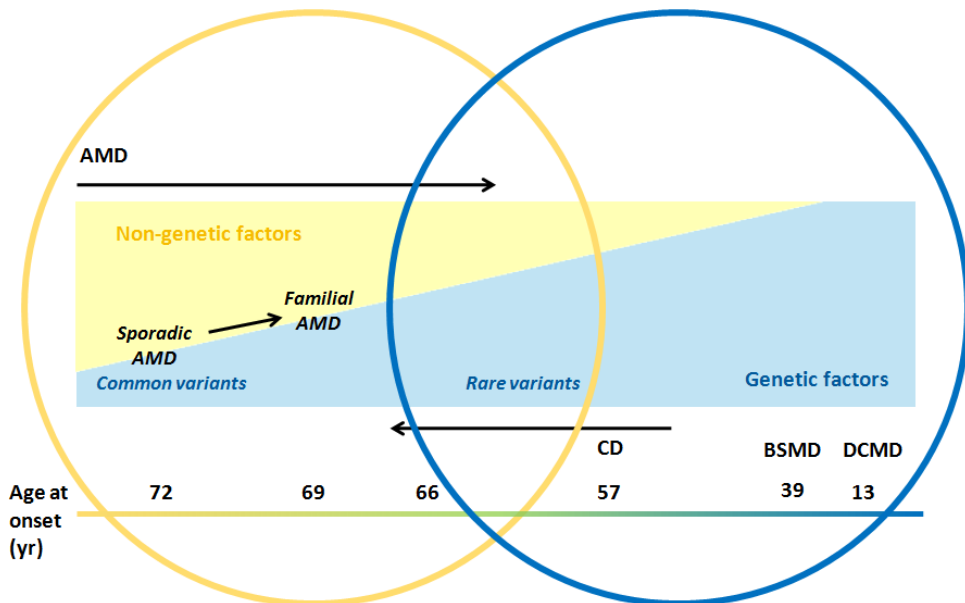


Figure 6.1 Contribution of non-genetic (i.e., environmental) and genetic factors in sporadic and familial age-related macular degeneration (AMD), cuticular drusen, and inherited macular dystrophies. Age-related macular degeneration (AMD) is a multifactorial disease caused by both non-genetic and genetic factors. In patients with a positive family history for AMD (familial AMD) and patients with cuticular drusen (CD), a subtype of AMD, genetic factors play a more important role than in sporadic AMD patients. In contrast to AMD, dominant cystoid macular dystrophy (DCMD) and butterfly-shaped pigment dystrophy (BSPD) are monogenic macular dystrophies with autosomal dominant inheritance. AMD patients with a positive family history have a significantly earlier onset of first symptoms than sporadic patients. The presence of a rare variant in the CFI, C9, or C3 gene results in a lower age at onset in AMD patients, and a rare variant in the CFH gene results in an earlier onset in patients with CD. This is consistent with the general finding of an inverse correlation between the degree to which genetics contributes to a disease and its age at onset. Therefore, monogenic diseases such as BSPD and DCMD are early-onset diseases, whereas multifactorial AMD is a late-onset disease.

6.1.2 Phenotype and genotype

AMD is a highly prevalent multifactorial degenerative disease of the macula that arises from a complex interaction between genetic susceptibility variants, environmental factors, and age-associated changes in the retina, retinal pigment epithelium (RPE), and choroid.³⁻⁶ Unlike inherited macular dystrophies—in which a highly penetrant mutation is the primary cause of the disease—several genetic variants are associated to a greater or lesser extent with the development of AMD (**Figure 6.1**). The extent to which genetic factors play a role in the development of AMD is generally correlated with the phenotype and the individual's family history of AMD (**Figure 6.1 and 6.2**). Studies have shown that related family members can present with strikingly similar phenotypes.^{7,8} In addition, we found a significantly higher prevalence of geographic atrophy (GA) in patients with familial AMD than in patients with sporadic AMD (**Chapter 3.1**). This finding suggests that genetics may play a larger role in

the development of GA than in the development of choroidal neovascularization (CNV). This notion is supported by the higher prevalence of non-exudative AMD compared to neovascular AMD in twins studied by Gottfredsdottir et al.⁷ On the other hand, neovascular AMD can also have high concordance in twins.⁹

Patients with familial AMD also present more frequently with cuticular drusen (**Chapter 3.1**), a subtype of AMD that often runs in families and has a relatively early age at onset. The cuticular drusen phenotype is more strongly associated with the *CFH* Y402H variant than AMD without cuticular drusen, whereas smoking is more strongly associated with the AMD phenotype without cuticular drusen.¹⁰ This is also the case for several environmental risk factors, which have a lower association with familial AMD than with sporadic AMD (**Figure 6.2**).

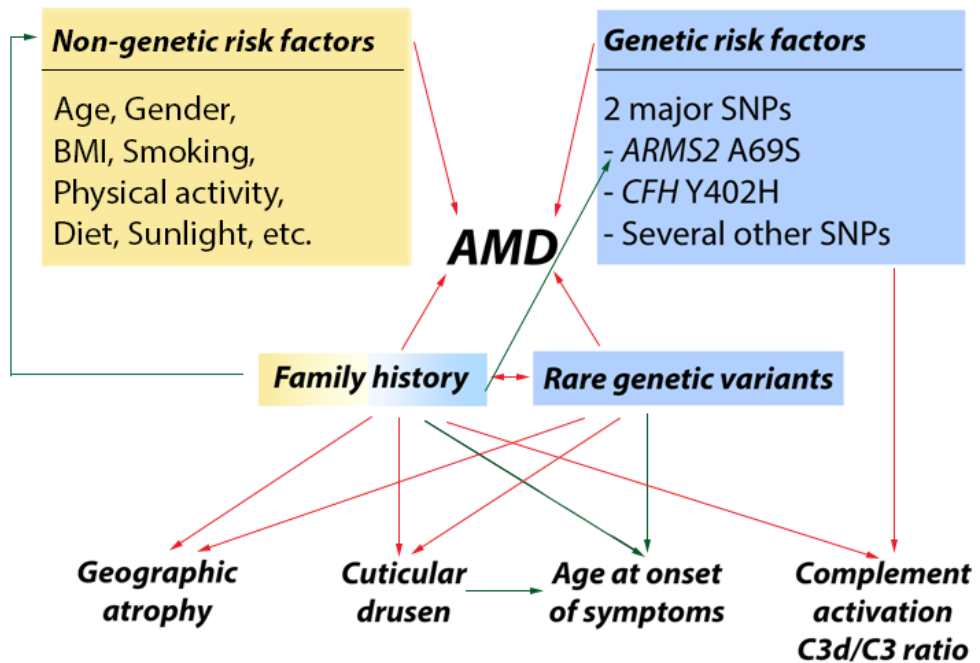


Figure 6.2 Schematic summary of the primary findings in this thesis with respect to familial AMD, showing the complex interplay between positive family history and rare genetic variants with risk factors and phenotypic characteristics. AMD is caused by a combination of both genetic and non-genetic factors. A positive family history for AMD results in a lower risk effect of several environmental risk factors and the *ARMS2* SNP. Patients carrying a rare variant in a complement gene (*CFH*, *CFI*, *C9*, or *C3*) frequently have a positive family history; however, thus far a rare genetic variant has been identified in only a minority of families with AMD. Patients with a positive family history and patients who carry a rare genetic variant are more likely to have geographic atrophy and cuticular drusen, and they may have higher levels of complement activation (i.e., a higher C3d/C3 ratio). The red arrows indicate an increased effect, and the green arrows indicate a decreased effect. BMI = body mass index; AMD = age-related macular degeneration; SNPs = single nucleotide polymorphisms



In contrast, the relatively common *ARMS2* SNP A69S, which confers a higher risk of developing CNV than GA,¹¹⁻¹³ is associated more strongly with sporadic AMD than familial AMD (**Chapter 3.3**). In addition to the previously identified rare variants in the *CFH*, *CFI*, *C9*, and *C3* complement genes,¹⁴⁻¹⁷ we also identified several novel, rare variants in the *CFH* gene (**Chapter 3.5**), and we demonstrated that rare variants are more common among individuals with a positive family history than among patients with sporadic AMD (**Figure 6.2**). Although several rare genetic variants that confer a high risk of AMD have been identified in familial AMD patients, most of these rare variants did not completely segregate within the families (**Chapter 3.4**). Together, these findings indicate that even in densely affected families, AMD is not strictly monogenic, but is also a multifactorial disease, with genetic factors playing a strong—but not exclusive—role.

The estimated heritability of AMD ranges from 45% (for early-stage disease) up to 70% (for advanced-stage disease).¹⁸ Many AMD-associated SNPs have been identified, and together these SNPs can account for up to 65% of AMD heritability.^{12,19} Furthermore, several rare genetic variants have been identified in AMD.^{14, 15, 20} Compared to common genetic variants, rare variants are more likely to play a causal role and may have a larger functional impact. Consequently, these rare genetic variants may offer more insight into disease pathophysiology and may provide more suitable targets for new therapies.²¹ Additional genetics research in AMD patients and families will likely reveal additional rare variants, thus explaining some of the currently ‘missing’ heritability. Gene-environment interactions and other genetic factors—for example, copy number variation, mitochondrial sequence variations, and epigenetics—may also play a role in the development of AMD;²² however, little is currently known regarding these putative additional genetic factors. Epigenetics refers to heritable modifications in gene activity due to a change in genomic structure and function without a change in the DNA sequence itself. Epigenetic mechanisms that regulate gene expression include DNA methylation, histone modifications, and microRNAs (small non-coding RNAs).^{22, 23} These mechanisms regulate gene transcription in a variety of ways, for example by affecting DNA accessibility, recruiting DNA-binding proteins, and post-transcriptional downregulation of gene expression.²³ Thus, epigenetic mechanisms may be a mechanistic link between environmental risk factors and the development of AMD,²⁴ and they may explain how interactions between genetics and the environment give rise to particular phenotypes.²² Although epigenetics may explain some of the remaining heritability, the extent to which these epigenetic effects contribute to AMD is currently unknown.

6.1.3 AMD risk prediction

The ability to accurately predict the risk of developing AMD is important in genetic counseling, particularly for individuals with affected family members. In addition, prediction models can help identify the high-risk patients who will benefit most from newly emerging preventive and therapeutic strategies. Furthermore, predictive tests can identify patients

who do not carry the known genetic risk factors and may therefore benefit from additional genetic testing in order to identify the underlying genetic cause(s).

Several commercial tests that assess the risk of developing advanced AMD are (or have been) available on the market. These tests are based on several common genetic risk factors (i.e., SNPs) and in some cases are used in combination with demographic data. However, these commercial prediction tests have only limited value and are not yet suitable for clinical applications in the general population,²⁵ as it is currently not possible to prevent the development of early or intermediate AMD. Nutritional supplements of the Age-Related Eye Disease Study (AREDS) formulation only prevent the progression to advanced AMD in AMD patients with extensive intermediate or large drusen, or in patients with advanced AMD in one eye.²⁶ Therefore, clinicians are confounded with respect to giving advice to individuals who have a high risk of developing advanced AMD but do not meet these clinical criteria.²⁵ Population-based risk prediction for AMD may become more justifiable if a preventive therapy becomes available, particularly if this therapy is suitable for all high-risk individuals. Additionally, population-based risk prediction will be more suitable for clinical use with the introduction of a preventive intervention that goes beyond good health practices (like quitting smoking, eating a balanced diet, exercising regularly, and taking nutritional supplements) and includes risk and cost elements that limit this intervention to individuals with increased risk.

In general, the relatives of patients with familial AMD tend to ask the most questions regarding their risk of developing AMD, as they are directly confronted with the disease and their family members' visual impairment. Although a positive family history is a significant risk factor for developing AMD, most research-based and commercial prediction models do not take family history into account; rather, they are based only on demographics, environmental factors, and common SNPs. Thus, patients who will develop AMD due to other factors (e.g., rare genetic variants, which play an important role in the development of AMD in (part of the) cases of familial AMD) will be missed by these models (**Chapter 3.4**). Incorporating family history into these AMD risk prediction tests will therefore improve their accuracy.

Previous studies have shown that including an extended set of genetic variants can improve a model's predictive ability.²⁷ Optimal prediction models currently have an area under the curve of 0.80-0.90, which is highly predictive but far from perfect.^{27,28} Adding rare genetic variants in addition to demographic, environmental, and common genetic factors may further refine personalized risk prediction.^{25,28} However, testing for rare genetic variants in prediction models may be problematic, as the occurrence of these variants may be limited to specific geographic regions and/or populations, or may even be specific to one family, making it difficult to determine their effect size for developing AMD. The prevalence of four rare variants in complement genes was considerably lower in the general AMD population compared to densely affected families with AMD (**Chapter 3.4**). Therefore, although rare variants may not account for a large percentage of AMD risk in the overall population, they



can have a strong effect on the risk of developing AMD in certain individuals and in AMD families, for whom the ability to predict AMD risk is highly desirable.²¹

The number of siblings and/or parents with AMD can also provide important information regarding one's risk of developing AMD. For example, belonging to a large, densely affected family markedly increases an individual's risk of AMD (**Chapter 3.2**). When a subject has three or more first-degree relatives with AMD, we found that adding SNP analyses to a model that already includes the subject's extended family history and several non-genetic factors does not increase the model's predictive value. This finding suggests that the risk effect of common SNPs may be smaller in familial AMD than in sporadic AMD, as suggested by the inverse interaction between family history and the major *ARMS2* allele (**Chapter 3.3**), and/or may indicate that the risk conferred by common variants is already included in the risk of a positive family history. Therefore, analyzing common AMD-associated risk SNPs may not be necessary in order to predict AMD risk in members of families with many affected relatives.

6.2 Future perspectives

6.2.1 Preventive and therapeutic options for AMD

6.2.1.1 Nutritional supplements

Nutritional supplements of the AREDS formulation (containing vitamin C, vitamin E, zinc, copper, lutein, and zeaxanthin) have been shown to reduce the risk of progressing to advanced AMD in high-risk patients by approximately 25%.²⁶ These high-risk patients had AREDS category 3 (intermediate AMD) or category 4 (unilateral advanced AMD) in at least one eye. The preventive effect of such nutritional supplements may depend on the patient's genotype,^{29,30} although this is somewhat controversial.³¹ Studies suggest that strong genetic predisposition to AMD conferred by the presence of two risk alleles in the *CFH* gene limits the benefits available from (supplements containing) zinc.^{29, 30} On the other hand, Chew et al.^{31,32} failed to confirm this interaction between genotype and the preventive effect of nutritional supplements in a replication and residual cohort, demonstrating that AREDS supplements reduced the rate of AMD progression in all genotype groups.

The Rotterdam Study found that high dietary intake of zinc and nutrients with antioxidant properties reduces the risk of early AMD selectively in patients with high genetic risk based on the presence of two *CFH* risk alleles and at least one *ARMS2* risk allele.³³ If future research can replicate these results, they may have clinical implications in terms of providing personalized medicine based on genotype-specific prevention. Because patients with familial AMD and unaffected family members have a higher frequency of the *CFH* Y402H and *ARMS2* A69S risk alleles than sporadic individuals (**Chapter 3.3**), these results suggest that consuming high amounts of zinc and nutrients with antioxidant properties can reduce the risk of developing AMD, particularly in individuals with a positive family history. Further research is needed in order to determine the beneficial effects of taking

antioxidants and zinc in familial subjects with a high genetic risk with respect to the ability to reduce their risk of developing early AMD and/or progressing to advanced AMD.

Recent studies indicate that nutritional supplements may affect the complement system, which plays a central role in the pathogenesis of AMD; for example, taking lutein supplements decreases levels of the complement activation products C5a and C3d in the serum.³⁴ In addition, zinc supplements decrease both C5a levels and the C3d/C3 ratio in AMD patients with elevated complement activation.³⁵ Rare variants in complement genes are more common among patients with familial AMD compared to sporadic AMD, (**Chapter 3.4**), and complement activation seems to play a more important role in the development of familial AMD (**Chapter 3.3**). Therefore, nutritional supplements may have a larger preventive effect in familial AMD than in sporadic AMD, making familial subjects particularly valuable for testing the effects of supplements. However, it will be challenging to prove such effects at a statistically significant level, since a large cohort size would be required.

Because AREDS nutritional supplements have been shown to reduce the risk of progressing to advanced AMD, and because subjects with a positive family history of advanced AMD have a ten-fold higher risk of developing advanced AMD than sporadic subjects,³⁶ individuals with familial AMD should be advised to take these nutritional supplements.

6.2.1.2 Complement modulation

The complement system plays an important role in the pathogenesis of AMD and is therefore a promising target for preventive and/or therapeutic interventions. The major *CFH* Y402H SNP is strongly associated with atrophic AMD,¹² and rare variants in complement genes were most often present in AMD patients with GA (**Chapter 3.4**), suggesting a strong association between the complement system and the development of GA. Currently, no therapy is available for treating or preventing GA, and therefore the development of treatments for GA is of great importance.

The complement system is a complex cascade that is tightly controlled by specific regulatory proteins and affects a wide range of target pathways (**Figure 6.3**). The complement system can be modulated by targeting these regulatory components.³⁷⁻⁴³ Several strategies for modulating complement activation in patients with GA are currently being evaluated in both clinical and pre-clinical trials.^{44, 45} Preliminary studies have been rather disappointing;^{37, 46} however, a phase II trial evaluating the effect of an antibody that blocks complement factor D (a regulator of the alternative complement pathway) has shown promising results in terms of inhibiting systemic complement activity and reducing the progression of GA.^{45, 47}



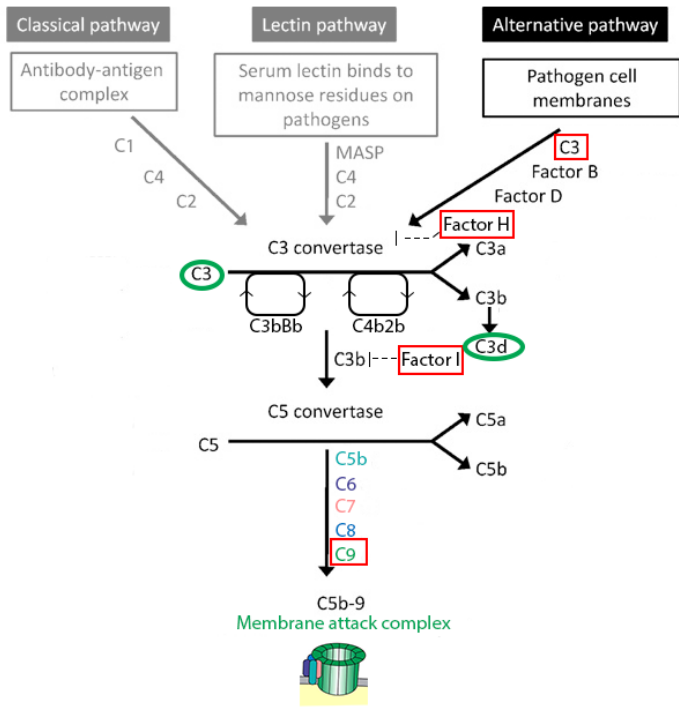


Figure 6.3 The complement system is a tightly regulated cascade that plays an important role in the pathogenesis of AMD. Several complement components have been identified in drusen, the hallmark of AMD. Moreover, the C3d/C3 ratio, a measure of complement activation, is elevated in AMD patients. In addition, many AMD-associated SNPs and rare genetic variants are located in genes that encode complement components. In this thesis, we focused on the C3d/C3 ratio (circled in green) and the presence of rare variants in the complement factor H (CFH), complement factor I (CFI), component 9 (C9), and component 3 (C3) genes (red boxes).

In addition to searching for new therapeutic options, researchers must determine in which patients—and at which disease stage—newly developed therapeutic options will provide the greatest benefit, thereby facilitating the implementation of personalized medicine.⁴⁴ The relatively high frequency of rare variants in complement genes among familial AMD patients—coupled with our finding that increased complement activation is more strongly associated with familial AMD than sporadic AMD—suggests that familial individuals may benefit most from complement-modulating therapies. Because many years of chronic local complement activation likely underlies the formation of drusen (and their associated complications in AMD), complement inhibitors are probably most effective after prolonged administration and before the disease has developed to an advanced stage. Individuals in families with AMD generally present early in the course of the disease due to their increased risk and their increased awareness of disease-associated visual symptoms. Therefore, in addition to reducing environmental risk factors (for example, by quitting

smoking, increasing physical activity, and eating a balanced diet, all of which will benefit all individuals, regardless of their family history), inhibiting the complement system in individuals with a family history of AMD may be more effective when started before the onset of irreversible visual loss.

Because the complement system is an essential component of the innate immune system, chronic treatment with complement inhibitors may increase one's susceptibility to infections. Therefore, in order to justify pharmaceutical modulation of the complement system in patients with early AMD, the likelihood of progressing to advanced AMD needs to be predicted with high accuracy, thus balancing the benefits against any possible adverse effects. This emphasizes the high importance of developing models that accurately predict progression to advanced AMD.

6.2.2 Genetics and therapeutic options for dominant cystoid macular dystrophy

We proposed a classification system for DCMD in which the disease can be classified into three stages, which correlated with age and visual acuity. Currently available treatment options for patients with DCMD are limited to carbonic anhydrase inhibitors, such as acetazolamide, and octreotide acetate, which reduce cystoid fluid collections, and the treatment of DCMD-associated complications such as angle-closure glaucoma (**Chapter 4**). Although the causative genetic mutation and the identity of the gene at the DCMD locus have not yet been identified, genetic testing of polymorphic markers at the DCMD locus can be used to confirm the diagnosis and allows for genetic counseling of family members who may be currently asymptomatic, as we observed that the disease haplotype at the DCMD locus has complete penetrance. Moreover, although the disease can potentially be prevented by taking steps to avoid passing the affected allele to the offspring, this approach has complicated ethical considerations. Nevertheless, identifying the causative gene can provide important clues regarding the pathogenesis of DCMD and may improve our understanding of the pathophysiological pathways underlying other diseases with cystoid macular edema, including retinal dystrophies, uveitis, diabetic macular edema, and after ophthalmic surgery. Identifying the affected gene and the downstream pathway may ultimately lead to the development of new treatment strategies that address the primary molecular defect underlying DCMD.

6.2.3 Genetics and therapeutic options in butterfly-shaped pigment dystrophy

Butterfly-shaped pigment dystrophy (BSPD) is inherited in an autosomal dominant fashion, and only in a fraction of patients a mutation in the *PRPH2* gene is identified.⁴⁸ Genetic counseling is only possible for relatives of patients who have an identified genetic cause. Therefore, our identification of mutations in the *CTNNA1* gene (**Chapter 5**) in BSPD patients who do not carry a mutation in the *PRPH2* gene is an important finding. However, only three of our 19 BSPD patients carry a mutation in the *CTNNA1* gene, thus explaining only a small fraction of these patients. Further research is needed in order to identify the genetic cause



of BSPD in patients who do not carry a mutation in either the *PRPH2* gene or the *CTNNA1* gene. Nevertheless, identifying the disease mechanism underlying *CTNNA1* mutations may provide important insight into the pathogenesis of BSPD and other RPE dystrophies and may ultimately lead to the development of new treatment strategies.

6.2.4 Gene-based therapy

Significant progress has been made towards understanding the genetic pathogenesis of retinal diseases, and ocular gene therapy research has improved the safety and specificity of vector-based ocular gene transfer methods, providing a major step forward in the development of gene replacement therapy.⁴⁹ The ultimate goal of gene replacement therapy is to replace the mutated gene with a fully functional gene, leading to normal levels of functional protein. In diseases caused by a loss-of-function mutation, which are common for autosomal recessive and X-linked disorders, introducing a normal copy of the missing or defective gene can provide cells with normal functioning proteins. The safety and putative efficacy of gene therapy strategies have been demonstrated in autosomal recessive Leber congenital amaurosis and X-linked choroideremia.⁵⁰⁻⁵² However, in the case of mutations that cause a gain-of-function or dominant-negative effect (for example, in most autosomal dominant diseases, perhaps including the DCMD and BSPD phenotypes described in this thesis), the mutant allele must be silenced in order to restore function.⁵³

Our identification of mutations in the *CTNNA1* gene in a subset of patients with BSPD (**Chapter 5**) together with the future identification of the causative gene in DCMD will likely provide gene-based therapeutic targets for treating these autosomal dominant macular dystrophies. Interestingly, a role for gene therapy has even been suggested for multifactorial AMD, as virus-encoded RNA-interference effector molecules can silence endogenous VEGF gene expression, thereby inhibiting neovascularization.^{54, 55} In advanced disease stages in which significant, irreversible retinal structural damage has already occurred (for example, in stage 3 DCMD and fovea-involving GA), replacing photoreceptors and/or RPE cells using stem cell therapy, an approach currently being tested at the experimental phase, may provide a promising therapeutic option in the future.^{49, 56, 57} Other artificial vision-restoring strategies such as electronic retinal implants are also being developed and may become available after future improvements for use in patients with severe visual impairment due to inherited macular diseases.⁵⁸

6.2.5 The importance of close collaboration between ophthalmology and genetics

Unraveling the genetic causes of retinal diseases and the emerging availability of advanced genetic sequencing techniques can help ophthalmologists to establish the correct clinical diagnosis. Therefore, a close collaboration between ophthalmologists and geneticists is essential for establishing procedures for diagnosing inherited eye diseases. In addition, genetic testing will likely be incorporated into personalized medicine in the future, as the onset of AMD, the progression of AMD to advanced stages, and the patient's treatment

response may depend on the patient's unique genotype with respect to several AMD risk-associated genes.^{13, 59-68}

Optimal personalized healthcare requires a complete overview of the patient's environmental, clinical, and genetic profile during diagnosis, during the course of the disease, and when evaluating therapeutic procedures. Therefore, combining the expertise of ophthalmologists with the power of genetics is essential in both patient care and scientific research.



REFERENCES

1. Shahid H, Khan JC, Cipriani V, et al. Age-related macular degeneration: the importance of family history as a risk factor. *Br J Ophthalmol* 2012;96:427-431.
2. Raychaudhuri S, Iartchouk O, Chin K, et al. A rare penetrant mutation in CFH confers high risk of age-related macular degeneration. *Nat Genet* 2011;43:1232-1236.
3. Hageman GS, Luthert PJ, Victor Chong NH, Johnson LV, Anderson DH, Mullins RF. An integrated hypothesis that considers drusen as biomarkers of immune-mediated processes at the RPE-Bruch's membrane interface in aging and age-related macular degeneration. *Prog Retin Eye Res* 2001;20:705-732.
4. Huang JD, Presley JB, Chimento MF, Curcio CA, Johnson M. Age-related changes in human macular Bruch's membrane as seen by quick-freeze/deep-etch. *Exp Eye Res* 2007;85:202-218.
5. Jager RD, Mieler WF, Miller JW. Age-related macular degeneration. *N Engl J Med* 2008;358:2606-2617.
6. Swaroop A, Chew EY, Rickman CB, Abecasis GR. Unraveling a multifactorial late-onset disease: from genetic susceptibility to disease mechanisms for age-related macular degeneration. *Annu Rev Genomics Hum Genet* 2009;10:19-43.
7. Gottfredsdottir MS, Sverrisson T, Musch DC, Stefansson E. Age related macular degeneration in monozygotic twins and their spouses in Iceland. *Acta Ophthalmol Scand* 1999;77:422-425.
8. Klein ML, Mauldin WM, Stoumbos VD. Heredity and age-related macular degeneration. Observations in monozygotic twins. *Arch Ophthalmol* 1994;112:932-937.
9. Melrose MA, Magargal LE, Lucier AC. Identical twins with subretinal neovascularization complicating senile macular degeneration. *Ophthalmic Surg* 1985;16:648-651.
10. van de Ven JP, Smailhodzic D, Boon CJ, et al. Association analysis of genetic and environmental risk factors in the cuticular drusen subtype of age-related macular degeneration. *Mol Vis* 2012;18:2271-2278.
11. Sobrin L, Reynolds R, Yu Y, et al. ARMS2/HTRA1 locus can confer differential susceptibility to the advanced subtypes of age-related macular degeneration. *Am J Ophthalmol* 2011;151:345-352 e343.
12. Fritsche LG, Chen W, Schu M, et al. Seven new loci associated with age-related macular degeneration. *Nat Genet* 2013;45:433-439, 439e431-432.
13. Seddon JM, Francis PJ, George S, Schultz DW, Rosner B, Klein ML. Association of CFH Y402H and LOC387715 A69S with progression of age-related macular degeneration. *Jama* 2007;297:1793-1800.
14. van de Ven JP, Nilsson SC, Tan PL, et al. A functional variant in the CFI gene confers a high risk of age-related macular degeneration. *Nat Genet* 2013;45:813-817.
15. Seddon JM, Yu Y, Miller EC, et al. Rare variants in CFI, C3 and C9 are associated with high risk of advanced age-related macular degeneration. *Nat Genet* 2013;45:1366-1370.
16. Duvvari MR, Paun CC, Buitendijk GH, et al. Analysis of rare variants in the C3 gene in patients with age-related macular degeneration. *PLoS One* 2014;9:e94165.
17. Helgason H, Sulem P, Duvvari MR, et al. A rare nonsynonymous sequence variant in C3 is associated with high risk of age-related macular degeneration. *Nat Genet* 2013;45:1371-1374.
18. Seddon JM, Cote J, Page WF, Aggen SH, Neale MC. The US twin study of age-related macular degeneration: relative roles of genetic and environmental influences. *Arch Ophthalmol* 2005;123:321-327.
19. Maller J, George S, Purcell S, et al. Common variation in three genes, including a noncoding variant in CFH, strongly influences risk of age-related macular degeneration. *Nat Genet* 2006;38:1055-1059.

20. Boon CJ, Klevering BJ, Hoyng CB, et al. Basal laminar drusen caused by compound heterozygous variants in the CFH gene. *Am J Hum Genet* 2008;82:516-523.
21. Sobrin L, Seddon JM. Nature and nurture- genes and environment- predict onset and progression of macular degeneration. *Prog Retin Eye Res* 2014;40:1-15.
22. Gemenetzi M, Lotery AJ. The role of epigenetics in age-related macular degeneration. *Eye (Lond)* 2014.
23. Liu MM, Chan CC, Tuo J. Epigenetics in ocular diseases. *Curr Genomics* 2013;14:166-172.
24. Jirtle RL, Skinner MK. Environmental epigenomics and disease susceptibility. *Nat Rev Genet* 2007;8:253-262.
25. Buitendijk GH, Amin N, Hofman A, van Duijn CM, Vingerling JR, Klaver CC. Direct-to-consumer personal genome testing for age-related macular degeneration. *Invest Ophthalmol Vis Sci* 2014;55:6167-6174.
26. Age-Related Eye Disease Study Research G. A randomized, placebo-controlled, clinical trial of high-dose supplementation with vitamins C and E, beta carotene, and zinc for age-related macular degeneration and vision loss: AREDS report no. 8. *Arch Ophthalmol* 2001;119:1417-1436.
27. Buitendijk GH, Rochtchina E, Myers C, et al. Prediction of age-related macular degeneration in the general population: the Three Continent AMD Consortium. *Ophthalmology* 2013;120:2644-2655.
28. Seddon JM, Reynolds R, Yu Y, Rosner B. Three new genetic loci (R1210C in CFH, variants in COL8A1 and RAD51B) are independently related to progression to advanced macular degeneration. *PLoS One* 2014;9:e87047.
29. Klein ML, Francis PJ, Rosner B, et al. CFH and LOC387715/ARMS2 genotypes and treatment with antioxidants and zinc for age-related macular degeneration. *Ophthalmology* 2008;115:1019-1025.
30. Awh CC, Hawken S, Zanke BW. Treatment Response to Antioxidants and Zinc Based on CFH and ARMS2 Genetic Risk Allele Number in the Age-Related Eye Disease Study. *Ophthalmology* 2015;122:162-169.
31. Chew EY, Klein ML, Clemons TE, Agron E, Abecasis GR. Genetic Testing in Persons with Age-Related Macular Degeneration and the Use of the AREDS Supplements: To Test or Not to Test? *Ophthalmology* 2015;122:212-215.
32. Chew EY, Klein ML, Clemons TE, et al. No Clinically Significant Association between CFH and ARMS2 Genotypes and Response to Nutritional Supplements: AREDS Report Number 38. *Ophthalmology* 2014;121:2173-2180.
33. Ho L, van Leeuwen R, Witteman JC, et al. Reducing the genetic risk of age-related macular degeneration with dietary antioxidants, zinc, and omega-3 fatty acids: the Rotterdam study. *Arch Ophthalmol* 2011;129:758-766.
34. Tian Y, Kijlstra A, van der Veen RL, Makridaki M, Murray IJ, Berendschot TT. The effect of lutein supplementation on blood plasma levels of complement factor D, C5a and C3d. *PLoS One* 2013;8:e73387.
35. Smailhodzic D, van Asten F, Blom AM, et al. Zinc supplementation inhibits complement activation in age-related macular degeneration. *PLoS One* 2014;9:e112682.
36. Klein BE, Klein R, Lee KE, Moore EL, Danforth L. Risk of incident age-related eye diseases in people with an affected sibling: The Beaver Dam Eye Study. *Am J Epidemiol* 2001;154:207-211.
37. Garcia Filho CA, Yehoshua Z, Gregori G, et al. Change in drusen volume as a novel clinical trial endpoint for the study of complement inhibition in age-related macular degeneration. *Ophthalmic surgery, lasers & imaging retina* 2014;45:18-31.
38. Do DV, Pieramici DJ, van Lookeren Campagne M, et al. A phase ia dose-escalation study of the anti-factor D monoclonal antibody fragment FCFD4514S in patients with geographic atrophy. *Retina* 2014;34:313-320.



39. Pauly D, Nagel BM, Reinders J, et al. A novel antibody against human properdin inhibits the alternative complement system and specifically detects properdin from blood samples. *PLoS One* 2014;9:e96371.
40. Biesecker G, Dihel L, Enney K, Bendele RA. Derivation of RNA aptamer inhibitors of human complement C5. *Immunopharmacology* 1999;42:219-230.
41. Murray-Rust TA, Kerr FK, Thomas AR, et al. Modulation of the proteolytic activity of the complement protease C1s by polyanions: implications for polyanion-mediated acceleration of interaction between C1s and SERPING1. *Biochem J* 2009;422:295-303.
42. Cicardi M, Zingale L, Zanichelli A, Pappalardo E, Cicardi B. C1 inhibitor: molecular and clinical aspects. *Springer Semin Immunopathol* 2005;27:286-298.
43. Kohl J. Drug evaluation: the C5a receptor antagonist PMX-53. *Curr Opin Mol Ther* 2006;8:529-538.
44. Holz FG, Strauss EC, Schmitz-Valckenberg S, van Lookeren Campagne M. Geographic atrophy: clinical features and potential therapeutic approaches. *Ophthalmology* 2014;121:1079-1091.
45. Weber BH, Charbel Issa P, Pauly D, Herrmann P, Grassmann F, Holz FG. The role of the complement system in age-related macular degeneration. *Dtsch Arztebl Int* 2014;111:133-138.
46. Yehoshua Z, de Amorim Garcia Filho CA, Nunes RP, et al. Systemic complement inhibition with eculizumab for geographic atrophy in age-related macular degeneration: the COMPLETE study. *Ophthalmology* 2014;121:693-701.
47. Loyet KM, Good J, Davancaze T, et al. Complement inhibition in cynomolgus monkeys by anti-factor d antigen-binding fragment for the treatment of an advanced form of dry age-related macular degeneration. *J Pharmacol Exp Ther* 2014;351:527-537.
48. Boon CJ, den Hollander AI, Hoyng CB, Cremers FP, Klevering BJ, Keunen JE. The spectrum of retinal dystrophies caused by mutations in the peripherin/RDS gene. *Prog Retin Eye Res* 2008;27:213-235.
49. Stieger K, Cronin T, Bennett J, Rolling F. Adeno-associated virus mediated gene therapy for retinal degenerative diseases. *Methods Mol Biol* 2011;807:179-218.
50. Bainbridge JW, Smith AJ, Barker SS, et al. Effect of gene therapy on visual function in Leber's congenital amaurosis. *N Engl J Med* 2008;358:2231-2239.
51. Hauswirth WW, Aleman TS, Kaushal S, et al. Treatment of leber congenital amaurosis due to RPE65 mutations by ocular subretinal injection of adeno-associated virus gene vector: short-term results of a phase I trial. *Hum Gene Ther* 2008;19:979-990.
52. Maguire AM, Simonelli F, Pierce EA, et al. Safety and efficacy of gene transfer for Leber's congenital amaurosis. *N Engl J Med* 2008;358:2240-2248.
53. Sundaram V, Moore AT, Ali RR, Bainbridge JW. Retinal dystrophies and gene therapy. *Eur J Pediatr* 2012;171:757-765.
54. Askou AL. Development of gene therapy for treatment of age-related macular degeneration. *Acta Ophthalmol* 2014;92 Thesis3:1-38.
55. Cashman SM, Ramo K, Kumar-Singh R. A non membrane-targeted human soluble CD59 attenuates choroidal neovascularization in a model of age related macular degeneration. *PLoS One* 2011;6:e19078.
56. West EL, Pearson RA, MacLaren RE, Sowden JC, Ali RR. Cell transplantation strategies for retinal repair. *Prog Brain Res* 2009;175:3-21.
57. Pan CK, Heilweil G, Lanza R, Schwartz SD. Embryonic stem cells as a treatment for macular degeneration. *Expert Opin Biol Ther* 2013;13:1125-1133.
58. Winter JO, Cogan SF, Rizzo JF, 3rd. Retinal prostheses: current challenges and future outlook. *J Biomater Sci Polym Ed* 2007;18:1031-1055.

59. Francis PJ, Hamon SC, Ott J, Weleber RG, Klein ML. Polymorphisms in C2, CFB and C3 are associated with progression to advanced age related macular degeneration associated with visual loss. *J Med Genet* 2009;46:300-307.
60. Klein ML, Ferris FL, 3rd, Francis PJ, et al. Progression of geographic atrophy and genotype in age-related macular degeneration. *Ophthalmology* 2010;117:1554-1559, 1559 e1551.
61. Caire J, Recalde S, Velazquez-Villoria A, et al. Growth of geographic atrophy on fundus autofluorescence and polymorphisms of CFH, CFB, C3, FHR1-3, and ARMS2 in age-related macular degeneration. *JAMA Ophthalmology* 2014;132:528-534.
62. Dietzel M, Pauleikhoff D, Arning A, et al. The contribution of genetic factors to phenotype and progression of drusen in early age-related macular degeneration. *Graefes Arch Clin Exp Ophthalmol* 2014;252:1273-1281.
63. Abedi F, Wickremasinghe S, Richardson AJ, Islam AF, Guymer RH, Baird PN. Genetic influences on the outcome of anti-vascular endothelial growth factor treatment in neovascular age-related macular degeneration. *Ophthalmology* 2013;120:1641-1648.
64. Finger RP, Wickremasinghe SS, Baird PN, Guymer RH. Predictors of anti-VEGF treatment response in neovascular age-related macular degeneration. *Surv Ophthalmol* 2014;59:1-18.
65. Veloso CE, de Almeida LN, Recchia FM, Pelayes D, Nehemy MB. VEGF gene polymorphism and response to intravitreal ranibizumab in neovascular age-related macular degeneration. *Ophthalmic Res* 2014;51:1-8.
66. Zhao L, Grob S, Avery R, et al. Common variant in VEGFA and response to anti-VEGF therapy for neovascular age-related macular degeneration. *Curr Mol Med* 2013;13:929-934.
67. Brantley MA, Jr., Fang AM, King JM, Tewari A, Kymes SM, Shiels A. Association of complement factor H and LOC387715 genotypes with response of exudative age-related macular degeneration to intravitreal bevacizumab. *Ophthalmology* 2007;114:2168-2173.
68. Kanoff J, Miller J. Pharmacogenetics of the treatment response of age-related macular degeneration with ranibizumab and bevacizumab. *Semin Ophthalmol* 2013;28:355-360.



Chapter 7

Summary / Samenvatting
List of publications
Dankwoord
About the author / PhD portfolio



SUMMARY

Degenerative diseases affecting the macula constitute a major cause of incurable vision loss and exhibit considerable clinical and genetic heterogeneity, ranging from early-onset monogenic diseases such as dominant cystoid macular dystrophy (DCMD) and butterfly-shaped pigment dystrophy (BSPD) to multifactorial late-onset age-related macular degeneration (AMD).

In the Western world, AMD is the most common cause of irreversible vision loss among the elderly. AMD is caused by a combination of demographic, environmental, and genetic risk factors. Despite its multifactorial etiology, AMD can run in families, although little is known regarding the clinical and genetic differences between familial AMD and sporadic AMD. The aim of this thesis is to increase our understanding of the clinical features of AMD and the contribution of environmental and genetic risk factors to the risk of developing AMD in patients with a family history of AMD. This information may provide individuals with more accurate information regarding their unique risk for developing AMD, particularly among relatives of patients with familial AMD, for whom this issue is highly relevant.

Chapter 1 provides a general introduction to the anatomy and function of the retina, the techniques commonly used to evaluate these features, and a brief background regarding the field of molecular genetics. We also describe the clinical and genetic features of AMD, DCMD, and BSPD.

Given its heterogeneous presentation, distinguishing AMD from other macular diseases that mimic the features of AMD can be challenging to clinicians. Importantly, this clinical overlap can potentially lead to misdiagnosis. In **Chapter 2**, we discuss the characteristics of AMD and the macular dystrophies that can mimic AMD, and we present an overview of overlapping and distinguishing clinical features. This information can help clinicians choose the most appropriate clinical and/or genetic tests in order to correctly diagnose patients. Furthermore, it can provide patients with more accurate prognostic information.

Approximately one-third of all patients with AMD have at least one first-degree relative with AMD; in such cases, the patient is diagnosed with familial AMD. In **Chapter 3**, we investigate the importance of having a positive family history of AMD with respect to both the clinical and genetic aspects.

Chapter 3.1 reports that the initial onset of symptoms in patients with familial AMD occurs an average of three years earlier than in patients with sporadic AMD. Although ageing and smoking are associated with both familial and sporadic AMD, low physical activity and daily consumption of red meat are significantly associated with only the sporadic form of AMD. Clinically, both geographic atrophy and cuticular drusen are nearly twice as prevalent among patients with familial AMD compared to patients with sporadic AMD; however, no difference was observed in early, intermediate, and neovascular AMD.



Chapter 3.2 discusses the important role that a positive family history of AMD plays in an individual's risk of developing AMD. Particularly in large, densely affected AMD families the positive family history can have a high impact on the risk of developing AMD. Therefore, we created a model for predicting AMD that includes family history, demographics, and environmental risk factors. This model was found to be valid for predicting both familial AMD and sporadic AMD. Extending the model by incorporating AMD-associated common genetic variants (also known as risk-associated single-nucleotide polymorphisms, or risk SNPs) increased the model's predictive value for sporadic AMD. In contrast, including common SNPs in the risk prediction model had no effect on the predictive value in individuals from AMD families with three or more affected relatives.

In **Chapter 3.3**, we tested two major AMD-associated SNPs (in the *CFH* and *ARMS2* genes), and the results indicate that the major risk SNP in *ARMS2* interacts with positive family history and does not play a role in the development of AMD in patients with familial AMD. In contrast, the levels of complement activation are slightly higher in patients with familial AMD (particularly in subjects with a densely affected family) than in patients with sporadic AMD.

Chapter 3.4 discusses our finding that 6.4% of patients with AMD carry a rare, highly penetrant gene variant in the *CFI*, *C9*, or *C3* gene. The presence of one of these rare variants is associated with a high familial occurrence, as more than half of all patients who carry such a rare variant report a positive family history for AMD, which is significantly more often than among affected non-carriers. However, these rare variants do not segregate fully with AMD in the affected families. Clinically, the initial onset of symptoms in carriers of these rare variants occurs an average of six years earlier than in non-carriers. In addition, these genetic rare variants are more prevalent among patients with advanced AMD and geographic atrophy than in patients with neovascular AMD.

In **Chapter 3.5**, we report that a rare variant in the *CFH* gene is present in 8.8% of patients with the cuticular drusen phenotype of AMD. The age at onset for carriers of this rare *CFH* variant is nine years earlier than among non-carriers.

DCMD is a rare form of macular dystrophy characterized by early-onset cystoid fluid collections, hyperopia, and chorioretinal atrophy. In **Chapter 4**, we present a clinical classification of the DCMD phenotype into three stages based on 97 affected individuals in one large family in the Netherlands. We also discuss therapeutic options and the efficacy of these therapies in reducing cystoid fluid collections in stage 1 and stage 2 patients.

BSPD is another rare macular dystrophy with autosomal dominant inheritance. BSPD has been identified in a large Dutch family. Until recently, BSPD was associated exclusively with mutations in the *PRPH2* gene; however mutations in the *PRPH2* gene—and several other genes commonly associated with retinal disease—were excluded in this family. **Chapter 5** presents the identification of a rare variant in the *CTNNA1* gene in this family; this variant segregates fully with the disease. In addition, variants in this gene have been detected in two other families with BSPD. These variants have also been identified in a

mutant mouse model. The fundi of these mice exhibits yellowish flecks in the center of the retina, and morphological studies revealed that the structure of the retinal pigment epithelium is highly disrupted. The identification of this gene as the cause of the disease aids genetic counseling in families with BSPD.

Chapter 6 provides a general discussion of the main findings in this thesis and their clinical implications. The importance of a positive family history of AMD is described with respect to clinical features, the ability to predict the risk of developing AMD, and the effect of environmental and genetic risk factors. In addition, we describe the clinical implications of a positive family history with respect to nutritional supplements and modulation of the complement system. We also discuss how the identification of new genes associated with macular diseases can improve genetic counseling, facilitate studies of disease pathogenesis, and create opportunities for developing and testing novel therapies. Finally, we discuss the importance of personalized healthcare and the benefits of establishing a close working relationship between clinical ophthalmologists and geneticists in providing medical care.



SAMENVATTING

Degeneratieve ziekten die de macula aantasten vormen een belangrijke oorzaak van onherstelbaar visusverlies. Ze vertonen een aanzienlijke klinische en genetische heterogeniteit, variërend van monogene ziektebeelden die op jonge leeftijd ontstaan, zoals dominante cystoïde macula dystrofie (DCMD) en ‘butterfly-shaped’ pigment dystrofie (BSPD), tot leeftijdsgebonden maculadegeneratie (LMD) welke multifactorieel is en op late leeftijd ontstaat. LMD is de meest voorkomende oorzaak van onherstelbaar visusverlies in de oudere populatie in de Westerse wereld en wordt veroorzaakt door zowel demografische- en omgevingsfactoren als genetische factoren. LMD komt soms voor in families, maar er is weinig bekend over klinische en genetische verschillen tussen familiale en sporadische LMD patiënten. Het doel van dit proefschrift is om inzicht te krijgen in klinische kenmerken en omgevings- en genetische factoren die een rol spelen bij het ontstaan van LMD bij patiënten met een positieve familiegeschiedenis voor LMD. Dit kan in de toekomst mogelijk leiden tot een betere voorspelling van het risico op LMD, in het bijzonder voor familieleden van LMD patiënten, voor wie deze vraag het meest dringend is.

Hoofdstuk 1 dient als een algemene introductie van de anatomie en functie van de retina en de technieken die worden gebruikt om deze zaken te analyseren, evenals een inleiding over genetica. Daarnaast beschrijft het de klinische en genetische aspecten van LMD, DCMD en BSPD.

Door de variabele presentatie van LMD kan het lastig zijn om LMD van diverse maculaire aandoeningen te onderscheiden die op LMD kunnen lijken. Deze klinische overlap kan leiden tot een verkeerde diagnose. In **Hoofdstuk 2** bespreken we de kenmerken van LMD en de maculadystrofieën die op LMD kunnen lijken en wordt een overzicht gepresenteerd van overlappende en onderscheidende klinische kenmerken. Dit helpt oogartsen om de juiste klinische en genetische diagnostische testen te gebruiken om tot de correcte diagnose te komen en om de patiënt van de juiste prognostische informatie te voorzien.

Ongeveer een derde van de LMD patiënten heeft tenminste één (genetisch gezien) eerstegraads familielid met LMD, wat wij definiëren als familiale LMD. In **Hoofdstuk 3** onderzoeken we het belang van een positieve familiegeschiedenis voor LMD en analyseren we klinische en genetische factoren in familiale en sporadische patiënten.

Hoofdstuk 3.1 toont dat de eerste visusklachten bij familiale LMD patiënten drie jaar eerder ontstaan dan bij sporadische patiënten. Hoewel een hogere leeftijd en roken zowel met familiale als met sporadische LMD zijn geassocieerd, zijn verminderde lichaamsbeweging en dagelijkse consumptie van rood vlees alleen met sporadische LMD geassocieerd. Klinische kenmerken zoals geografische atrofie en cuticulaire drusen komen bijna tweemaal zo vaak voor in familiale patiënten als in sporadische patiënten, maar er werd geen verschil gevonden voor vroege, intermediaire en neovasculaire LMD.

Hoofdstuk 3.2 onderzoekt de invloed van een positieve familiegeschiedenis op het risico om LMD te ontwikkelen. Vooral in grote families waarin veel familieleden zijn

aangedaan is een positieve familiegeschiedenis sterk geassocieerd met een verhoogd risico om LMD te ontwikkelen. Op basis hiervan hebben wij een voorspellend model voor het ontwikkelen van LMD ontworpen, waarin naast demografische- en omgevingsfactoren ook de familiegeschiedenis is meegenomen. Het model was toepasbaar op zowel familiale als sporadische individuen en uitbreiding van het model met LMD geassocieerde genetische varianten (SNPs) gaf een betere voorspellende waarde bij sporadische patiënten, maar niet bij personen die drie of meer aangedane familieleden hebben.

In **Hoofdstuk 3.3** zijn de twee belangrijkste LMD-geassocieerde SNPs in *CFH* en *ARMS2* getest. De genetische variant in *ARMS2* vertoont een interactie met een positieve familiegeschiedenis en speelt daarbij geen rol in de ontwikkeling van LMD bij familiale patiënten. Daarentegen lijkt een verhoogde activiteit van het complementsysteem een belangrijkere rol te spelen bij familiale patiënten dan bij sporadische patiënten, met name bij familiale patiënten met veel aangedane familieleden.

Hoofdstuk 3.4 toont de aanwezigheid van drie LMD-geassocieerde zeldzame genetische varianten in het *CFI*-, *C9*- of *C3*-gen in 6,4% van de patiënten met LMD. Deze drie zeldzame genetische varianten komen vaker voor in familiale LMD patiënten en meer dan de helft van de patiënten die een zeldzame genetische variant dragen hebben een positieve familie-anamnese voor LMD. Dit is beduidend meer dan bij patiënten die deze drie zeldzame varianten niet dragen. Deze zeldzame genetische varianten segregeren echter niet volledig met de ziekte in deze families. Bij patiënten die een zeldzame genetische variant dragen starten de visusklachten zes jaar eerder dan bij patiënten zonder een zeldzame genetische variant. Patiënten met geografische atrofie dragen vaker een zeldzame genetische variant dan patiënten met neovasculaire LMD.

In **Hoofdstuk 3.5** presenteren we zeldzame varianten in het *CFH*-gen in 8,8% van de LMD patiënten met het cuticulaire drusen subtype. Bij patiënten met een zeldzame genetische variant in het *CFH*-gen ontstaan de eerste visusklachten negen jaar eerder dan bij patiënten zonder een zeldzame variant.

DCMD is een zeldzame maculadystrofie, gekenmerkt door cystoïde vochtophopingen op jonge leeftijd, hypermetropie en chorioretinale atrofie. In **Hoofdstuk 4** presenteren we een klinische classificatie van het DCMD fenotype in 3 stadia op basis van de bevindingen bij 97 personen uit één grote Nederlandse familie met DCMD. Verder gaan we in op de therapeutische opties en de effectiviteit om de cystoïde vochtophopingen te verminderen in patiënten met stadium 1 en 2 DCMD.

BSPD is ook een zeldzame maculadystrofie, die onder andere voorkomt in een grote Nederlandse familie met een autosomaal dominant overervingspatroon. Tot dusver zijn alleen mutaties in het *PRPH2*-gen geassocieerd met BSPD. Mutaties in dit gen en in diverse andere genen zijn echter uitgesloten in deze Nederlandse BSPD familie. **Hoofdstuk 5** beschrijft de identificatie van een zeldzame variant in het *CTNNA1*-gen, die segregiert met de ziekte in deze familie. Daarnaast hebben we varianten in dit gen gevonden in twee andere families met BSPD en in een gemuteerd muismodel. Deze muizen vertonen gele



vlekken in de centrale retina en morfologische studies tonen een verstoorde structuur van het retinaal pigment epitheel. De identificatie van dit gen als nieuwe genetische oorzaak van deze ziekte kan genetische counseling bij families met BSPD verbeteren.

Hoofdstuk 6 is een algemene discussie van de belangrijkste bevindingen in dit proefschrift en de klinische implicaties daarvan. Het belang van een positieve familiegeschiedenis voor LMD wordt beschreven voor de klinische kenmerken, risico-predictie en voor het effect van omgevingsfactoren en genetische factoren. Vervolgens worden de klinische implicaties voor het gebruik van voedingssupplementen en modulatie van het complementsysteem besproken ten aanzien van een positieve familiegeschiedenis voor LMD. De identificatie van nieuwe genen in aandoeningen van de macula kan genetische counseling en de opheldering van de pathogenese faciliteren en mogelijkheden bieden voor nieuwe therapieën. Tenslotte wordt besproken dat gepersonaliseerde gezondheidszorg de kwaliteit van zorg zal verbeteren, waarbij een goede samenwerking tussen oogartsen en genetici essentieel is.

LIST OF PUBLICATIONS

Mutations in α -catenin 1 cause butterfly-shaped pigment dystrophy and perturbed retinal pigment epithelium integrity.

N.T.M. Saksens, M.P. Krebs, F.E. Schoenmaker-Koller, W. Hicks, M. Yu, L. Shi, L. Rowe, S.J. Letteboer, K. Neveling, T.W. van Moorsel, S. Abu-Ltaif, E. De Baere, S. Walraedt, S. Banfi, F. Simonelli, F.P.M. Cremers, C.J.F. Boon, R. Roepman, B.P. Leroy, N.S. Peachey, C.B. Hoyng, P.M. Nishina, A.I. den Hollander.

Nature Genetics. accepted.

Analysis of risk alleles and complement activation levels in familial and non-familial age-related macular degeneration.

N.T.M. Saksens, Y.T.E. Lechanteur, S.K. Verbakel, J.M.M. Groenewoud, M.R. Daha, T. Schick, S. Fauser, C.J.F. Boon, C.B. Hoyng, A.I. den Hollander.

PLoS One. Under review.

Discovery of novel candidate genes for normal tension glaucoma by whole exome sequencing in a large multiplex family.

S. Micheal, N.T.M. Saksens, B.F. Hogewind, C.B. Hoyng, A.I. den Hollander

Journal of Medical Genetics. Submitted.

Rare variants associated with age-related macular degeneration result in a lower age at onset and higher familial occurrence.

N.T.M. Saksens, M.J. Geerlings, B. Bakker, T. Schick, M.R. Daha, S. Fauser, C.J.F. Boon, E.K. de Jong, C.B. Hoyng, A.I. den Hollander.

JAMA Ophthalmology. Under review.

Whole exome sequencing in patients with the cuticular drusen subtype of age-related macular degeneration.

M.R. Duvvari, J.P.H. van de Ven, M.J. Geerlings, N.T.M. Saksens, B. Bakker, A. Henkes, K. Neveling, D. Westra, L.P.W.J. van den Heuvel, T. Schick, S. Fauser, C.J.F. Boon, C.B. Hoyng, E.K. de Jong, A.I. den Hollander

PLoS One. Under review.

Past sunlight exposure is a risk factor for age-related macular degeneration.

T. Schick, L. Ersoy, Y.T. Lechanteur, N.T.M. Saksens, A.I. den Hollander, S. Fauser

Retina. Accepted.



Physical Activity and Age-related Macular Degeneration: A systematic literature review and meta-analysis.

J. Le, M.B. Mcguinness, E. Cerin, N.T.M. Saksens, R.H. Guymer, R.P. Finger.
Ophthalmology. Under review.

Insights into Rare Genetic Variation: From a Large Study of Age-Related Macular Degeneration.

L.G. Fritsche, W. Igl, J.N. Cooke Bailey, F. Grassman, S. Sengupta, J.L. Bragg-Gresham, K.P. Burdon, S.J. Hebring, C. Wen, M. Gorski, I.K. Kim, D. Cho, D. Zack, E. Souied, H.P.N. Scholl, E. Bala, K.E. Lee, D.I. Chasman, R. Sardell, P. Mitchell, J.E. Merriam, V. Cipriani, J.D. Hoffman, T. Schick, Y.T.E. Lechanteur, R.H. Guymer, M.P. Johnson, Y. Jiang, C. Stanton, G.H.S. Buitendijk, X. Zhan, A.M. Kwong, A. Boleda, M. Brooks, L. Gieser, R. Ratnapriya, K.E. Branham, J.R. Foerster, J.R. Heckenlively, M.I. Othman, B.J. Vote, H. Hai Liang, E. Souzeau, I.L. McAllister, T. Isaacs, J. Hall, S. Lake, D.A. Mackey, I.J. Constable, J.E. Craig, T.E. Kitcher, Z. Yang, Z. Su, H. Luo, D. Chen, H. Ouyang, K. Flagg, D. Lin, G. Mao, H. Ferreyra, K. Stark, C.N. von Strachwitz, A. Wolf, C. Brandl, G. Rudolph, M. Olden, M.A. Morrison, D.J. Morgan, M. Schu, J. Ahn, G. Silvestri, E.E. Tsironi, K. Hyung Park, L.A. Farrer, A. Orlin, A. Brucker, M. Li, C. Curcio, S. Mohand-Saïd, J. Sahel, I. Audo, M. Benchaboune, A. Cree, C. Rennie, S. Goverdhan, M. Grunin, S. Hagbi-Levi, P. Campochiaro, N. Katsanis, F.G. Holz, F. Blond, H. Blanché, J. Deneuve, R.P. Igo Jr, B. Truitt, N. Peachey, S.M. Meuer, C.E. Myers, E.L. Moore, R. Klein, D. Hunter, M.D. Courtenay, S.G. Schwartz, J.L. Kovach, W.K. Scott, G. Liew, A.G. Tan, B. Gopinath, J.C. Merriam, R.T. Smith, J. Khan, H. Shahid, A.T. Moore, J.A. McGrath, R. Laux, M.A. Brantley, A. Agarwal, L. Ersoy, A. Caramoy, T. Langmann, N.T.M. Saksens, E.K. de Jong, C.B. Hoyng, M.S. Cain, A.J. Richardson, T.M. Martin, J. Blangero, D.E. Weeks, B. Dhillon, C.M. van Duijn, K.F. Doheny, J. Romm, the GIANT consortium, the CKDGen consortium, C.C.W. Klaver, C. Hayward, M.B. Gorin, M.L. Klein, P.N. Baird, A.I. den Hollander, S. Fauser, J.R.W. Yates, R. Allikmets, J.J. Wang, D.A. Schaumberg, B.E. K. Klein, S. Hagstrom, I. Chowers, A. Lotery, T. Léveillard, K. Zhang, M.H. Brilliant, A.W. Hewitt, A. Swaroop, E.Y. Chew, M.A. Pericak-Vance, M. DeAngelis, D. Stambolian, J.L. Haines, S.K. Iyengar, B.H.F. Weber, G.R. Abecasis, I.M. Heid.

Nature genetics. Accepted.

Analysis of rare variants in the *CFH* gene in patients with the cuticular drusen subtype of age-related macular degeneration.

M.R. Duvvari, N.T.M. Saksens, J.P.H. van de Ven, Y. de Jong-Hesse, T. Schick, W.M. Nillesen, S. Fauser, L.H. Hoefsloot, C.B. Hoyng, E.K. de Jong, A.I. den Hollander.

Molecular Vision 2015;21:285-292.

Dominant cystoid macular dystrophy.

N.T.M. Saksens, R.A. van Huet, J.J. van Lith-Verhoeven, A.I. den Hollander, C.B. Hoyng, C.J.F. Boon.
Ophthalmology 2015;122(1):180-191.

Clinical characteristics of familial and sporadic age-related macular degeneration: differences and similarities.

N.T.M. Saksens, E. Kersten, J.M.M. Groenewoud, M.J. van Grinsven, J.P.H. van de Ven, C.I. Sánchez, T. Schick, S. Fauser, A.I. den Hollander, C.B. Hoyng, C.J.F. Boon.
Investigative Ophthalmology & Visual Science 2014;9:7085-7092.

Analysis of rare variants in the C3 gene in patients with age-related macular degeneration.

M.R. Duvvari, C.C. Paun, G.H. Buitendijk, N.T.M. Saksens, E.B. Volokhina, T. Ristau, F.E. Schoenmaker-Koller, J.P.H. van de Ven, J.M.M. Groenewoud, L.P. van den Heuvel, A. Hofman, S. Fauser, A.G. Uitterlinden, C.C.W. Klaver, C.B. Hoyng, E.K. de Jong, A.I. den Hollander.
PLoS One 2014;15:9(4).

Macular dystrophies mimicking age-related macular degeneration.

N.T.M. Saksens, M. Fleckenstein, S. Schmitz-Valckenberg, F.G. Holz, A.I. den Hollander, J.E.E. Keunen, C.J.F. Boon, C.B. Hoyng.
Progress in Retinal and Eye Research 2014;9:2-57.

Smoking behavior and attitudes in patients undergoing cardiac surgery. The Radboud experience.

N.T.M. Saksens, L. Noyez
Interactive Cardiovascular and Thoracic Surgery 2010;10:195-199.



DANKWOORD

Een promotieonderzoek kost veel energie en vergt doorzettingsvermogen, maar het geeft ook voldoening. Daarom zou ik mijn promotietraject willen vergelijken met mijn ontwikkeling in het hardlopen. Tijdens het promotieonderzoek heb ik in het oogheekunde team van het RadboudUMC aan diverse hardloopwedstrijden deelgenomen, waaronder de Zevenheuvelenloop (15km). De eerste 5 kilometer ging snel voorbij, wat overeenkomt met mijn 1^e promotiejaar, waarin ik alle AMD families heb verzameld. De tweede 5 kilometer gaat over de zware Zevenheuvelenweg en karakteriseert mijn 2^e promotiejaar, waarin de exome sequencing van de verzamelde familieleden wat vertraging opliep, maar waarin ik veel heb geleerd in Oxford en mijn eerste artikel werd geaccepteerd. De laatste 5 kilometer gaat vals plat naar beneden, waardoor je kunt versnellen, overeenkomstig met mijn laatste promotiejaar. Het blijft dan echter wel goed opletten dat je niet struikelt, want er zitten hobbels in de weg en het wordt steeds drukker op het parcours. Daar staan ook steeds meer mensen aan de kant van de weg om aan te moedigen, wat het mogelijk maakt om dan nog de eindsprint in te zetten.

Gedurende het gehele traject van trainen, voorbereidingen en hardloopwedstrijden werd ik bijgestaan door heel veel mensen. Zo ook gedurende mijn promotietraject. Het is dan ook een onmogelijke taak om iedereen persoonlijk te bedanken die op welke manier dan ook bij mijn promotieonderzoek betrokken is geweest. Daarom wil ik hierbij iedereen bedanken! Echter, in het bijzonder wil ik de volgende mensen bedanken:

Beste Prof. dr. Hoyng, beste Carel, door jouw klinische ervaring wist je altijd het klinisch belang van het onderzoek voorop te stellen, iets wat bij wetenschappelijk onderzoek soms wordt vergeten. Je bent een man met humor die overal juist de mogelijkheden in ziet. Jij hebt me geholpen bij het verzamelen van familiale AMD patiënten en de middelen geboden die nodig waren voor het onderzoek. Daarnaast heb jij mij ook de vrijheid gegeven om mezelf te ontwikkelen en de kans gegeven om me te bewijzen als onderzoeker. Ik wil je bedanken voor je vertrouwen in mij en mijn onderzoek.

Beste Prof. dr. Den Hollander, beste Anneke, jij keek mijn manuscripten altijd met grote precisie na. Je weet dingen zo te formuleren dat ik vaak bij het doornemen van jouw revisies dacht ‘ja, dat is precies wat ik bedoelde’, maar daar kwam ik dan zelf niet op. Jouw vermogen om onderzoeksplannen te schrijven en daarmee subsidies te werven en het vormen van de brug tussen genetica en de oogheekunde is van groot belang geweest bij mijn onderzoeken. Tijdens mijn onderzoek ben jij tot professor benoemd, waardoor ik ineens twee promotoren had. Bedankt dat jouw deur altijd voor mij open stond en dat je altijd op de hoogte was van mijn projecten. Je was de constante factor in de begeleiding van mijn promotietraject.

Beste dr. Boon, beste Camiel, jouw grote kennis op het gebied van erfelijke retinale aandoeningen en jouw enthousiasme maken jou tot een uitstekende co-promotor. Dit, samen met je prettige klinische begeleiding en altijd positieve instelling waren voor mij

telkens weer een grote inspiratiebron. Ook toen je Nijmegen verliet bleef je me op afstand begeleiden of kwam ik naar je toe, zoals in Oxford. Dat was een leerzame en onvergetelijke periode voor mij, waarin ik de kunst van het schrijven (in zekere mate) van jou heb mogen leren. Bedankt voor je bijna 24-uur non-stop begeleiding, want zelfs 's avonds en in de weekenden hadden we regelmatig skype-meetings en een mail werd vrijwel altijd diezelfde dag (of nacht) nog door jou beantwoord. Dank voor je enthousiasme en steun waar ik altijd op kon rekenen.

Beste Prof. dr. Keunen, tijdens klinische besprekingen en het schrijven van mijn review heb ik uw motiverende begeleiding, enorme kennis en expertise mogen ervaren. Hartelijk dank daarvoor.

Beste Prof. dr. Klaver, beste Caroline, de combinatie van genetica, epidemiologie en het klinisch beeld maakte mijn onderzoek complex, maar deze combinatie is aan jou helemaal toevertrouwd. Bedankt voor jouw ideeën, begeleiding en inspiratie op de momenten dat ik zelf niet meer wist hoe ik verder moest gaan.

Beste Prof. Daha, dank dat u met uw expertise op het gebied van het complement systeem mij wilde bijstaan in de complement analyses binnen de diverse onderzoeken naar maculadegeneratie.

Dear Prof. dr Holz, dr. Monica Fleckenstein and dr. Steffen Schmitz-Valckenberg: I'm really thankful for our nice collaboration in writing the impressive review for the journal *Progress in Retinal and Eye Research*.

I am also grateful to my German colleagues in the EUGENDA database for our close collaboration.

Dear Patsy Nishina, Mark Krebs and the analysts of the Jackson Laboratory: thank you for our collaboration which has strengthened our findings in humans and mice, leading to a great result. I am also grateful to the Belgian and Italian groups of Prof. dr. Bart Leroy and dr. Sandro Banfi, respectively, for providing us with clinical data of patients with pattern dystrophy.

Kornelia Neveling, Stef Letteboer en Ronald Roepman, ik wil jullie bedanken voor jullie bijdrage in het functionele onderzoek naar patroon dystrofie. Dat toont maar weer dat onderzoek doen niet iets is wat je alleen doet, maar een samenwerking van allerlei expertises vereist.

Bij wetenschappelijk onderzoek vind je meestal niet in één keer het antwoord op de vraag, maar dit gaat vaak stapsgewijs. Beste dr. Van Lith-Verhoeven, beste Janneke, jouw onderzoek naar 'butterfly-shaped' pigment dystrofie en dominante cystoïde macula dystrofie vormde een goede basis voor mijn vervolg onderzoek. Dank hiervoor.

Vervolgens een speciale plek voor mijn collega-promovendi. Myrte, Ramon, John, Dženita, Yara, Freekje, Nathalie, Stanley, Michel, Eveline, Constantin, Mahesh, Maartje, Shazia en Mark, bedankt voor jullie betrokkenheid en samenwerking, maar ook voor de gezelligheid samen. Met de klinische collega's hoop ik in de kliniek weer fijn samen te mogen werken als arts-assistent.



Frederieke, Bjorn, Tamara, en Eiko, hoewel ik niet altijd begreep waarom sommige genetische processen zoveel tijd in beslag namen en ik soms ongeduldig werd van jullie uiterst gedetailleerde verslaglegging van werkelijk alles wat jullie deden, is jullie genetische ondersteuning en begeleiding voor mij van groot belang geweest. En Frederieke, ik kan het nog steeds niet bevatten dat jij mij hebt kunnen overtuigen het onzichtbare te pipetteren en dat we daarmee uiteindelijk een nieuwe genetisch oorzaak voor 'Butterfly-shaped pigment dystrofie' hebben geïdentificeerd.

Bert, Tiny, en Saskia, hoewel jullie werk zich vooral achter de schermen plaatsvindt, gaf het me altijd een goed gevoel de bloedmonsters bij jullie af te kunnen leveren, want bij jullie was het in goede handen voor de verwerking ervan.

Beste Arjen, jouw bio-informatische ondersteuning was onmisbaar om met de enorme hoeveelheid exome sequencing data van aangedane families te kunnen werken. Bedankt.

Beste drs. Groenewoud, beste Hans. Jouw statistische kennis en inzicht hebben mij geholpen mijn enorme data bestanden te analyseren en te komen tot de resultaten van dit proefschrift. Tussen alle analyses door waren jouw boeiende verhalen over vlinders en de natuur telkens weer een gezellige en leerzame afleiding. Dank voor alles.

Het hele optometristenteam, en in het bijzonder Liesbeth en Jack, wil ik bedanken voor de goede ondersteuning bij de onderzoeken van mijn patiënten. Altijd kon ik bij jullie terecht voor het maken van extra afbeeldingen en het uitvoeren van extra testen, zelfs al was daar eigenlijk geen tijd voor.

Dames van het trialcentrum, bedankt voor jullie ondersteuning bij het verzamelen van mijn onderzoekspatiënten, in het bijzonder Anne voor al het belwerk voor de AMD dagen, maar ook voor jullie gezelligheid.

Collega's van de verpleegpost, de administratie en het stafsecretariaat oogheelkunde bedankt voor de gezelligheid en jullie ondersteuning bij het maken van alle afspraken met de patiënten en met mijn begeleiders.

De studenten Sanne, Eveline en Leonie wie ik tijdens mijn promotieonderzoek heb mogen begeleiden: naast een leerzame periode voor jullie, was het voor mij ook leerzaam om jullie te begeleiden.

Arts-assistenten oogheelkunde, bedankt voor jullie gezelligheid en prettige samenwerking van afgelopen jaar, waarin ik mijn opleiding tot oogarts ben gestart en mijn proefschrift heb afgerond. Wat fijn om jullie als collega's te hebben.

Hardloopgroep B van Running-Elst, bedankt voor de ontspanning en hardlooptechniek.

Uiteraard ben ik alle patiënten die hebben deelgenomen aan het onderzoek uiterst dankbaar, want zonder hun medewerking was mijn onderzoek onmogelijk. Hun blijk van waardering dat je onderzoek doet naar hetgeen wat voor hen van groot belang is, geeft mij energie om door te zetten. Het klinisch belang van wetenschappelijk onderzoek mag namelijk nooit uit het oog worden verloren en is uiteindelijk hetgeen waar je het allemaal voor doet!

Al mijn vriendinnen, in het bijzonder Marieke, Ilse, Nicole en Manon, dank voor jullie belangstelling, steun en afleiding ondanks jullie eigen drukke agenda's. We hebben het altijd erg gezellig, maar het is ook fijn om te weten dat we er altijd voor elkaar zijn. Vriendschap is een waardevol goed; het verdubbelt de vreugde en deelt de frustraties.

Gary, José, Iris, Tim en Rogier, ik wil jullie bedanken voor alle gezelligheid en jullie oprechte interesse in mij als jullie 'Nicolovic' van het gezin. Het is mooi te zien dat Iris naast het piano spelen ook mijn passie voor de geneeskunde deelt.

Mijn paranimfen Ilse en Myrte, wat fijn dat jullie op deze belangrijke dag naast mij willen staan, zoals jullie mij ook tijdens mijn promotieonderzoek altijd hebben bijgestaan. Met vragen of problemen kunnen we bij elkaar terecht en bieden we een luisterend oor. We hebben de hoogtepunten van het onderzoek samen gevierd en samen heel veel plezier gehad. Bedankt.

Als laatste, mijn lieve familie, welke voor mij heel belangrijk is. In het bijzonder mijn ouders, die mij hebben geleerd door te zetten en er alles uit te halen wat erin zit, want dat is waar 'een echte Saksens' voor staat en waar ik trots op ben. Jullie steunen me in mijn keuzes en alles wat ik doe, zo ook tijdens mijn promotieonderzoek. Jullie staan altijd voor jullie kinderen klaar, hebben samen veel bereikt en zijn een groot voorbeeld voor mij. Daarnaast wil ik ook Ramon, Erik, Tanja en mijn schoonfamilie bedanken voor alle gezelligheid, steun en interesse in alles wat ik doe. En Tanja, ik kan oprecht zeggen: jij ben de allerliefste zus die ik me kan wensen.

Lieve Roderik, met jouw liefdevolle ondersteuning en vermogen om mij op de juiste momenten af te remmen, heb ik dit proefschrift kunnen volbrengen, mijzelf verder kunnen ontwikkelen en ben ik trots dat jij mijn man bent.



ABOUT THE AUTHOR

Nicole Theresia Maria Saksens was born on the 3rd of January 1987 in Haaksbergen, the Netherlands. She graduated *cum laude* from secondary school at Gymnasium Het Assink in Haaksbergen in 2005. She studied Medicine at the Faculty of Medicine of the Radboud University Nijmegen, where she received the Bachelor of Science (BSc) degree *cum laude* in 2008; in 2011, she received her Master of Science (MSc)/ Medical Doctor (MD) degree with *bene meritum* distinction. During her study, Nicole worked as a research student in the Department of Physiology, where she investigated the effect of physical activity in patients with metabolic syndrome. Her particular interest in ophthalmology emerged in the third year of her medicine study, when she attended a lecture on the visual pathway and the anatomy of the eye given by Prof. dr. J.R.M. Cruysberg. An internship in Ophthalmology further deepened her interest in this field of study. During her senior-internship in the Department of Ophthalmology, Nicole investigated familial normal-tension glaucoma. In October 2011, Nicole initiated her PhD research on familial macular diseases, which resulted in this thesis, in the Department of Ophthalmology at the RadboudUMC in Nijmegen under the supervision of Prof. dr. C.B. Hoyng, Prof. dr. A.I. den Hollander, and dr. C.J.F. Boon. During her PhD, Nicole was a co-initiator and co-organizer of the 'Dutch Ophthalmology PhD-Students' (DOPS) congress, a committee member of the 'Association for Research in Vision and Ophthalmology Netherlands' (ARVO-NED) chapter committee, and the recipient of an 'ARVO-International Travel Grant' for her oral presentation given at the ARVO congress in Fort Lauderdale, Florida. Nicole visited the University of Oxford in March and April 2013 for her research activities, which was supported by the 'Prins Bernhard Cultuurfonds' grant she received. In December 2014, she started her residency in ophthalmology at the RadboudUMC, under the auspices of dr. B.J. Klevering and Prof. dr. J.E.E. Keunen.



A handwritten signature in black ink, appearing to read 'N. Saksens', enclosed within a large, stylized oval flourish.



PHD PORTFOLIO

Name PhD student: <i>Nicole T.M. Saksens</i>	PhD period: <i>01-10-2011 – 31-10-2014</i>
Department: <i>Ophthalmology</i>	Promotors: <i>Prof. Dr. C.B. Hoyng,</i>
Graduate School: <i>Radboud Institute for Health Sciences</i>	<i>Prof. Dr. A.I. den Hollander</i>
	<i>Co-promotor: Dr. C.J.F. Boon</i>

	TRAINING ACTIVITIES	Year(s)	ECTS
a)	Courses & Workshops		
-	<i>Medical library: endnote</i>	2011	0.1
-	<i>Cambridge course, advanced graduate</i>	2012	4.5
-	<i>NIHES: Principles of Research in Medicine; Rotterdam</i>	2012	0.7
-	<i>NIHES: Principles of Genetic Epidemiology; Rotterdam</i>	2012	0.7
-	<i>IGMD: Poster presentation workshop</i>	2012	0.2
-	<i>IGMD: How to write a medical scientific paper</i>	2012	0.2
-	<i>IGMD: How to organize your data</i>	2012	0.2
-	<i>ARVO-NED: Research Course Emerging Therapies; Amsterdam</i>	2012	0.2
-	<i>Academic writing</i>	2013	2.0
-	<i>Advanced conversation</i>	2013	3.0
-	<i>Presentation skills</i>	2013	1.5
-	<i>Basiscursus Regelgeving en Organisatie voor Klinisch onderzoekers (BROK)</i>	2013	1.5
-	<i>SPSS course</i>	2013	0.6
-	<i>The art of presenting science</i>	2013	1.5
-	<i>Course in Eye Genetics; Gent</i>	2013	0.6
-	<i>How to design your thesis</i>	2014	0.2
b)	Seminars & lectures[^]		
-	<i>Masterclass: novel therapies in retinal dystrophies</i>	2014	0.3
-	<i>ARVO WEAVR</i>	2012, 2013	
-	<i>Referring / imaging evening department of Ophthalmology</i>	2012, 2013, 2014	
-	<i>PhD-defences/Orations</i>	2011,2012,2013,2014	
c)	Symposia & congresses[^]		
-	<i>NOG</i>	2011, 2012# - 2014#	1.2
-	<i>OOG/ZOG</i>	2011 - 2013	0.4
-	<i>ARVO-congress</i>	2012#, 2013 [^]	3.0
-	<i>DOPS</i>	2012 - 2014#	1.5
-	<i>IGMD Science day</i>	2013	0.4
d)	Other		
-	<i>Eugenda retreat; Cologne/Nijmegen</i>	2011,2012#,2013#	0.1
-	<i>FFB center grant meetings</i>	2012#-2014#	1.5
-	<i>LVAO study day; Utrecht</i>	2014	0.3
-	<i>Radboud Research Round Sensory Disorders</i>	2014	
	TEACHING ACTIVITIES		
e)	Lecturing		
-	<i>MD-patient organization</i>	2011#, 2013#	
-	<i>DCMD-family day</i>	2012#	
f)	Supervision of internships / other		
-	<i>Teaching 5KMP1 Medical biotechnology</i>	2014	0.3
-	<i>Supervision scientific research: Sanne Verbakel, Leonie Bogaard, and Eveline Kersten</i>	2013, 2014	
	TOTAL		26.7

